POLITECNICO DI TORINO
Repository ISTITUZIONALE

Effective elasto(visco)plastic coefficients of a biphasic composite material with scaledependent size effects

Original
Effective elasto(visco)plastic coefficients of a biphasic composite material with scaledependent size effects / Giammarini, A., Ramíreztorres, A., Grillo, A.. - In: MATHEMATICAL METHODS IN THE APPLIED SCIENCES. - ISSN 0170-4214. - 48:1(2025), pp. 926-979. [10.1002/mma.10367]

Availability:
This version is available at: 11583/2993590 since: 2024-10-22T15:55:25Z

Publisher:
Wiley

Published
DOI:10.1002/mma.10367

Terms of use:

This article is made available under terms and conditions as specified in the corresponding bibliographic description in the repository

Publisher copyright

(Article begins on next page)

25 November 2026

Check for updates

Received: 23 January 2024 | Revised: 11 June 2024 | Accepted: 13 July 2024

DOI: 10.1002/mma.10367

RESEARCH ARTICLE

WILEY

Effective elasto-(visco)plastic coefficients of a bi-phasic composite material with scale-dependent size effects

Alessandro Giammarini[1] | **Ariel Ramírez-Torres**[2] | **Alfio Grillo**[1]

[1]Dipartimento di Scienze Matematiche "G. L. Lagrange", Politecnico di Torino, Turin, Italy

[2]School of Mathematics & Statistics, University of Glasgow, Glasgow, UK

Correspondence
Alfio Grillo, Dipartimento di Scienze Matematiche "G. L. Lagrange", Politecnico di Torino, Turin 10129, Italy.
Email: alfio.grillo@polito.it

Communicated by: P. A. Mariano

Funding information
A. Grillo is partially supported by MIUR (Italian Ministry of Education, University and Research) through the PRIN project n. 2017KL4EF3 on "Mathematics of active materials: From mechanobiology to smart devices" and the PRIN project n. 2020F3NCPX on "Mathematics for industry 4.0 (Math4I4)." A. Grillo's research group is funded by the European Union—Next Generation EU. A. Grillo and A. Giammarini have been supported by the Research Project Prin2022 PNRR of National Relevance P2022KHFNB on "Innovative multiscale approaches, possibly based on Fractional Calculus, for the effective constitutive modeling of cell mechanics, engineered tissues, and metamaterials in Biomedicine and related fields" granted by the Italian MUR. A. Ramírez-Torres is supported by the Engineering and Physical Sciences Research Council (Grant EP/Y001583/1). This grant is funded by the International Science Partnerships Fund (ISPF) and the UK Research and Innovation (UKRI).

We employ the theory of asymptotic homogenization (AH) to study the elasto-plastic behavior of a composite medium comprising two solid phases, separated by a sharp interface and characterized by mechanical properties, such as elastic coefficients and "initial yield stresses" (i.e., a threshold stress above which remodeling is triggered), that may differ up to several orders of magnitude. We speak of "plastic" behavior because we have in mind a material behavior that, to a certain extent, resembles plasticity, although, for biological systems, it embraces a much wider class of inelastic phenomena. In particular, we are interested in studying the influence of gradient effects in the remodeling variable on the homogenized mechanical properties of the composite. The jump of the mechanical properties from one phase to the other makes the composite highly heterogeneous and calls for the determination of *effective properties*, that is, properties that are associated with a homogenized "version" of the original composite, and that are obtained through a suitable averaging procedure. The determination of the effective properties results convenient, in particular, when it comes to the multiscale description of inelastic processes, such as remodeling in soft or hard tissues, like bones. To accomplish this task with the aid of AH, we assume that the length scale over which the heterogeneities manifest themselves is several orders of magnitude smaller than the characteristic length scale of the composite as a whole. We identify both a *fine-scale* problem and a *coarse-scale* problem, each of which characterizes the elasto-plastic dynamics of the composite at the corresponding scale, and we discuss how they are reciprocally coupled through a transfer of information from one scale to the other. In particular, we highlight how the coarse-scale plastic distortions influence the fine-scale problem. Moreover, in the limit of negligible hysteresis effects, we individuate two viscoplastic effective coefficients that encode the information of the two-scale nature of the composite medium in the upscaled equations. Finally, to deal with a case study tractable semi-analytically, we consider a multilayered composite material with an initial yield stress that is constant in each

This is an open access article under the terms of the Creative Commons Attribution License, which permits use, distribution and reproduction in any medium, provided the original work is properly cited.
© 2024 The Author(s). Mathematical Methods in the Applied Sciences published by John Wiley & Sons Ltd.

phase. Such investigation is meant to contribute to the constitution of a robust framework for devising the effective properties of hierarchical biological media.

KEYWORDS

asymptotic homogenization, biological composites, constraints, effective coefficients, nonlinear composites, remodeling, strain-gradient plasticity

MSC CLASSIFICATION

74Q05, 74Q15, 74C10, 74C15, 74A40, 74E30, 35J05, 35J57

1 | INTRODUCTION

Biological systems exhibit the innate capability of modifying actively their internal structure in response to interactions that may be either internal or external to them and that are expressed in the form of signaling pathways of various type, involving both genetic and epigenetic factors [1], among which the most common ones are of chemo-mechanical origin. Relevant instances of the reorganization of biological media involve, for example, cellular migration [2], the rupture and restoration of the adhesive links among the cells [3], and the agglomeration of cellular aggregates, with characteristics depending on the environment in which the cells are cultured [4]. These specific phenomena are manifestations of more general classes of internal transformations of biological tissues, which, in turn, comprise morphogenesis and pattern formation [1], aging [5, 6], damage [7], growth [1, 8], and remodeling [1].

Each of the aforementioned processes expresses a peculiar type of *symmetry breaking* for the tissue in which it occurs. In particular, damage, growth, and remodeling share the feature of being inherently *anelastic* [1], in the sense that they involve the commencement and evolution of structural transformations that cannot be resolved in terms of mere changes of shape of the medium hosting the transformations themselves. This issue is closely related to two main problems: on the one hand, the necessity for generalizing the notion of "configuration" in a way capable of accounting for the defects and residual stresses that typically originate from the structural evolution of a body [9–16] (this can be achieved by switching to a non-Euclidean geometry [9, 10, 16–18]); on the other hand, the necessity for introducing suitable tensor fields for describing the fact that, as is the case for plasticity (see, e.g., [9]), a structural transformation experienced by a body is, in general, neither a deformation nor the tangent map of a deformation (i.e., a "deformation gradient"). Because of this property, a structural transformation is often identified with an *incompatible deformation* (for a discussion on incompatibility, the reader is referred, e.g., to [16]), and we shall refer to it as *distortion* in the sequel.

Other common features of damage, growth, and remodeling are their being intrinsically multiscale phenomena, and the fact that they typically induce variations of the mechanical properties of the media in which they take place, for example, by varying their stiffness. The multiscale nature of the processes listed above combines with the complex architecture of biological tissues, which consists of several constituents differing in shape, functionality, and mechanical properties (e.g., protein fibers, osteoblasts, nuclei, cellular membranes, and extra-cellular matrix).

In this work, by expanding the framework developed in [19], our focus is on the formulation of a multiscale description of *remodeling* in a tissue characterized by a microstructure that, as is often assumed in the case of bone, can be taken to be periodic [20, 21]. For our purposes, we consider only two scales, which we refer to as the microscale (or fine scale) and the macroscale (or coarse scale), respectively, and we hypothesize that remodeling occurs at both scales. Specifically, "remodeling" here is meant to be the complex of transformations of the internal structure of the medium under study that, at the finest scale considered, produce *anelastic distortions* resembling the incompatible deformations associated with the irreversible strains occurring in bone tissue [22–24]. Indeed, various experiments performed on bone [25, 26], like torsion, ultrasound, and nano-indentation, highlight the onset and accumulation of anelastic distortions both at the scale of the osteons and at that of the tissue as a whole. In particular, such anelastic distortions are often related to the "*formation of microcracks in diseased or injured tissues*" [27] (see also [7, 26, 28]), and concur to alter the fine-scale mechanical properties of the material itself, such as its elastic coefficients, thereby providing a motivation for investigating how the concomitant microstructural reorganizations impact the macroscopic mechanical properties of the tissue. Indeed, the anelastic distortions introduced at the fine scale are upscaled to the coarse scale, and so is also their influence on the material's elasticity moduli, which are then expressed through a tensor field that is referred to as *tensor of effective elastic coefficients* [19, 29, 30]. The benefit of this study, although being at the level of a conjecture for the time being, could be

10991476, 2025, 1, Downloaded from https://onlinelibrary.wiley.com/doi/10.1002/mma.10367 by Politecnico Di Torino Sist. Bibl Del Polit Di Torino, Wiley Online Library on [12/02/2025]. See the Terms and Conditions (https://onlinelibrary.wiley.com/terms-and-conditions) on Wiley Online Library for rules of use; OA articles are governed by the applicable Creative Commons License

a better characterization of the mechanical properties of hierarchical biological media [31–33]. More generally, indeed, the type of remodeling described here for the bone tissue can manifest itself also in a variety of other tissues, such as multicellular aggregates [34], malignant tissue [35], and focal adhesions [36], involving different scales.

In the sequel, we consider a biphasic, solid–solid composite medium, the internal structure of which undergoes remodeling, and by employing the asymptotic homogenization (AH) theory [37–41], we examine how its mechanical properties vary in response to the considered remodeling process. Within the characterization of homogenized systems, we believe that one of the main novelties of our work is the contextualization of the flow rule introduced by Gurtin and Anand [42] for plastic distortions to the study of remodeling and, in particular, the characterization of this phenomenon in a two-scale setting. We pursue this goal in a way that, by employing AH, size effects are explicitly taken into account at both the microscale and the macroscale of the composite. More in detail, although the original formulation of the flow rule proposed in [42] is conceived within the theory of plasticity, we adapt it to our biomechanical framework in order to describe the remodeling distortions. To this end, the anelastic deformations arising in the constituents of the composite as a result of their remodeling are formally described as if they were plastic distortions in a non-biological material. This approach has been proven to be successful in many situations addressed in the literature to describe remodeling and growth (see, e.g., [34, 35, 43–49]). On the basis of these considerations, in our work we will use the terminologies "remodeling distortions" and "plastic distortions" as equivalent. Moreover, as will be explained in Remark 4.1 below, we shall be dealing with a class of flow rules that is suitable for a type of remodeling sharing formal analogies with viscoplasticity rather than with plasticity. However, when there is no room for confusion, for the sake of conciseness we shall not distinguish between these two terms.

Building upon the investigations conducted in [19], we aim to shed light on the impact that, within the context of remodeling, higher order gradient effects may have on the overall behavior of composite media. For example, these effects should be taken into account, both at the microscale and at the macroscale, when considering indentation, torsion, bending, or uni-axial tests (see, e.g., [50] for a review on the topic).

To proceed with our work, we will take inspiration from the theory of strain-gradient plasticity. This theory was originally conceived to study the size effects due to the accumulation of geometrical dislocations in the lattices of metals [51], or to study the localization of inelastic distortions in materials, such as metals and polymers, exhibiting the formation of shear bands [52]. To resolve the spatial distribution of the plastic distortions, and to weigh their influence on the overall behavior of an elasto-plastic medium, it is necessary to identify the length scales characterizing the gradients of such distortions, and to let them feature explicitly in suitably formulated constitutive theories. For example, in [50], it has been shown that the length scales of plastic distortions, disregarded in conventional theories of plasticity [53], capture the phenomenology at the basis of the hardness–strain curves observed experimentally for several materials. Furthermore, a rather thorough examination of the role of these length scales was conducted, for example, in [54], where a relation among the intrinsic length of plastic dissipation, grain size, and spatial distribution of the deformation field is proposed.

In the literature, also, other homogenization approaches have been proposed for strain-gradient plasticity. For example, in [55], a homogenized version of the Gurtin and Anand [42] microforce balance is put forward on the basis of the Hill–Mandel condition. In fact, in the context delineated in [55], although the author distinguishes between the mesoscopic scale and the macroscopic scale of the medium studied in his work, the case of poor scale separation is considered. This aspect notwithstanding, it is demonstrated that the homogenized model predicts very closely the experimental data [55]. On the same principle, Gudmundson's strain-gradient theory of plasticity [56] is homogenized in [57]. Okumura et al. [58] proposed a grain-based homogenization strategy capable of accommodating for a low separation between the number of grains and the characteristic length scale associated with the Bauschinger effect. Moreover, investigations of the macroscopic mechanical properties of non-biological composites, being, for example, metallic, stiff, or generic materials, are carried out in [59–62], while other studies [63, 64] focus on the determination of effective mechanical properties. Besides, Grillo et al. [65] propose an adaptation of the theory of Anand et al. [52] to address a problem of biological growth and remodeling within the context of tumor mechanics, although no AH is used in that work.

In our work, by imitating the theory of Gurtin and Anand [42], the evolution of the remodeling distortions is viewed as the evolution of a descriptor, defined as a tensor field, that represents the structural degrees of freedom of the composite medium undergoing remodeling. Moreover, the kinematics of the overall remodeling process is depicted both at microscale and at the macroscale of the composite under investigation. In particular, our concern is the study of the relationship between the remodeling at the macroscale and the remodeling at the microscale (see Section 7), thereby trying to contribute to understand how the two phenomena are interweaved, as is the case, for example, of bones [28, 66].

10991476, 2025, 1, Downloaded from https://onlinelibrary.wiley.com/doi/10.1002/mma.10367 by Politecnico Di Torino Sist. Bibl Del Polit Di Torino, Wiley Online Library on [12/02/2025]. See the Terms and Conditions (https://onlinelibrary.wiley.com/terms-and-conditions) on Wiley Online Library for rules of use; OA articles are governed by the applicable Creative Commons License

In our approach, the microscale remodeling distortions are captured as if they were a locally periodic perturbation of the macroscopic ones, and are represented by a two-scale asymptotic expansion of the remodeling tensor and its rate. Moreover, in the present context, remodeling is assumed not to involve changes of the body mass, and we describe it as an isochoric process (this hypothesis, however, can be relaxed). In addition, following [42], we assume no plastic spin. In particular, by picking up some ideas from [67, 68], the isochoricity and the hypothesis of null plastic spin are treated as kinematic constraints and are then expanded asymptotically for coherence with the AH approach. Thus, we obtain two conditions for the macroscopic remodeling tensor and two conditions for the microscopic one, which concur to formulate the homogenized problem and the cell problem, respectively.

We also aim to study the role that the microscopic structure of the composite under investigation has on its macroscopic remodeling. This is done by taking into account the ordering and repetitiveness of the composite's constituents, which identify the so-called *periodic cell* of the composite itself (see, e.g., [40, 69, 70]), and the shape of the cell defined this way. Then, by means of AH, these items of information are transferred to the macroscale, where they appear in the macroscopic balance laws through suitable *effective coefficients*, and are combined with the information about the overall shape and size of the composite as a whole.

In its original formulation in the context of the theory of plasticity, the microforce balance put forward by Gurtin and Anand [42] can describe hysteresis phenomena, like the Bauschinger effect, and can be interpreted as a generalization of the Allen–Cahn equation [71] involving the remodeling rate tensor and the so-called Burgers tensor. In [42], the latter tensor is associated with a "defect" energy, which leads to the definition of a generalized backstress, but which is disregarded if one wishes to concentrate on the merely dissipative aspects of remodeling. By adhering to this hypothesis, we immerse the aforementioned microforce balance in the framework of AH, by assuming that it holds in the repetitive microstructure of the medium under study and, more specifically, in its periodic cell. This approach leads to the statement of a microscopic dynamic equation for the remodeling rate tensor that, by entailing the upscaling of a tensorial Allen–Cahn equation, requires the identification of the *remodeling effective coefficients* determining the macroscopic remodeling. This constitutes, to the best of our knowledge, a novelty in the field of AH applied to elasto-viscoplastic composites, and it is one of the major results of our work. Indeed, it shows how the microstructural information on the gradient part of remodeling is self-consistently upscaled. Moreover, as it is typical in the AH framework, this is done at a minimal cost, because one can solve the upscaled equation, rather than running simulations at a microstructural level.

For our purposes, we consider a multilayered composite material undergoing axial stretch under the hypothesis that the elastic and viscoplastic coefficients are spatially homogeneous within each constituents. Such considerations simplify considerably the problem, so that the solutions to the cell problems can be found analytically and the effective coefficients can be expressed explicitly. The homogenized dynamic equations are then simulated for realistic parameters, and the magnitude of the effects related to the gradient of the remodeling rate are evaluated.

2 | DIMENSIONAL ANALYSIS

We deem it necessary to begin our work with a dimensional consideration on the characteristic lengths involved in the study of the hypothetical composite material taken as target in our work. In fact, we should specify up to four characteristic lengths: Two are associated with the microscopic and macroscopic geometric features of the composite, respectively, and we denote them by ℓ_0 and L_0; the other two, indicated by ℓ_η and L_η, are associated with the dissipative and the non-dissipative processes described in the ηth constituent by strain-gradient plasticity.

Of the first two lengths, ℓ_0 is associated with the size of the periodic elementary cell, while L_0 is related to the size of the composite as a whole. Within the framework of AH, ℓ_0 and L_0 are usually introduced to identify the well-separated scales on which the cell problem and the homogenized problem [38, 40] are studied. However, the introduction of the other two lengths, relative to the strain-gradient plasticity, poses a dilemma: Is the microscopic scale still determined by ℓ_0, or is it identified by the minimum between ℓ_η and L_η?

The quantification of ℓ_η or L_η depends on the specific process that is taking place in the composite and, ultimately, on the physics that is being described. Moreover, ℓ_η and L_η appear naturally in the equation for strain-gradient plasticity that we rely on in the sequel [42], so that they should be compared with ℓ_0 prior to the homogenization of the flow rule. When the effects related to strain-gradient plasticity are visible only at relatively small characteristic lengths, that is, when they are comparable with, or smaller than, ℓ_0, the homogenization approach followed in the sequel leads to the conclusion that the gradients of the plastic-like tensorial variable are not resolved at the homogenized model (in other words, we could say that, in this case, the homogenization eliminates the macroscale effects of the strain gradient, since

10991476, 2025, 1, Downloaded from https://onlinelibrary.wiley.com/doi/10.1002/mma.10367 by Politecnico Di Torino Sist. Bibl Del Polit Di Torino, Wiley Online Library on [12/02/2025]. See the Terms and Conditions (https://onlinelibrary.wiley.com/terms-and-conditions) on Wiley Online Library for rules of use; OA articles are governed by the applicable Creative Commons License

it is conducted only inside each representative cell). Still, there are indications that these higher order contributions can be included even in the case of comparatively small values of ℓ_η or L_η [72].

In spite of the considerations reported above, in this work, we consider the technically simpler situation in which the microscopic scale is still determined by ℓ_0, which means that ℓ_η and/or L_η are greater than ℓ_0. Albeit this is a very peculiar circumstance, there exist cases in which it is verified. A representative example is given by [73], in which the plasticity of bone tissue is studied, and the authors write:

> *[…] the plastic zone size is found to be 0.0168* mm. *[…] Since the thickness of a lamella in bone is 3–12* μm, *the plastic zone evidently extends over 1–5 lamellae.*

Other papers reporting on the extension of the plastic zone at the tip of microcracks in bones are, for example, [74–76]. In the context of these works, a "plastic zone" is a region of bone tissue that forms in the proximity of crack-like defects, or cracks, and in which plastic distortions have occurred in response to the intensification of the mechanical stress due to the presence of the defects or cracks themselves. The generation of such zones and the concomitant development of plastic distortions are mechanisms capable of dissipating the mechanical energy introduced in the bone by the load to which it is subjected and, thus, to compete against the propagation of the defects or cracks [74].

Since the bone is a hierarchical material for which it is possible to identify a representative cell (see, e.g., [77]), the plastic zone may include various lamellae, which may result into a diffuse plastic interface of characteristic length greater than the one associated with the representative cell. Moreover, at the level of the microscale, the plastic zone envelops different constituents, each with its own material properties, thereby determining a heterogeneous microstructure.

The considerations done so far, which refer to bone tissue, serve to provide a biologically relevant situation that can justify the employment of the theory of AH to strain-gradient plasticity. However, in the sequel, we shall be dealing with a hypothetical composite material, which is assumed to have a very simple microstructure (not comparable with that of bone), and we shall focus solely on the role that material heterogeneities play in the identification of the effective coefficients of the composite itself.

Within the context delineated above, the novelty of our study is, to the best of our knowledge, in the quantitative determination of the influence of strain-gradient plasticity on the composite's effective coefficients. Indeed, a study of plasticity of grade zero in composite materials conducted by means of AH has been done in [19, 78] (here, "plasticity of grade zero" refers to the theory of plasticity that does not involve the gradient of the tensor of plastic distortions). To accomplish this task, we base our investigations on a hypothesis put forward by Okumura et al. [58] in one of the scenarios studied in their work, which relies on the condition that the length of the representative cell of a metallic material is sufficiently smaller than the characteristic length of the spatially resolved dissipative processes associated with strain-gradient plasticity. In our notation, upon setting $\ell_m := \min\{\ell_1, \ell_2\}$, this condition reads $\ell_0 < \ell_m$, where we recall that ℓ_0 is the characteristic length of the representative cell of the composite material hereafter taken as target.

Since our target composite medium is meant to be an idealization of a biological tissue, we shall adopt Gurtin's theory of strain-gradient plasticity [42] to describe the biological process of *structural remodeling*, which, as anticipated in Section 1, consists in the rearrangement of the tissue's internal structure and in the evolution of its mechanical properties. For this reason, we shall speak of *strain-gradient remodeling* as a synonym of "strain-gradient plasticity." Within this setting, we would like to study the effect of the heterogeneities of our idealized medium on the macroscale spatial distribution of the homogenized remodeling descriptor, and *not* the contrary, which instead would be the case of interest if the dissipative length ℓ_m were shorter than the cell length ℓ_0. Consequently, we evaluate how the medium's heterogeneities influence the macroscopic evolution of the medium itself, since we expect them to play a relevant role in its evolution, also because of the assumed shape of the reference cell and of the spatial distribution of the constituents. However, we wish to remark that this work is to be intended as an intermediate step with respect to a further homogenization approach.

We also draw a parallelism between our approach and the one followed by [58]. In the work by Okumura et al. [58], the role of the grain size of the metal considered therein is investigated in order to establish the elasto-plastic response of the metal itself under uniform stress, while giving prominence to microstructural effects. Moreover, even though the authors employ a strategy for homogenization that is different from ours, they study the cases characterized by the conditions $\ell_m/\ell_0 = 1$ and $\ell_m/\ell_0 = 2 \cdot 10^1$ (in our notation). In our work, we weaken these two conditions by hypothesizing $\ell_m/\ell_0 \leq 1$, and $\ell_m/\ell_0 \geq k \cdot 10^1$ with $k > 1$ being a case-dependent real number, respectively. In particular, when the second condition is fulfilled, it suggests that strain-gradient plasticity in a composite with periodic microstructure can be approached by means of AH, which requires that all the physical quantities related to the phenomenon of interest are expanded in asymptotic series of the smallness parameter $\varepsilon := \ell_0/L_0$, with ℓ_0 and L_0 being the characteristic length of the

10991476, 2025, 1, Downloaded from https://onlinelibrary.wiley.com/doi/10.1002/mma.10367 by Politecnico Di Torino Sist. Bibl Del Polit Di Torino, Wiley Online Library on [12/02/2025]. See the Terms and Conditions (https://onlinelibrary.wiley.com/terms-and-conditions) on Wiley Online Library for rules of use; OA articles are governed by the applicable Creative Commons License

periodic reference cell and the characteristic length of the composite, respectively. In the sequel, we assume the validity of the condition $\ell_m/\ell_0 \geq k \cdot 10^1$, with $k > 1$, and we do perform AH, since, for the time being, we concentrate on problems that, although technically simpler, have a biological relevance which we are aware of, as is the case for the study of the plastic zones in bones. This has a twofold advantage: First, our choice offers the possibility to contribute to the foundations of the theory of AH and of the theory of Grade 1 plasticity together, by reviewing, in particular, the main results of Gurtin and Anand [42], and especially the constraints, in the framework of AH; second, our study supplies a benchmark in which it is possible to observe and quantify how the microstructural dynamics influences the macroscopic physics through the relevant *effective coefficients* of the composite (which, by definition, encode the geometrical and material properties of the composite).

3 | THEORETICAL BACKGROUND

In this section, we provide the background for addressing the main goal of our work. We begin with recalling the rationale behind the hypothesis of scale separation, and we specialize it to the type of composite materials examined in the sequel. Then, we review the main consequences of this hypothesis in the description of the two-scale spatial variability of the physical quantities that are relevant for our study. Furthermore, since we aim at the mechanical characterization of the composite material under investigation, we summarize the definitions of continuum kinematics that are essential for our purposes. Finally, since the main novelty of our work is related to the formulation and adaptation of Gurtin and Anand's theory of strain-gradient elasto-plasticity [42] to composite materials, we summarize how the fundamentals of AH apply to the problem at hand.

3.1 | Topology and kinematics

To describe the kinematics of the composite material under study, we begin with the introduction of its reference placement, that is, a subset $\mathscr{B}_R$ of the three-dimensional Euclidean space $\mathscr{S}$, in which the composite is ideally placed, and from which its changes of shape and internal structure are observed.

We hypothesize that $\mathscr{B}_R$ is partitioned into two disjoint open subsets $\mathscr{B}_{R\eta}$, with $\eta = 1, 2$, each of which is occupied by a continuum body, and corresponds to a phase, or constituent, of the biphasic composite under consideration. In general, $\mathscr{B}_{R\eta}$, with $\eta = 1, 2$, need not be connected, and thus, $\mathscr{B}_{R1}$ and $\mathscr{B}_{R2}$ may be separated from one another by several interfaces. We indicate with Γ_R the set of all interfaces separating $\mathscr{B}_{R1}$ from $\mathscr{B}_{R2}$, and we suppose that there are no voids in $\mathscr{B}_R$. Each surface of Γ_R is supposed to be contourless. Hence, we may write $\mathscr{B}_R = \mathscr{B}_{R1} \cup \mathscr{B}_{R2} \cup \Gamma_R$, $\overline{\mathscr{B}_{R1}} \cap \mathscr{B}_{R2} = \emptyset$ and $\mathscr{B}_{R1} \cap \overline{\mathscr{B}_{R2}} = \emptyset$, where the superimposed bar stands for the topological closure of the set to which it is applied.

We denote by $\mathscr{B}(t) \subset \mathscr{S}$ the subset of $\mathscr{S}$ occupied by the composite as a whole at the time t, and similarly to the description provided for $\mathscr{B}_R$, we call $\mathscr{B}_1(t) \subset \mathscr{S}$ and $\mathscr{B}_2(t) \subset \mathscr{S}$ the two disjoint open subsets of $\mathscr{S}$ occupied by the composite's phases at time t, and we let $\Gamma(t)$ be the set of all interfaces between $\mathscr{B}_1(t)$ and $\mathscr{B}_2(t)$. Moreover, as reported above, we write $\mathscr{B}_1(t) \cup \mathscr{B}_2(t) \cup \Gamma(t) = \mathscr{B}(t)$, $\overline{\mathscr{B}_1(t)} \cap \mathscr{B}_2(t) = \emptyset$, and $\mathscr{B}_1(t) \cap \overline{\mathscr{B}_2(t)} = \emptyset$.

By selecting an interval of time $\mathscr{I} = [t_{in}, t_{fin}[$, we describe the motion of the composite at hand by means of the injective maps $\chi_\eta : \mathscr{B}_{R\eta} \times \mathscr{I} \to \mathscr{S}$, with $\eta = 1, 2$. For every $t \in \mathscr{I}$, $\chi_\eta(\cdot, t)$ determines the placement of the ηth phase of the composite at time t, that is, $\mathscr{B}_\eta(t) = \chi_\eta(\mathscr{B}_{R\eta}, t)$. Note that, throughout this work, the maps χ_η, with $\eta = 1, 2$, are assumed to be at least of class C^2 in each of their variables.

For each $\eta = 1, 2$, and for a given pair $(X, t) \in \mathscr{B}_{R\eta} \times \mathscr{I}$, the deformation gradient tensor $\boldsymbol{F}_\eta(X, t)$ is the tangent map of $\chi_\eta(\cdot, t)$ at $X \in \mathscr{B}_{R\eta}$ [79], that is, $\boldsymbol{F}_\eta(X, t) := T\chi_\eta(X, t)$, and maps vectors of the tangent space $T_X\mathscr{B}_{R\eta}$ into vectors of the tangent space $T_x\mathscr{S}$, with $x = \chi_\eta(X, t)$.

Suitable conditions on the kinematics will be prescribed in the following sections in order to ensure that the motions of the constituents are compatible with the properties of $\mathscr{B}_\eta(t)$ enunciated above, that is, that the two constituents of the composite do not overlap in the course of their evolution, thereby maintaining the composite's original topology. Moreover, renouncing to the mathematical complexity of a differential geometry formalism in view of a sufficiently simple, yet rigorous, presentation of the AH, we adhere to the theoretical framework outlined in [19, 80]. Hence, upon adopting Cartesian coordinates, the deformation gradient $\boldsymbol{F}_\eta$ of the ηth constituent can be conveniently written in terms of the displacement field $\boldsymbol{u}_\eta$ of the same constituent as

$$\boldsymbol{F}_\eta = \boldsymbol{I} + \mathrm{Grad}\boldsymbol{u}_\eta, \quad \eta = 1, 2, \tag{1}$$

10991476, 2025, 1, Downloaded from https://onlinelibrary.wiley.com/doi/10.1002/nma.10367 by Politecnico Di Torino Sist. Bibl Del Polit Di Torino, Wiley Online Library on [12/02/2025]. See the Terms and Conditions (https://onlinelibrary.wiley.com/terms-and-conditions) on Wiley Online Library for rules of use; OA articles are governed by the applicable Creative Commons License

where $\boldsymbol{I}$ is the second-order identity tensor. More precisely, for each pair $(X,t) \in \mathscr{B}_{\mathrm{R}\eta} \times \mathscr{I}$, $\boldsymbol{I}(X,t)$ should be regarded as the shifter [79] from the tangent space of $\mathscr{B}_{\mathrm{R}\eta}$ at X to the tangent space of the three-dimensional Euclidean space at $\chi_\eta(X,t)$. However, as remarked above, since this geometric characterization is out of the scopes of our work, we do not dwell into the details that such a characterization would require, and we formulate the remainder of this study only in the Cartesian setting.

In elasto-plasticity, several inelastic processes, such as the structural reorganization of the internal structure of a medium, can be described with the aid of the multiplicative decomposition of the deformation gradient tensor known as the *Bilby–Kröner–Lee (BKL) decomposition* (see, e.g., [9]). Specialized to each constituent of the composite under consideration, the descriptor of the inelastic distortions is a tensor field $\boldsymbol{K}_\eta$ that is generally not integrable, that is, that cannot be written as the deformation gradient of an embedding. The presence of $\boldsymbol{K}_\eta$ is associated with the identification of a natural state, which is by definition stress free, and is attained by means of an *"ideal tearing process"* [9].

Accordingly to the BKL decomposition, the deformation gradient of the ηth constituent is written as

$$\boldsymbol{F}_\eta = \boldsymbol{F}_{\mathrm{e}\eta}\boldsymbol{K}_\eta, \quad \eta = 1,2. \tag{2}$$

This amounts to breaking up the overall deformation gradient of the continuum body into a purely elastic contribution, accommodated by the tensor field $\boldsymbol{F}_{\mathrm{e}\eta}$, and into an inelastic contribution, modeled by $\boldsymbol{K}_\eta$, that modifies the mechanical properties of the internal structure of the ηth constituent, thereby altering the mechanical properties of the composite as a whole. In the context of biomechanics, in which the BKL decomposition has been employed by several authors [16, 27, 81–87], the kinematic variable $\boldsymbol{K}_\eta$ is also referred to as *remodeling tensor*.

3.2 | Separation of scales

A necessary condition for the employment of AH is that the length scales that characterize a given material with respect to some peculiar phenomena are well separated. Here, we identify two characteristic length scales: one, denoted by ℓ_0, concerns the local structure, and the other one, denoted by L_0, characterizes the material as a whole. These two characteristic lengths are such that

$$0 < \varepsilon := \frac{\ell_0}{L_0} \ll 1. \tag{3}$$

By letting X denote the collection of coordinates that, in a given Cartesian coordinate frame, identify univocally a point of the composite, we rely on the standard procedure of AH [39, 40, 70] that introduces the two non-dimensional collections of coordinates $\tilde{X} := L_0^{-1}X$ and $\tilde{Y} := \ell_0^{-1}X$, so that $\tilde{X} = \varepsilon^{-1}\tilde{Y}$. These resolve the coarse and the fine-scale inhomogeneities of the composite, respectively. We recall, in addition, that $\tilde{X}$ is also referred to as the *slow*, or *macroscopic*, variable, while $\tilde{Y}$ is said to be the *fast*, or *microscopic*, variable [37, 41]. Moreover, both $\tilde{X}$ and $\tilde{Y}$ are associated with the composite's reference placement $\mathscr{B}_{\mathrm{R}}$.

Any scalar, vector or tensor field Φ depending on X can be formally written as $\Phi(X) = \Phi_{\mathrm{c}}\Phi^\epsilon(\tilde{X},\tilde{Y})$ [70], where Φ_{c} is a characteristic value of Φ. Accordingly, the gradient of Φ is

$$\mathrm{Grad}\Phi(X) = \frac{\Phi_{\mathrm{c}}}{L_0}[\mathrm{Grad}_{\tilde{X}}\Phi^\epsilon(\tilde{X},\tilde{Y}) + \varepsilon^{-1}\mathrm{Grad}_{\tilde{Y}}\Phi^\epsilon(\tilde{X},\tilde{Y})]. \tag{4}$$

Similarly, the divergence of a tensor field $\boldsymbol{T}$ reads

$$\mathrm{Div}\boldsymbol{T}(X) = \frac{T_{\mathrm{c}}}{L_0}[\mathrm{Div}_{\tilde{X}}\boldsymbol{T}^\epsilon(\tilde{X},\tilde{Y}) + \varepsilon^{-1}\mathrm{Div}_{\tilde{Y}}\boldsymbol{T}^\epsilon(\tilde{X},\tilde{Y})], \tag{5}$$

with T_{c} being the scale characterizing $\boldsymbol{T}$.

We notice that, when the physical quantity Φ is specifically associated with a given constituent of the composite, so that we write Φ_η, with $\eta = 1,2$, also its characteristic value depends, in principle, on the composite's same constituent, and one should adopt the notation $\Phi_{\mathrm{c}\eta}$. However, to avoid the sprouting of too many indices, we select for each physical quantity of interest one characteristic value for all the composite's constituents, and we denote this value by Φ_{c}. Moreover, we remark that in addition to the rescaling $\Phi(X) = \Phi_{\mathrm{c}}\Phi^\epsilon(\tilde{X},\tilde{Y})$ and $\boldsymbol{T}(X) = T_{\mathrm{c}}\boldsymbol{T}^\epsilon(\tilde{X},\tilde{Y})$, which requires $\Phi^\epsilon(\tilde{X},\tilde{Y})$ and $\boldsymbol{T}^\epsilon(\tilde{X},\tilde{Y})$ to be non-dimensional, we find it convenient to introduce also the writing $\boldsymbol{Q}(X) = \boldsymbol{Q}^\epsilon(\tilde{X},\tilde{Y})$, in which $\boldsymbol{Q}^\epsilon(\tilde{X},\tilde{Y})$ is provided as a function of the non-dimensional spatial variables $\tilde{X}$ and $\tilde{Y}$, but it *is not* non-dimensional *per se*.

10991476, 2025, 1, Downloaded from https://onlinelibrary.wiley.com/doi/10.1002/nma.10367 by Politecnico Di Torino Sist. Bibl Del Polit Di Torino, Wiley Online Library on [12/02/2025]. See the Terms and Conditions (https://onlinelibrary.wiley.com/terms-and-conditions) on Wiley Online Library for rules of use; OA articles are governed by the applicable Creative Commons License

Before going further, we summarize in the remarks below two fundamental hypotheses which the forthcoming discussion relies on.

Remark 3.1 (Periodic cell)**.** By following a rather standard praxis of AH [37, 39, 70, 88], we assume that the composite under study admits the existence of a *reference* or elementary cell $\mathscr{Y}_{\mathrm{R}}$, that is, a suitably chosen subset of the reference placement $\mathscr{B}_{\mathrm{R}}$ that is *representative* of the composite's microstructure. In this respect, the composite is also hypothesized to be microscopically *periodic*, in the sense that it is ideally generated by replicating $\mathscr{Y}_{\mathrm{R}}$ throughout $\mathscr{B}_{\mathrm{R}}$, thereby obtaining a periodic representation of it (for a discussion on some topological aspects on the topic, the interested reader is referred to, e.g., [88]). In addition, we assume that the microscopic periodicity of the composite is "maintained" by its kinematics, so that it is possible to find also for $\mathscr{B}(t)$ a representative cell $\mathscr{Y}(t) \subset \mathscr{B}(t)$ that inherits the properties of $\mathscr{Y}_{\mathrm{R}}$. Finally, we assume that the periodic cell $\mathscr{Y}_{\mathrm{R}}$ of $\mathscr{B}_{\mathrm{R}}$ comprises the two constituents of the composite and, thus, that it consists of the points of $\mathscr{B}_{\mathrm{R}1}$ and $\mathscr{B}_{\mathrm{R}2}$, as well as of the points of the interface Γ_{R} separating $\mathscr{B}_{\mathrm{R}1}$ from $\mathscr{B}_{\mathrm{R}2}$, denoted by $\Gamma_{\mathscr{Y}_{\mathrm{R}}}$. Hence, we write $\mathscr{Y}_{\mathrm{R}} = \mathscr{Y}_{\mathrm{R}1} \cup \mathscr{Y}_{\mathrm{R}2} \cup \Gamma_{\mathscr{Y}_{\mathrm{R}}}$, where $\mathscr{Y}_{\mathrm{R}1}$ and $\mathscr{Y}_{\mathrm{R}2}$ are identified with $\mathscr{Y}_{\mathrm{R}1} = \mathscr{B}_{\mathrm{R}1} \cap \mathscr{Y}_{\mathrm{R}}$ and $\mathscr{Y}_{\mathrm{R}2} = \mathscr{B}_{\mathrm{R}2} \cap \mathscr{Y}_{\mathrm{R}}$.

Remark 3.2 (Macroscopic uniformity)**.** On the trail of some previous works (see, e.g., [77, 80, 88–90]), also in the remainder of this study, we enforce the hypothesis of macroscopic uniformity [91–93]. As pointed out in [88], this means that with reference to a rescaled periodic cell, denoted by $\tilde{\mathscr{Y}}_{\mathrm{R}} := \mathscr{Y}_{\mathrm{R}}/\ell_0$, $\tilde{\mathscr{Y}}_{\mathrm{R}}$ does not depend on the slow variable $\tilde{X}$. This property, in fact, makes $\tilde{\mathscr{Y}}_{\mathrm{R}}$ even more representative of the composite's microstructure, since it can be selected "once for all" for the entire composite. Note that within $\tilde{\mathscr{Y}}_{\mathrm{R}}$, the spatial variability of any physical quantity of interest for our problem is resolved by fixing $\tilde{X}$ and letting $\tilde{Y}$ vary in $\tilde{\mathscr{Y}}_{\mathrm{R}}$.

In terms of the rescaled space variables, the periodic cell $\tilde{\mathscr{Y}}_{\mathrm{R}}$ is written as $\tilde{\mathscr{Y}}_{\mathrm{R}} = \tilde{\mathscr{Y}}_{\mathrm{R}1} \cup \tilde{\mathscr{Y}}_{\mathrm{R}2} \cup \tilde{\Gamma}_{\mathscr{Y}_{\mathrm{R}}}$, where $\tilde{\Gamma}_{\mathscr{Y}_{\mathrm{R}}}$ is the rescaled interface. Consistently with this description, we write $\Phi_\eta(X) = \Phi_{\mathrm{c}}\Phi^\epsilon_\eta(\tilde{X}, \tilde{Y})$ to indicate that a given physical quantity is associated with the constituent occupying the rescaled subset $\tilde{\mathscr{Y}}_{\mathrm{R}\eta}$ of $\tilde{\mathscr{Y}}_{\mathrm{R}}$ and is defined therein. Often, however, it is also required that Φ^ϵ_1 and Φ^ϵ_2 satisfy *no-jump* conditions at $\tilde{\Gamma}_{\mathscr{Y}_{\mathrm{R}}}$, which means that each of these functions can be prolonged by continuity on $\tilde{\Gamma}_{\mathscr{Y}_{\mathrm{R}}}$. This result, in turn, allows to reconstruct a unique function Φ^ϵ, defined at all points of $\tilde{\mathscr{Y}}_{\mathrm{R}}$, such that its restriction to $\tilde{\mathscr{Y}}_{\mathrm{R}\eta}$ provides $\Phi^\epsilon_\eta(\tilde{X}, \tilde{Y})$, for each $\eta = 1, 2$, and uniformly in $\tilde{X}$ (see Remark 3.2), while its restriction to $\tilde{\Gamma}_{\mathscr{Y}_{\mathrm{R}}}$ provides the values that the prolongations of Φ^ϵ_1 and Φ^ϵ_2 take when both functions are evaluated on the common interface. Having recourse to the prolonged function Φ^ϵ, when it exists, is sometimes preferable to simplify the description of the composite. Throughout this work, we shall hypothesize that it is always possible to determine the prolonged function Φ^ϵ.

We remark that there are situations in which it is not possible to find a continuous prolongation of a given physical quantity when the interface between the two phases of a cell cannot be modeled as ideal. Indeed, in such a situation, the no-jump conditions are not suitable for describing the physics of the problem. Similar cases occur, for example, in cancerous tissues [94, 95] or in the periodontal ligament in which, as reported in [19], there exists a *"thin layer between the cementum of the tooth to the adjacent alveolar bone [96]."*

Whenever the interface is not ideal, the interface conditions have to be reformulated [97–102]. A biologically relevant case in which a composite material with non-ideal surfaces is studied with the tools of AH is provided in the work by Guinovart-Díaz et al. [103], which addresses the imperfect contact between the matrix of the composite and the fibers embedded within it.

As anticipated in Remark 3.1, all the quantities of interest for the present study will be assumed to be periodic over $\tilde{\mathscr{Y}}_{\mathrm{R}}$. In terms of the generic physical quantity Φ^ϵ, this condition is characterized by the equality

$$\Phi^\epsilon(\tilde{X}, \tilde{Y}_{\mathrm{b}}) = \Phi^\epsilon(\tilde{X}, \tilde{Y}_{\mathrm{b}} + \mathcal{E}_A), \qquad \forall \tilde{X} \text{ and } \forall \tilde{Y}_{\mathrm{b}} \in \partial\tilde{\mathscr{Y}}_{\mathrm{R}} \backslash (\partial\tilde{\mathscr{Y}}_{\mathrm{R}} \cap \tilde{\Gamma}_{\mathscr{Y}_{\mathrm{R}}}) \text{ such that } \tilde{Y}_{\mathrm{b}} + \mathcal{E}_A \in \partial\tilde{\mathscr{Y}}_{\mathrm{R}} \backslash (\partial\tilde{\mathscr{Y}}_{\mathrm{R}} \cap \tilde{\Gamma}_{\mathscr{Y}_{\mathrm{R}}}), \tag{6}$$

with $\mathcal{E}_A$, $A = 1, 2, 3$, being the Ath unit vector of the local Cartesian frame associated with the periodic cell (some topologies of periodic cells have been studied in [80]). Note that in the just given periodicity condition, the evaluations of Φ^ϵ at $\tilde{Y}_{\mathrm{b}}$ and $\tilde{Y}_{\mathrm{b}} + \mathcal{E}_A$ have to be understood as limits from the inner points of a periodic cell towards the points $\tilde{Y}_{\mathrm{b}}$ and $\tilde{Y}_{\mathrm{b}} + \mathcal{E}_A$ of its boundary.

In passing, we also notice that the integral over the periodic cell of a physical quantity Φ^ϵ obtained by prolonging Φ^ϵ_1 and Φ^ϵ_2 by continuity on $\tilde{\Gamma}_{\mathscr{Y}_{\mathrm{R}}}$ can be written as

$$\int_{\tilde{\mathscr{Y}}_{\mathrm{R}}} \Phi^\epsilon(\tilde{X}, \tilde{Y}) \mathrm{dV}(\tilde{Y}) = \int_{\tilde{\mathscr{Y}}_{\mathrm{R}1}} \Phi^\epsilon_1(\tilde{X}, \tilde{Y}) \mathrm{dV}(\tilde{Y}) + \int_{\tilde{\mathscr{Y}}_{\mathrm{R}2}} \Phi^\epsilon_2(\tilde{X}, \tilde{Y}) \mathrm{dV}(\tilde{Y}). \tag{7}$$

10991476, 2025, 1, Downloaded from https://onlinelibrary.wiley.com/doi/10.1002/nme.10367 by Politecnico Di Torino Sist. Bibl Del Polit Di Torino, Wiley Online Library on [12/02/2025]. See the Terms and Conditions (https://onlinelibrary.wiley.com/terms-and-conditions) on Wiley Online Library for rules of use; OA articles are governed by the applicable Creative Commons License

This result brings us to the following definition.

Definition 3.1 (Cell averages [70])**.** Within the Cartesian context followed in this work, and under the hypothesis of macroscopic uniformity [91–93], we define three averages for any generic physical quantity (be it a scalar-, vector-, or tensor-valued field) rewritten as a two-scale function Φ^ϵ_η and associated with $\tilde{\mathscr{Y}}_{\mathrm{R}\eta} = \tilde{\mathscr{Y}}_{\mathrm{R}} \cap \tilde{\mathscr{B}}_{\mathrm{R}\eta}$, where $\tilde{\mathscr{B}}_{\mathrm{R}\eta}$ being the rescaled version of the set $\mathscr{B}_{\mathrm{R}\eta}$:

Intrinsic average of Φ^ϵ_η *over* $\tilde{\mathscr{Y}}_{\mathrm{R}\eta}$.

$$\langle \Phi^\epsilon_\eta \rangle^\eta_\eta(\tilde{X}) := \frac{1}{|\tilde{\mathscr{Y}}_{\mathrm{R}\eta}|} \int\limits_{\tilde{\mathscr{Y}}_{\mathrm{R}\eta}} \Phi^\epsilon_\eta(\tilde{X},\tilde{Y})\ \mathrm{dV}(\tilde{Y}) = \frac{1}{|\tilde{\mathscr{Y}}_{\mathrm{R}\eta}|} \int\limits_{\tilde{\mathscr{Y}}_{\mathrm{R}}} \Phi^\epsilon(\tilde{X},\tilde{Y})\vartheta_\eta(\tilde{Y})\ \mathrm{dV}(\tilde{Y}), \tag{8}$$

where ϑ_η is the characteristic function of $\tilde{\mathscr{Y}}_{\mathrm{R}\eta}$, that is, $\vartheta_\eta(\tilde{Y}) = 1$ for $\tilde{Y} \in \tilde{\mathscr{Y}}_{\mathrm{R}\eta}$ and $\vartheta_\eta(\tilde{Y}) = 0$ for $\tilde{Y} \in \tilde{\mathscr{Y}}_{\mathrm{R}} \backslash \tilde{\mathscr{Y}}_{\mathrm{R}\eta}$, and for each $\eta = 1, 2$, we denote by $\Phi^\epsilon(\tilde{X},\tilde{Y})\vartheta_\eta(\tilde{Y}) \equiv \Phi^\epsilon_{\eta\mathrm{p}}(\tilde{X},\tilde{Y})$ the *prolongation* of $\Phi^\epsilon_\eta(\tilde{X},\tilde{Y})$—which is defined only for $\tilde{Y} \in \tilde{\mathscr{Y}}_{\mathrm{R}\eta}$—to the whole periodic cell $\tilde{\mathscr{Y}}_{\mathrm{R}}$ through the quantity $\Phi^\epsilon(\tilde{X},\tilde{Y}) := \sum_{\eta=1,2} \Phi^\epsilon_{\eta\mathrm{p}}(\tilde{X},\tilde{Y})$.

Apparent average of Φ^ϵ_η *over* $\tilde{\mathscr{Y}}_{\mathrm{R}}$.

$$\langle \Phi^\epsilon_\eta \rangle_\eta(\tilde{X}) := \frac{1}{|\tilde{\mathscr{Y}}_{\mathrm{R}}|} \int\limits_{\tilde{\mathscr{Y}}_{\mathrm{R}\eta}} \Phi^\epsilon_\eta(\tilde{X},\tilde{Y})\ \mathrm{dV}(\tilde{Y}) \equiv \varphi_\eta \langle \Phi^\epsilon_\eta \rangle^\eta_\eta(\tilde{X}), \tag{9}$$

where $\varphi_\eta := |\tilde{\mathscr{Y}}_{\mathrm{R}\eta}|/|\tilde{\mathscr{Y}}_{\mathrm{R}}|$ is the volumetric fraction of the ηth constituent in the periodic cell, and because of the hypothesis of macroscopic uniformity, it is constant in this work (note that both in Equations (8) and (9), the notation for the averages has been taken from [104]).

Cell average of Φ^ϵ *over* $\tilde{\mathscr{Y}}_{\mathrm{R}}$.

$$\langle \Phi^\epsilon \rangle(\tilde{X}) := \sum_{\eta=1,2} \langle \Phi^\epsilon_\eta \rangle_\eta(\tilde{X}) = \sum_{\eta=1,2} \varphi_\eta \langle \Phi^\epsilon_\eta \rangle^\eta_\eta(\tilde{X}). \tag{10}$$

3.3 | Two-scale kinematics for a gradient theory of remodeling

We solve the inelastic processes introduced in Section 3.1 by accounting for $\boldsymbol{K}_\eta$ and its gradient in the model. We do this by adapting Gurtin and Anand's [42] theory of strain-gradient plasticity to the context of composite media (see also [56, 60, 105–109]). For example, boundary effects and/or aspects of remodeling that are explicitly associated with length scales relevant for these phenomena can be described by accounting for "first neighborhood" interactions. This means that the elasto-plastic response of the ηth phase at a given point $X \in \mathscr{B}_{\mathrm{R}\eta}$ is influenced both by the punctual or local value of $\boldsymbol{K}_\eta$ and, through the gradient of $\boldsymbol{K}_\eta$, by the mechanical state of the points in a neighborhood of X contained in $\mathscr{B}_{\mathrm{R}\eta}$.

We study the kinematics of the constituents in $\mathscr{Y}_{\mathrm{R}}$ through their corresponding maps of motion χ_η, with $\eta = 1, 2$, restricted to the reference cell, although we shall use the associated displacements $\boldsymbol{u}_\eta$ in the forthcoming calculations. Recalling the formalism introduced in Section 3.2, the motion and the displacement of the ηth constituent are rewritten as $\chi_\eta(X,t) = \chi_{\mathrm{c}}\chi^\epsilon_\eta(\tilde{X},\tilde{Y},t)$ and $\boldsymbol{u}_\eta(X,t) = u_{\mathrm{c}}\boldsymbol{u}^\epsilon_\eta(\tilde{X},\tilde{Y},t)$, with respect to the coordinates $\tilde{X}$ and $\tilde{Y}$ introduced by the two-scale formalism.

Finally, the multiplicative decomposition of the deformation gradient tensor $\boldsymbol{F}_\eta(X,t)$ can be rephrased in terms of $\boldsymbol{F}^\epsilon_\eta(\tilde{X},\tilde{Y},t)$ as

$$\begin{aligned} \boldsymbol{F}_\eta(X,t) = \boldsymbol{F}_{\mathrm{e}\eta}(X,t)\boldsymbol{K}_\eta(X,t) \ &\Rightarrow\ F_{\mathrm{c}}\boldsymbol{F}^\epsilon_\eta(\tilde{X},\tilde{Y},t) = F_{\mathrm{ec}}\boldsymbol{F}^\epsilon_{\mathrm{e}\eta}(\tilde{X},\tilde{Y},t)K_{\mathrm{c}}\boldsymbol{K}^\epsilon_\eta(\tilde{X},\tilde{Y},t) \\ &\Rightarrow\ \boldsymbol{F}^\epsilon_\eta(\tilde{X},\tilde{Y},t) = \boldsymbol{F}^\epsilon_{\mathrm{e}\eta}(\tilde{X},\tilde{Y},t)\boldsymbol{K}^\epsilon_\eta(\tilde{X},\tilde{Y},t)\ \eta = 1, 2, \end{aligned} \tag{11}$$

where the relation $F_{\mathrm{c}} = F_{\mathrm{ec}}K_{\mathrm{c}}$ exists among the characteristic values of the tensors featuring in the BKL decomposition. In particular, since F_{c} can be related to the characteristic scale of the displacement, that is, u_{c}, while K_{c} is the characteristic value of $\boldsymbol{K}$, which is a primary variable for the model at hand, then F_{ec} can be deduced as $F_{\mathrm{ec}} = F_{\mathrm{c}}/K_{\mathrm{c}}$. We remark that both $\boldsymbol{F}^\epsilon_{\mathrm{e}\eta}$ and $\boldsymbol{K}^\epsilon_\eta$ have strictly positive determinants $J^\epsilon_{\mathrm{e}\eta} = \det \boldsymbol{F}^\epsilon_{\mathrm{e}\eta} > 0$ and $J^\epsilon_{\boldsymbol{K}\eta} = \det \boldsymbol{K}^\epsilon_\eta > 0$.

In the case of structural reorganization in soft tissues, cellular aggregates, and early stage tumor masses (i.e., prior to vascularization), the inelastic process of remodeling is often assumed to be isochoric, since the distortions associated with it mainly consist of rearrangements of cells, extra-cellular matrix, and inter-cellular adhesion bonds, which are believed

10991476, 2025, 1, Downloaded from https://onlinelibrary.wiley.com/doi/10.1002/nme.13067 by Politecnico Di Torino Sist. Bibl Del Polit Di Torino, Wiley Online Library on [12/02/2025]. See the Terms and Conditions (https://onlinelibrary.wiley.com/terms-and-conditions) on Wiley Online Library for rules of use; OA articles are governed by the applicable Creative Commons License

not to involve appreciable volume variations. Therefore, the condition $J_{\boldsymbol{K}\eta} \equiv \det \boldsymbol{K}_\eta = 1$ is prescribed. This condition, in fact, can be treated explicitly as a holonomic constraint, as done in the following sections. In this respect, it also applies that $\det(K_c \boldsymbol{K}_\eta^\varepsilon) = K_c^3 \det \boldsymbol{K}_\eta^\varepsilon = 1$ and, without loss of generality, we can take $K_c = 1$ and $\det \boldsymbol{K}_\eta^\varepsilon = 1$.

Since we are working in a simplified Cartesian framework, the spatial gradient of the remodeling tensor in the reference placement can be explicitly written as

$$\text{Grad } \boldsymbol{K}_\eta(X,t) = \frac{1}{L_0}\left[\text{Grad}_{\tilde{X}} \boldsymbol{K}_\eta^\varepsilon(\tilde{X},\tilde{Y},t) + \varepsilon^{-1}\text{Grad}_{\tilde{Y}} \boldsymbol{K}_\eta^\varepsilon(\tilde{X},\tilde{Y},t)\right]. \tag{12}$$

4 | FORMULATION OF THE PROBLEM

In this section, we present the equations that govern the dynamics of the composite under study, which is assumed to undergo elasto-viscoplastic distortions.

4.1 | Momentum balance law and microforce balance

The viscoplastic distortions occurring in the two phases of the composite under study must satisfy certain equations in the tensor variable $\boldsymbol{K}_\eta$, with $\eta = 1, 2$, that are usually referred to as *flow rules* (see, e.g., [42, 53, 108]). These must be solved in conjunction with the equations of motion for χ_η, which allow determining $\boldsymbol{F}_\eta$, so that also the elastic distortions can be computed a posteriori as $\boldsymbol{F}_{e\eta} = \boldsymbol{F}_\eta \boldsymbol{K}_\eta^{-1}$.

In the remainder of this subsection, we recall the fundamental model equations, and we focus on the formulation of the flow rule selected for our purposes. To this end, we begin with the balance of the forces that are power conjugate with $\dot{\chi}_\eta$, and by neglecting all body forces, we write

$$\text{Div } \boldsymbol{P}_\eta = \boldsymbol{0}, \quad \text{with } \eta = 1, 2, \tag{13}$$

where $\boldsymbol{P}_\eta$ is the first Piola–Kirchhoff stress tensor of the ηth constituent [79].

For the statement of the flow rule, we rely on the framework established in [42]. In the view of Gurtin and Anand [42], the tensor $\boldsymbol{K}_\eta$, its rate $\boldsymbol{L}_{\boldsymbol{K}\eta} := \dot{\boldsymbol{K}}_\eta \boldsymbol{K}_\eta^{-1}$, and the gradient Grad $\boldsymbol{L}_{\boldsymbol{K}\eta}$ are the *kinematic descriptors* associated with the structural degrees of freedom of the microstructure of each constituent, and suitable generalized forces power conjugate with $\boldsymbol{L}_{\boldsymbol{K}\eta} = \dot{\boldsymbol{K}}_\eta \boldsymbol{K}_\eta^{-1}$ and Grad $\boldsymbol{L}_{\boldsymbol{K}\eta}$ are introduced and balanced. Although we have slightly adjusted the formulation outlined in [42] to our problem, above all to perform the AH procedure, we do not review it here. Rather, we start with the balance of the generalized forces power conjugate to $\boldsymbol{L}_{\boldsymbol{K}\eta}$, which, in [42], is put in the form

$$\text{DevSym}\{\boldsymbol{T}_\eta - J_{\boldsymbol{K}\eta}\boldsymbol{\Sigma}_\eta - \text{Div}\mathbb{K}_\eta\} = \boldsymbol{O}, \qquad \eta = 1, 2, \tag{14}$$

with, however, $J_{\boldsymbol{K}\eta} = 1$, and where $\boldsymbol{O}$ is the second-order null tensor. Here, DevSym is the operator that extracts the symmetric-deviatoric part of a given second-order tensor; $\boldsymbol{\Sigma}_\eta := J_{\boldsymbol{K}\eta}^{-1} \boldsymbol{K}_\eta^{-\mathrm{T}} \boldsymbol{F}_\eta^{\mathrm{T}} \boldsymbol{P}_\eta \boldsymbol{K}_\eta^{\mathrm{T}}$ is the Mandel stress tensor associated with the natural state; $\boldsymbol{T}_\eta$ is a second-order stress tensor power conjugate with the plastic rate $\boldsymbol{L}_{\boldsymbol{K}\eta} = \dot{\boldsymbol{K}}_\eta \boldsymbol{K}_\eta^{-1}$; and $\mathbb{K}_\eta$ is the third-order tensor dual in power to Grad $\boldsymbol{L}_{\boldsymbol{K}\eta}$. According to Gurtin and Anand's formulation [42], both $\boldsymbol{T}_\eta$ and $\mathbb{K}_\eta$ represent generalized stresses and Equation (14) is also called *"microforce balance"* [42]. Before proceeding, we emphasize that Equation (14) is taken from [42] *as is* (apart, of course, from the subscript η and the presence of $J_{\boldsymbol{K}\eta}$ in spite of it being unitary), since the purpose of this work of ours is not deriving it, but only approaching it within the framework of AH.

With respect to the plastic flow rule proposed in [42], which is obtained by working out the expression that we have reported in Equation (14) with the slight changes mentioned above, we emphasize the presence of the DevSym operator. In the referenced paper, indeed, the generalized stress tensors $\boldsymbol{T}_\eta$ and $\text{Div}\mathbb{K}_\eta$ are originally assumed to be deviatoric and symmetric, prior to any constitutive characterization of $\boldsymbol{T}_\eta$ and $\mathbb{K}_\eta$. Thus, apart from the explicit presence of the DevSym operator, and since $J_{\boldsymbol{K}\eta} = 1$, the balance law (14) is equivalent to the one originally stated by Gurtin and Anand [42] for strain-gradient plasticity.

Even though Equation (14) is fully tensorial and equivalent to a system of 9 scalar equations, the DevSym operator extracts only five linearly independent scalar equations. Thus, since we aim at solving for the remodeling tensor $\boldsymbol{K}_\eta$ under some constitutive assumptions for $\boldsymbol{T}_\eta$ and $\mathbb{K}_\eta$, we solve explicitly the kinematic constraints of isochoricity (in differential

10991476, 2025, 1, Downloaded from https://onlinelibrary.wiley.com/doi/10.1002/mma.10367 by Politecnico Di Torino Sist. Bibl Del Polit Di Torino, Wiley Online Library on [12/02/2025]. See the Terms and Conditions (https://onlinelibrary.wiley.com/terms-and-conditions) on Wiley Online Library for rules of use; OA articles are governed by the applicable Creative Commons License

form) and of null spin of the remodeling distortions [42], that is,

$$\dot{\boldsymbol{K}}_\eta : \boldsymbol{K}_\eta^{-\mathrm{T}} = 0, \qquad \text{with } \eta = 1, 2, \tag{15a}$$

$$\dot{\boldsymbol{K}}_\eta \boldsymbol{K}_\eta^{-1} - \boldsymbol{K}_\eta^{-\mathrm{T}} \dot{\boldsymbol{K}}_\eta^{\mathrm{T}} = \mathbf{O}, \qquad \text{with } \eta = 1, 2, \tag{15b}$$

where the symbol ":" indicates the double contraction between two second-order tensors, that is, $\dot{\boldsymbol{K}}_\eta : \boldsymbol{K}_\eta^{-\mathrm{T}} \equiv \mathrm{tr}(\dot{\boldsymbol{K}}_\eta \boldsymbol{K}_\eta^{-1})$. Note that in the original derivation of the model of Gurtin and Anand [42], the constraints in Equations (15a) and (15b) were accounted for by enforcing them directly in the dynamic equations of the problem. On the contrary, the idea of exploiting these constraints as additional equations of the model is ours (see [67, 68]), and in the present framework, it is motivated by the fact that in our opinion, they simplify the forthcoming study based on AH. We also remark that Equations (15a) and (15b) fulfill, by construction, the essential aspect of the theory according to which the constraints, being intrinsic, must be independent of the choice of the composite's reference placement. This property, indeed, is satisfied automatically by Equations (15a) and (15b), as can be seen upon performing the transformation $\boldsymbol{K}_\eta \mapsto \boldsymbol{K}_\eta \boldsymbol{\Xi}$, where $\boldsymbol{\Xi}$ is the (nonsingular) tangent map of a diffeomorphism describing a given and time constant change of reference placement of the composite.

Equations (15a) and (15b) amount to four linearly independent scalar equations that, with the five linearly independent equations from Equation (14), constitute a system of 9 linearly independent scalar equations. Therefore, after providing constitutive relations for $\boldsymbol{T}_\eta$ and $\mathbb{K}_\eta$, the problem is closed.

4.2 | Constitutive framework and final form of the microforce balance

To develop the constitutive framework, we start with the introduction of the Helmholtz free energy per unit volume of the natural state of each constituent, which can be decomposed additively as the sum of the hyperelastic strain energy $\psi_{\mathrm{e}\eta}$, and a "defect" energy $\psi_{\mathrm{d}\eta}$, which accounts for the accumulation of the geometrical incompatibilities associated with remodeling (see [42] for details), that is,

$$\psi_\eta(\boldsymbol{F}_\eta, \boldsymbol{K}_\eta, \mathrm{Grad}\ \boldsymbol{K}_\eta) := \psi_{\mathrm{e}\eta}(\boldsymbol{F}_{\mathrm{e}\eta}) + \psi_{\mathrm{d}\eta}(\boldsymbol{K}_\eta, \mathrm{Grad}\ \boldsymbol{K}_\eta), \tag{16}$$

where $\boldsymbol{F}_{\mathrm{e}\eta}$ is understood here as a function of $\boldsymbol{F}_\eta$ and $\boldsymbol{K}_\eta$ through the relation $\boldsymbol{F}_{\mathrm{e}\eta} = \boldsymbol{F}_\eta \boldsymbol{K}_\eta^{-1}$. We notice that since $\psi_{\mathrm{e}\eta}$ depends on $\boldsymbol{F}_\eta$ and $\boldsymbol{K}_\eta$ through $\boldsymbol{F}_{\mathrm{e}\eta}$, it is in fact invariant under transformations of the reference placement, since these leave $\boldsymbol{F}_{\mathrm{e}\eta}$ unaffected. On the same footing, to ensure that also $\psi_{\mathrm{d}\eta}$ (and, thus, ψ_η, too) is invariant under transformations of the reference placement (see [110] for details), Cermelli and Gurtin [110] assume that $\psi_{\mathrm{d}\eta}$ depends on $\boldsymbol{K}_\eta$ and Grad $\boldsymbol{K}_\eta$ through the quantity [110]

$$\mathfrak{B}_\eta := J_{\boldsymbol{K}_\eta}^{-1} \boldsymbol{K}_\eta \mathrm{Curl}\ \boldsymbol{K}_\eta. \tag{17}$$

Indeed, this second-order tensor field, referred to as *Burgers tensor* [110], is by construction invariant under transformations of the reference placement. Note also that Curl $\boldsymbol{K}_\eta$ is a second-order tensor field that, in Cartesian coordinates, is defined as $(\mathrm{Curl}\ \boldsymbol{K}_\eta)_{AB} = \mathfrak{e}_{ACD}(\mathrm{Grad}\ \boldsymbol{K}_\eta)_{BDC}$ in [111], where $\mathfrak{e}$ is the Levi-Civita symbol (we use the symbol "$\mathfrak{e}$" in lieu of the classical "ε" because the latter symbol is already employed as the smallness parameter for the AH theory). Finally, we emphasize that the Burgers tensor represents a "measure" of the action of remodeling.

To extract constitutive information from Equation (16), it may be convenient to express the Helmholtz free energy density per unit volume of the reference placement, that is, in terms of the quantity $\psi_{\mathrm{R}\eta} := J_{\boldsymbol{K}\eta} \psi_\eta$, which yields $\psi_{\mathrm{Re}\eta} := J_{\boldsymbol{K}\eta} \psi_{\mathrm{e}\eta}$ and $\psi_{\mathrm{Rd}\eta} := J_{\boldsymbol{K}\eta} \psi_{\mathrm{d}\eta}$. By doing so, we can make the following identifications between quantities defined in the reference placement and in the natural state, through the push-forward induced by $\boldsymbol{K}_\eta$:

$$\psi_{\mathrm{Re}\eta}(\boldsymbol{F}_\eta, \boldsymbol{K}_\eta) \equiv J_{\boldsymbol{K}\eta} \psi_{\mathrm{e}\eta}(\boldsymbol{F}_{\mathrm{e}\eta}), \tag{18a}$$

$$\psi_{\mathrm{Rd}\eta}(\boldsymbol{K}_\eta, \mathrm{Grad}\ \boldsymbol{K}_\eta) \equiv J_{\boldsymbol{K}\eta} \psi_{\mathrm{d}\eta}(\mathfrak{B}_\eta). \tag{18b}$$

Hence, by exploiting the dissipation inequality (not shown here for the sake of brevity, but taken from [42, 112]), we determine the constitutive expression of the Mandel stress tensor $\boldsymbol{\Sigma}_\eta$ as (see, e.g., [113])

10991476, 2025, 1, Downloaded from https://onlinelibrary.wiley.com/doi/10.1002/nma.10367 by Politecnico Di Torino Sist. Bibl Del Polit Di Torino, Wiley Online Library on [12/02/2025]. See the Terms and Conditions (https://onlinelibrary.wiley.com/terms-and-conditions) on Wiley Online Library for rules of use; OA articles are governed by the applicable Creative Commons License

$$\boldsymbol{\Sigma}_\eta = \frac{1}{J_{\boldsymbol{K}\eta}} \boldsymbol{K}_\eta^{-\mathrm{T}} \boldsymbol{F}_\eta^{\mathrm{T}} \boldsymbol{P}_\eta \boldsymbol{K}_\eta^{\mathrm{T}} = \boldsymbol{F}_{\mathrm{e}\eta}^{\mathrm{T}} \left(\frac{\partial \psi_{\mathrm{e}\eta}}{\partial \boldsymbol{F}_{\mathrm{e}\eta}} (\boldsymbol{F}_{\mathrm{e}\eta}) \right), \ \boldsymbol{P}_\eta := J_{\boldsymbol{K}\eta} \left(\frac{\partial \psi_{\mathrm{e}\eta}}{\partial \boldsymbol{F}_{\mathrm{e}\eta}} (\boldsymbol{F}_{\mathrm{e}\eta}) \right) \boldsymbol{K}_\eta^{-\mathrm{T}}. \tag{19}$$

Note that to obtain Equation (19), use has been made of the following relations:

$$\begin{aligned} \dot{\overline{\psi_{\mathrm{Re}\eta}(\boldsymbol{F}_\eta, \boldsymbol{K}_\eta)}} &= \left(\frac{\partial \psi_{\mathrm{Re}\eta}}{\partial \boldsymbol{F}_\eta} (\boldsymbol{F}_\eta, \boldsymbol{K}_\eta) \right) : \dot{\boldsymbol{F}}_\eta + \left(\frac{\partial \psi_{\mathrm{Re}\eta}}{\partial \boldsymbol{K}_\eta} (\boldsymbol{F}_\eta, \boldsymbol{K}_\eta) \right) : \dot{\boldsymbol{K}}_\eta \\ &= J_{\boldsymbol{K}\eta} \left(\frac{\partial \psi_{\mathrm{e}\eta}}{\partial \boldsymbol{F}_{\mathrm{e}\eta}} (\boldsymbol{F}_{\mathrm{e}\eta}) \right) : \left(\dot{\boldsymbol{F}}_\eta \boldsymbol{K}_\eta^{-1} - \boldsymbol{F}_\eta \boldsymbol{K}_\eta^{-1} \dot{\boldsymbol{K}}_\eta \boldsymbol{K}_\eta^{-1} \right) = \boldsymbol{P}_\eta : \dot{\boldsymbol{F}}_\eta - J_{\boldsymbol{K}\eta} \boldsymbol{\Sigma}_\eta : \boldsymbol{L}_{\boldsymbol{K}\eta}, \end{aligned} \tag{20a}$$

$$\begin{aligned} \dot{\overline{\psi_{\mathrm{Rd}\eta}(\boldsymbol{K}_\eta, \mathrm{Grad}\ \boldsymbol{K}_\eta)}} &= \left(\frac{\partial \psi_{\mathrm{Rd}\eta}}{\partial \boldsymbol{K}_\eta} (\boldsymbol{K}_\eta, \mathrm{Grad}\ \boldsymbol{K}_\eta) \right) : \dot{\boldsymbol{K}}_\eta + \left(\frac{\partial \psi_{\mathrm{Rd}\eta}}{\partial\ \mathrm{Grad}\ \boldsymbol{K}_\eta} (\boldsymbol{K}_\eta, \mathrm{Grad}\ \boldsymbol{K}_\eta) \right) : \mathrm{Grad}\ \dot{\boldsymbol{K}}_\eta \\ &= J_{\boldsymbol{K}\eta} \left(\frac{\partial \psi_{\mathrm{d}\eta}}{\partial \mathfrak{B}_\eta} (\mathfrak{B}_\eta) \right) : \dot{\mathfrak{B}}_\eta \\ &= J_{\boldsymbol{K}\eta} \left(\left(\frac{\partial \psi_{\mathrm{d}\eta}}{\partial \mathfrak{B}_\eta} (\mathfrak{B}_\eta) \right)^{\mathrm{T}} \mathfrak{B}_\eta + \left(\frac{\partial \psi_{\mathrm{d}\eta}}{\partial \mathfrak{B}_\eta} (\mathfrak{B}_\eta) \right) \mathfrak{B}_\eta^{\mathrm{T}} \right) : \boldsymbol{L}_{\boldsymbol{K}\eta} \\ &\quad + J_{\boldsymbol{K}\eta} \left(\left(\frac{\partial \psi_{\mathrm{d}\eta}}{\partial \mathfrak{B}_\eta} (\mathfrak{B}_\eta) \right)^{\mathrm{T}} \times \boldsymbol{K}_\eta^{-1} \right)^{(\mathrm{t},\cdot)} \vdots\ \mathrm{Grad}\ \boldsymbol{L}_{\boldsymbol{K}\eta}, \end{aligned} \tag{20b}$$

in which the symbol "$\vdots$" indicates the triple contraction between two third-order tensors $\mathbb{A}$ and $\mathbb{B}$, that is,

$$\mathbb{A} \vdots \mathbb{B} = [\mathbb{A}]_{MNL} [\mathbb{B}]_{MNL}, \tag{21}$$

the cross product "$\times$" between two second-order tensors $\boldsymbol{Q}$ and $\boldsymbol{R}$ is defined as $[\boldsymbol{Q} \times \boldsymbol{R}]_{ABC} = \mathfrak{e}_{ADE} [\boldsymbol{Q}]_{BD} [\boldsymbol{R}]_{CE}$ [42, 110], and the symbol $(\boldsymbol{Q} \times \boldsymbol{R})^{(\mathrm{t},\cdot)}$ means transposition with respect to the first pair of indices, that is, $[(\boldsymbol{Q} \times \boldsymbol{R})^{(\mathrm{t},\cdot)}]_{ABC} = [\boldsymbol{Q} \times \boldsymbol{R}]_{BAC}$. Finally, we recall that to obtain Equations (20a) and (20b), the hypothesis of isochoric remodeling distortions has been invoked, thereby implying that the time derivative of $J_{\boldsymbol{K}\eta}$ vanishes identically for consistency with Equation (15a).

By following the study of the dissipation inequality conducted in [42], and slightly adapting it to our framework, the tensors $\boldsymbol{T}_\eta$ and $\mathbb{K}_\eta$ are written as

$$\boldsymbol{T}_\eta = \boldsymbol{T}_{\mathrm{en}\eta} + \boldsymbol{T}_{\mathrm{dis}\eta}, \tag{22a}$$

$$\mathbb{K}_\eta = \mathbb{K}_{\mathrm{en}\eta} + \mathbb{K}_{\mathrm{dis}\eta}, \tag{22b}$$

where $\boldsymbol{T}_{\mathrm{en}\eta}$ and $\mathbb{K}_{\mathrm{en}\eta}$ are said to be the *"energetic"* [42], or *non-dissipative*, contributions to $\boldsymbol{T}_\eta$ and $\mathbb{K}_\eta$, respectively, and are identified with the constitutive relations [42]

$$\boldsymbol{T}_{\mathrm{en}\eta} = J_{\boldsymbol{K}\eta} \left(\left(\frac{\partial \psi_{\mathrm{d}\eta}}{\partial \mathfrak{B}_\eta} (\mathfrak{B}_\eta) \right)^{\mathrm{T}} \mathfrak{B}_\eta + \left(\frac{\partial \psi_{\mathrm{d}\eta}}{\partial \mathfrak{B}_\eta} (\mathfrak{B}_\eta) \right) \mathfrak{B}_\eta^{\mathrm{T}} \right), \tag{23a}$$

$$\mathbb{K}_{\mathrm{en}\eta} = J_{\boldsymbol{K}\eta} \left(\left(\frac{\partial \psi_{\mathrm{d}\eta}}{\partial \mathfrak{B}_\eta} (\mathfrak{B}_\eta) \right)^{\mathrm{T}} \times \boldsymbol{K}_\eta^{-1} \right)^{(\mathrm{t},\cdot)}, \tag{23b}$$

while $\boldsymbol{T}_{\mathrm{dis}\eta}$ and $\mathbb{K}_{\mathrm{dis}\eta}$ represent their *dissipative* counterparts and are prescribed to be [42]

$$\boldsymbol{T}_{\mathrm{dis}\eta} = \sigma_\eta \tau_\eta \boldsymbol{L}_{\boldsymbol{K}\eta}, \tag{24a}$$

$$\mathbb{K}_{\mathrm{dis}\eta} = \ell_\eta^2 \sigma_\eta \tau_\eta\ \mathrm{Grad}\ \boldsymbol{L}_{\boldsymbol{K}\eta}, \tag{24b}$$

where σ_η is a scalar having physical units of stress and representing the *initial yield stress* of the material, τ_η is a *characteristic time scale* of the remodeling distortions, and ℓ_η (refer to Section 2) is a *characteristic length scale* associated with $\boldsymbol{L}_{\boldsymbol{K}\eta}$.

10991476, 2025, 1, Downloaded from https://onlinelibrary.wiley.com/doi/10.1002/nme.10367 by Politecnico Di Torino Sist. Bibl Del Polit Di Torino, Wiley Online Library on [12/02/2025]. See the Terms and Conditions (https://onlinelibrary.wiley.com/terms-and-conditions) on Wiley Online Library for rules of use; OA articles are governed by the applicable Creative Commons License

By putting together the results obtained so far, the microforce balance given in Equation (14) reads

$$\mathrm{DevSym}\left\{\boldsymbol{T}_{\mathrm{en}\eta}-\mathrm{Div}\mathbb{K}_{\mathrm{en}\eta}+\sigma_\eta\tau_\eta\boldsymbol{L}_{\boldsymbol{K}\eta}-J_{\boldsymbol{K}\eta}\boldsymbol{\Sigma}_\eta-\mathrm{Div}\left(\ell_\eta^2\sigma_\eta\tau_\eta\mathrm{Grad}\ \boldsymbol{L}_{\boldsymbol{K}\eta}\right)\right\}=\boldsymbol{O},\qquad \eta=1,2, \tag{25}$$

where the explicit expressions of $\boldsymbol{T}_{\mathrm{en}\eta}$ and $\mathbb{K}_{\mathrm{en}\eta}$ have not been substituted into Equation (25) in order to keep it as short as possible.

Note that the term $\mathrm{Div}\mathbb{K}_{\mathrm{en}\eta}$ in Equation (25) leads to *"energetic backstress effects"* and *"Bauschinger-like phenomena"* [42], while the terms $\sigma_\eta\tau_\eta\boldsymbol{L}_{\boldsymbol{K}\eta}$ and $\mathrm{Div}(\ell_\eta^2\sigma_\eta\tau_\eta\mathrm{Grad}\boldsymbol{L}_{\boldsymbol{K}\eta})$ represent the dissipative contributions capturing how the inelastic distortions due to remodeling evolve over time and distribute throughout each constituent of the composite.

To conclude the presentation of Gurtin and Anand's model [42], we specify for each constituent of the composite that $\psi_{\mathrm{e}\eta}$ is a De Saint-Venant strain energy density, while $\psi_{\mathrm{d}\eta}$ is quadratic in the Burgers tensor, thereby obtaining

$$\psi_{\mathrm{e}\eta}(\boldsymbol{F}_{\mathrm{e}\eta})=\frac{1}{2}\boldsymbol{E}_{\mathrm{e}\eta}\ :\ C_\eta\ :\ \boldsymbol{E}_{\mathrm{e}\eta},\qquad \eta=1,2, \tag{26a}$$

$$\psi_{\mathrm{d}\eta}(\mathfrak{B}_\eta)=\frac{1}{2}\mu_\eta L_\eta^2||\mathfrak{B}_\eta||^2,\qquad \eta=1,2, \tag{26b}$$

with $\boldsymbol{E}_{\mathrm{e}\eta}=\frac{1}{2}[\boldsymbol{F}_{\mathrm{e}\eta}^{\mathrm{T}}\boldsymbol{F}_{\mathrm{e}\eta}-\boldsymbol{I}]$ being the elastic Green–Lagrange strain tensor, and C_η the positive definite fourth-order elasticity tensor. Furthermore, L_η is a *"constant energetic length scale"* [42] (refer to Section 2), and μ_η is the *"elastic shear modulus"* [42] of the ηth constituent.

Although the presentation considered so far allows for a rather comprehensive model of strain-gradient inelastic phenomena, from here on we simplify Gurtin and Anand's framework [42] by assuming that the energetic contributions $\boldsymbol{T}_{\mathrm{en}\eta}$ and $\mathbb{K}_{\mathrm{en}\eta}$ featuring in Equation (25) vanish identically. This can be achieved by setting the energy density $\psi_{\mathrm{d}\eta}$ equal to zero for each $\eta=1,2$, as done by Gurtin and Anand [42] themselves, when they hypothesize that the characteristic lengths L_η, with $\eta=1,2$, are zero from the outset. This implies that the Burgers tensors $\mathfrak{B}_\eta$ disappear from the model equations, and amounts to requiring that the plastic behavior of the material is exclusively dissipative. We do this simplification in order to focus the theory of AH applied to Equation (25) only on the dissipative contributions to remodeling, even though we would like to dedicate another work to the study of the energetic terms in a multiscale context, again with the aid of AH.

According to the simplifications proposed, the dynamic equation of the periodic cell problem, that is, Equation (25), reduces to

$$\mathrm{DevSym}\left\{\sigma_\eta\tau_\eta\boldsymbol{L}_{\boldsymbol{K}\eta}-J_{\boldsymbol{K}\eta}\boldsymbol{\Sigma}_\eta-\mathrm{Div}\left(\ell_\eta^2\sigma_\eta\tau_\eta\mathrm{Grad}\ \boldsymbol{L}_{\boldsymbol{K}\eta}\right)\right\}=\boldsymbol{O},\qquad \eta=1,2. \tag{27}$$

We emphasize that with respect to the original work of Gurtin and Anand [42], we have made the following main changes, motivated both by the necessity of maintaining the presentation at a minimal level of complexity, and by the search for a notation as essential as possible, also in light of the calculations related to AH. For these purposes, we make two assumptions. First, here and in the sequel, we hypothesize that the yield stresses of the two phases of the composite under study do not change in time. This, indeed, allows to eliminate the equation for the evolution of the yield stresses from our model. Second, we are slightly modifying the notation in order to avoid the sprouting of too many indices. Hence, we use σ_η to indicate the yield stress, although this quantity would read $\sigma_{\mathrm{y}\eta}$ if the notation of [42] were to be used. Furthermore, instead of normalizing $\boldsymbol{L}_{\boldsymbol{K}\eta}$ and $\mathrm{Grad}\boldsymbol{L}_{\boldsymbol{K}\eta}$ by means of the characteristic rate of plastic distortions, denoted by "d_0" in [42], we find it convenient to multiply the yield stress by the characteristic time scale of plastic distortions τ_η, thereby identifying the scaling term d_0^{-1} of Gurtin and Anand [42] with τ_η. This way, the product $\sigma_\eta\tau_\eta$ acquires the meaning of a generalized viscosity, whose origin is related to the physical quantities σ_η and τ_η that are measurable and already present in standard models of plasticity [53] and, more generally, of biological remodeling (see, e.g., the description of remodeling in multicellular spheroids [34, 35, 114–118]). It is also worth to notice that, in our setting, each phase of the composite is characterized by its own initial yield stress σ_η, which should thus be understood as a fine-scale feature of the system at hand. Still, it describes a "macroscopic" quantity for each phase, which is regarded as a continuum, and indeed, it is referred to as *"coarse-grain yield strength"* in [42]. Finally, some considerations on a possible physical meaning of ℓ_η will be given in Remark 4.2 below.

Before closing this section, the following two remarks are in order.

Remark 4.1 (Plastic and viscoplastic)**.** We emphasize that Equations (24a) and (24b) are obtained as particular cases among different possible options suggested in [42]. A consequence of our choice, however, is that each phase of the composite behaves as a *viscoplastic* medium. In other words, if the constitutive expressions of $\boldsymbol{T}_{\mathrm{dis}\eta}$ and $\mathbb{K}_{\mathrm{dis}\eta}$ are substituted in Equation (14), one finds that, although plastic distortions are stress driven, plasticity is not modeled as a

10991476, 2025, 1, Downloaded from https://onlinelibrary.wiley.com/doi/10.1002/mma.10367 by Politecnico Di Torino Sist. Bibl Del Polit Di Torino, Wiley Online Library on [12/02/2025]. See the Terms and Conditions (https://onlinelibrary.wiley.com/terms-and-conditions) on Wiley Online Library for rules of use; OA articles are governed by the applicable Creative Commons License

threshold phenomenon, as is instead the case in perfect, rate-independent plasticity, in which plastic flow commences when the stress equals the yield stress [53]. In this respect, the terminology that we are reserving for σ_η, referred to as "yield stress" in our work, is inherited from [42], in which this quantity has indeed the physical meaning of a yield stress. The reason for our modeling assumption, which leads to flow rules simpler than those involving threshold phenomena and the related Karush–Kuhn–Tucker formalism (see, e.g., [53, 119]), is that we need a manageable problem in view of the intricate calculations that are unavoidable when AH is performed. In addition, we mention a paper by Anand et al. [52] in which the authors warn about the fact that gradient models of plasticity accounting for a transition between a plastic and an elastic domain inside the material involve moving *"elastic-plastic boundaries"* [52] on which *"higher-order boundary conditions need to be imposed"* [52].

Remark 4.2 (The characteristic length ℓ_η in Equation (24b))**.** When Gurtin and Anand [42] introduce the characteristic length ℓ_η in the equation corresponding to our Equation (24b), they refer to ℓ_η as a *"phenomenological parameter."* However, Anand et al. [52], although addressing a different context, propose to associate the characteristic length ℓ_η with the manifestation of *shear bands* (i.e., regions of strongly localized plastic distortions forming band-shaped domains), which may occur in metals and polymers. As mentioned in Section 2, this situation may constitute the case in which the plastic processes take place at a length scale much smaller than the cell's characteristic length $\ell_{\mathrm{m}} = \min_\eta \ell_\eta$ considered in our work. Although we do not study such processes in the sequel, we emphasize that the formation of shear bands is a phenomenon of relevance for composite materials. More generally, physical situations in which inelastic distortions, such as those related to remodeling and/or growth [65] in biomechanical problems, are inhomogeneously distributed, and may concentrate on narrow regions, occur, for example, in bones [120] and multicellular aggregates [121, 122]. For bones, however, also the converse is true, see, for example [73], and it may happen that the plastic zone "covers" multiple cells. All these scenarios provide a physical motivation to further expand our work in the future, especially when AH is employed to determine the effective coefficients of the material from the knowledge of its microstructure.

4.3 | Summary of the model and interface conditions

As anticipated in the previous sections, we consider a composite material comprising two distinct solid phases, each of which undergoes remodeling, understood here as an elasto-plastic process characterized by the hyperelastic Helmholtz free energy density defined in (26a) and by the accumulation of inelastic distortions.

The dynamics of the composite is accounted for by considering two balances of forces for each phase, augmented by suitable interface conditions. One force balance is the momentum balance law of "classical" continuum mechanics, while the other one is the balance of micro-forces introduced in [42]. By collecting all the hypotheses discussed in the previous sections, the balances of forces read:

$$\mathrm{Div}\boldsymbol{P}_\eta = \boldsymbol{0}, \qquad \text{in } \mathscr{B}_{\mathrm{R}\eta}, \tag{28a}$$

$$\mathrm{DevSym}\{\boldsymbol{T}_{\mathrm{dis}\eta} - \boldsymbol{\Sigma}_\eta - \mathrm{Div}\mathbb{K}_{\mathrm{dis}\eta}\} = \boldsymbol{O}, \qquad \text{in } \mathscr{B}_{\mathrm{R}\eta}, \tag{28b}$$

where $\boldsymbol{O}$ is the second-order null tensor, $\boldsymbol{P}_\eta$ and $\boldsymbol{\Sigma}_\eta$ have been defined in Equation (19), while $\boldsymbol{T}_{\mathrm{dis}\eta}$ and $\mathbb{K}_{\mathrm{dis}\eta}$ have been declared in Equations (24a) and (24b), and we have explicitly set $J_{\boldsymbol{K}\eta} = 1$. Along with the force balances (28a) and (28b), the kinematic constraints for $\boldsymbol{K}_\eta$, with $\eta = 1, 2$, put in differential form, are

$$\dot{\boldsymbol{K}}_\eta : \boldsymbol{K}_\eta^{-\mathrm{T}} = 0, \qquad \text{in } \mathscr{B}_{\mathrm{R}\eta}, \tag{29a}$$

$$\dot{\boldsymbol{K}}_\eta \boldsymbol{K}_\eta^{-1} - \boldsymbol{K}_\eta^{-\mathrm{T}} \dot{\boldsymbol{K}}_\eta^{\mathrm{T}} = \boldsymbol{O}, \qquad \text{in } \mathscr{B}_{\mathrm{R}\eta}. \tag{29b}$$

On the interface between the constituents, the following interface conditions are prescribed:

$$\boldsymbol{u}_1 = \boldsymbol{u}_2, \qquad \text{on } \Gamma_{\mathrm{R}}, \tag{30a}$$

$$\boldsymbol{P}_1 \boldsymbol{N}_{\Gamma_{\mathrm{R}}} = \boldsymbol{P}_2 \boldsymbol{N}_{\Gamma_{\mathrm{R}}}, \qquad \text{on } \Gamma_{\mathrm{R}}, \tag{30b}$$

$$\boldsymbol{L}_{\boldsymbol{K}1} = \boldsymbol{L}_{\boldsymbol{K}2} \qquad \text{on } \Gamma_{\mathrm{R}}, \tag{30c}$$

$$(\mathrm{DevSym}\mathbb{K}_{\mathrm{dis}1})\boldsymbol{N}_{\Gamma_{\mathrm{R}}} = (\mathrm{DevSym}\mathbb{K}_{\mathrm{dis}2})\boldsymbol{N}_{\Gamma_{\mathrm{R}}}, \qquad \text{on } \Gamma_{\mathrm{R}}. \tag{30d}$$

10991476, 2025, 1, Downloaded from https://onlinelibrary.wiley.com/doi/10.1002/nma.10367 by Politecnico Di Torino Sist. Bibl Del Polit Di Torino, Wiley Online Library on [12/02/2025]. See the Terms and Conditions (https://onlinelibrary.wiley.com/terms-and-conditions) on Wiley Online Library for rules of use; OA articles are governed by the applicable Creative Commons License

Here, Equation (30a) states that the displacements of the two constituents are congruent at the interface, and Equations (30b) and (30d) impose that the contact forces at the interface are transferred from one phase to the other. In particular, the latter two conditions are obtained as a consequence of the principle of virtual power, by imposing that the mechanical power is transferred without jumps from one constituent to the other. In addition, Equation (30c) requires the rates $\boldsymbol{L}_{\boldsymbol{K}1}$ and $\boldsymbol{L}_{\boldsymbol{K}2}$ to be equal to each other at the interface (in fact, due to the constraints (29a) and (29b), this condition applies to the deviatoric-symmetric parts of $\boldsymbol{L}_{\boldsymbol{K}1}$ and $\boldsymbol{L}_{\boldsymbol{K}2}$, rather than to the full tensors). Finally, Equation (30d) imposes a no-jump condition only on the deviatoric-symmetric part of $\mathbb{K}_{\text{dis}1}$ and of $\mathbb{K}_{\text{dis}2}$, and descends from the fact that the operators DevSym and Div commute.

We treat a problem that is different from [19] in view of the different choice of the evolution law for the remodeling distortions. In particular, the difference is twofold: (i) Here, we investigate a theory of remodeling of grade one in the anelastic distortions, whereas the theory adopted in [19] was of grade zero in these variables; and (ii), even in the case of negligible gradient of the anelastic distortions, the flow rule (28b) is different from the one in [19] because we employ here a linear constitutive law relating the dissipative generalized stress $\boldsymbol{T}_{\text{dis}\eta}$ with the remodeling rate $\boldsymbol{L}_{\boldsymbol{K}\eta}$, whereas in [19] the remodeling rate was expressed as a nonlinear function of the Mandel stress tensor. The dynamic Equation (28a), the associated interface conditions (30a) and (30b), and the choice of the elastic energy (26a) mirror that of [19].

Remark 4.3 (On the interface conditions on the variable $\boldsymbol{K}_{\eta}$)**.** We deem it worthwhile to discuss the reason why we prescribe the interface condition (30d), which imposes that $(\text{DevSym}\mathbb{K}_{\text{dis}1})\boldsymbol{N}_{\Gamma_{\text{R}}}$ and $(\text{DevSym}\mathbb{K}_{\text{dis}2})\boldsymbol{N}_{\Gamma_{\text{R}}}$ are equal to each other on the contact surface between the corresponding constituents. To explain the rationale behind this choice, we briefly review the condition that Gurtin and Anand [42] assign in their original paper, in which a single continuum is studied and no AH is done. In their framework, Gurtin and Anand [42] give the condition $(\text{DevSym}\mathbb{K})\boldsymbol{N} = \boldsymbol{O}$ on the boundary of the body that they consider, or on a portion of it, as opposite to another possible choice, which amounts to set (in our notation) $\boldsymbol{D}_{\boldsymbol{K}} = \boldsymbol{O}$ on the same boundary, or on the portion complementary to the one on which $(\text{DevSym}\mathbb{K})\boldsymbol{N} = \boldsymbol{O}$ is prescribed. In doing this, Gurtin and Anand [42] call *"microscopically hard"* the surface on which $\boldsymbol{D}_{\boldsymbol{K}}$ is set equal to the null tensor, whereas they refer to the surface on which $(\text{DevSym}\mathbb{K})\boldsymbol{N}$ vanishes as to *"microscopically free."* Physically, a *"microscopically hard"* surface means that no evolution of plastic distortions may occur on that surface, whereas a *"microscopically free"* surface implies that the plastic descriptors of the body, that is, $\boldsymbol{K}$ and $\boldsymbol{L}_{\boldsymbol{K}}$, do not communicate with the world surrounding the body through any contact force. In this respect, if we imported the point of view of the *"microscopically free"* boundary into our context, and if we applied it to each constituent of the composite that we are considering, then each side of Equation (30d) could be assumed to vanish independently of the other one, as if each constituent would have a *"microscopically free"* surface. However, in our opinion, and to the best of our understanding, even though this approach works for the theory of plasticity of Gurtin and Anand [42], in the case of internal boundaries that are in contact with each other, and in the case of the biological process of remodeling, it could be too stringent. Indeed, if one allows that the structural degrees of freedom of the body can be activated also by external interactions, which need not be of strict mechanical nature, but that may be represented by generalized forces, then the hypothesis of *"microscopically free"* surface ceases to apply. Hence, one may presume a boundary condition of the type $(\text{DevSym}\mathbb{K}_{\text{dis}\eta})\boldsymbol{N}_{\eta} = \mathfrak{E}_{\text{rem},\eta}$ on the outer boundary of the ηth constituent, where $\mathfrak{E}_{\text{rem},\eta}$ is a second-order tensor having the physical dimensions of energy per unit area (or force per unit length), and describing an external source or sink of energy that is transferred through the body's boundary. Within this approach, it seems to us natural to suppose that an interaction of this type propagates through the interface of the two constituents under consideration, thereby leading to Equation (30d).

Note that boundary conditions of the type (30d) are referred to as "natural boundary conditions" in theories based on variational methods [123]. In fact, by prescribing no-jump conditions at the interface for the remodeling rates $\boldsymbol{L}_{\boldsymbol{K}1}$ and $\boldsymbol{L}_{\boldsymbol{K}2}$ with the constraints (29a) and (29b), the condition of no-jump for the symmetric and deviatoric part of the generalized stresses through the interface appears naturally.

5 | ASYMPTOTIC HOMOGENIZATION OF THE MICROFORCE BALANCE

In this section, we focus on the homogenization of Equations (28a), (28b), (29a), and (29b). Particular relevance will be given to Equations (28b), (29a), and (29b), although, to make our work self-contained, we shall report also the most

10991476, 2025, 1, Downloaded from https://onlinelibrary.wiley.com/doi/10.1002/mma.10367 by Politecnico Di Torino Sist. Bibl Del Polit Di Torino, Wiley Online Library on [12/02/2025]. See the Terms and Conditions (https://onlinelibrary.wiley.com/terms-and-conditions) on Wiley Online Library for rules of use; OA articles are governed by the applicable Creative Commons License

fundamental steps of the homogenization of the linear momentum balance law (28a), since we follow here a path that is different from the one outlined in [19].

For our purposes, we perform the asymptotic expansion of the linear momentum balance (28a), of the microforce balance (28b), and of the kinematic constraints (29a) and (29b), which determine, in a two-scale setting, the motion, or the displacement, of the composite's constituents and the evolution of their remodeling tensor $\boldsymbol{K}_\eta^\varepsilon(\tilde{X},\tilde{Y},t)$, with ε being the ratio introduced in Equation (3), and where the notation $\boldsymbol{K}_\eta^\varepsilon(\tilde{X},\tilde{Y},t)$ is intended as in Section 3.2.

Before starting the expansions of the fields of interest in asymptotic series, we should notice that the smallness parameter ε has been defined in Equation (3) as the ratio between the characteristic length scale of the microstructure, that is, ℓ_0, and the length scale L_0 characterizing the composite as a whole. In accordance with the discussion above, ℓ_0 is the finest length scale of the problem at hand, since the length scales associated with the plastic distortions, that is, ℓ_η, with $\eta = 1, 2$ (see Equation (24b)), are taken such that $\ell_\eta > \ell_0$. Hence, in our study, we are not solving the inhomogeneities of the remodeling distortions inside the portions of the constituents composing the reference cell of the composite.

5.1 | Asymptotic expansion of displacement, remodeling tensor, and related fields

The formal expansions for the displacement $\boldsymbol{u}_\eta$, displacement gradient tensor Grad $\boldsymbol{u}_\eta$, and remodeling tensor $\boldsymbol{K}_\eta$ are written as (see, e.g., [19])

$$\boldsymbol{u}_\eta(X,t) \equiv u_c \boldsymbol{u}_\eta^\varepsilon(\tilde{X},\tilde{Y},t) = u_c \sum_{l=0}^{\infty} \varepsilon^l \boldsymbol{u}_\eta^{(l)}(\tilde{X},\tilde{Y},t) = u_c \left\{ \boldsymbol{u}_\eta^{(0)}(\tilde{X},\tilde{Y},t) + \varepsilon\, \boldsymbol{u}_\eta^{(1)}(\tilde{X},\tilde{Y},t) \right\} + o(\varepsilon), \tag{31a}$$

$$\begin{aligned} \text{Grad}\ \boldsymbol{u}_\eta(X,t) &= \frac{u_c}{L_0} \left\{ \text{Grad}_{\tilde{X}} \boldsymbol{u}_\eta^\varepsilon(\tilde{X},\tilde{Y},t) + \varepsilon^{-1} \text{Grad}_{\tilde{Y}} \boldsymbol{u}_\eta^\varepsilon(\tilde{X},\tilde{Y},t) \right\} \\ &= \frac{u_c}{L_0} \left\{ \sum_{l=0}^{\infty} \varepsilon^l \text{Grad}_{\tilde{X}} \boldsymbol{u}_\eta^{(l)}(\tilde{X},\tilde{Y},t) + \sum_{l=0}^{\infty} \varepsilon^{l-1} \text{Grad}_{\tilde{Y}} \boldsymbol{u}_\eta^{(l)}(\tilde{X},\tilde{Y},t) \right\} \\ &= \varepsilon^{-1} \frac{u_c}{L_0} \text{Grad}_{\tilde{Y}} \boldsymbol{u}_\eta^{(0)}(\tilde{X},\tilde{Y},t) + \frac{u_c}{L_0} \left(\text{Grad}_{\tilde{X}} \boldsymbol{u}_\eta^{(0)}(\tilde{X},\tilde{Y},t) + \text{Grad}_{\tilde{Y}} \boldsymbol{u}_\eta^{(1)}(\tilde{X},\tilde{Y},t) \right) \\ &\quad + \varepsilon \frac{u_c}{L_0} \left(\text{Grad}_{\tilde{X}} \boldsymbol{u}_\eta^{(1)}(\tilde{X},\tilde{Y},t) + \text{Grad}_{\tilde{Y}} \boldsymbol{u}_\eta^{(2)}(\tilde{X},\tilde{Y},t) \right) + o(\varepsilon), \end{aligned} \tag{31b}$$

$$\boldsymbol{K}_\eta(X,t) = \boldsymbol{K}_\eta^\varepsilon(\tilde{X},\tilde{Y},t) = \sum_{l=0}^{\infty} \varepsilon^l \boldsymbol{K}_\eta^{(l)}(\tilde{X},\tilde{Y},t) = \boldsymbol{K}_\eta^{(0)}(\tilde{X},\tilde{Y},t) + \varepsilon \boldsymbol{K}_\eta^{(1)}(\tilde{X},\tilde{Y},t) + o(\varepsilon), \tag{31c}$$

$$\begin{aligned} \text{Grad}\ \boldsymbol{K}_\eta(X,t) &= \varepsilon^{-1} \frac{1}{L_0} \text{Grad}_{\tilde{Y}} \boldsymbol{K}_\eta^{(0)}(\tilde{X},\tilde{Y},t) + \frac{1}{L_0} \left(\text{Grad}_{\tilde{X}} \boldsymbol{K}_\eta^{(0)}(\tilde{X},\tilde{Y},t) + \text{Grad}_{\tilde{Y}} \boldsymbol{K}_\eta^{(1)}(\tilde{X},\tilde{Y},t) \right) \\ &\quad + \varepsilon \frac{1}{L_0} \left(\text{Grad}_{\tilde{X}} \boldsymbol{K}_\eta^{(1)}(\tilde{X},\tilde{Y},t) + \text{Grad}_{\tilde{Y}} \boldsymbol{K}_\eta^{(2)}(\tilde{X},\tilde{Y},t) \right) + o(\varepsilon), \end{aligned} \tag{31d}$$

for $\varepsilon \to 0$. Here, $\boldsymbol{u}_\eta^{(l)}$ and $\boldsymbol{K}_\eta^{(l)}$ are the generic lth-order terms of the formal expansions of the non-dimensional displacement and remodeling tensor, respectively. Similar results have been obtained for the case of heat conduction for the temperature field in [69].

Other two kinematic descriptors related to $\boldsymbol{K}_\eta$ that are relevant for our two-scale problem are the inverse of the remodeling tensor $(\boldsymbol{K}_\eta)^{-1}$ and the plastic rate $\boldsymbol{L}_{\boldsymbol{K}\eta}$. For the inverse of the remodeling tensor, we introduce the notation $\boldsymbol{Z}_\eta(X,t) := (\boldsymbol{K}_\eta(X,t))^{-1}$ and write its formal expansion as

$$\boldsymbol{Z}_\eta(X,t) = \boldsymbol{Z}_\eta^\varepsilon(\tilde{X},\tilde{Y},t) = \sum_{l=0}^{\infty} \varepsilon^l \boldsymbol{Z}_\eta^{(l)}(\tilde{X},\tilde{Y},t) = \boldsymbol{Z}_\eta^{(0)}(\tilde{X},\tilde{Y},t) + \varepsilon \boldsymbol{Z}_\eta^{(1)}(\tilde{X},\tilde{Y},t) + o(\varepsilon), \tag{32}$$

where we characterize $\boldsymbol{Z}_\eta^{(0)}(\tilde{X},\tilde{Y},t)$ and $\boldsymbol{Z}_\eta^{(1)}(\tilde{X},\tilde{Y},t)$ by virtue of the Cayley–Hamilton theorem. Indeed, by introducing the principal invariants of $\boldsymbol{K}_\eta$, that is,

$$I_{1\boldsymbol{K}_\eta} := \text{tr}\boldsymbol{K}_\eta, \qquad I_{2\boldsymbol{K}_\eta} := \frac{1}{2}\left((\text{tr}\boldsymbol{K}_\eta)^2 - \text{tr}((\boldsymbol{K}_\eta)^2) \right), \qquad I_{3\boldsymbol{K}_\eta} := \det \boldsymbol{K}_\eta, \tag{33}$$

the tensor $(\boldsymbol{K}_\eta)^{-1}$ satisfies the relation

$$I_{3\boldsymbol{K}_\eta} (\boldsymbol{K}_\eta)^{-1} = (\boldsymbol{K}_\eta)^2 - I_{1\boldsymbol{K}_\eta} \boldsymbol{K}_\eta + I_{2\boldsymbol{K}_\eta} \boldsymbol{I}. \tag{34}$$

10991476, 2025, 1, Downloaded from https://onlinelibrary.wiley.com/doi/10.1002/nma.10367 by Politecnico Di Torino Sist. Bibl Del Polit Di Torino, Wiley Online Library on [12/02/2025]. See the Terms and Conditions (https://onlinelibrary.wiley.com/terms-and-conditions) on Wiley Online Library for rules of use; OA articles are governed by the applicable Creative Commons License

By recalling the constraint of isochoric remodeling distortions, which reads here $I_{3\boldsymbol{K}_\eta} = 1$, and invoking the formal two-scale expansion of $\boldsymbol{K}_\eta(X,t) = \boldsymbol{K}_\eta^\varepsilon(\tilde{X},\tilde{Y},t)$ and of $\boldsymbol{Z}_\eta(X,t) = \boldsymbol{Z}_\eta^\varepsilon(\tilde{X},\tilde{Y},t)$, both truncated at the first order in ε, we obtain the following identifications through Equation (34):

$$\boldsymbol{Z}_\eta^{(0)} := \left(\boldsymbol{K}_\eta^{(0)}\right)^{-1}, \tag{35a}$$

$$\boldsymbol{Z}_\eta^{(1)} := \boldsymbol{K}_\eta^{(0)}\boldsymbol{K}_\eta^{(1)} + \boldsymbol{K}_\eta^{(1)}\boldsymbol{K}_\eta^{(0)} - \mathrm{tr}\left(\boldsymbol{K}_\eta^{(0)}\right)\boldsymbol{K}_\eta^{(1)} - \mathrm{tr}\left(\boldsymbol{K}_\eta^{(1)}\right)\boldsymbol{K}_\eta^{(0)} + \left(\mathrm{tr}\left(\boldsymbol{K}_\eta^{(0)}\right)\mathrm{tr}\left(\boldsymbol{K}_\eta^{(1)}\right) - \mathrm{tr}\left(\boldsymbol{K}_\eta^{(0)}\boldsymbol{K}_\eta^{(1)}\right)\right)\boldsymbol{I}. \tag{35b}$$

We also notice that, in general, $\boldsymbol{K}_\eta^{(1)}$ and $\boldsymbol{Z}_\eta^{(1)}$ can be singular. For instance, if $\boldsymbol{K}_\eta^\varepsilon \equiv \boldsymbol{I}$, which is a relevant case, since it is often assumed as an initial condition for the dynamic equation of $\boldsymbol{K}$, we have $\boldsymbol{K}_\eta^{(0)} = \boldsymbol{I}$, $\boldsymbol{Z}_\eta^{(0)} = \boldsymbol{I}$, $\boldsymbol{K}_\eta^{(1)} = \boldsymbol{O}$, and $\boldsymbol{Z}_\eta^{(1)} = \boldsymbol{O}$.

Another consideration follows from the expansion of $\boldsymbol{K}_\eta$. In fact, if we take the determinant of Equation (31c), we obtain

$$\begin{aligned}
\det(\boldsymbol{K}_\eta^\varepsilon) &= \det\left(\boldsymbol{K}_\eta^{(0)} + \varepsilon\boldsymbol{K}_\eta^{(1)} + o(\varepsilon)\right)\\
&= \det\left(\boldsymbol{K}_\eta^{(0)}\left(\boldsymbol{I} + \varepsilon\boldsymbol{Z}_\eta^{(0)}\boldsymbol{K}_\eta^{(1)} + o(\varepsilon)\right)\right)\\
&= \det\left(\boldsymbol{K}_\eta^{(0)}\right)\det\left(\boldsymbol{I} + \varepsilon\boldsymbol{Z}_\eta^{(0)}\boldsymbol{K}_\eta^{(1)} + o(\varepsilon)\right)\\
&= \det\left(\boldsymbol{K}_\eta^{(0)}\right)\left(1 + \varepsilon\ \mathrm{tr}\left(\boldsymbol{Z}_\eta^{(0)}\boldsymbol{K}_\eta^{(1)}\right) + o(\varepsilon)\right),
\end{aligned} \tag{36}$$

in which the last equality is found by having recourse to the Taylor expansion of the determinant in a neighborhood of the identity tensor $\boldsymbol{I}$. Moreover, since the remodeling does not involve changes of volume in the present setting, we have that $\det(\boldsymbol{K}_\eta^\varepsilon) = 1$, independently of the smallness parameter ε. Consequently, from Equation (36), by taking into consideration higher terms in the Taylor expansion of the determinant, we obtain the conditions

$$\det\left(\boldsymbol{K}_\eta^{(0)}\right) = 1, \tag{37a}$$

$$\mathrm{tr}\left(\boldsymbol{Z}_\eta^{(0)}\boldsymbol{K}_\eta^{(1)}\right) = 0, \tag{37b}$$

$$2\mathrm{tr}\left(\boldsymbol{Z}_\eta^{(0)}\boldsymbol{K}_\eta^{(2)}\right) - \mathrm{tr}\left(\left(\boldsymbol{Z}_\eta^{(0)}\boldsymbol{K}_\eta^{(1)}\right)^2\right) = 0, \tag{37c}$$

which represent the isochoricity constraint of $\boldsymbol{K}_\eta$ in our two-scale framework and lead to the conclusion that the first-order term $\boldsymbol{K}_\eta^{(1)}$ is *orthogonal* to $(\boldsymbol{Z}_\eta^{(0)})^{\mathrm{T}}$, whereas at the second order, we obtain a balance between the volumetric contributions made by $\boldsymbol{Z}_\eta^{(0)}\boldsymbol{K}_\eta^{(1)}$ and $\boldsymbol{Z}_\eta^{(0)}\boldsymbol{K}_\eta^{(2)}$. Such constraints can also be expressed in differential form, which is more convenient for our purposes. To this end, we introduce the formal two-scale expansion of the plastic rate $\boldsymbol{L}_{\boldsymbol{K}\eta}$, that is,

$$\boldsymbol{L}_{\boldsymbol{K}\eta}(X,t) = \boldsymbol{L}_{\boldsymbol{K}\eta}^\varepsilon(\tilde{X},\tilde{Y},t) = \sum_{l=0}^{\infty}\varepsilon^l\boldsymbol{L}_{\boldsymbol{K}\eta}^{(l)}(\tilde{X},\tilde{Y},t) = \boldsymbol{L}_{\boldsymbol{K}\eta}^{(0)}(\tilde{X},\tilde{Y},t) + \varepsilon\boldsymbol{L}_{\boldsymbol{K}\eta}^{(1)}(\tilde{X},\tilde{Y},t) + o(\varepsilon), \tag{38}$$

where $\boldsymbol{L}_{\boldsymbol{K}\eta}^{(l)}$ is the generic lth-order term of the formal expansion of $\boldsymbol{L}_{\boldsymbol{K}\eta}$, while $\boldsymbol{L}_{\boldsymbol{K}\eta}^{(0)}$ and $\boldsymbol{L}_{\boldsymbol{K}\eta}^{(1)}$ are the zeroth- and first-order term of this expansion. We emphasize that to avoid the introduction of further symbols, we do not perform any non-dimensionalization for the asymptotic expansion of $\boldsymbol{L}_{\boldsymbol{K}\eta}$. Thus, $\boldsymbol{L}_{\boldsymbol{K}\eta}^\varepsilon$ and each term $\boldsymbol{L}_{\boldsymbol{K}\eta}^{(l)}$, for $l \geq 0$, have physical dimension of the reciprocal of time.

Next, we provide a characterization of $\boldsymbol{L}_{\boldsymbol{K}\eta}^{(0)}$ and $\boldsymbol{L}_{\boldsymbol{K}\eta}^{(1)}$ by writing $\boldsymbol{L}_{\boldsymbol{K}\eta}$ as a function of the two-scale formal expansions of $\boldsymbol{K}_\eta$ and $\boldsymbol{Z}_\eta$, and singling out the tensorial expressions associated with ε^0 and ε^1. So, by writing

$$\boldsymbol{L}_{\boldsymbol{K}\eta}(X,t) = \boldsymbol{L}_{\boldsymbol{K}\eta}^\varepsilon(\tilde{X},\tilde{Y},t) = \dot{\boldsymbol{K}}_\eta^\varepsilon(\tilde{X},\tilde{Y},t)(\boldsymbol{K}_\eta^\varepsilon(\tilde{X},\tilde{Y},t))^{-1} = \left(\sum_{i=0}^{\infty}\varepsilon^i\dot{\boldsymbol{K}}_\eta^{(i)}(\tilde{X},\tilde{Y},t)\right)\left(\sum_{j=0}^{\infty}\varepsilon^j\boldsymbol{Z}_\eta^{(j)}(\tilde{X},\tilde{Y},t)\right), \tag{39}$$

we can make the following identifications:

$$\boldsymbol{L}_{\boldsymbol{K}\eta}^{(0)} := \dot{\boldsymbol{K}}_\eta^{(0)}\boldsymbol{Z}_\eta^{(0)}, \tag{40a}$$

10991476, 2025, 1, Downloaded from https://onlinelibrary.wiley.com/doi/10.1002/nme.10367 by Politecnico Di Torino Sist. Bibl Del Polit Di Torino, Wiley Online Library on [12/02/2025]. See the Terms and Conditions (https://onlinelibrary.wiley.com/terms-and-conditions) on Wiley Online Library for rules of use; OA articles are governed by the applicable Creative Commons License

$$\boldsymbol{L}_{\boldsymbol{K}\eta}^{(1)} := \dot{\boldsymbol{K}}_{\eta}^{(0)}\boldsymbol{Z}_{\eta}^{(1)} + \dot{\boldsymbol{K}}_{\eta}^{(1)}\boldsymbol{Z}_{\eta}^{(0)}, \tag{40b}$$

$$\boldsymbol{L}_{\boldsymbol{K}\eta}^{(2)} := \dot{\boldsymbol{K}}_{\eta}^{(0)}\boldsymbol{Z}_{\eta}^{(2)} + \dot{\boldsymbol{K}}_{\eta}^{(1)}\boldsymbol{Z}_{\eta}^{(1)} + \dot{\boldsymbol{K}}_{\eta}^{(2)}\boldsymbol{Z}_{\eta}^{(0)}. \tag{40c}$$

Next, we introduce the expansion of $\mathrm{Grad}\boldsymbol{L}_{\boldsymbol{K}\eta}$, that is,

$$\begin{aligned}\mathrm{Grad}\ \boldsymbol{L}_{\boldsymbol{K}\eta}(X,t) &= \frac{1}{L_0}\left\{\mathrm{Grad}_{\tilde{X}}\boldsymbol{L}_{\boldsymbol{K}\eta}^{\varepsilon}(\tilde{X},\tilde{Y},t) + \varepsilon^{-1}\mathrm{Grad}_{\tilde{Y}}\boldsymbol{L}_{\boldsymbol{K}\eta}^{\varepsilon}(\tilde{X},\tilde{Y},t)\right\}\\ &= \varepsilon^{-1}\frac{1}{L_0}\mathrm{Grad}_{\tilde{Y}}\boldsymbol{L}_{\boldsymbol{K}\eta}^{(0)}(\tilde{X},\tilde{Y},t) + \frac{1}{L_0}\left(\mathrm{Grad}_{\tilde{X}}\boldsymbol{L}_{\boldsymbol{K}\eta}^{(0)}(\tilde{X},\tilde{Y},t) + \mathrm{Grad}_{\tilde{Y}}\boldsymbol{L}_{\boldsymbol{K}\eta}^{(1)}(\tilde{X},\tilde{Y},t)\right)\\ &\quad + \varepsilon\frac{1}{L_0}\left(\mathrm{Grad}_{\tilde{X}}\boldsymbol{L}_{\boldsymbol{K}\eta}^{(1)}(\tilde{X},\tilde{Y},t) + \mathrm{Grad}_{\tilde{Y}}\boldsymbol{L}_{\boldsymbol{K}\eta}^{(2)}(\tilde{X},\tilde{Y},t)\right) + o(\varepsilon),\end{aligned} \tag{41}$$

for $\varepsilon \to 0$, where $\boldsymbol{L}_{\boldsymbol{K}\eta}^{(2)}$ is defined in Equation (40c). Note that the gradients of $\boldsymbol{K}_{\eta}^{(0)}$, $\boldsymbol{K}_{\eta}^{(1)}$, and $\boldsymbol{K}_{\eta}^{(2)}$ in Equation (31d) can be used to express explicitly the gradients of $\boldsymbol{L}_{\boldsymbol{K}\eta}^{(0)}$, $\boldsymbol{L}_{\boldsymbol{K}\eta}^{(1)}$, and $\boldsymbol{L}_{\boldsymbol{K}\eta}^{(2)}$ of Equation (41), although we omit these lengthy calculations for the sake of conciseness.

Finally, we perform the asymptotic expansion of the kinematic constraints (15a) and (15b), thereby obtaining the conditions that interweave the zeroth- and the first-order terms of the two-scale expansion of $\boldsymbol{K}_{\eta}$. Hence, the constraint of isochoricity and the constraint of null plastic spin lead to the equations

$$\mathrm{tr}\boldsymbol{L}_{\boldsymbol{K}\eta}^{(0)} = 0, \qquad \mathrm{tr}\boldsymbol{L}_{\boldsymbol{K}\eta}^{(1)} = 0, \tag{42a}$$

$$\boldsymbol{L}_{\boldsymbol{K}\eta}^{(0)} - \left(\boldsymbol{L}_{\boldsymbol{K}\eta}^{(0)}\right)^{\mathrm{T}} = \boldsymbol{O}, \qquad \boldsymbol{L}_{\boldsymbol{K}\eta}^{(1)} - \left(\boldsymbol{L}_{\boldsymbol{K}\eta}^{(1)}\right)^{\mathrm{T}} = \boldsymbol{O}. \tag{42b}$$

5.2 | Cell problems

The scope of this section is to present the asymptotic expansion of the system of Equations (28a) and (28b). In this respect, we notice that while the constitutive expressions of $\boldsymbol{T}_{\mathrm{dis}\eta}$ and $\mathbb{K}_{\mathrm{dis}\eta}$ are already linear in $\boldsymbol{L}_{\boldsymbol{K}\eta}$ and Grad $\boldsymbol{L}_{\boldsymbol{K}\eta}$, respectively, those defining the first Piola–Kirchhoff stress tensor $\boldsymbol{P}_{\eta}$ and the Mandel stress tensor $\boldsymbol{\Sigma}_{\eta}$ depend on their arguments, namely, $\boldsymbol{F}_{\eta}$ and $\boldsymbol{K}_{\eta}$, in a nonlinear way. For this reason, and since for the purposes of our work we would like our calculations to be as analytical as possible, we proceed with a linearization of the constituting functions of $\boldsymbol{P}_{\eta}$ and $\boldsymbol{\Sigma}_{\eta}$. To this end, we follow the procedure outlined in [19], thereby substituting $\boldsymbol{P}_{\eta}$ in Equation (28a) and $\boldsymbol{\Sigma}_{\eta}$ in Equation (28b) with their linearizations performed with respect to the displacement gradient $\boldsymbol{H}_{\eta} := \mathrm{Grad}\ \boldsymbol{u}_{\eta}$ in a neighborhood of $\boldsymbol{H}_{\eta} = \boldsymbol{O}$, that is,

$$\boldsymbol{P}_{\eta\mathrm{lin}} = \mathcal{C}_{\mathrm{R}\eta} : \mathrm{sym}\boldsymbol{H}_{\eta} - (\boldsymbol{I} + \boldsymbol{H}_{\eta})(\mathcal{C}_{\mathrm{R}\eta} : \boldsymbol{E}_{\boldsymbol{K}\eta}), \tag{43a}$$

$$\boldsymbol{\Sigma}_{\eta\mathrm{lin}} = \frac{1}{J_{\boldsymbol{K}\eta}}\boldsymbol{K}_{\eta}^{-\mathrm{T}}\left\{\mathcal{C}_{\mathrm{R}\eta} : \mathrm{sym}\boldsymbol{H}_{\eta} - (\boldsymbol{I} + 2\mathrm{sym}\boldsymbol{H}_{\eta})(\mathcal{C}_{\mathrm{R}\eta} : \boldsymbol{E}_{\boldsymbol{K}\eta})\right\}\boldsymbol{K}_{\eta}^{\mathrm{T}}, \tag{43b}$$

where we have used the De Saint-Venant strain energy density introduced in Equation (26a), the definition of the elasticity tensor $\mathcal{C}_{\mathrm{R}\eta}$ associated with the reference placement, that is,

$$\mathcal{C}_{\mathrm{R}\eta} := J_{\boldsymbol{K}\eta}\left\{\boldsymbol{K}_{\eta}^{-1}\underline{\otimes}\boldsymbol{K}_{\eta}^{-1} : \mathcal{C}_{\eta} : \boldsymbol{K}_{\eta}^{-\mathrm{T}}\underline{\otimes}\boldsymbol{K}_{\eta}^{-\mathrm{T}}\right\}, \tag{44}$$

where $\left[\boldsymbol{A}\underline{\otimes}\boldsymbol{B}\right]_{KLMN} = [\boldsymbol{A}]_{KM}[\boldsymbol{B}]_{LN}$ and $[\boldsymbol{A}\overline{\otimes}\boldsymbol{B}]_{KLMN} = [\boldsymbol{A}]_{KN}[\boldsymbol{B}]_{LM}$ [124], and the Green–Lagrange strain tensor $\boldsymbol{E}_{\boldsymbol{K}\eta}$ due to the remodeling distortions, that is,

$$\boldsymbol{E}_{\boldsymbol{K}\eta} = \frac{1}{2}\left[\boldsymbol{K}_{\eta}^{\mathrm{T}}\boldsymbol{K}_{\eta} - \boldsymbol{I}\right]. \tag{45}$$

We notice that in the present framework, we do not linearize with respect to the remodeling tensor $\boldsymbol{K}_{\eta}$. Accordingly, we obtain

10991476, 2025, 1, Downloaded from https://onlinelibrary.wiley.com/doi/10.1002/nma.10367 by Politecnico Di Torino Sist. Bibl Del Polit Di Torino, Wiley Online Library on [12/02/2025]. See the Terms and Conditions (https://onlinelibrary.wiley.com/terms-and-conditions) on Wiley Online Library for rules of use; OA articles are governed by the applicable Creative Commons License

$$\mathrm{Div}\boldsymbol{P}_{\eta\mathrm{lin}} = \boldsymbol{0}, \qquad \text{in } \mathscr{B}_{\mathrm{R}\eta}, \tag{46a}$$

$$\mathrm{DevSym}\{\boldsymbol{T}_{\mathrm{dis}\eta} - \boldsymbol{\Sigma}_{\eta\mathrm{lin}} - \mathrm{Div}\mathbb{K}_{\mathrm{dis}\eta}\} = \boldsymbol{O}, \qquad \text{in } \mathscr{B}_{\mathrm{R}\eta}. \tag{46b}$$

Looking at the constitutive expressions of $\boldsymbol{T}_{\mathrm{dis}\eta}$ and $\mathbb{K}_{\mathrm{dis}\eta}$ in Equations (24a) and (24b), and of $\boldsymbol{P}_{\eta\mathrm{lin}}$ and $\boldsymbol{\Sigma}_{\eta\mathrm{lin}}$ in Equations (43a) and (43b), we notice that the force balances (46a) and (46b) are coupled with each other, and that this coupling emerges through the stress tensors $\boldsymbol{P}_{\eta\mathrm{lin}}$ and $\boldsymbol{\Sigma}_{\eta\mathrm{lin}}$. In particular, the balance (46a) influences (46b) through the dependence of $\boldsymbol{\Sigma}_{\eta\mathrm{lin}}$ on the deformation, whereas the "flow rule" (46b) influences the equilibrium equation (46a) through the dependence of $\boldsymbol{P}_{\eta\mathrm{lin}}$ on $\boldsymbol{K}_\eta$. However, if there existed a certain regime in which the contribution of the Mandel stress tensor were negligible with respect to the other generalized forces featuring in Equation (46b), then, for each phase, the tensor of remodeling distortions $\boldsymbol{K}_\eta$ could be determined independently on the deformation (and of Mandel stress) in our model.[2] The converse, however, is not true, since $\boldsymbol{K}_\eta$ influences the (linearized) first Piola–Kirchhoff stress tensor through the dependence of the latter on the remodeling distortions.

The coupling just discussed has also the important peculiarity of being scale dependent, in the sense that it manifests in different ways at different length scales, as can be seen through the study of Equations (46a) and (46b) with the aid of AH.

To proceed with the homogenization of Equations (46a) and (46b), we need to recast them in the following form:

$$\frac{1}{L_0}\left(\mathrm{Div}_{\tilde{X}} + \frac{1}{\varepsilon}\mathrm{Div}_{\tilde{Y}}\right)\boldsymbol{P}^{\varepsilon}_{\eta\mathrm{lin}} = \boldsymbol{0}, \qquad \text{in } \mathscr{B}_{\mathrm{R}\eta}, \tag{47a}$$

$$\mathrm{DevSym}\left\{\boldsymbol{T}^{\varepsilon}_{\mathrm{dis}\eta} - \boldsymbol{\Sigma}^{\varepsilon}_{\eta\mathrm{lin}} - \frac{1}{L_0}\left(\mathrm{Div}_{\tilde{X}} + \frac{1}{\varepsilon}\mathrm{Div}_{\tilde{Y}}\right)\mathbb{K}^{\varepsilon}_{\mathrm{dis}\eta}\right\} = \boldsymbol{O}, \qquad \text{in } \mathscr{B}_{\mathrm{R}\eta}, \tag{47b}$$

where we set

$$\boldsymbol{P}^{\varepsilon}_{\eta\mathrm{lin}} = C^{\varepsilon}_{\mathrm{R}\eta} : \frac{u_\mathrm{c}}{L_0}\boldsymbol{H}^{\varepsilon}_{\eta} - \left(\boldsymbol{I} + \frac{u_\mathrm{c}}{L_0}\boldsymbol{H}^{\varepsilon}_{\eta}\right)\left(C^{\varepsilon}_{\mathrm{R}\eta} : \boldsymbol{E}^{\varepsilon}_{\boldsymbol{K}\eta}\right), \tag{48a}$$

$$\boldsymbol{T}^{\varepsilon}_{\mathrm{dis}\eta} = \sigma^{\varepsilon}_{\eta}\tau^{\varepsilon}_{\eta}\boldsymbol{L}^{\varepsilon}_{\boldsymbol{K}\eta}, \tag{48b}$$

$$\boldsymbol{\Sigma}^{\varepsilon}_{\eta\mathrm{lin}} = \frac{1}{\det\boldsymbol{K}^{\varepsilon}_{\eta}}(\boldsymbol{Z}^{\varepsilon}_{\eta})^{\mathrm{T}}\left\{C^{\varepsilon}_{\mathrm{R}\eta} : \frac{u_\mathrm{c}}{L_0}\boldsymbol{H}^{\varepsilon}_{\eta} - \left(\boldsymbol{I} + 2\frac{u_\mathrm{c}}{L_0}\boldsymbol{H}^{\varepsilon}_{\eta}\right)\left(C^{\varepsilon}_{\mathrm{R}\eta} : \boldsymbol{E}^{\varepsilon}_{\boldsymbol{K}\eta}\right)\right\}(\boldsymbol{K}^{\varepsilon}_{\eta})^{\mathrm{T}}, \tag{48c}$$

$$\mathbb{K}^{\varepsilon}_{\mathrm{dis}\eta} = \ell^2_{\eta}\sigma^{\varepsilon}_{\eta}\tau^{\varepsilon}_{\eta}\frac{1}{L_0}\left(\mathrm{Grad}_{\tilde{X}} + \frac{1}{\varepsilon}\mathrm{Grad}_{\tilde{Y}}\right)\boldsymbol{L}^{\varepsilon}_{\boldsymbol{K}\eta}, \tag{48d}$$

with the expansion of $\boldsymbol{L}^{\varepsilon}_{\boldsymbol{K}\eta}$ being given in Equation (38) and $\boldsymbol{H}^{\varepsilon}_{\eta}$ being defined through Equation (31b) as

$$\begin{aligned}\boldsymbol{H}^{\varepsilon}_{\eta}(\tilde{X},\tilde{Y},t) :&= \mathrm{Grad}_{\tilde{X}}\boldsymbol{u}^{\varepsilon}_{\eta}(\tilde{X},\tilde{Y},t) + \varepsilon^{-1}\mathrm{Grad}_{\tilde{Y}}\boldsymbol{u}^{\varepsilon}_{\eta}(\tilde{X},\tilde{Y},t)\\ &= \varepsilon^{-1}\mathrm{Grad}_{\tilde{Y}}\boldsymbol{u}^{(0)}_{\eta}(\tilde{X},\tilde{Y},t) + \varepsilon^{0}\left(\mathrm{Grad}_{\tilde{X}}\boldsymbol{u}^{(0)}_{\eta}(\tilde{X},\tilde{Y},t) + \mathrm{Grad}_{\tilde{Y}}\boldsymbol{u}^{(1)}_{\eta}(\tilde{X},\tilde{Y},t)\right)\\ &\quad + \varepsilon\left(\mathrm{Grad}_{\tilde{X}}\boldsymbol{u}^{(1)}_{\eta}(\tilde{X},\tilde{Y},t) + \mathrm{Grad}_{\tilde{Y}}\boldsymbol{u}^{(2)}_{\eta}(\tilde{X},\tilde{Y},t)\right) + o(\varepsilon),\end{aligned} \tag{49}$$

for $\varepsilon \to 0$. Note that in Equations (48a) and (48c) we have taken advantage of the minor symmetries of $C^{\varepsilon}_{\mathrm{R}\eta}$ to replace $\mathrm{sym}\boldsymbol{H}^{\varepsilon}_{\eta}$ with $\boldsymbol{H}^{\varepsilon}_{\eta}$.

To render the asymptotic homogenization of Equations (47a) and (47b) and (48a)–(48d) more tractable, we make now the following hypotheses:

(Hp.1) The material parameters σ_η and τ_η as well as the elasticity tensor C_η are constant in space and time in the corresponding ηth constituent. Accordingly, the expansions $\sigma^{\varepsilon}_{\eta}$ and $\tau^{\varepsilon}_{\eta}$ become unnecessary, and they will be simply written as σ_η and τ_η, with the understanding that these quantities are constant. On the other hand, the expansion of the elasticity tensor in the reference placement, that is, $C^{\varepsilon}_{\mathrm{R}\eta}$, remains, because it depends on the remodeling tensor, which is expanded as $\boldsymbol{K}^{\varepsilon}_{\eta}$. However, a strong simplification is attained thanks to the following hypothesis.

[2]This hypothetical behavior is profoundly different from standard plasticity, which is essentially stress driven, but it has been suggested in [125] for a model of the evolution of defects in solids, based on a theoretical framework different from the one considered in our present work.

10991476, 2025, 1, Downloaded from https://onlinelibrary.wiley.com/doi/10.1002/mma.10367 by Politecnico Di Torino Sist. Bibl Del Polit Di Torino, Wiley Online Library on [12/02/2025]. See the Terms and Conditions (https://onlinelibrary.wiley.com/terms-and-conditions) on Wiley Online Library for rules of use; OA articles are governed by the applicable Creative Commons License

(Hp.2) In Equations (48a) and (48c), the expansions of $C^{\varepsilon}_{\mathrm{R}\eta}$, $\boldsymbol{K}^{\varepsilon}_{\eta}$, $\boldsymbol{Z}^{\varepsilon}_{\eta}$, $\boldsymbol{E}^{\varepsilon}_{\boldsymbol{K}\eta}$, and $\det \boldsymbol{K}^{\varepsilon}_{\eta}$ are directly replaced with $C^{(0)}_{\mathrm{R}\eta}$, $\boldsymbol{K}^{(0)}_{\eta}$, $\boldsymbol{Z}^{(0)}_{\eta}$, $\boldsymbol{E}^{(0)}_{\boldsymbol{K}\eta}$, and $\det \boldsymbol{K}^{(0)}_{\eta}$, where $C^{(0)}_{\mathrm{R}\eta}$ and $\boldsymbol{E}^{(0)}_{\boldsymbol{K}\eta}$ are defined by

$$C^{(0)}_{\mathrm{R}\eta} = (\det \boldsymbol{K}^{(0)}_{\eta})\, \boldsymbol{Z}^{(0)}_{\eta} \underline{\otimes} \boldsymbol{Z}^{(0)}_{\eta} \,:\, \mathcal{C}_{\eta} \,:\, (\boldsymbol{Z}^{(0)}_{\eta})^{\mathrm{T}} \underline{\otimes} (\boldsymbol{Z}^{(0)}_{\eta})^{\mathrm{T}}, \qquad \text{with} \quad \det \boldsymbol{K}^{(0)}_{\eta} = 1, \tag{50a}$$

$$\boldsymbol{E}^{(0)}_{\boldsymbol{K}\eta} = \frac{1}{2}\left[\left(\boldsymbol{K}^{(0)}_{\eta}\right)^{\mathrm{T}} \boldsymbol{K}^{(0)}_{\eta} - \boldsymbol{I}\right]. \tag{50b}$$

The hypotheses given above add themselves to the "classical" assumption of AH, by which each term of the expansions (31a)–(31d), (38), and (41) is required to be periodic in the fine-scale variable $\tilde{Y}$. We remark, in this respect, that whereas the hypothesis of $\tilde{Y}$-periodicity for the displacement is well established in the context of composite materials (see, e.g., [38, 70]), the assumption of $\tilde{Y}$-periodicity in the remodeling variable requires some words of explanation. There are examples in the literature (see, e.g., [55, 58]) in which the homogenization of composite materials, subjected to microforce balance laws based on Gurtin and Anand, and Gurtin's theory [42, 106, 108], is carried out by admitting such $\tilde{Y}$-periodicity also for the plastic contribution in the case of *"macroscopically uniform stress or strain"* [58] applied to the composite.

The orders of the Mandel stress tensor associated with ε^{-1} and ε^{0} are given by

$$\boldsymbol{\Sigma}^{(-1)}_{\eta\mathrm{lin}} = \frac{1}{\det \boldsymbol{K}^{(0)}_{\eta}}\left(\boldsymbol{Z}^{(0)}_{\eta}\right)^{\mathrm{T}} \left\{ C^{(0)}_{\mathrm{R}\eta} \,:\, \frac{u_{\mathrm{c}}}{L_0}\mathrm{Grad}_{\tilde{Y}} \boldsymbol{u}^{(0)}_{\eta} - 2\frac{u_{\mathrm{c}}}{L_0}\left(\mathrm{Grad}_{\tilde{Y}} \boldsymbol{u}^{(0)}_{\eta}\right)\left(C^{(0)}_{\mathrm{R}\eta} \,:\, \boldsymbol{E}^{(0)}_{\boldsymbol{K}\eta}\right)\right\}\left(\boldsymbol{K}^{(0)}_{\eta}\right)^{\mathrm{T}}. \tag{51a}$$

$$\begin{aligned}\boldsymbol{\Sigma}^{(0)}_{\eta\mathrm{lin}} = {} & \frac{1}{\det \boldsymbol{K}^{(0)}_{\eta}}\left(\boldsymbol{Z}^{(0)}_{\eta}\right)^{\mathrm{T}} \left\{ C^{(0)}_{\mathrm{R}\eta} \,:\, \frac{u_{\mathrm{c}}}{L_0}\left(\mathrm{Grad}_{\tilde{X}} \boldsymbol{u}^{(0)}_{\eta} + \mathrm{Grad}_{\tilde{Y}} \boldsymbol{u}^{(1)}_{\eta}\right) - 2\frac{u_{\mathrm{c}}}{L_0}\left(\mathrm{Grad}_{\tilde{X}} \boldsymbol{u}^{(0)}_{\eta} + \mathrm{Grad}_{\tilde{Y}} \boldsymbol{u}^{(1)}_{\eta}\right)\left(C^{(0)}_{\mathrm{R}\eta} \,:\, \boldsymbol{E}^{(0)}_{\boldsymbol{K}\eta}\right)\right\}\left(\boldsymbol{K}^{(0)}_{\eta}\right)^{\mathrm{T}} \\ & - \frac{1}{\det \boldsymbol{K}^{(0)}_{\eta}}\left(\boldsymbol{Z}^{(0)}_{\eta}\right)^{\mathrm{T}} \left\{ C^{(0)}_{\mathrm{R}\eta} \,:\, \boldsymbol{E}^{(0)}_{\boldsymbol{K}\eta}\right\}\left(\boldsymbol{K}^{(0)}_{\eta}\right)^{\mathrm{T}}.\end{aligned} \tag{51b}$$

Now, by exploiting hypotheses Hp.1 and Hp.2, we substitute Equations (49), (50a), and (50b) into Equation (48a), and the resulting expression into Equation (47a), and upon collecting the coefficients of ε^{-2}, ε^{-1}, and ε^{0}, we obtain

$$\begin{aligned}&\text{Order } \varepsilon^{-2}: \\ &\frac{u_{\mathrm{c}}}{L_0^2}\mathrm{Div}_{\tilde{Y}}\left\{ C^{(0)}_{\mathrm{R}\eta} \,:\, \mathrm{Grad}_{\tilde{Y}} \boldsymbol{u}^{(0)}_{\eta} - (\mathrm{Grad}_{\tilde{Y}} \boldsymbol{u}^{(0)}_{\eta})\left(C^{(0)}_{\mathrm{R}\eta} \,:\, \boldsymbol{E}^{(0)}_{\boldsymbol{K}\eta}\right)\right\} = \boldsymbol{0},\end{aligned} \tag{52a}$$

$$\begin{aligned}&\text{Order } \varepsilon^{-1}: \\ &\frac{u_{\mathrm{c}}}{L_0^2}\mathrm{Div}_{\tilde{X}}\left\{ C^{(0)}_{\mathrm{R}\eta} \,:\, \mathrm{Grad}_{\tilde{Y}} \boldsymbol{u}^{(0)}_{\eta} - (\mathrm{Grad}_{\tilde{Y}} \boldsymbol{u}^{(0)}_{\eta})\left(C^{(0)}_{\mathrm{R}\eta} \,:\, \boldsymbol{E}^{(0)}_{\boldsymbol{K}\eta}\right)\right\} \\ &+ \frac{u_{\mathrm{c}}}{L_0^2}\mathrm{Div}_{\tilde{Y}}\left\{ C^{(0)}_{\mathrm{R}\eta} \,:\, \left(\mathrm{Grad}_{\tilde{X}} \boldsymbol{u}^{(0)}_{\eta} + \mathrm{Grad}_{\tilde{Y}} \boldsymbol{u}^{(1)}_{\eta}\right) - \frac{L_0}{u_{\mathrm{c}}} C^{(0)}_{\mathrm{R}\eta} \,:\, \boldsymbol{E}^{(0)}_{\boldsymbol{K}\eta} - \left(\mathrm{Grad}_{\tilde{X}} \boldsymbol{u}^{(0)}_{\eta} + \mathrm{Grad}_{\tilde{Y}} \boldsymbol{u}^{(1)}_{\eta}\right)\left(C^{(0)}_{\mathrm{R}\eta} \,:\, \boldsymbol{E}^{(0)}_{\boldsymbol{K}\eta}\right)\right\} = \boldsymbol{0},\end{aligned} \tag{52b}$$

$$\begin{aligned}&\text{Order } \varepsilon^{0}: \\ &\frac{u_{\mathrm{c}}}{L_0^2}\mathrm{Div}_{\tilde{X}}\left\{ C^{(0)}_{\mathrm{R}\eta} \,:\, \left(\mathrm{Grad}_{\tilde{X}} \boldsymbol{u}^{(0)}_{\eta} + \mathrm{Grad}_{\tilde{Y}} \boldsymbol{u}^{(1)}_{\eta}\right) - \frac{L_0}{u_{\mathrm{c}}} C^{(0)}_{\mathrm{R}\eta} \,:\, \boldsymbol{E}^{(0)}_{\boldsymbol{K}\eta} - \left(\mathrm{Grad}_{\tilde{X}} \boldsymbol{u}^{(0)}_{\eta} + \mathrm{Grad}_{\tilde{Y}} \boldsymbol{u}^{(1)}_{\eta}\right)\left(C^{(0)}_{\mathrm{R}\eta} \,:\, \boldsymbol{E}^{(0)}_{\boldsymbol{K}\eta}\right)\right\} \\ &+ \frac{u_{\mathrm{c}}}{L_0^2}\mathrm{Div}_{\tilde{Y}}\left\{ C^{(0)}_{\mathrm{R}\eta} \,:\, \left(\mathrm{Grad}_{\tilde{X}} \boldsymbol{u}^{(1)}_{\eta} + \mathrm{Grad}_{\tilde{Y}} \boldsymbol{u}^{(2)}_{\eta}\right) - \left(\mathrm{Grad}_{\tilde{X}} \boldsymbol{u}^{(1)}_{\eta} + \mathrm{Grad}_{\tilde{Y}} \boldsymbol{u}^{(2)}_{\eta}\right)\left(C^{(0)}_{\mathrm{R}\eta} \,:\, \boldsymbol{E}^{(0)}_{\boldsymbol{K}\eta}\right)\right\} = \boldsymbol{0}.\end{aligned} \tag{52c}$$

On the same footing, Equation (47b) is approximated by the following system of equations:

$$\begin{aligned}&\text{Order } \varepsilon^{-2}: \\ &\mathrm{DevSym}\left\{ -\mathrm{Div}_{\tilde{Y}}\left[\frac{\ell_\eta^2}{L_0^2}\sigma_\eta \tau_\eta \mathrm{Grad}_{\tilde{Y}} \boldsymbol{L}^{(0)}_{\boldsymbol{K}\eta}\right]\right\} = \boldsymbol{O},\end{aligned} \tag{53a}$$

$$\begin{aligned}&\text{Order } \varepsilon^{-1}: \\ &\mathrm{DevSym}\left\{ -\boldsymbol{\Sigma}^{(-1)}_{\eta\mathrm{lin}} - \mathrm{Div}_{\tilde{X}}\left[\frac{\ell_\eta^2}{L_0^2}\sigma_\eta \tau_\eta \mathrm{Grad}_{\tilde{Y}} \boldsymbol{L}^{(0)}_{\boldsymbol{K}\eta}\right] - \mathrm{Div}_{\tilde{Y}}\left[\frac{\ell_\eta^2}{L_0^2}\sigma_\eta \tau_\eta \left(\mathrm{Grad}_{\tilde{X}} \boldsymbol{L}^{(0)}_{\boldsymbol{K}\eta} + \mathrm{Grad}_{\tilde{Y}} \boldsymbol{L}^{(1)}_{\boldsymbol{K}\eta}\right)\right]\right\} = \boldsymbol{O},\end{aligned} \tag{53b}$$

10991476, 2025, 1, Downloaded from https://onlinelibrary.wiley.com/doi/10.1002/nma.10367 by Politecnico Di Torino Sist. Bibl Del Polit Di Torino, Wiley Online Library on [12/02/2025]. See the Terms and Conditions (https://onlinelibrary.wiley.com/terms-and-conditions) on Wiley Online Library for rules of use; OA articles are governed by the applicable Creative Commons License

$$\text{Order } \varepsilon^0 :$$
$$\text{DevSym}\left\{\sigma_\eta\tau_\eta \boldsymbol{L}^{(0)}_{\boldsymbol{K}\eta} - \boldsymbol{\Sigma}^{(0)}_{\eta\text{lin}} - \text{Div}_{\tilde{X}}\left[\frac{\ell_\eta^2}{L_0^2}\sigma_\eta\tau_\eta\left(\text{Grad}_{\tilde{X}}\boldsymbol{L}^{(0)}_{\boldsymbol{K}\eta} + \text{Grad}_{\tilde{Y}}\boldsymbol{L}^{(1)}_{\boldsymbol{K}\eta}\right)\right]\right.$$
$$\left. - \text{Div}_{\tilde{Y}}\left[\frac{\ell_\eta^2}{L_0^2}\sigma_\eta\tau_\eta\left(\text{Grad}_{\tilde{X}}\boldsymbol{L}^{(1)}_{\boldsymbol{K}\eta} + \text{Grad}_{\tilde{Y}}\boldsymbol{L}^{(2)}_{\boldsymbol{K}\eta}\right)\right]\right\} = \mathbf{O}. \tag{53c}$$

The coupling discussed after Equations (46a) and (46b) has now been expanded coherently with the ε-expansions of the fields involved in the current model, and this leads to the following conclusions.

C1. According to the two-scale asymptotic homogenization analysis conducted in this work, the ε^{-2}-order of the flow rule, reported in Equation (53a), decouples the microscale evolution of the leading term of $\boldsymbol{L}_{\boldsymbol{K}\eta}$, that is, $\boldsymbol{L}^{(0)}_{\boldsymbol{K}\eta}$, from the Mandel stress tensor. This implies that at the order ε^{-2}, the spatial distribution of $\boldsymbol{L}^{(0)}_{\boldsymbol{K}\eta}$ is governed solely by the vanishing of the $\tilde{Y}$-divergence of the ε^{-1}-term of $\mathbb{K}^{\varepsilon}_{\text{dis}\eta}$, that is, $\mathbb{K}^{(-1)}_{\text{dis}\eta} := (\ell_\eta^2/L_0)\sigma_\eta\tau_\eta\text{Grad}_{\tilde{Y}}\boldsymbol{L}^{(0)}_{\boldsymbol{K}\eta}$, while no stress-driven evolution due to the Mandel stress appears. This is, to us, a major difference with respect to models of anelastic processes that do not account for the gradient of the rate of anelastic distortions in their constitutive framework.

C2. Starting from Equation (53a), it is possible to prove that, with the approach followed in this work, $\boldsymbol{L}^{(0)}_{\boldsymbol{K}\eta}$ is constant with respect to the fine variable $\tilde{Y}$, that is, it is such that $\text{Grad}_{\tilde{Y}}\boldsymbol{L}^{(0)}_{\boldsymbol{K}\eta}(\tilde{X},\tilde{Y},t) = \mathbb{0}_3$, where $\mathbb{0}_3$ represents the null tensor in the space of the third-order tensors,[3] for $\eta = 1,2$, for all $\tilde{Y} \in \tilde{\mathscr{Y}}_{\text{R}}$, and uniformly with respect to $\tilde{X}$ and time. A proof of this statement can be obtained by rephrasing the proof provided by Auriault [69] for the case of the homogenization of a temperature field in a biphasic medium, which we adapt to our framework as follows. Let us introduce the functional space

$$\mathscr{V} := \left\{\mathfrak{L} \in (H^1(\tilde{\mathscr{Y}}_{\text{R}}))^{3,3} : \mathfrak{L} \text{ is } \tilde{\mathscr{Y}}_{\text{R}}\text{-periodic, and with null integral over } \tilde{\mathscr{Y}}_{\text{R}}, \text{ that is, } \int_{\tilde{\mathscr{Y}}_{\text{R}}} \mathfrak{L}(\tilde{Y})\text{dV}(\tilde{Y}) = \mathbf{O}\right\}, \tag{54}$$

where $(H^1(\tilde{\mathscr{Y}}_{\text{R}}))^{3,3}$ is the Sobolev space of order one constituted by all the functions defined in $\tilde{\mathscr{Y}}_{\text{R}}$ and valued in the space of second-order tensors.[4] Let us then take a function $\mathfrak{L} \in \mathscr{V}$, and for each $\eta = 1,2$, let us construct the weak form associated with Equation (53a), that is,

$$-\int_{\partial\tilde{\mathscr{Y}}_{\text{R}\eta}} \mathfrak{L} : \left[\left(\frac{\ell_\eta^2}{L_0^2}\sigma_\eta\tau_\eta\text{Grad}_{\tilde{Y}}\boldsymbol{L}^{(0)}_{\boldsymbol{K}\eta}\right)\boldsymbol{N}_\eta\right] + \int_{\tilde{\mathscr{Y}}_{\text{R}\eta}} \left[\frac{\ell_\eta^2}{L_0^2}\sigma_\eta\tau_\eta\text{Grad}_{\tilde{Y}}\boldsymbol{L}^{(0)}_{\boldsymbol{K}\eta}\right] \vdots \text{Grad}_{\tilde{Y}}\mathfrak{L} = 0, \tag{55}$$

where $\boldsymbol{N}_\eta$ is the unit normal vector pointing towards the exterior of $\tilde{\mathscr{Y}}_{\text{R}\eta}$. Next, since the boundary $\partial\tilde{\mathscr{Y}}_{\text{R}\eta}$ can be written as $\partial\tilde{\mathscr{Y}}_{\text{R}\eta} = \tilde{\Gamma}_{\mathscr{Y}_{\text{R}}} \cup \left(\partial\tilde{\mathscr{Y}}_{\text{R}} \cap \partial\tilde{\mathscr{Y}}_{\text{R}\eta}\right)$, and since the intersection between $\tilde{\Gamma}_{\mathscr{Y}_{\text{R}}}$ and $\partial\tilde{\mathscr{Y}}_{\text{R}} \cap \partial\tilde{\mathscr{Y}}_{\text{R}\eta}$ has zero measure, Equation (55) becomes

$$-\int_{\tilde{\Gamma}_{\mathscr{Y}_{\text{R}}}} \mathfrak{L} : \left[\left(\frac{\ell_\eta^2}{L_0^2}\sigma_\eta\tau_\eta\text{Grad}_{\tilde{Y}}\boldsymbol{L}^{(0)}_{\boldsymbol{K}\eta}\right)\boldsymbol{N}_\eta\right] - \int_{\partial\tilde{\mathscr{Y}}_{\text{R}}\cap\partial\tilde{\mathscr{Y}}_{\text{R}\eta}} \mathfrak{L} : \left[\left(\frac{\ell_\eta^2}{L_0^2}\sigma_\eta\tau_\eta\text{Grad}_{\tilde{Y}}\boldsymbol{L}^{(0)}_{\boldsymbol{K}\eta}\right)\boldsymbol{N}_\eta\right]$$
$$+\int_{\tilde{\mathscr{Y}}_{\text{R}\eta}} \left[\frac{\ell_\eta^2}{L_0^2}\sigma_\eta\tau_\eta\text{Grad}_{\tilde{Y}}\boldsymbol{L}^{(0)}_{\boldsymbol{K}\eta}\right] \vdots \text{Grad}_{\tilde{Y}}\mathfrak{L} = 0. \tag{56}$$

[3]Here and in the sequel, we denote by $\mathbb{0}_d$ the null tensor in the space of the tensors of order $d \in \mathbb{N}$, $d \geq 3$.
[4]Note that, according to the theory of Sobolev's immersions (see, e.g., [126]), if $\mathfrak{L}$ belongs to a Sobolev space of at least exponent 2, its periodicity in the sense specified in Remark 3.1 and Equation (6) can be imposed without additional requests of regularity.

10991476, 2025, 1, Downloaded from https://onlinelibrary.wiley.com/doi/10.1002/nme.10367 by Politecnico Di Torino Sist. Bibl Del Polit Di Torino, Wiley Online Library on [12/02/2025]. See the Terms and Conditions (https://onlinelibrary.wiley.com/terms-and-conditions) on Wiley Online Library for rules of use; OA articles are governed by the applicable Creative Commons License

Thus, by summing Equation (56) over $\eta = 1, 2$, enforcing the no-jump condition (30d) on $\mathrm{DevSym}\mathbb{K}^{(-1)}_{\mathrm{dis}\eta}\boldsymbol{N}_\eta$ along with the constraints (42a) and (42b), and invoking the periodicity hypothesis on the cell boundary, we obtain

$$\sum_{\eta=1,2}\int_{\tilde{\mathscr{Y}}_{\mathrm{R}\eta}}\left[\frac{\ell_\eta^2}{L_0^2}\sigma_\eta\tau_\eta\mathrm{Grad}_{\tilde{Y}}\boldsymbol{L}^{(0)}_{\boldsymbol{K}\eta}\right]\vdots\,\mathrm{Grad}_{\tilde{Y}}\mathfrak{L} = 0. \tag{57}$$

Since the functional space $\mathscr{V}$ is a Hilbert space, Equation (57) defines a scalar product between $\boldsymbol{L}^{(0)}_{\boldsymbol{K}\eta}$ and $\mathfrak{L}$, weighted by the positive quantities $(\ell_\eta^2/L_0^2)\sigma_\eta\tau_\eta$, and since this scalar product has to vanish for any choice of $\mathfrak{L}\in\mathscr{V}$, then it must hold true that $\mathrm{Grad}_{\tilde{Y}}\boldsymbol{L}^{(0)}_{\boldsymbol{K}\eta} = \mathbb{0}_3$ almost everywhere in $\tilde{\mathscr{Y}}_{\mathrm{R}\eta}$. Hence, $\boldsymbol{L}^{(0)}_{\boldsymbol{K}\eta}$ must be almost everywhere constant with respect to $\tilde{Y}$ for each $\eta = 1, 2$, and because of the no-jump condition on $\boldsymbol{L}^{(0)}_{\boldsymbol{K}\eta}$ at the interface, it must also be independent of η. Therefore, for each $\eta = 1, 2$, we set $\boldsymbol{L}^{(0)}_{\boldsymbol{K}\eta}(\tilde{X},\tilde{Y},t)\equiv\boldsymbol{L}^{(0)}_{\boldsymbol{K}}(\tilde{X},t)$, and for the sake of simpler formalism, we will commit the light abuse of notation consisting in regarding $\boldsymbol{L}^{(0)}_{\boldsymbol{K}}$ either as a function of $(\tilde{X},t)$ or as a function of $(\tilde{X},\tilde{Y},t)$, depending on the context.

C3. We combine now the just obtained result with the hypothesis that the initial value of $\boldsymbol{K}^{(0)}_\eta(\tilde{X},\tilde{Y},t)$ is constant with respect to $\tilde{Y}$. This implies, indeed, that also $\boldsymbol{K}^{(0)}_\eta$ is constant with respect to $\tilde{Y}$, so that we can write $\boldsymbol{K}^{(0)}_\eta(\tilde{X},\tilde{Y},t)\equiv\boldsymbol{K}^{(0)}(\tilde{X},t)$. In addition, the same property is inherited by $\boldsymbol{E}^{(0)}_{\boldsymbol{K}\eta}(\tilde{X},\tilde{Y},t)$, which, thus, becomes $\boldsymbol{E}^{(0)}_{\boldsymbol{K}\eta}(\tilde{X},\tilde{Y},t)\equiv\boldsymbol{E}^{(0)}_{\boldsymbol{K}}(\tilde{X},t)$. Then, since the terms between braces in Equation (52a) can be recast in the form

$$\mathcal{C}^{(0)}_{\mathrm{R}\eta}\,\vdots\,\mathrm{Grad}_{\tilde{Y}}\boldsymbol{u}^{(0)}_\eta - \left(\mathrm{Grad}_{\tilde{Y}}\boldsymbol{u}^{(0)}_\eta\right)\left(\mathcal{C}^{(0)}_{\mathrm{R}\eta}\,\vdots\,\boldsymbol{E}^{(0)}_{\boldsymbol{K}}\right) = \left(\mathcal{C}^{(0)}_{\mathrm{R}\eta} - \boldsymbol{I}\underline{\otimes}\left(\mathcal{C}^{(0)}_{\mathrm{R}\eta}\,\vdots\,\boldsymbol{E}^{(0)}_{\boldsymbol{K}}\right)\right)\vdots\,\mathrm{Grad}_{\tilde{Y}}\boldsymbol{u}^{(0)}_\eta, \tag{58}$$

applying the same reasoning shown in conclusion C2 to Equation (52a) leads to the conclusion that also $\boldsymbol{u}^{(0)}_\eta$ is constant with respect to $\tilde{Y}$, that is, we can write $\boldsymbol{u}^{(0)}_\eta(\tilde{X},\tilde{Y},t)\equiv\boldsymbol{u}^{(0)}(\tilde{X},t)$. Note that from now on, we will commit for $\boldsymbol{u}^{(0)}$ the same abuse of notation that we have declared for $\boldsymbol{L}^{(0)}_{\boldsymbol{K}}$.

The right-hand side of Equation (58) is notationally "confortable" because of the compact expression given to the fourth-order tensor double contracted with $\mathrm{Grad}_{\tilde{Y}}\boldsymbol{u}^{(0)}_\eta$. However, whereas it can be shown that the elasticity tensor $\mathcal{C}^{(0)}_{\mathrm{R}\eta}$ is strongly elliptic [79] for all $\boldsymbol{K}^{(0)}_\eta$ (since its strong ellipticity is inherited from that of $\mathcal{C}_\eta$, here given for granted), it is difficult to establish a priori whether or not the rescaled elasticity tensor $\mathcal{C}^{(0)}_{\mathrm{R}\eta} - \boldsymbol{I}\underline{\otimes}\left(\mathcal{C}^{(0)}_{\mathrm{R}\eta}\,\vdots\,\boldsymbol{E}^{(0)}_{\boldsymbol{K}}\right)$ is strongly elliptic, with all the consequences that failing to meet this property may have. For this reason, we use the right-hand side of Equation (58) just for compacting the algebraic calculations and we will discuss the issue of strong ellipticity when necessary.

By putting together the results commented above, Equations (52a)–(52c) simplify to

$$\begin{aligned}&\text{Order } \varepsilon^{-1}:\\ &\frac{u_\mathrm{c}}{L_0^2}\mathrm{Div}_{\tilde{Y}}\left\{\left(\mathcal{C}^{(0)}_{\mathrm{R}\eta} - \boldsymbol{I}\underline{\otimes}\left(\mathcal{C}^{(0)}_{\mathrm{R}\eta}\,\vdots\,\boldsymbol{E}^{(0)}_{\boldsymbol{K}}\right)\right)\vdots\left(\mathrm{Grad}_{\tilde{X}}\boldsymbol{u}^{(0)} + \mathrm{Grad}_{\tilde{Y}}\boldsymbol{u}^{(1)}_\eta\right)\right\} = \boldsymbol{0},\end{aligned} \tag{59a}$$

$$\begin{aligned}&\text{Order } \varepsilon^{0}:\\ &\frac{u_\mathrm{c}}{L_0^2}\mathrm{Div}_{\tilde{X}}\left\{\left(\mathcal{C}^{(0)}_{\mathrm{R}\eta} - \boldsymbol{I}\underline{\otimes}\left(\mathcal{C}^{(0)}_{\mathrm{R}\eta}\,\vdots\,\boldsymbol{E}^{(0)}_{\boldsymbol{K}}\right)\right)\vdots\left(\mathrm{Grad}_{\tilde{X}}\boldsymbol{u}^{(0)} + \mathrm{Grad}_{\tilde{Y}}\boldsymbol{u}^{(1)}_\eta\right) - \frac{L_0}{u_\mathrm{c}}\mathcal{C}^{(0)}_{\mathrm{R}\eta}\,\vdots\,\boldsymbol{E}^{(0)}_{\boldsymbol{K}}\right\}\\ &+\frac{u_\mathrm{c}}{L_0^2}\mathrm{Div}_{\tilde{Y}}\left\{\left(\mathcal{C}^{(0)}_{\mathrm{R}\eta} - \boldsymbol{I}\underline{\otimes}\left(\mathcal{C}^{(0)}_{\mathrm{R}\eta}\,\vdots\,\boldsymbol{E}^{(0)}_{\boldsymbol{K}}\right)\right)\vdots\left(\mathrm{Grad}_{\tilde{X}}\boldsymbol{u}^{(1)}_\eta + \mathrm{Grad}_{\tilde{Y}}\boldsymbol{u}^{(2)}_\eta\right)\right\} = \boldsymbol{0},\end{aligned} \tag{59b}$$

while Equations (53a)–(53c) become

$$\begin{aligned}&\text{Order } \varepsilon^{-1}:\\ &\mathrm{DevSym}\left\{-\mathrm{Div}_{\tilde{Y}}\left[\frac{\ell_\eta^2}{L_0^2}\sigma_\eta\tau_\eta\left(\mathrm{Grad}_{\tilde{X}}\boldsymbol{L}^{(0)}_{\boldsymbol{K}} + \mathrm{Grad}_{\tilde{Y}}\boldsymbol{L}^{(1)}_{\boldsymbol{K}\eta}\right)\right]\right\} = \mathbf{O},\end{aligned} \tag{60a}$$

10991476, 2025, 1, Downloaded from https://onlinelibrary.wiley.com/doi/10.1002/nma.10367 by Politecnico Di Torino Sist. Bibl Del Polit Di Torino, Wiley Online Library on [12/02/2025]. See the Terms and Conditions (https://onlinelibrary.wiley.com/terms-and-conditions) on Wiley Online Library for rules of use; OA articles are governed by the applicable Creative Commons License

Order ε^0 :

$$\text{DevSym}\left\{\sigma_\eta\tau_\eta\boldsymbol{L}_{\boldsymbol{K}}^{(0)}-\boldsymbol{\Sigma}_{\eta\text{lin}}^{(0)}-\text{Div}_{\tilde{X}}\left[\frac{\ell_\eta^2}{L_0^2}\sigma_\eta\tau_\eta\left(\text{Grad}_{\tilde{X}}\boldsymbol{L}_{\boldsymbol{K}}^{(0)}+\text{Grad}_{\tilde{Y}}\boldsymbol{L}_{\boldsymbol{K}\eta}^{(1)}\right)\right]\right.$$
$$\left.-\text{Div}_{\tilde{Y}}\left[\frac{\ell_\eta^2}{L_0^2}\sigma_\eta\tau_\eta\left(\text{Grad}_{\tilde{X}}\boldsymbol{L}_{\boldsymbol{K}\eta}^{(1)}+\text{Grad}_{\tilde{Y}}\boldsymbol{L}_{\boldsymbol{K}\eta}^{(2)}\right)\right]\right\}=\boldsymbol{O}, \tag{60b}$$

where $\boldsymbol{\Sigma}_{\eta\text{lin}}^{(-1)}$ disappears from Equation (60a) because $\text{Grad}_{\tilde{Y}}\boldsymbol{u}_\eta^{(0)}(\tilde{X},\tilde{Y},t)\equiv\text{Grad}_{\tilde{Y}}\boldsymbol{u}^{(0)}(\tilde{X},t)\equiv\boldsymbol{O}$.

Before proceeding, we recall that according to the theory of AH, the fields $\boldsymbol{u}^{(0)}$ and $\boldsymbol{L}_{\boldsymbol{K}}^{(0)}$ are unknowns that will be determined by averaging Equations (59b) and (60b). To do this, it is necessary to solve Equations (59a) and (60a), which make it evident as the macroscale dynamics couple with the microscopic ones through the displacement gradients $\text{Grad}_{\tilde{Y}}\boldsymbol{u}_\eta^{(1)}$ and $\text{Grad}_{\tilde{X}}\boldsymbol{u}^{(0)}$, and through the rates of anelastic distortions $\boldsymbol{L}_{\boldsymbol{K}\eta}^{(1)}$ and $\boldsymbol{L}_{\boldsymbol{K}}^{(0)}$.

Remark 5.1 (Solvability condition and Fredholm alternative)**.** We remark that Equations (59a) and (60a) constitute the cell problems for $\boldsymbol{u}_\eta^{(1)}$ and $\boldsymbol{L}_{\boldsymbol{K}\eta}^{(1)}$, for $\eta=1,2$. By rewriting them as

$$\frac{u_\text{c}}{L_0^2}\text{Div}_{\tilde{Y}}\left\{\left(\mathcal{C}_{\text{R}\eta}^{(0)}-\boldsymbol{I}\underline{\otimes}\left(\mathcal{C}_{\text{R}\eta}^{(0)}:\boldsymbol{E}_{\boldsymbol{K}}^{(0)}\right)\right):\text{Grad}_{\tilde{Y}}\boldsymbol{u}_\eta^{(1)}\right\}=-\frac{u_\text{c}}{L_0^2}\text{Div}_{\tilde{Y}}\left\{\left(\mathcal{C}_{\text{R}\eta}^{(0)}-\boldsymbol{I}\underline{\otimes}\left(\mathcal{C}_{\text{R}\eta}^{(0)}:\boldsymbol{E}_{\boldsymbol{K}}^{(0)}\right)\right):\text{Grad}_{\tilde{X}}\boldsymbol{u}^{(0)}\right\}, \tag{61a}$$

$$\text{DevSym}\left\{-\text{Div}_{\tilde{Y}}\left[\frac{\ell_\eta^2}{L_0^2}\sigma_\eta\tau_\eta\text{Grad}_{\tilde{Y}}\boldsymbol{L}_{\boldsymbol{K}\eta}^{(1)}\right]\right\}=\text{DevSym}\left\{\text{Div}_{\tilde{Y}}\left[\frac{\ell_\eta^2}{L_0^2}\sigma_\eta\tau_\eta\text{Grad}_{\tilde{X}}\boldsymbol{L}_{\boldsymbol{K}}^{(0)}\right]\right\}, \tag{61b}$$

they are put in a form that is typical in homogenization theory. Quoting from [127], *"by the Fredholm alternative,"* Equations (61a) and (61b) have *"a solution if and only if"* their right-hand sides have zero integral over the unit cell. In [127], this condition is referred to as *"solvability condition"* since it guarantees the existence of solutions, but not their uniqueness. In fact, the right-hand sides of Equations (61a) and (61b) satisfy automatically the solvability condition for the cell problem since the arguments of the $\text{Div}_{\tilde{Y}}$ operator are constants with respect to $\tilde{Y}$. Therefore, our problems admit solution.

Pavliotis and Stuart [127] report this result in the context of AH for elliptic operators and under the assumption of $\tilde{Y}$-periodicity, that is, periodicity in the $\tilde{Y}$ variable, referred to as *"1-periodicity"* in [127]. Hence, if the rescaled elasticity tensor $\mathcal{C}_{\text{R}\eta}^{(0)}-\boldsymbol{I}\underline{\otimes}\left(\mathcal{C}_{\text{R}\eta}^{(0)}:\boldsymbol{E}_{\boldsymbol{K}}^{(0)}\right)$ is strongly elliptic (as is the case for the benchmark problem analyzed below), and since the coefficients σ_η and τ_η are positive for both constituents, the aforementioned existence criterion based on the solvability condition can be applied. The uniqueness of the solution is not granted at this stage because the solution is identified up to a constant with respect to $\tilde{Y}$. However, this issue will be removed by imposing further conditions, as discussed in the following.

6 | CELL PROBLEMS

This section is devoted to the solution of Equations (59a), (59b), (60a), and (60b). By adapting the theory of AH to our setting, and, in particular, by taking inspiration from the homogenization of diffusion problems [70], we enforce now the two following *Ansätze*. Since Equation (59a) is linear in $\text{Grad}_{\tilde{Y}}\boldsymbol{u}_\eta^{(1)}$, and Equation (60a) is linear with respect to $\boldsymbol{L}_{\boldsymbol{K}\eta}^{(1)}$, we enforce the tentative solutions

$$\boldsymbol{u}_\eta^{(1)}(\tilde{X},\tilde{Y},t)=\boldsymbol{\xi}_\eta(\tilde{X},\tilde{Y},t):\text{Grad}_{\tilde{X}}\boldsymbol{u}^{(0)}(\tilde{X},t)+\boldsymbol{\omega}_\eta(\tilde{X},\tilde{Y},t), \tag{62a}$$

$$\boldsymbol{L}_{\boldsymbol{K}\eta}^{(1)}(\tilde{X},\tilde{Y},t):=\boldsymbol{\Lambda}_\eta(\tilde{X},\tilde{Y},t)\vdots\text{Grad}_{\tilde{X}}\boldsymbol{L}_{\boldsymbol{K}}^{(0)}(\tilde{X},t), \tag{62b}$$

in which $\boldsymbol{\xi}_\eta$ is a third-order tensor field, $\boldsymbol{\omega}_\eta$ is a vector field [19], and $\boldsymbol{\Lambda}_\eta$ is a *fifth-order* tensor field. Note that each of these fields is locally periodic in the microscopic variable $\tilde{Y}$ and defined within the ηth constituent of the composite material under study. We also notice that, at variance with the *Ansatz* introduced for the displacement, in the *Ansatz* specifying the guessed functional form of $\boldsymbol{L}_{\boldsymbol{K}\eta}^{(1)}$, we do not add any further unknown second-order tensor field playing the role that

10991476, 2025, 1, Downloaded from https://onlinelibrary.wiley.com/doi/10.1002/nma.10367 by Politecnico Di Torino Sist. Bibl Del Polit Di Torino, Wiley Online Library on [12/02/2025]. See the Terms and Conditions (https://onlinelibrary.wiley.com/terms-and-conditions) on Wiley Online Library for rules of use; OA articles are governed by the applicable Creative Commons License

$\boldsymbol{\omega}_\eta$ plays in Equation (62a). However, $\boldsymbol{\Lambda}_\eta$ contains the topological and geometrical information about the ηth constituent of the reference cell $\tilde{\mathscr{Y}}_{\mathrm{R}\eta}$.

By substituting Equation (62a) into Equation (59a), and (62b) into (60a), we obtain the following system of equations in the auxiliary tensor variables $\boldsymbol{\xi}_\eta$, $\boldsymbol{\omega}_\eta$, and $\boldsymbol{\Lambda}_\eta$:

$$\begin{aligned}&\mathrm{Div}_{\tilde{Y}}\left\{\left(\boldsymbol{C}^{(0)}_{\mathrm{R}\eta}-\boldsymbol{I}\underline{\otimes}\left(\boldsymbol{C}^{(0)}_{\mathrm{R}\eta}:\boldsymbol{E}^{(0)}_{\boldsymbol{K}}\right)\right):\left(\mathrm{Grad}_{\tilde{X}}\boldsymbol{u}^{(0)}+\mathrm{Grad}_{\tilde{Y}}\boldsymbol{u}^{(1)}_\eta\right)\right\}\\&\equiv\mathrm{Div}_{\tilde{Y}}\left\{\left(\boldsymbol{C}^{(0)}_{\mathrm{R}\eta}-\boldsymbol{I}\underline{\otimes}\left(\boldsymbol{C}^{(0)}_{\mathrm{R}\eta}:\boldsymbol{E}^{(0)}_{\boldsymbol{K}}\right)\right):\left(\mathbb{I}_4+T\mathrm{Grad}_{\tilde{Y}}\boldsymbol{\xi}_\eta\right):\mathrm{Grad}_{\tilde{X}}\boldsymbol{u}^{(0)}+\left(\boldsymbol{C}^{(0)}_{\mathrm{R}\eta}-\boldsymbol{I}\underline{\otimes}\left(\boldsymbol{C}^{(0)}_{\mathrm{R}\eta}:\boldsymbol{E}^{(0)}_{\boldsymbol{K}}\right)\right):\mathrm{Grad}_{\tilde{Y}}\boldsymbol{\omega}_\eta\right\}=\boldsymbol{0},\end{aligned}\tag{63a}$$

$$\begin{aligned}&\mathrm{DevSym}\left\{-\mathrm{Div}_{\tilde{Y}}\left[\frac{\ell_\eta^2}{L_0^2}\sigma_\eta\tau_\eta\left(\mathrm{Grad}_{\tilde{X}}\boldsymbol{L}^{(0)}_{\boldsymbol{K}}+\mathrm{Grad}_{\tilde{Y}}\boldsymbol{L}^{(1)}_{\boldsymbol{K}\eta}\right)\right]\right\}\\&\equiv\mathrm{DevSym}\left\{-\mathrm{Div}_{\tilde{Y}}\left[\frac{\ell_\eta^2}{L_0^2}\sigma_\eta\tau_\eta\left(\mathbb{I}_6+T\mathrm{Grad}_{\tilde{Y}}\boldsymbol{\Lambda}_\eta\right)\vdots\mathrm{Grad}_{\tilde{X}}\boldsymbol{L}^{(0)}_{\boldsymbol{K}}\right]\right\}=\mathbf{O},\end{aligned}\tag{63b}$$

where we have introduced the symbols $\mathbb{I}_4$ and $\mathbb{I}_6$ to denote the fourth-order and the sixth-order identity tensor, respectively, and we have defined the quantities [19]

$$T\mathrm{Grad}_{\tilde{Y}}\boldsymbol{\xi}_\eta:=[T\mathrm{Grad}_{\tilde{Y}}\boldsymbol{\xi}_\eta]_{AB\boxed{CD}}\,\boldsymbol{\mathcal{E}}_A\otimes\boldsymbol{\mathcal{E}}_B\otimes\boxed{\boldsymbol{\mathcal{E}}_C\otimes\boldsymbol{\mathcal{E}}_D}=\frac{\partial[\boldsymbol{\xi}_\eta]_{A\boxed{CD}}}{\partial\tilde{Y}_B}\,\boldsymbol{\mathcal{E}}_A\otimes\boldsymbol{\mathcal{E}}_B\otimes\boxed{\boldsymbol{\mathcal{E}}_C\otimes\boldsymbol{\mathcal{E}}_D},\tag{64a}$$

$$\begin{aligned}T\mathrm{Grad}_{\tilde{Y}}\boldsymbol{\Lambda}_\eta&:=[T\mathrm{Grad}_{\tilde{Y}}\boldsymbol{\Lambda}_\eta]_{MNP\boxed{JK}}\,\boldsymbol{\mathcal{E}}_M\otimes\boldsymbol{\mathcal{E}}_N\otimes\boldsymbol{\mathcal{E}}_P\otimes\boxed{\boldsymbol{\mathcal{E}}_I\otimes\boldsymbol{\mathcal{E}}_J\otimes\boldsymbol{\mathcal{E}}_K}\\&=\frac{\partial[\boldsymbol{\Lambda}_\eta]_{MN\boxed{JK}}}{\partial\tilde{Y}_P}\,\boldsymbol{\mathcal{E}}_M\otimes\boldsymbol{\mathcal{E}}_N\otimes\boldsymbol{\mathcal{E}}_P\otimes\boxed{\boldsymbol{\mathcal{E}}_I\otimes\boldsymbol{\mathcal{E}}_J\otimes\boldsymbol{\mathcal{E}}_K},\end{aligned}\tag{64b}$$

with $\mathrm{Grad}_{\tilde{Y}}\boldsymbol{\xi}_\eta$ and $\mathrm{Grad}_{\tilde{Y}}\boldsymbol{\Lambda}_\eta$ being given by

$$\mathrm{Grad}_{\tilde{Y}}\boldsymbol{\xi}_\eta=[\mathrm{Grad}_{\tilde{Y}}\boldsymbol{\xi}_\eta]_{A\boxed{CD}B}\,\boldsymbol{\mathcal{E}}_A\otimes\boxed{\boldsymbol{\mathcal{E}}_C\otimes\boldsymbol{\mathcal{E}}_D}\otimes\boldsymbol{\mathcal{E}}_B=\frac{\partial[\boldsymbol{\xi}_\eta]_{A\boxed{CD}}}{\partial\tilde{Y}_B}\,\boldsymbol{\mathcal{E}}_A\otimes\boxed{\boldsymbol{\mathcal{E}}_C\otimes\boldsymbol{\mathcal{E}}_D}\otimes\boldsymbol{\mathcal{E}}_B,\tag{65a}$$

$$\begin{aligned}\mathrm{Grad}_{\tilde{Y}}\boldsymbol{\Lambda}_\eta&=[\mathrm{Grad}_{\tilde{Y}}\boldsymbol{\Lambda}_\eta]_{MN\boxed{JK}P}\,\boldsymbol{\mathcal{E}}_M\otimes\boldsymbol{\mathcal{E}}_N\otimes\boxed{\boldsymbol{\mathcal{E}}_I\otimes\boldsymbol{\mathcal{E}}_J\otimes\boldsymbol{\mathcal{E}}_K}\otimes\boldsymbol{\mathcal{E}}_P\\&=\frac{\partial[\boldsymbol{\Lambda}_\eta]_{MN\boxed{JK}}}{\partial\tilde{Y}_P}\,\boldsymbol{\mathcal{E}}_M\otimes\boldsymbol{\mathcal{E}}_N\otimes\boxed{\boldsymbol{\mathcal{E}}_I\otimes\boldsymbol{\mathcal{E}}_J\otimes\boldsymbol{\mathcal{E}}_K}\otimes\boldsymbol{\mathcal{E}}_P.\end{aligned}\tag{65b}$$

In Equations (64a)–(65b), the rectangles are used to highlight the components that are left untouched by the transposition operation.

Finally, we notice that Equation (63a) has been obtained by exploiting the symmetry of the second-order tensor $\boldsymbol{C}^{(0)}_{\mathrm{R}\eta}:\boldsymbol{E}^{(0)}_{\boldsymbol{K}}$, that is, $\boldsymbol{C}^{(0)}_{\mathrm{R}\eta}:\boldsymbol{E}^{(0)}_{\boldsymbol{K}}=\left(\boldsymbol{C}^{(0)}_{\mathrm{R}\eta}:\boldsymbol{E}^{(0)}_{\boldsymbol{K}}\right)^{\mathrm{T}}$, and the identity

$$\left(\mathrm{Grad}_{\tilde{X}}\boldsymbol{u}^{(0)}+\mathrm{Grad}_{\tilde{Y}}\boldsymbol{u}^{(1)}_\eta\right)\left(\boldsymbol{C}^{(0)}_{\mathrm{R}\eta}:\boldsymbol{E}^{(0)}_{\boldsymbol{K}}\right)\equiv\left[\boldsymbol{I}\underline{\otimes}\left(\boldsymbol{C}^{(0)}_{\mathrm{R}\eta}:\boldsymbol{E}^{(0)}_{\boldsymbol{K}}\right)\right]:\left(\mathrm{Grad}_{\tilde{X}}\boldsymbol{u}^{(0)}+\mathrm{Grad}_{\tilde{Y}}\boldsymbol{u}^{(1)}_\eta\right),\tag{66}$$

which, in index notation, reads

$$\begin{aligned}\left(\frac{\partial[\boldsymbol{u}^{(0)}]_A}{\partial\tilde{X}_D}+\frac{\partial\left[\boldsymbol{u}^{(1)}_\eta\right]_A}{\partial\tilde{Y}_D}\right)\left(\boldsymbol{C}^{(0)}_{\mathrm{R}\eta}:\boldsymbol{E}^{(0)}_{\boldsymbol{K}}\right)_{DB}&=\delta_{AC}\left(\boldsymbol{C}^{(0)}_{\mathrm{R}\eta}:\boldsymbol{E}^{(0)}_{\boldsymbol{K}}\right)_{BD}\left(\frac{\partial[\boldsymbol{u}^{(0)}]_C}{\partial\tilde{X}_D}+\frac{\partial\left[\boldsymbol{u}^{(1)}_\eta\right]_C}{\partial\tilde{Y}_D}\right)\\&=\left[\boldsymbol{I}\underline{\otimes}\left(\boldsymbol{C}^{(0)}_{\mathrm{R}\eta}:\boldsymbol{E}^{(0)}_{\boldsymbol{K}}\right)\right]_{ABCD}\left(\frac{\partial[\boldsymbol{u}^{(0)}]_C}{\partial\tilde{X}_D}+\frac{\partial\left[\boldsymbol{u}^{(1)}_\eta\right]_C}{\partial\tilde{Y}_D}\right).\end{aligned}\tag{67}$$

To clarify Equation (63b), we make the following Remark:

10991476, 2025, 1, Downloaded from https://onlinelibrary.wiley.com/doi/10.1002/nme.10367 by Politecnico Di Torino Sist. Bibl Del Polit Di Torino, Wiley Online Library on [12/02/2025]. See the Terms and Conditions (https://onlinelibrary.wiley.com/terms-and-conditions) on Wiley Online Library for rules of use; OA articles are governed by the applicable Creative Commons License

Remark 6.1 (DevSym-, Skew-, and Tr-operator applied to tensor fields of any order ≥ 2)**.** An equivalent formulation of Equation (63b) can be obtained by factorizing $\mathrm{Grad}_{\tilde{X}}\boldsymbol{L}_{\boldsymbol{K}}^{(0)}$ and exploiting the commutativity of the operators DevSym and $\mathrm{Div}_{\tilde{Y}}$. The latter property, in particular, holds true because DevSym operates only on the first pair of indices of any tensor field of order greater than, or equal to, 2 (this is due to the fact that in Equation (60a), which is the starting point of these considerations, the DevSym operator is applied to a second-order tensor field). In this respect, we recall that, for any given tensor $\mathbf{U}$ of order greater than, or equal to, 2, that is, $\mathbf{U} = \mathsf{U}_{AB\ldots}\mathcal{E}_A \otimes \mathcal{E}_B \otimes \ldots$, the expression $\mathrm{DevSym}\mathbf{U}$ means

$$[\mathrm{DevSym}\mathbf{U}]_{AB\ldots} := \left(\frac{\delta_{AM}\delta_{BN} + \delta_{AN}\delta_{BM}}{2} - \frac{1}{3}\delta_{AB}\delta_{MN}\right)[\mathbf{U}]_{MN\ldots} = \frac{\mathsf{U}_{AB\ldots} + \mathsf{U}_{BA\ldots}}{2} - \frac{1}{3}\delta_{AB}\mathsf{U}_{MM\ldots}, \tag{68}$$

where summation over $M = 1, 2, 3$ is understood in $\mathsf{U}_{MM\ldots}$. Moreover, to provide explicit expressions of $\mathrm{DevSym}\mathbb{I}_6$ and $\mathrm{DevSym}(T\mathrm{Grad}_{\tilde{Y}}\boldsymbol{\Lambda}_\eta)$, we work in index notation. In particular, the identity tensor $\mathbb{I}_6$ reads

$$[\mathbb{I}_6]_{ABCIJK} = \delta_{AI}\delta_{BJ}\delta_{CK}, \tag{69}$$

so that, for every third-order tensor $\boldsymbol{\beta} = \beta_{IJK}\mathcal{E}_I \otimes \mathcal{E}_J \otimes \mathcal{E}_K$, it applies that

$$[\mathbb{I}_6]_{ABCIJK}\beta_{IJK} = \delta_{AI}\delta_{BJ}\delta_{CK}\beta_{IJK} = \beta_{ABC}. \tag{70}$$

In addition, in this work, the Sym operator applied to a third-order tensor is defined in such a way that the resulting tensor is symmetric in its first two indices. To do this, it is necessary to define the symmetrization of a sixth-order tensor in its first two indices. To this end, in index notation, we write

$$[\mathrm{Sym}\mathbb{I}_6]_{ABCIJK} = \frac{\delta_{AI}\delta_{BJ} + \delta_{AJ}\delta_{BI}}{2}\delta_{CK} \;\Rightarrow\; [\mathrm{Sym}\mathbb{I}_6]_{ABCIJK}\beta_{IJK} = \frac{\beta_{ABC} + \beta_{BAC}}{2}. \tag{71}$$

On the same footing, in our work, $\mathrm{DevSym}\mathbb{I}_6$ is defined as

$$[\mathrm{DevSym}\mathbb{I}_6]_{ABCIJK} = \left[\frac{\delta_{AI}\delta_{BJ} + \delta_{AJ}\delta_{BI}}{2} - \frac{1}{3}\delta_{AB}\delta_{IJ}\right]\delta_{CK} \Rightarrow [\mathrm{DevSym}\mathbb{I}_6]_{ABCIJK}\beta_{IJK} = \frac{\beta_{ABC} + \beta_{BAC}}{2} - \frac{1}{3}\delta_{AB}\beta_{MMC}, \tag{72}$$

where summation over M is understood in β_{MMC}.

Analogously, since DevSym commutes also with $T\mathrm{Grad}_{\tilde{Y}}$ (the reason is the same as that for which it commutes with $\mathrm{Div}_{\tilde{Y}}$, as explained at the beginning of this remark), it holds that

$$\mathrm{DevSym}\left(T\mathrm{Grad}_{\tilde{Y}}\boldsymbol{\Lambda}_\eta\right) = T\mathrm{Grad}_{\tilde{Y}}\left(\mathrm{DevSym}\boldsymbol{\Lambda}_\eta\right), \tag{73}$$

where, in index notation, $\mathrm{DevSym}\boldsymbol{\Lambda}_\eta$ and $T\mathrm{Grad}_{\tilde{Y}}\left(\mathrm{DevSym}\boldsymbol{\Lambda}_\eta\right)$ read (cf. Equation (68))

$$[\mathrm{DevSym}\boldsymbol{\Lambda}_\eta]_{ABIJK} = \frac{[\boldsymbol{\Lambda}_\eta]_{ABIJK} + [\boldsymbol{\Lambda}_\eta]_{BAIJK}}{2} - \frac{1}{3}\delta_{AB}[\boldsymbol{\Lambda}_\eta]_{MMIJK}, \tag{74a}$$

$$\left[T\mathrm{Grad}_{\tilde{Y}}\left(\mathrm{DevSym}\boldsymbol{\Lambda}_\eta\right)\right]_{ABCIJK} = \frac{1}{2}\left(\frac{\partial[\boldsymbol{\Lambda}_\eta]_{ABIJK}}{\partial\tilde{Y}_C} + \frac{\partial[\boldsymbol{\Lambda}_\eta]_{BAIJK}}{\partial\tilde{Y}_C}\right) - \frac{1}{3}\delta_{AB}\frac{\partial[\boldsymbol{\Lambda}_\eta]_{MMIJK}}{\partial\tilde{Y}_C}. \tag{74b}$$

To complete the picture, we introduce also the definitions of the quantities $\mathrm{Skew}\boldsymbol{\Lambda}_\eta$ and $\mathrm{Tr}\boldsymbol{\Lambda}_\eta$, which are employed in the formulation of the cell problem that has to be solved for determining $\boldsymbol{\Lambda}_\eta$. In components, we define

$$[\mathrm{Skew}\boldsymbol{\Lambda}_\eta]_{ABIJK} := \frac{[\boldsymbol{\Lambda}_\eta]_{ABIJK} - [\boldsymbol{\Lambda}_\eta]_{BAIJK}}{2}, \tag{75a}$$

$$[\mathrm{Tr}\boldsymbol{\Lambda}_\eta]_{IJK} := [\boldsymbol{\Lambda}_\eta]_{AAIJK} \equiv \sum_{A=1}^{3}[\boldsymbol{\Lambda}_\eta]_{AAIJK}. \tag{75b}$$

10991476, 2025, 1, Downloaded from https://onlinelibrary.wiley.com/doi/10.1002/nme.10367 by Politecnico Di Torino Sist. Bibl Del Polit Di Torino, Wiley Online Library on [12/02/2025]. See the Terms and Conditions (https://onlinelibrary.wiley.com/terms-and-conditions) on Wiley Online Library for rules of use; OA articles are governed by the applicable Creative Commons License

We notice that $\mathrm{Tr}\boldsymbol{\Lambda}_\eta$ is obtained by contracting the first two indices of $\boldsymbol{\Lambda}_\eta$ and, thus, it is a third-order tensor field, rather than a scalar.

On the basis of the considerations above, Equation (63b) can be rewritten as

$$\mathrm{Grad}_{\tilde{X}}\boldsymbol{L}_{\boldsymbol{K}}^{(0)} \vdots \left\{ -\mathrm{Div}_{\tilde{Y}} \left[\frac{\ell_\eta^2}{L_0^2}\sigma_\eta\tau_\eta \left(\mathrm{DevSym}\mathbb{I}_6 + \mathrm{DevSym}(T\mathrm{Grad}_{\tilde{Y}}\boldsymbol{\Lambda}_\eta)\right)^{\mathrm{T}} \right] \right\} = \mathbf{O}, \tag{76}$$

where the DevSym operator is now applied to the first pair of indices of the sixth-order tensors $\mathbb{I}_6$ and $T\mathrm{Grad}_{\tilde{Y}}\boldsymbol{\Lambda}_\eta$, and the transpose $(\dots)^{\mathrm{T}}$ of the sixth-order tensor field in parentheses has to be understood as follows (in index notation)

$$[(\dots)^{\mathrm{T}}]_{IJKABC} = [\dots]_{ABCIJK}, \tag{77}$$

so that in components, Equation (76) reads

$$\begin{aligned} &- \left[\mathrm{Grad}_{\tilde{X}}\boldsymbol{L}_{\boldsymbol{K}}^{(0)}\right]_{IJK} \frac{\partial}{\partial\tilde{Y}_C} \left\{ \frac{\ell_\eta^2}{L_0^2}\sigma_\eta\tau_\eta \left[\frac{\delta_{IA}\delta_{JB}+\delta_{JA}\delta_{IB}}{2}\delta_{KC} - \frac{1}{3}\delta_{IJ}\delta_{KC}\delta_{AB} \right.\right. \\ &\left.\left. + \frac{\partial}{\partial\tilde{Y}_C}\left(\frac{[\boldsymbol{\Lambda}_\eta]_{ABIJK}+[\boldsymbol{\Lambda}_\eta]_{BAIJK}}{2} \right) - \frac{1}{3}\frac{\partial[\boldsymbol{\Lambda}_\eta]_{MMIJK}}{\partial\tilde{Y}_C}\delta_{AB} \right] \right\} = 0. \end{aligned} \tag{78}$$

6.1 | Cell problems

We notice that consistently with the general theory of AH (see, e.g., [37–41]), Equation (63a) can be split into one equation for $\boldsymbol{\xi}_\eta$ and one for $\boldsymbol{\omega}_\eta$ [19], which thus constitute a sufficient condition for the verification of Equation (63a), while Equation (63b) solves $\boldsymbol{\Lambda}_\eta$, so that the system (63a)–(63b) becomes

$$\mathrm{Div}_{\tilde{Y}} \left\{ \left(\mathcal{C}_{\mathrm{R}\eta}^{(0)} - \boldsymbol{I}\underline{\otimes}\left(\mathcal{C}_{\mathrm{R}\eta}^{(0)} : \boldsymbol{E}_{\boldsymbol{K}}^{(0)} \right) \right) : \left(\mathbb{I}_4 + T\mathrm{Grad}_{\tilde{Y}}\boldsymbol{\xi}_\eta \right) : \mathrm{Grad}_{\tilde{X}}\boldsymbol{u}^{(0)} \right\} = \mathbf{0}, \tag{79a}$$

$$\mathrm{Div}_{\tilde{Y}} \left\{ \left(\mathcal{C}_{\mathrm{R}\eta}^{(0)} - \boldsymbol{I}\underline{\otimes}\left(\mathcal{C}_{\mathrm{R}\eta}^{(0)} : \boldsymbol{E}_{\boldsymbol{K}}^{(0)} \right) \right) : \mathrm{Grad}_{\tilde{Y}}\boldsymbol{\omega}_\eta \right\} = \mathbf{0}, \tag{79b}$$

$$\mathrm{DevSym} \left\{ -\mathrm{Div}_{\tilde{Y}} \left[\frac{\ell_\eta^2}{L_0^2}\sigma_\eta\tau_\eta \left(\mathbb{I}_6 + T\mathrm{Grad}_{\tilde{Y}}\boldsymbol{\Lambda}_\eta \right) \vdots \mathrm{Grad}_{\tilde{X}}\boldsymbol{L}_{\boldsymbol{K}}^{(0)} \right] \right\} = \mathbf{O}. \tag{79c}$$

Each of these equations generates its own cell problem, which is defined by taking into account the boundary conditions at the interface $\tilde{\Gamma}_{\mathscr{Y}_{\mathrm{R}}}$ within the rescaled periodic cell $\tilde{\mathscr{Y}}_{\mathrm{R}}$. Such conditions, in fact, can be obtained by specializing Equations (30a)–(30d) to $\tilde{\mathscr{Y}}_{\mathrm{R}}$, and by performing the two-scale expansion of Equations (30a) and (30b) for the displacement fields $\boldsymbol{u}_1$ and $\boldsymbol{u}_2$, and of Equations (30c) and (30d) for the remodeling tensors $\boldsymbol{K}_1$ and $\boldsymbol{K}_2$. However, by virtue of the *Ansätze* (62a) and (62b), these expansions can be rephrased in terms of the auxiliary tensor fields $\boldsymbol{\xi}_\eta$, $\boldsymbol{\omega}_\eta$, and $\boldsymbol{\Lambda}_\eta$, with $\eta = 1, 2$. We notice that Equation (79a) is the form of the equation for the auxiliary third-order tensor field $\boldsymbol{\xi}_\eta$ prior to the factorization of $\mathrm{Grad}_{\tilde{X}}\boldsymbol{u}^{(0)}$. Usually, in homogenization theory, $\mathrm{Grad}_{\tilde{X}}\boldsymbol{u}^{(0)}$ is assumed to be arbitrary, and it is factorized out of Equation (79a), so that an equation corresponding to eq. (43a) of [19] is obtained. In the present work, however, we follow a different path since we consider a special case in which only few entries of $\mathrm{Grad}_{\tilde{X}}\boldsymbol{u}^{(0)}$ are non-null (see Remark 6.2 for detailed explanation on this issue).

6.1.1 | Interface conditions for the cell problems associated with each $\boldsymbol{u}_\eta$, $\eta = 1, 2$

By having recourse to the asymptotic expansion (31a) and to conclusion C3 in Section 5.2, the two-scale expansion of the interface condition (30a) reads

$$u_{\mathrm{c}} \left\{ \boldsymbol{u}^{(0)}(\tilde{X}, t) + \varepsilon\,\boldsymbol{u}_1^{(1)}(\tilde{X}, \tilde{Y}, t) \right\} + o(\varepsilon) = u_{\mathrm{c}} \left\{ \boldsymbol{u}^{(0)}(\tilde{X}, t) + \varepsilon\,\boldsymbol{u}_2^{(1)}(\tilde{X}, \tilde{Y}, t) \right\} + o(\varepsilon), \qquad u_{\mathrm{c}} > 0, \qquad \varepsilon \to 0, \text{on } \tilde{\Gamma}_{\mathscr{Y}_{\mathrm{R}}}. \tag{80}$$

10991476, 2025, 1, Downloaded from https://onlinelibrary.wiley.com/doi/10.1002/nma.10367 by Politecnico Di Torino Sist. Bibl Del Polit Di Torino, Wiley Online Library on [12/02/2025]. See the Terms and Conditions (https://onlinelibrary.wiley.com/terms-and-conditions) on Wiley Online Library for rules of use; OA articles are governed by the applicable Creative Commons License

Hence, by singling out the coefficients of ε^0 and ε^1, and noticing that, because of the discussion done at the end of Section 5.2, Equation (80) is automatically satisfied by $\boldsymbol{u}^{(0)}$, the no-jump condition on the interface $\tilde{\Gamma}_{\mathscr{Y}_{\mathrm{R}}}$ reduces to

$$\boldsymbol{u}_1^{(1)}(\tilde{X},\tilde{Y}_{\mathrm{b}},t)=\boldsymbol{u}_2^{(1)}(\tilde{X},\tilde{Y}_{\mathrm{b}},t), \qquad \text{for all } \tilde{Y}_{\mathrm{b}}\in\tilde{\Gamma}_{\mathscr{Y}_{\mathrm{R}}}, \tag{81}$$

and, on each side, it has to be understood as the limit of $\boldsymbol{u}_\eta^{(1)}(\tilde{X},\tilde{Y},t)$, with $\eta=1,2$, for $\tilde{Y}$ tending towards a given $\tilde{Y}_{\mathrm{b}}\in\tilde{\Gamma}_{\mathscr{Y}_{\mathrm{R}}}$. Moreover, since the *Ansatz* (62a) expresses $\boldsymbol{u}_\eta^{(1)}$ in terms of $\boldsymbol{\xi}_\eta$ and $\boldsymbol{\omega}_\eta$, Equation (81) becomes:

$$\boldsymbol{\xi}_1(\tilde{X},\tilde{Y}_{\mathrm{b}},t)\,:\,\mathrm{Grad}_{\tilde{X}}\boldsymbol{u}^{(0)}(\tilde{X},t)+\boldsymbol{\omega}_1(\tilde{X},\tilde{Y}_{\mathrm{b}},t)=\boldsymbol{\xi}_2(\tilde{X},\tilde{Y}_{\mathrm{b}},t)\,:\,\mathrm{Grad}_{\tilde{X}}\boldsymbol{u}^{(0)}(\tilde{X},t)+\boldsymbol{\omega}_2(\tilde{X},\tilde{Y}_{\mathrm{b}},t), \qquad \text{for all } \tilde{Y}_{\mathrm{b}}\in\tilde{\Gamma}_{\mathscr{Y}_{\mathrm{R}}}, \tag{82}$$

which can be split into one condition for $\boldsymbol{\xi}_\eta$ and one for $\boldsymbol{\omega}_\eta$, that is,

$$\boldsymbol{\xi}_1(\tilde{X},\tilde{Y}_{\mathrm{b}},t)\,:\,\mathrm{Grad}_{\tilde{X}}\boldsymbol{u}^{(0)}(\tilde{X},t)=\boldsymbol{\xi}_2(\tilde{X},\tilde{Y}_{\mathrm{b}},t)\,:\,\mathrm{Grad}_{\tilde{X}}\boldsymbol{u}^{(0)}(\tilde{X},t), \qquad \text{for all } \tilde{Y}_{\mathrm{b}}\in\tilde{\Gamma}_{\mathscr{Y}_{\mathrm{R}}}, \tag{83a}$$

$$\boldsymbol{\omega}_1(\tilde{X},\tilde{Y}_{\mathrm{b}},t)=\boldsymbol{\omega}_2(\tilde{X},\tilde{Y}_{\mathrm{b}},t), \qquad \text{for all } \tilde{Y}_{\mathrm{b}}\in\tilde{\Gamma}_{\mathscr{Y}_{\mathrm{R}}}. \tag{83b}$$

Within the two-scale, elasto-plastic framework delineated so far, Equation (30b) is studied for the linearized first Piola–Kirchhoff stress tensor $\boldsymbol{P}_{\eta\mathrm{lin}}$ given in Equation (43a), and it is thus rephrased as $\boldsymbol{P}_{1\mathrm{lin}}\boldsymbol{N}_{\tilde{\Gamma}_{\mathscr{Y}_{\mathrm{R}}}}=\boldsymbol{P}_{2\mathrm{lin}}\boldsymbol{N}_{\tilde{\Gamma}_{\mathscr{Y}_{\mathrm{R}}}}$, thereby approximating the no-jump condition on the contact forces exchanged by the constituents at the interface inside the periodic cell. Furthermore, by enforcing the two-scale expansion of $\boldsymbol{P}_{\eta\mathrm{lin}}$, the latter condition is rewritten as $\boldsymbol{P}^{\varepsilon}_{1\mathrm{lin}}\boldsymbol{N}_{\tilde{\Gamma}_{\mathscr{Y}_{\mathrm{R}}}}=\boldsymbol{P}^{\varepsilon}_{2\mathrm{lin}}\boldsymbol{N}_{\tilde{\Gamma}_{\mathscr{Y}_{\mathrm{R}}}}$. Now, we truncate this equality at the first order in ε, and we exploit Equation (49) for the expression of the asymptotic expansion of the displacement gradient. Then, by invoking the hypothesis Hp.2, along with the properties of $\boldsymbol{u}^{(0)}$ and $\boldsymbol{K}^{(0)}$ of being constant with respect to $\tilde{Y}$ and independent of η, we obtain

$$\boldsymbol{P}^{(0)}_{1\mathrm{lin}}\boldsymbol{N}_{\tilde{\Gamma}_{\mathscr{Y}_{\mathrm{R}}}}=\boldsymbol{P}^{(0)}_{2\mathrm{lin}}\boldsymbol{N}_{\tilde{\Gamma}_{\mathscr{Y}_{\mathrm{R}}}}, \qquad \text{on } \tilde{\Gamma}_{\mathscr{Y}_{\mathrm{R}}} \tag{84a}$$

$$\boldsymbol{P}^{(1)}_{1\mathrm{lin}}\boldsymbol{N}_{\tilde{\Gamma}_{\mathscr{Y}_{\mathrm{R}}}}=\boldsymbol{P}^{(1)}_{2\mathrm{lin}}\boldsymbol{N}_{\tilde{\Gamma}_{\mathscr{Y}_{\mathrm{R}}}}, \qquad \text{on } \tilde{\Gamma}_{\mathscr{Y}_{\mathrm{R}}}, \tag{84b}$$

where

$$\boldsymbol{P}^{(0)}_{\eta\mathrm{lin}}=\left(C^{(0)}_{\mathrm{R}\eta}-\boldsymbol{I}\underline{\otimes}\left(C^{(0)}_{\mathrm{R}\eta}:\boldsymbol{E}^{(0)}_{\boldsymbol{K}}\right)\right):\left(\mathrm{Grad}_{\tilde{X}}\boldsymbol{u}^{(0)}+\mathrm{Grad}_{\tilde{Y}}\boldsymbol{u}^{(1)}_\eta\right)-\frac{L_0}{u_{\mathrm{c}}}C^{(0)}_{\mathrm{R}\eta}:\boldsymbol{E}^{(0)}_{\boldsymbol{K}}, \tag{85a}$$

$$\boldsymbol{P}^{(1)}_{\eta\mathrm{lin}}=\left(C^{(0)}_{\mathrm{R}\eta}-\boldsymbol{I}\underline{\otimes}\left(C^{(0)}_{\mathrm{R}\eta}:\boldsymbol{E}^{(0)}_{\boldsymbol{K}}\right)\right):\left(\mathrm{Grad}_{\tilde{X}}\boldsymbol{u}^{(1)}_\eta+\mathrm{Grad}_{\tilde{Y}}\boldsymbol{u}^{(2)}_\eta\right). \tag{85b}$$

Note that only Equation (85a) is needed to formulate the cell problem for the displacement, whereas Equation (85b) will be used later, when the averaged momentum balance law is obtained. Hence, we start focusing on Equation (85a), and by substituting the *Ansatz* (62a) into Equation (85a), the interface condition (84a) splits into one condition for $\boldsymbol{\xi}_\eta$ and one for $\boldsymbol{\omega}_\eta$, that is,

$$\left[\!\left[\left(C^{(0)}_{\mathrm{R}\eta}-\boldsymbol{I}\underline{\otimes}\left(C^{(0)}_{\mathrm{R}\eta}:\boldsymbol{E}^{(0)}_{\boldsymbol{K}}\right)\right):\left(\mathbb{I}_4+T\mathrm{Grad}_{\tilde{Y}}\boldsymbol{\xi}_\eta\right):\mathrm{Grad}_{\tilde{X}}\boldsymbol{u}^{(0)}\right]\!\right]\boldsymbol{N}_{\tilde{\Gamma}_{\mathscr{Y}_{\mathrm{R}}}}=\boldsymbol{0}, \qquad \text{on } \tilde{\Gamma}_{\mathscr{Y}_{\mathrm{R}}}, \tag{86a}$$

$$\left[\!\left[\left(C^{(0)}_{\mathrm{R}\eta}-\boldsymbol{I}\underline{\otimes}\left(C^{(0)}_{\mathrm{R}\eta}:\boldsymbol{E}^{(0)}_{\boldsymbol{K}}\right)\right):\mathrm{Grad}_{\tilde{Y}}\boldsymbol{\omega}_\eta-\frac{L_0}{u_{\mathrm{c}}}\left(C^{(0)}_{\mathrm{R}\eta}:\boldsymbol{E}^{(0)}_{\boldsymbol{K}}\right)\right]\!\right]\boldsymbol{N}_{\tilde{\Gamma}_{\mathscr{Y}_{\mathrm{R}}}}=\boldsymbol{0}, \qquad \text{on } \tilde{\Gamma}_{\mathscr{Y}_{\mathrm{R}}}, \tag{86b}$$

where, for a generic field Φ_η, the brackets $[\![\Phi_\eta]\!]:=(\Phi_1-\Phi_2)|_{\tilde{\Gamma}_{\mathscr{Y}_{\mathrm{R}}}}$ indicate the jump of Φ_η across the interface.

By putting together the interface conditions (83a) and (86a) with Equation (79a), which, for each $\eta=1,2$, is defined in the interior points of $\tilde{\mathscr{Y}}_{\mathrm{R}\eta}$, and the conditions (83b) and (86b) with Equation (79b), which, again, is defined in the bulk of $\tilde{\mathscr{Y}}_{\mathrm{R}\eta}$, we obtain two independent cell problems for the fields $\boldsymbol{\xi}_\eta$ and $\boldsymbol{\omega}_\eta$, with $\eta=1,2$. The cell problem for $\boldsymbol{\xi}_\eta$ reads

$$\begin{cases}\mathrm{Div}_{\tilde{Y}}\left\{\left(C^{(0)}_{\mathrm{R}\eta}-\boldsymbol{I}\underline{\otimes}\left(C^{(0)}_{\mathrm{R}\eta}:\boldsymbol{E}^{(0)}_{\boldsymbol{K}}\right)\right):\left(\mathbb{I}_4+T\mathrm{Grad}_{\tilde{Y}}\boldsymbol{\xi}_\eta\right):\mathrm{Grad}_{\tilde{X}}\boldsymbol{u}^{(0)}\right\}=\boldsymbol{0}, & \text{in } \tilde{\mathscr{Y}}_{\mathrm{R}\eta},\\ [\![\boldsymbol{\xi}_\eta]\!]:\mathrm{Grad}_{\tilde{X}}\boldsymbol{u}^{(0)}=\boldsymbol{0}, & \text{on } \tilde{\Gamma}_{\mathscr{Y}_{\mathrm{R}}},\\ \left[\!\left[\left(C^{(0)}_{\mathrm{R}\eta}-\boldsymbol{I}\underline{\otimes}\left(C^{(0)}_{\mathrm{R}\eta}:\boldsymbol{E}^{(0)}_{\boldsymbol{K}}\right)\right):\left(\mathbb{I}_4+T\mathrm{Grad}_{\tilde{Y}}\boldsymbol{\xi}_\eta\right):\mathrm{Grad}_{\tilde{X}}\boldsymbol{u}^{(0)}\right]\!\right]\boldsymbol{N}_{\tilde{\Gamma}_{\mathscr{Y}_{\mathrm{R}}}}=\boldsymbol{0}, & \text{on } \tilde{\Gamma}_{\mathscr{Y}_{\mathrm{R}}}.\end{cases} \tag{87}$$

10991476, 2025, 1, Downloaded from https://onlinelibrary.wiley.com/doi/10.1002/nma.10367 by Politecnico Di Torino Sist. Bibl Del Polit Di Torino, Wiley Online Library on [12/02/2025]. See the Terms and Conditions (https://onlinelibrary.wiley.com/terms-and-conditions) on Wiley Online Library for rules of use; OA articles are governed by the applicable Creative Commons License

Analogously, the cell problem for $\boldsymbol{\omega}_\eta$ is given by

$$\begin{cases} \mathrm{Div}_{\tilde{Y}} \left\{ \left(\boldsymbol{C}^{(0)}_{\mathrm{R}\eta} - \boldsymbol{I} \underline{\otimes} (\boldsymbol{C}^{(0)}_{\mathrm{R}\eta} : \boldsymbol{E}^{(0)}_{\boldsymbol{K}}) \right) : \mathrm{Grad}_{\tilde{Y}} \boldsymbol{\omega}_\eta \right\} = \boldsymbol{0}, & \text{in } \tilde{\mathscr{Y}}_{\mathrm{R}\eta}, \\ [\![\boldsymbol{\omega}_\eta]\!] = \boldsymbol{0}, & \text{on } \tilde{\Gamma}_{\mathscr{Y}_{\mathrm{R}}}, \\ \left[\!\!\left[\left(\boldsymbol{C}^{(0)}_{\mathrm{R}\eta} - \boldsymbol{I} \underline{\otimes} (\boldsymbol{C}^{(0)}_{\mathrm{R}\eta} : \boldsymbol{E}^{(0)}_{\boldsymbol{K}}) \right) : \mathrm{Grad}_{\tilde{Y}} \boldsymbol{\omega}_\eta - \frac{L_0}{u_c} \left(\boldsymbol{C}^{(0)}_{\mathrm{R}\eta} : \boldsymbol{E}^{(0)}_{\boldsymbol{K}} \right) \right]\!\!\right] \boldsymbol{N}_{\tilde{\Gamma}_{\mathscr{Y}_{\mathrm{R}}}} = \boldsymbol{0}, & \text{on } \tilde{\Gamma}_{\mathscr{Y}_{\mathrm{R}}}. \end{cases} \tag{88}$$

By following the argument highlighted in Remark 5.1, and assuming the rescaled elasticity tensor to be strongly elliptic, we conclude that both cell problems (87) and (88) satisfy the solvability condition and, thus, admit a solution.

Remark 6.2 (Equivalent formulation of the cell problem for $\boldsymbol{\xi}_\eta$)**.** The first and the last equation of the cell problem for $\boldsymbol{\xi}_\eta$ are often written in a form that differs from the one presented in Equation (87) and that is obtained by factorizing $\mathrm{Grad}_{\tilde{X}} \boldsymbol{u}^{(0)}$, and requiring the vanishing of the expression multiplying $\mathrm{Grad}_{\tilde{X}} \boldsymbol{u}^{(0)}$, provided that $\mathrm{Grad}_{\tilde{X}} \boldsymbol{u}^{(0)}$ is regarded as arbitrary. If, in addition, the parentheses double contracted with the sum $\mathbb{I}_4 + T\mathrm{Grad}_{\tilde{Y}} \boldsymbol{\xi}_\eta$ are unfolded, we obtain (for each $\eta = 1, 2$)

$$\begin{cases} \mathrm{Div}_{\tilde{Y}} \left\{ \boldsymbol{C}^{(0)}_{\mathrm{R}\eta} : T\mathrm{Grad}_{\tilde{Y}} \boldsymbol{\xi}_\eta - T \left(\mathrm{Grad}_{\tilde{Y}} \boldsymbol{\xi}_\eta \left(\boldsymbol{C}^{(0)}_{\mathrm{R}\eta} : \boldsymbol{E}^{(0)}_{\boldsymbol{K}} \right) \right) \right\} = -\mathrm{Div}_{\tilde{Y}} \left[\boldsymbol{C}^{(0)}_{\mathrm{R}\eta} - \boldsymbol{I} \underline{\otimes} \left(\boldsymbol{C}^{(0)}_{\mathrm{R}\eta} : \boldsymbol{E}^{(0)}_{\boldsymbol{K}} \right) \right], & \text{in } \tilde{\mathscr{Y}}_{\mathrm{R}\eta}, \\ [\![\boldsymbol{\xi}_\eta]\!] = \mathbb{0}_3, & \text{on } \tilde{\Gamma}_{\mathscr{Y}_{\mathrm{R}}}, \\ \left[\!\!\left[\left\{ \boldsymbol{C}^{(0)}_{\mathrm{R}\eta} : T\mathrm{Grad}_{\tilde{Y}} \boldsymbol{\xi}_\eta - T \left(\mathrm{Grad}_{\tilde{Y}} \boldsymbol{\xi}_\eta \left(\boldsymbol{C}^{(0)}_{\mathrm{R}\eta} : \boldsymbol{E}^{(0)}_{\boldsymbol{K}} \right) \right) + \boldsymbol{C}^{(0)}_{\mathrm{R}\eta} - \boldsymbol{I} \underline{\otimes} \left(\boldsymbol{C}^{(0)}_{\mathrm{R}\eta} : \boldsymbol{E}^{(0)}_{\boldsymbol{K}} \right) \right\} \right]\!\!\right] \boldsymbol{N}_{\tilde{\Gamma}_{\mathscr{Y}_{\mathrm{R}}}} = \mathbb{0}_3, & \text{on } \tilde{\Gamma}_{\mathscr{Y}_{\mathrm{R}}}, \end{cases} \tag{89}$$

where the term $T \left(\mathrm{Grad}_{\tilde{Y}} \boldsymbol{\xi}_\eta \left(\boldsymbol{C}^{(0)}_{\mathrm{R}\eta} : \boldsymbol{E}^{(0)}_{\boldsymbol{K}} \right) \right)$ featuring in the first and third equation of the system (89) is defined by

$$\begin{aligned} T \left(\mathrm{Grad}_{\tilde{Y}} \boldsymbol{\xi}_\eta \left(\boldsymbol{C}^{(0)}_{\mathrm{R}\eta} : \boldsymbol{E}^{(0)}_{\boldsymbol{K}} \right) \right) &= \left[T \left(\mathrm{Grad}_{\tilde{Y}} \boldsymbol{\xi}_\eta \left(\boldsymbol{C}^{(0)}_{\mathrm{R}\eta} : \boldsymbol{E}^{(0)}_{\boldsymbol{K}} \right) \right) \right]_{ABPQ} \mathcal{E}_A \otimes \mathcal{E}_B \otimes \mathcal{E}_P \otimes \mathcal{E}_Q \\ &= \left[\mathrm{Grad}_{\tilde{Y}} \boldsymbol{\xi}_\eta \left(\boldsymbol{C}^{(0)}_{\mathrm{R}\eta} : \boldsymbol{E}^{(0)}_{\boldsymbol{K}} \right) \right]_{APQB} \mathcal{E}_A \otimes \mathcal{E}_B \otimes \mathcal{E}_P \otimes \mathcal{E}_Q, \end{aligned} \tag{90}$$

and the symbol $\mathbb{0}_3$ is the third-order null tensor. It is worth remarking that in the first equation of the system (89), the divergence operator $\mathrm{Div}_{\tilde{Y}}$ contracts with the second index of the fourth-order tensors to which it is applied, and the normal unit vector $\boldsymbol{N}_{\tilde{\Gamma}_{\mathscr{Y}_{\mathrm{R}}}}$ in the third equation behaves accordingly.

The form (89) of the cell problem for $\boldsymbol{\xi}_\eta$ requires, for each $\eta = 1, 2$, the determination of the 27 functions that represent the components of the third-order tensor field $\boldsymbol{\xi}_\eta$. However, apart from possible material symmetries that simplify the elasticity tensor $\boldsymbol{C}^{(0)}_{\mathrm{R}\eta}$, a strong reduction occurs when the macroscale boundary-value problem imposes particularly simple boundary conditions on the macroscopic displacement field $\boldsymbol{u}^{(0)}$. Indeed, such conditions allow to infer a priori how $\boldsymbol{u}^{(0)}$ depends on the macroscopic spatial variable $\tilde{X}$ and, from this information, which components of $\mathrm{Grad}_{\tilde{X}} \boldsymbol{u}^{(0)}$ are null. This way, indeed, only the coefficients of the nonzero components of $\mathrm{Grad}_{\tilde{X}} \boldsymbol{u}^{(0)}$ remain in Equation (87). We will take advantage from these simplifications in the next sections.

Another remark pertains to the property of $\boldsymbol{K}^{(0)}$ and, thus, of $\boldsymbol{E}^{(0)}_{\boldsymbol{K}}$, of being constant with $\tilde{Y}$, and to the specific assumption that the elastic coefficients of each constituent of the composite material under study are independent of the microscopic variable $\tilde{Y}$ (although they jump considerably when switching from one constituent to the other). These facts, indeed, allow to conclude that the right-hand side of the first equation of the cell problem (89) is null. Hence, the cell problem for $\boldsymbol{\xi}_\eta$ becomes

$$\begin{cases} \mathrm{Div}_{\tilde{Y}} \left\{ \boldsymbol{C}^{(0)}_{\mathrm{R}\eta} : T\mathrm{Grad}_{\tilde{Y}} \boldsymbol{\xi}_\eta - T \left(\mathrm{Grad}_{\tilde{Y}} \boldsymbol{\xi}_\eta \left(\boldsymbol{C}^{(0)}_{\mathrm{R}\eta} : \boldsymbol{E}^{(0)}_{\boldsymbol{K}} \right) \right) \right\} = \mathbb{0}_3, & \text{in } \tilde{\mathscr{Y}}_{\mathrm{R}\eta}, \\ [\![\boldsymbol{\xi}_\eta]\!] = \mathbb{0}_3, & \text{on } \tilde{\Gamma}_{\mathscr{Y}_{\mathrm{R}}}, \\ \left[\!\!\left[\boldsymbol{C}^{(0)}_{\mathrm{R}\eta} : T\mathrm{Grad}_{\tilde{Y}} \boldsymbol{\xi}_\eta - T \left(\mathrm{Grad}_{\tilde{Y}} \boldsymbol{\xi}_\eta \left(\boldsymbol{C}^{(0)}_{\mathrm{R}\eta} : \boldsymbol{E}^{(0)}_{\boldsymbol{K}} \right) \right) + \boldsymbol{C}^{(0)}_{\mathrm{R}\eta} - \boldsymbol{I} \underline{\otimes} \left(\boldsymbol{C}^{(0)}_{\mathrm{R}\eta} : \boldsymbol{E}^{(0)}_{\boldsymbol{K}} \right) \right]\!\!\right] \boldsymbol{N}_{\tilde{\Gamma}_{\mathscr{Y}_{\mathrm{R}}}} = \mathbb{0}_3, & \text{on } \tilde{\Gamma}_{\mathscr{Y}_{\mathrm{R}}}. \end{cases} \tag{91}$$

10991476, 2025, 1, Downloaded from https://onlinelibrary.wiley.com/doi/10.1002/nma.10367 by Politecnico Di Torino Sist. Bibl Del Polit Di Torino, Wiley Online Library on [12/02/2025]. See the Terms and Conditions (https://onlinelibrary.wiley.com/terms-and-conditions) on Wiley Online Library for rules of use; OA articles are governed by the applicable Creative Commons License

Thus, in a sense, with respect to the "classical" problems of AH [40, 70], in which no remodeling is considered, but the microscale variability of the elastic coefficients serves as a forcing term for $\boldsymbol{\xi}_\eta$ and $\boldsymbol{\omega}_\eta$, the attention of our study is shifted towards the role played by the remodeling distortions on $\boldsymbol{\xi}_\eta$ and $\boldsymbol{\omega}_\eta$, for $\eta = 1, 2$, and, at the macroscale, on the displacement field $\boldsymbol{u}^{(0)}$ through the identification of the so-called effective elastic coefficients [70].

A last consideration is about the role of the remodeling distortions, which is twofold. Indeed, it manifests itself: (i) in the definition of $\mathcal{C}^{(0)}_{\mathrm{R}\eta}$ as the algebraic pull-back, through the tensor map $\boldsymbol{K}^{(0)}$, of the elasticity tensor $\mathcal{C}_\eta$ associated with the natural state of the ηth constituent of the composite material under study (see Equation (50a)); (ii) in the definition of the "rescaled" elasticity tensor $\mathcal{C}^{(0)}_{\mathrm{R}\eta} - \boldsymbol{I} \underline{\otimes} \left(\mathcal{C}^{(0)}_{\mathrm{R}\eta} : \boldsymbol{E}^{(0)}_{\boldsymbol{K}} \right)$, which has been introduced with the linearization of the first Piola–Kirchhoff stress tensor, and appears in the system (91) by reassembling the terms under divergence on the left-hand side of the first equation. Note, in this respect, that in our work, which relies on the hypotheses of isotropic constituents and isochoric remodeling distortions, the rescaled elasticity tensor is in general nonsingular also for $\boldsymbol{E}^{(0)}_{\boldsymbol{K}} \neq \boldsymbol{O}$. Accordingly, it can be shown that the problems (88) and (91) can be viewed as generalized, microscopic Cauchy–Navier equations for the fields $\boldsymbol{\xi}_\eta$ and $\boldsymbol{\omega}_\eta$ in the "fast" variable $\tilde{Y}$.

6.1.2 | Interface conditions and kinematic constraints for the cell problem associated with $\boldsymbol{K}_\eta$

We focus now on the ε^{-1}-order of the flow rule given in Equation (60a) (and rewritten in Equation (79c)), and on the interface conditions (30c) and (30d), which are to be stated for the asymptotic expansions $\boldsymbol{L}^{\varepsilon}_{\boldsymbol{K}\eta}$ and $\mathbb{K}^{\varepsilon}_{\mathrm{dis}\eta}$, and have to be specialized to the interface $\tilde{\Gamma}_{\mathscr{Y}_{\mathrm{R}}}$ contained in the periodic cell. For this purpose, following a reasoning analogous to the one reported in section 6.1.1, we start with the no-jump condition on $\boldsymbol{L}^{\varepsilon}_{\boldsymbol{K}\eta} = \boldsymbol{L}^{(0)}_{\boldsymbol{K}} + \varepsilon \boldsymbol{L}^{(1)}_{\boldsymbol{K}\eta} + o(\varepsilon)$, for $\varepsilon \to 0$, and $\eta = 1, 2$. Then, by recalling that $\boldsymbol{L}^{(0)}_{\boldsymbol{K}}$ is constant with respect to $\tilde{Y}$, and enforcing the *Ansatz* (62b), we obtain

$$\begin{aligned} &\boldsymbol{L}^{(0)}_{\boldsymbol{K}}(\tilde{X}, t) + \varepsilon \boldsymbol{L}^{(1)}_{\boldsymbol{K}1}(\tilde{X}, \tilde{Y}, t) + o(\varepsilon) = \boldsymbol{L}^{(0)}_{\boldsymbol{K}}(\tilde{X}, t) + \varepsilon \boldsymbol{L}^{(1)}_{\boldsymbol{K}2}(\tilde{X}, \tilde{Y}, t) + o(\varepsilon), \ \varepsilon \to 0, \qquad \text{on } \tilde{\Gamma}_{\mathscr{Y}_{\mathrm{R}}} \\ &\Rightarrow \quad \boldsymbol{L}^{(1)}_{\boldsymbol{K}1}(\tilde{X}, \tilde{Y}, t) = \boldsymbol{L}^{(1)}_{\boldsymbol{K}2}(\tilde{X}, \tilde{Y}, t) \quad \Rightarrow \quad [\![\boldsymbol{\Lambda}_\eta(\tilde{X}, \tilde{Y}, t)]\!] \vdots \mathrm{Grad}_{\tilde{X}} \boldsymbol{L}^{(0)}_{\boldsymbol{K}}(\tilde{X}, t) = \boldsymbol{O}, \qquad \text{on } \tilde{\Gamma}_{\mathscr{Y}_{\mathrm{R}}}. \end{aligned} \tag{92}$$

Moreover, the no-jump condition on $\tilde{\Gamma}_{\mathscr{Y}_{\mathrm{R}}}$ applied to the third-order generalized stress tensor $\mathrm{DevSym}\mathbb{K}^{\varepsilon}_{\mathrm{dis}\eta}$, being automatically satisfied by $\mathbb{K}^{(-1)}_{\mathrm{dis}\eta}$, yields

$$\left(\mathrm{DevSym}\mathbb{K}^{(0)}_{\mathrm{dis}1} \right) \boldsymbol{N}_{\tilde{\Gamma}_{\mathscr{Y}_{\mathrm{R}}}} = \left(\mathrm{DevSym}\mathbb{K}^{(0)}_{\mathrm{dis}2} \right) \boldsymbol{N}_{\tilde{\Gamma}_{\mathscr{Y}_{\mathrm{R}}}}, \qquad \text{on } \tilde{\Gamma}_{\mathscr{Y}_{\mathrm{R}}}, \tag{93a}$$

$$\left(\mathrm{DevSym}\mathbb{K}^{(1)}_{\mathrm{dis}1} \right) \boldsymbol{N}_{\tilde{\Gamma}_{\mathscr{Y}_{\mathrm{R}}}} = \left(\mathrm{DevSym}\mathbb{K}^{(1)}_{\mathrm{dis}2} \right) \boldsymbol{N}_{\tilde{\Gamma}_{\mathscr{Y}_{\mathrm{R}}}}, \qquad \text{on } \tilde{\Gamma}_{\mathscr{Y}_{\mathrm{R}}}, \tag{93b}$$

with

$$\mathbb{K}^{(0)}_{\mathrm{dis}\eta} := \frac{\ell_\eta^2}{L_0} \sigma_\eta \tau_\eta \left(\mathrm{Grad}_{\tilde{X}} \boldsymbol{L}^{(0)}_{\boldsymbol{K}} + \mathrm{Grad}_{\tilde{Y}} \boldsymbol{L}^{(1)}_{\boldsymbol{K}\eta} \right), \tag{94a}$$

$$\mathbb{K}^{(1)}_{\mathrm{dis}\eta} := \frac{\ell_\eta^2}{L_0} \sigma_\eta \tau_\eta \left(\mathrm{Grad}_{\tilde{X}} \boldsymbol{L}^{(1)}_{\boldsymbol{K}\eta} + \mathrm{Grad}_{\tilde{Y}} \boldsymbol{L}^{(2)}_{\boldsymbol{K}\eta} \right). \tag{94b}$$

Equations (93a) and (93b), in turn, lead to the following conditions on the gradients of the remodeling tensor:

$$\begin{aligned} &\left[\!\!\left[\frac{\ell_\eta^2}{L_0} \sigma_\eta \tau_\eta \mathrm{DevSym} \left(\mathrm{Grad}_{\tilde{X}} \boldsymbol{L}^{(0)}_{\boldsymbol{K}} + \mathrm{Grad}_{\tilde{Y}} \boldsymbol{L}^{(1)}_{\boldsymbol{K}\eta} \right) \right]\!\!\right] \boldsymbol{N}_{\tilde{\Gamma}_{\mathscr{Y}_{\mathrm{R}}}} = \boldsymbol{O} \\ &\Rightarrow \ \left\{ \left[\!\!\left[\frac{\ell_\eta^2}{L_0} \sigma_\eta \tau_\eta \mathrm{DevSym} \left(\mathbb{I}_6 + T \mathrm{Grad}_{\tilde{Y}} \boldsymbol{\Lambda}_\eta \right) \right]\!\!\right] \vdots \mathrm{Grad}_{\tilde{X}} \boldsymbol{L}^{(0)}_{\boldsymbol{K}} \right\} \boldsymbol{N}_{\tilde{\Gamma}_{\mathscr{Y}_{\mathrm{R}}}} = \boldsymbol{O}, \qquad \text{on } \tilde{\Gamma}_{\mathscr{Y}_{\mathrm{R}}}, \end{aligned} \tag{95a}$$

$$\left[\!\!\left[\frac{\ell_\eta^2}{L_0} \sigma_\eta \tau_\eta \mathrm{DevSym} \left(\mathrm{Grad}_{\tilde{X}} \boldsymbol{L}^{(1)}_{\boldsymbol{K}\eta} + \mathrm{Grad}_{\tilde{Y}} \boldsymbol{L}^{(2)}_{\boldsymbol{K}\eta} \right) \right]\!\!\right] \boldsymbol{N}_{\tilde{\Gamma}_{\mathscr{Y}_{\mathrm{R}}}} = \boldsymbol{O}, \qquad \text{on } \tilde{\Gamma}_{\mathscr{Y}_{\mathrm{R}}}, \tag{95b}$$

where the term between the braces in Equation (95a) is a third-order tensor field that, applied to $\boldsymbol{N}_{\tilde{\Gamma}_{\mathscr{Y}_{\mathrm{R}}}}$, returns a tensor field of the second order.

10991476, 2025, 1, Downloaded from https://onlinelibrary.wiley.com/doi/10.1002/nma.10367 by Politecnico Di Torino Sist. Bibl Del Polit Di Torino, Wiley Online Library on [12/02/2025]. See the Terms and Conditions (https://onlinelibrary.wiley.com/terms-and-conditions) on Wiley Online Library for rules of use; OA articles are governed by the applicable Creative Commons License

To complete the formulation of the cell problem for $\boldsymbol{L}^{(1)}_{\boldsymbol{K}\eta}$, and express it in terms of the fifth-order tensor field $\boldsymbol{\Lambda}_\eta$, it is necessary to rewrite the constraints (42a) and (42b) by enforcing the *Ansatz* (62b), that is,

$$\mathrm{tr}\boldsymbol{L}^{(1)}_{\boldsymbol{K}\eta} = \mathrm{tr}\left(\boldsymbol{\Lambda}_\eta \vdots \mathrm{Grad}_{\tilde{X}}\boldsymbol{L}^{(0)}_{\boldsymbol{K}}\right) = \mathrm{Tr}\boldsymbol{\Lambda}_\eta \vdots \mathrm{Grad}_{\tilde{X}}\boldsymbol{L}^{(0)}_{\boldsymbol{K}} = 0, \tag{96a}$$

$$\mathrm{Skew}\boldsymbol{L}^{(1)}_{\boldsymbol{K}\eta} = \mathrm{Skew}\left(\boldsymbol{\Lambda}_\eta \vdots \mathrm{Grad}_{\tilde{X}}\boldsymbol{L}^{(0)}_{\boldsymbol{K}}\right) = \mathrm{Skew}\boldsymbol{\Lambda}_\eta \vdots \mathrm{Grad}_{\tilde{X}}\boldsymbol{L}^{(0)}_{\boldsymbol{K}} = \boldsymbol{O}. \tag{96b}$$

We can now formulate the cell problem for $\boldsymbol{L}^{(1)}_{\boldsymbol{K}\eta}$ in terms of the fifth-order tensor field $\boldsymbol{\Lambda}_\eta$ by taking into account Equation (79c), the interface conditions (92) and (95a), and the constraints, that is,

$$\begin{cases} \mathrm{Grad}_{\tilde{X}}\boldsymbol{L}^{(0)}_{\boldsymbol{K}} \vdots \left\{-\mathrm{Div}_{\tilde{Y}}\left[\frac{\ell_\eta^2}{L_0^2}\sigma_\eta\tau_\eta\left(\mathrm{DevSym}\mathbb{I}_6 + \mathrm{DevSym}(T\mathrm{Grad}_{\tilde{Y}}\boldsymbol{\Lambda}_\eta)\right)^{\mathrm{T}}\right]\right\} = \boldsymbol{O}, & \text{in } \tilde{\mathscr{Y}}_{\mathrm{R}\eta}, \\ [\![\boldsymbol{\Lambda}_\eta]\!] \vdots \mathrm{Grad}_{\tilde{X}}\boldsymbol{L}^{(0)}_{\boldsymbol{K}} = \boldsymbol{O}, & \text{on } \tilde{\Gamma}_{\mathscr{Y}_{\mathrm{R}}}, \\ \left\{\left[\!\left[\frac{\ell_\eta^2}{L_0}\sigma_\eta\tau_\eta\mathrm{DevSym}\left(\mathbb{I}_6 + T\mathrm{Grad}_{\tilde{Y}}\boldsymbol{\Lambda}_\eta\right)\right]\!\right] \vdots \mathrm{Grad}_{\tilde{X}}\boldsymbol{L}^{(0)}_{\boldsymbol{K}}\right\}\boldsymbol{N}_{\tilde{\Gamma}_{\mathscr{Y}_{\mathrm{R}}}} = \boldsymbol{O}, & \text{on } \tilde{\Gamma}_{\mathscr{Y}_{\mathrm{R}}}, \\ \mathrm{Tr}\boldsymbol{\Lambda}_\eta \vdots \mathrm{Grad}_{\tilde{X}}\boldsymbol{L}^{(0)}_{\boldsymbol{K}} = 0, & \text{in } \tilde{\mathscr{Y}}_{\mathrm{R}\eta}, \\ \mathrm{Skew}\boldsymbol{\Lambda}_\eta \vdots \mathrm{Grad}_{\tilde{X}}\boldsymbol{L}^{(0)}_{\boldsymbol{K}} = \boldsymbol{O}, & \text{in } \tilde{\mathscr{Y}}_{\mathrm{R}\eta}. \end{cases} \tag{97}$$

We notice that since the term $\mathrm{DevSym}\mathbb{I}_6$ of the bulk equation in cell problem (97) is constant with respect to $\tilde{Y}$, the criterion leading to the solvability condition of Remark 5.1 is satisfied. As done for the displacement, Equation (95b) will be used when the homogenized equation for $\boldsymbol{L}^{(0)}_{\boldsymbol{K}}$ is determined. Moreover, as noticed in Remark 6.2, when $\mathrm{Grad}_{\tilde{X}}\boldsymbol{L}^{(0)}_{\boldsymbol{K}}$ can be regarded as arbitrary, the cell problem (97) can be recast in the equivalent form

$$\begin{cases} -\mathrm{Div}_{\tilde{Y}}\left[\frac{\ell_\eta^2}{L_0^2}\sigma_\eta\tau_\eta\left(\mathrm{DevSym}\mathbb{I}_6 + \mathrm{DevSym}(T\mathrm{Grad}_{\tilde{Y}}\boldsymbol{\Lambda}_\eta)\right)^{\mathrm{T}}\right] = \mathbb{0}_5, & \text{in } \tilde{\mathscr{Y}}_{\mathrm{R}\eta}, \\ [\![\boldsymbol{\Lambda}_\eta]\!] = \mathbb{0}_5, & \text{on } \tilde{\Gamma}_{\mathscr{Y}_{\mathrm{R}}}, \\ \left[\!\left[\frac{\ell_\eta^2}{L_0}\sigma_\eta\tau_\eta\left(\mathrm{DevSym}\mathbb{I}_6 + \mathrm{DevSym}(T\mathrm{Grad}_{\tilde{Y}}\boldsymbol{\Lambda}_\eta)\right)^{\mathrm{T}}\right]\!\right]\boldsymbol{N}_{\tilde{\Gamma}_{\mathscr{Y}_{\mathrm{R}}}} = \mathbb{0}_5, & \text{on } \tilde{\Gamma}_{\mathscr{Y}_{\mathrm{R}}}, \\ \mathrm{Tr}\boldsymbol{\Lambda}_\eta = \mathbb{0}_3, & \text{in } \tilde{\mathscr{Y}}_{\mathrm{R}\eta}, \\ \mathrm{Skew}\boldsymbol{\Lambda}_\eta = \mathbb{0}_5, & \text{in } \tilde{\mathscr{Y}}_{\mathrm{R}\eta}, \end{cases} \tag{98}$$

where $\mathbb{0}_3$ and $\mathbb{0}_5$ represent the null tensors in the spaces of the third- and of the fifth-order tensors, respectively.

6.2 | Homogenized balance laws and effective coefficients

To determine the homogenized balance laws, we have to compute the apparent averages of Equations (59b) and (60b) over the periodic cell $\tilde{\mathscr{Y}}_{\mathrm{R}}$. According to the definition (9), this means integrating Equations (59b) and (60b) over $\tilde{\mathscr{Y}}_{\mathrm{R}\eta}$ and dividing the result by the size of the periodic cell, that is, by $|\tilde{\mathscr{Y}}_{\mathrm{R}}|$.

6.2.1 | Homogenization of the momentum balance law

We first perform the homogenization of the momentum balance law (59b), for which we review the procedure outlined in [19], adding some slight notational changes. To this end, we look at Equations (85a) and (85b), and we recognize that the arguments of $\mathrm{Div}_{\tilde{X}}$ and $\mathrm{Div}_{\tilde{Y}}$ featuring in Equation (59b) are the zeroth- and the first-order terms of the asymptotic expansion of the first Piola–Kirchhoff stress tensor of the ηth constituent of the composite under study. Hence, we start the homogenization procedure by rewriting Equation (59b), up to the factor u_{c}/L_0^2, as

$$\mathrm{Div}_{\tilde{X}}\boldsymbol{P}^{(0)}_{\eta\mathrm{lin}} + \mathrm{Div}_{\tilde{Y}}\boldsymbol{P}^{(1)}_{\eta\mathrm{lin}} = \boldsymbol{0}. \tag{99}$$

Next, we compute the apparent average of Equation (99). Hence, by recalling the hypothesis of *macroscopic uniformity*, which allows to exchange the order of the $\tilde{X}$-divergence operator with the (apparent) average operator, we obtain:

$$\left\langle \mathrm{Div}_{\tilde{X}}\boldsymbol{P}^{(0)}_{\eta\mathrm{lin}}\right\rangle_\eta + \left\langle \mathrm{Div}_{\tilde{Y}}\boldsymbol{P}^{(1)}_{\eta\mathrm{lin}}\right\rangle_\eta = \mathrm{Div}_{\tilde{X}}\left\langle \boldsymbol{P}^{(0)}_{\eta\mathrm{lin}}\right\rangle_\eta + \left\langle \mathrm{Div}_{\tilde{Y}}\boldsymbol{P}^{(1)}_{\eta\mathrm{lin}}\right\rangle_\eta = \boldsymbol{0}. \tag{100}$$

10991476, 2025, 1, Downloaded from https://onlinelibrary.wiley.com/doi/10.1002/nme.10367 by Politecnico Di Torino Sist. Bibl Del Polit Di Torino, Wiley Online Library on [12/02/2025]. See the Terms and Conditions (https://onlinelibrary.wiley.com/terms-and-conditions) on Wiley Online Library for rules of use; OA articles are governed by the applicable Creative Commons License

We exploit now the explicit definition of the apparent average operator, Gauss' theorem, the fact that the boundary $\partial\tilde{\mathscr{Y}}_{\mathrm{R}\eta}$ can be written as $\partial\tilde{\mathscr{Y}}_{\mathrm{R}\eta} \equiv \tilde{\Gamma}_{\mathscr{Y}_{\mathrm{R}}} \cup \left(\partial\tilde{\mathscr{Y}}_{\mathrm{R}\eta} \backslash \tilde{\Gamma}_{\mathscr{Y}_{\mathrm{R}}}\right)$, and the hypothesis of $\tilde{Y}$-periodicity of the fields involved in Equation (100), thereby achieving the following chain of equalities:

$$\begin{aligned}
&\mathrm{Div}_{\tilde{X}}\left\langle \boldsymbol{P}^{(0)}_{\eta\mathrm{lin}} \right\rangle_{\eta} + \left\langle \mathrm{Div}_{\tilde{Y}} \boldsymbol{P}^{(1)}_{\eta\mathrm{lin}} \right\rangle_{\eta} = \mathrm{Div}_{\tilde{X}}\left\langle \boldsymbol{P}^{(0)}_{\eta\mathrm{lin}} \right\rangle_{\eta} + \frac{1}{|\tilde{\mathscr{Y}}_{\mathrm{R}}|} \int\limits_{\tilde{\mathscr{Y}}_{\mathrm{R}\eta}} \mathrm{Div}_{\tilde{Y}} \boldsymbol{P}^{(1)}_{\eta\mathrm{lin}} \mathrm{dV}(\tilde{Y}) \\
&= \mathrm{Div}_{\tilde{X}}\left\langle \boldsymbol{P}^{(0)}_{\eta\mathrm{lin}} \right\rangle_{\eta} + \frac{1}{|\tilde{\mathscr{Y}}_{\mathrm{R}}|} \int\limits_{\partial\tilde{\mathscr{Y}}_{\mathrm{R}\eta}} \boldsymbol{P}^{(1)}_{\eta\mathrm{lin}} \boldsymbol{N}_{\partial\tilde{\mathscr{Y}}_{\mathrm{R}\eta}} \mathrm{dA}(\tilde{Y}) \\
&= \mathrm{Div}_{\tilde{X}}\left\langle \boldsymbol{P}^{(0)}_{\eta\mathrm{lin}} \right\rangle_{\eta} + \frac{1}{|\tilde{\mathscr{Y}}_{\mathrm{R}}|} \int\limits_{\tilde{\Gamma}_{\mathscr{Y}_{\mathrm{R}}}} \boldsymbol{P}^{(1)}_{\eta\mathrm{lin}} \boldsymbol{N}_{\tilde{\Gamma}_{\mathscr{Y}_{\mathrm{R}}}} \mathrm{dA}(\tilde{Y}) + \frac{1}{|\tilde{\mathscr{Y}}_{\mathrm{R}}|} \int\limits_{\partial\tilde{\mathscr{Y}}_{\mathrm{R}\eta} \backslash \tilde{\Gamma}_{\mathscr{Y}_{\mathrm{R}}}} \boldsymbol{P}^{(1)}_{\eta\mathrm{lin}} \boldsymbol{N}_{\partial\tilde{\mathscr{Y}}_{\mathrm{R}\eta}} \mathrm{dA}(\tilde{Y}) = \boldsymbol{0},
\end{aligned} \tag{101}$$

where we omitted the dependence of the integrands on the triples $(\tilde{X}, \tilde{Y}, t)$ to reduce the length of the mathematical formulae.

Now, we take advantage of the explicit expression of $\boldsymbol{P}^{(0)}_{\eta\mathrm{lin}}$, of the *Ansatz* (62a), and of the hypothesis according to which the remodeling distortions are constant with respect to $\tilde{Y}$. Therefore, the apparent average $\left\langle \boldsymbol{P}^{(0)}_{\eta\mathrm{lin}} \right\rangle_{\eta}$ reads

$$\begin{aligned}
\left\langle \boldsymbol{P}^{(0)}_{\eta\mathrm{lin}} \right\rangle_{\eta} &= \frac{1}{|\tilde{\mathscr{Y}}_{\mathrm{R}}|} \int\limits_{\tilde{\mathscr{Y}}_{\mathrm{R}\eta}} \boldsymbol{P}^{(0)}_{\eta\mathrm{lin}} \mathrm{dV}(\tilde{Y}) \\
&= \frac{1}{|\tilde{\mathscr{Y}}_{\mathrm{R}}|} \int\limits_{\tilde{\mathscr{Y}}_{\mathrm{R}\eta}} \left\{ \left(\mathcal{C}^{(0)}_{\mathrm{R}\eta} - \boldsymbol{I} \underline{\otimes} \left(\mathcal{C}^{(0)}_{\mathrm{R}\eta} : \boldsymbol{E}^{(0)}_{\boldsymbol{K}} \right) \right) : \left(\mathbb{I}_4 + T\mathrm{Grad}_{\tilde{Y}} \boldsymbol{\xi}_{\eta} \right) : \mathrm{Grad}_{\tilde{X}} \boldsymbol{u}^{(0)} - \frac{L_0}{u_{\mathrm{c}}} \left(\mathcal{C}^{(0)}_{\mathrm{R}\eta} : \boldsymbol{E}^{(0)}_{\boldsymbol{K}} \right) \right\} \mathrm{dV}(\tilde{Y}) \\
&\quad + \frac{1}{|\tilde{\mathscr{Y}}_{\mathrm{R}}|} \int\limits_{\tilde{\mathscr{Y}}_{\mathrm{R}\eta}} \left\{ \left(\mathcal{C}^{(0)}_{\mathrm{R}\eta} - \boldsymbol{I} \underline{\otimes} \left(\mathcal{C}^{(0)}_{\mathrm{R}\eta} : \boldsymbol{E}^{(0)}_{\boldsymbol{K}} \right) \right) : \mathrm{Grad}_{\tilde{Y}} \boldsymbol{\omega}_{\eta} \right\} \mathrm{dV}(\tilde{Y}) \\
&= \left(\mathcal{C}^{(0)}_{\mathrm{R}\eta} - \boldsymbol{I} \underline{\otimes} \left(\mathcal{C}^{(0)}_{\mathrm{R}\eta} : \boldsymbol{E}^{(0)}_{\boldsymbol{K}} \right) \right) : \left(\varphi_{\eta} \mathbb{I}_4 + \langle T\mathrm{Grad}_{\tilde{Y}} \boldsymbol{\xi}_{\eta} \rangle_{\eta} \right) : \mathrm{Grad}_{\tilde{X}} \boldsymbol{u}^{(0)} - \varphi_{\eta} \frac{L_0}{u_{\mathrm{c}}} \left(\mathcal{C}^{(0)}_{\mathrm{R}\eta} : \boldsymbol{E}^{(0)}_{\boldsymbol{K}} \right) \\
&\quad + \left(\mathcal{C}^{(0)}_{\mathrm{R}\eta} - \boldsymbol{I} \underline{\otimes} \left(\mathcal{C}^{(0)}_{\mathrm{R}\eta} : \boldsymbol{E}^{(0)}_{\boldsymbol{K}} \right) \right) : \langle \mathrm{Grad}_{\tilde{Y}} \boldsymbol{\omega}_{\eta} \rangle_{\eta}.
\end{aligned} \tag{102}$$

Thus, by introducing the notation

$$\mathcal{C}^{\mathrm{eff}}_{\mathrm{R}\eta} := \left(\mathcal{C}^{(0)}_{\mathrm{R}\eta} - \boldsymbol{I} \underline{\otimes} \left(\mathcal{C}^{(0)}_{\mathrm{R}\eta} : \boldsymbol{E}^{(0)}_{\boldsymbol{K}} \right) \right) : \left(\varphi_{\eta} \mathbb{I}_4 + \langle T\mathrm{Grad}_{\tilde{Y}} \boldsymbol{\xi}_{\eta} \rangle_{\eta} \right), \tag{103a}$$

$$\hat{\boldsymbol{D}}_{\mathrm{R}\eta} := -\varphi_{\eta} \frac{L_0}{u_{\mathrm{c}}} \left(\mathcal{C}^{(0)}_{\mathrm{R}\eta} : \boldsymbol{E}^{(0)}_{\boldsymbol{K}} \right) + \left(\mathcal{C}^{(0)}_{\mathrm{R}\eta} - \boldsymbol{I} \underline{\otimes} \left(\mathcal{C}^{(0)}_{\mathrm{R}\eta} : \boldsymbol{E}^{(0)}_{\boldsymbol{K}} \right) \right) : \langle \mathrm{Grad}_{\tilde{Y}} \boldsymbol{\omega}_{\eta} \rangle_{\eta}, \tag{103b}$$

and plugging these expressions into Equation (101), the apparent average of the linear momentum balance law becomes

$$\mathrm{Div}_{\tilde{X}} \left[\mathcal{C}^{\mathrm{eff}}_{\mathrm{R}\eta} : \mathrm{Grad}_{\tilde{X}} \boldsymbol{u}^{(0)} \right] + \mathrm{Div}_{\tilde{X}} \hat{\boldsymbol{D}}_{\mathrm{R}\eta} + \frac{1}{|\tilde{\mathscr{Y}}_{\mathrm{R}}|} \int\limits_{\tilde{\Gamma}_{\mathscr{Y}_{\mathrm{R}}}} \boldsymbol{P}^{(1)}_{\eta\mathrm{lin}} \boldsymbol{N}_{\tilde{\Gamma}_{\mathscr{Y}_{\mathrm{R}}}} \mathrm{dA}(\tilde{Y}) + \frac{1}{|\tilde{\mathscr{Y}}_{\mathrm{R}}|} \int\limits_{\partial\tilde{\mathscr{Y}}_{\mathrm{R}\eta} \backslash \tilde{\Gamma}_{\mathscr{Y}_{\mathrm{R}}}} \boldsymbol{P}^{(1)}_{\eta\mathrm{lin}} \boldsymbol{N}_{\partial\tilde{\mathscr{Y}}_{\mathrm{R}\eta}} \mathrm{dA}(\tilde{Y}) = \boldsymbol{0}. \tag{104}$$

Finally, by summing Equation (104) over $\eta = 1, 2$, enforcing the no-jump condition at $\tilde{\Gamma}_{\mathscr{Y}_{\mathrm{R}}}$ and the $\tilde{Y}$-periodicity at $\partial\tilde{\mathscr{Y}}_{\mathrm{R}\eta} \backslash \tilde{\Gamma}_{\mathscr{Y}_{\mathrm{R}}}$ (see, e.g., [88]) for $\boldsymbol{P}^{(1)}_{\eta\mathrm{lin}}$, and defining the quantities

$$\mathcal{C}^{\mathrm{eff}}_{\mathrm{R}} := \sum_{\eta=1,2} \mathcal{C}^{\mathrm{eff}}_{\mathrm{R}\eta}, \tag{105a}$$

$$\hat{\boldsymbol{D}}_{\mathrm{R}} := \sum_{\eta=1,2} \hat{\boldsymbol{D}}_{\mathrm{R}\eta}, \tag{105b}$$

10991476, 2025, 1, Downloaded from https://onlinelibrary.wiley.com/doi/10.1002/nme.10367 by Politecnico Di Torino Sist. Bibl Del Polit Di Torino, Wiley Online Library on [12/02/2025]. See the Terms and Conditions (https://onlinelibrary.wiley.com/terms-and-conditions) on Wiley Online Library for rules of use; OA articles are governed by the applicable Creative Commons License

the *homogenized balance of linear momentum* for the composite as a whole can be cast in the form

$$\mathrm{Div}_{\tilde{X}}\left[\mathcal{C}_{\mathrm{R}}^{\mathrm{eff}} : \mathrm{Grad}_{\tilde{X}}\boldsymbol{u}^{(0)}\right] + \mathrm{Div}_{\tilde{X}}\hat{\boldsymbol{D}}_{\mathrm{R}} = \boldsymbol{0}. \tag{106}$$

We emphasize that the fourth-order tensor $\mathcal{C}_{\mathrm{R}}^{\mathrm{eff}}$ found this way [19] is referred to as *effective elasticity tensor* of the composite material under study. It is also worth to recall that the effect of the microstructure of the composite on the macroscopic displacement $\boldsymbol{u}^{(0)}$ is transferred to Equation (106) through $\mathcal{C}_{\mathrm{R}}^{\mathrm{eff}}$ and $\hat{\boldsymbol{D}}_{\mathrm{R}}$. In particular, while the possibility of defining the effective elasticity tensor is a rather standard result in the theory of AH, the presence of the term $\hat{\boldsymbol{D}}_{\mathrm{R}}$ is a byproduct of the combined effect of the remodeling distortions, accounted for through $\boldsymbol{E}_{\boldsymbol{K}}^{(0)}$, and the microstructure, whose contribution emerges by means of the average of $\langle \mathrm{Grad}_{\tilde{Y}}\boldsymbol{\omega}\rangle_{\eta}$.

6.2.2 | Homogenization of the flow rule

We concentrate now on the homogenization of the flow rule given in Equation (60b), and, by invoking the *Ansatz* (62b), we rewrite it as

$$\mathrm{DevSym}\left\{\sigma_{\eta}\tau_{\eta}\boldsymbol{L}_{\boldsymbol{K}}^{(0)} - \boldsymbol{\Sigma}_{\eta\mathrm{lin}}^{(0)} - \mathrm{Div}_{\tilde{X}}\left[\frac{\ell_{\eta}^{2}}{L_{0}^{2}}\sigma_{\eta}\tau_{\eta}\left(\mathbb{I}_{6} + T\mathrm{Grad}_{\tilde{Y}}\boldsymbol{\Lambda}_{\eta}\right) \vdots \mathrm{Grad}_{\tilde{X}}\boldsymbol{L}_{\boldsymbol{K}}^{(0)}\right] - \mathrm{Div}_{\tilde{Y}}\mathbb{K}_{\mathrm{dis}\eta}^{(1)}\right\} = \mathbf{O}. \tag{107}$$

Then, following the path shown in Section 6.2.1, we apply the apparent average operator to Equation (107), and bearing in mind the simplifications due to the macroscopic uniformity of the composite, and the assumption that σ_{η}, τ_{η}, and $\boldsymbol{L}_{\boldsymbol{K}}^{(0)}$ are constant with respect to $\tilde{Y}$, we put the averaged equation in the form

$$\mathrm{DevSym}\left\{\varphi_{\eta}\sigma_{\eta}\tau_{\eta}\boldsymbol{L}_{\boldsymbol{K}}^{(0)} - \left\langle\boldsymbol{\Sigma}_{\eta\mathrm{lin}}^{(0)}\right\rangle_{\eta} - \mathrm{Div}_{\tilde{X}}\left[\frac{\ell_{\eta}^{2}}{L_{0}^{2}}\sigma_{\eta}\tau_{\eta}\left(\varphi_{\eta}\mathbb{I}_{6} + \langle T\mathrm{Grad}_{\tilde{Y}}\boldsymbol{\Lambda}_{\eta}\rangle_{\eta}\right) \vdots \mathrm{Grad}_{\tilde{X}}\boldsymbol{L}_{\boldsymbol{K}}^{(0)}\right] - \left\langle\mathrm{Div}_{\tilde{Y}}\mathbb{K}_{\mathrm{dis}\eta}^{(1)}\right\rangle_{\eta}\right\} = \mathbf{O}. \tag{108}$$

Then, we look into the apparent average of $\mathrm{Div}_{\tilde{Y}}\mathbb{K}_{\mathrm{dis}\eta}^{(1)}$, and by having recourse to Gauss' theorem, we obtain

$$\left\langle\mathrm{Div}_{\tilde{Y}}\mathbb{K}_{\mathrm{dis}\eta}^{(1)}\right\rangle_{\eta} = \frac{1}{|\tilde{\mathscr{Y}}_{\mathrm{R}}|}\int_{\tilde{\mathscr{Y}}_{\mathrm{R}\eta}}\mathrm{Div}_{\tilde{Y}}\mathbb{K}_{\mathrm{dis}\eta}^{(1)}\mathrm{dV}(\tilde{Y}) = \frac{1}{|\tilde{\mathscr{Y}}_{\mathrm{R}}|}\int_{\tilde{\Gamma}_{\mathscr{Y}_{\mathrm{R}}}}\mathbb{K}_{\mathrm{dis}\eta}^{(1)}\boldsymbol{N}_{\tilde{\Gamma}_{\mathscr{Y}_{\mathrm{R}}}}\mathrm{dA}(\tilde{Y}) + \frac{1}{|\tilde{\mathscr{Y}}_{\mathrm{R}}|}\int_{\partial\tilde{\mathscr{Y}}_{\mathrm{R}}\setminus\tilde{\Gamma}_{\mathscr{Y}_{\mathrm{R}}}}\mathbb{K}_{\mathrm{dis}\eta}^{(1)}\boldsymbol{N}_{\partial\tilde{\mathscr{Y}}_{\mathrm{R}}}\mathrm{dA}(\tilde{Y}). \tag{109}$$

Moreover, by substituting this result into Equation (108), adding over $\eta = 1, 2$, and, thus, exploiting the no-jump interface conditions and the $\tilde{Y}$-periodic conditions on $\mathbb{K}_{\mathrm{dis}\eta}^{(1)}$ (see Equation (93b)), we determine the homogenized flow rule for a gradient theory of remodeling, that is,

$$\mathrm{DevSym}\left\{\gamma^{\mathrm{eff}}\boldsymbol{L}_{\boldsymbol{K}}^{(0)} - \sum_{\eta=1,2}\left\langle\boldsymbol{\Sigma}_{\eta\mathrm{lin}}^{(0)}\right\rangle_{\eta} - \frac{1}{L_{0}^{2}}\mathrm{Div}_{\tilde{X}}\left[\mathbb{D}^{\mathrm{eff}} \vdots \mathrm{Grad}_{\tilde{X}}\boldsymbol{L}_{\boldsymbol{K}}^{(0)}\right]\right\} = \mathbf{O}, \tag{110}$$

where we have introduced an *effective viscosity* γ^{eff} and an *effective generalized viscosity tensor* $\mathbb{D}^{\mathrm{eff}}$ defined as

$$\gamma^{\mathrm{eff}} := \sum_{\eta=1,2}\varphi_{\eta}\sigma_{\eta}\tau_{\eta}, \tag{111a}$$

$$\mathbb{D}^{\mathrm{eff}} := \sum_{\eta=1,2}\ell_{\eta}^{2}\sigma_{\eta}\tau_{\eta}\left(\varphi_{\eta}\mathbb{I}_{6} + \langle T\mathrm{Grad}_{\tilde{Y}}\boldsymbol{\Lambda}_{\eta}\rangle_{\eta}\right). \tag{111b}$$

Note that, in spite of the resemblance of the last term of Equation (110) with a diffusive flux in the tensor variable $\boldsymbol{L}_{\boldsymbol{K}}^{(0)}$, there is no diffusion related to $\boldsymbol{L}_{\boldsymbol{K}}^{(0)}$ in the present framework. Rather, there is a balance of forces that generalizes the Allen–Cahn model proposed by Gurtin [71] to the elasto-viscoplastic context developed in our work.

10991476, 2025, 1, Downloaded from https://onlinelibrary.wiley.com/doi/10.1002/mma.10367 by Politecnico Di Torino Sist. Bibl Del Polit Di Torino, Wiley Online Library on [12/02/2025]. See the Terms and Conditions (https://onlinelibrary.wiley.com/terms-and-conditions) on Wiley Online Library for rules of use; OA articles are governed by the applicable Creative Commons License

The averaged, linearized Mandel stress tensor that features in Equation (110) can be reformulated in terms of the quantities $C^{\text{eff}}_{\text{R}\eta}$ and $\hat{\boldsymbol{D}}_{\text{R}\eta}$ introduced in Equations (103a) and (103b), that is,

$$\begin{aligned}\left\langle \boldsymbol{\Sigma}^{(0)}_{\eta\text{lin}} \right\rangle_\eta &= \frac{1}{\det \boldsymbol{K}^{(0)}} (\boldsymbol{Z}^{(0)})^{\text{T}} \frac{u_{\text{c}}}{L_0} \left\{ C^{\text{eff}}_{\text{R}\eta} : \text{Grad}_{\tilde{X}} \boldsymbol{u}^{(0)} + \hat{\boldsymbol{D}}_{\text{R}\eta} \right\} (\boldsymbol{K}^{(0)})^{\text{T}} \\ &+ \frac{1}{\det \boldsymbol{K}^{(0)}} (\boldsymbol{Z}^{(0)})^{\text{T}} \frac{u_{\text{c}}}{L_0} \left\{ \left[C^{\text{eff}}_{\text{R}\eta} - C^{(0)}_{\text{R}\eta} : \left(\varphi_\eta \mathbb{I}_4 + \langle T\text{Grad}_{\tilde{Y}} \boldsymbol{\xi}_\eta \rangle_\eta \right) \right] : \text{Grad}_{\tilde{X}} \boldsymbol{u}^{(0)} \right\} (\boldsymbol{K}^{(0)})^{\text{T}} \\ &+ \frac{1}{\det \boldsymbol{K}^{(0)}} (\boldsymbol{Z}^{(0)})^{\text{T}} \frac{u_{\text{c}}}{L_0} \left\{ \hat{\boldsymbol{D}}_{\text{R}\eta} + \varphi_\eta \frac{L_0}{u_{\text{c}}} \left(C^{(0)}_{\text{R}\eta} : \boldsymbol{E}^{(0)}_{\boldsymbol{K}} \right) - C^{(0)}_{\text{R}\eta} : \langle \text{Grad}_{\tilde{Y}} \boldsymbol{\omega} \rangle_\eta \right\} (\boldsymbol{K}^{(0)})^{\text{T}}. \end{aligned} \tag{112}$$

Therefore, the sum $\sum_{\eta=1,2} \left\langle \boldsymbol{\Sigma}^{(0)}_{\eta\text{lin}} \right\rangle_\eta$ yields

$$\begin{aligned}\sum_{\eta=1,2} \left\langle \boldsymbol{\Sigma}^{(0)}_{\eta\text{lin}} \right\rangle_\eta &= \frac{1}{\det \boldsymbol{K}^{(0)}} (\boldsymbol{Z}^{(0)})^{\text{T}} \frac{u_{\text{c}}}{L_0} \left\{ C^{\text{eff}}_{\text{R}} : \text{Grad}_{\tilde{X}} \boldsymbol{u}^{(0)} + \hat{\boldsymbol{D}}_{\text{R}} \right\} (\boldsymbol{K}^{(0)})^{\text{T}} \\ &+ \frac{1}{\det \boldsymbol{K}^{(0)}} (\boldsymbol{Z}^{(0)})^{\text{T}} \frac{u_{\text{c}}}{L_0} \left\{ \left[C^{\text{eff}}_{\text{R}} - \sum_{\eta=1,2} C^{(0)}_{\text{R}\eta} : \left(\varphi_\eta \mathbb{I}_4 + \langle T\text{Grad}_{\tilde{Y}} \boldsymbol{\xi}_\eta \rangle_\eta \right) \right] : \text{Grad}_{\tilde{X}} \boldsymbol{u}^{(0)} \right\} (\boldsymbol{K}^{(0)})^{\text{T}} \\ &+ \frac{1}{\det \boldsymbol{K}^{(0)}} (\boldsymbol{Z}^{(0)})^{\text{T}} \frac{u_{\text{c}}}{L_0} \left\{ \hat{\boldsymbol{D}}_{\text{R}} + \sum_{\eta=1,2} \varphi_\eta \frac{L_0}{u_{\text{c}}} \left(C^{(0)}_{\text{R}\eta} : \boldsymbol{E}^{(0)}_{\boldsymbol{K}} \right) - \sum_{\eta=1,2} C^{(0)}_{\text{R}\eta} : \langle \text{Grad}_{\tilde{Y}} \boldsymbol{\omega} \rangle_\eta \right\} (\boldsymbol{K}^{(0)})^{\text{T}}. \end{aligned} \tag{113}$$

By plugging this expression of $\sum_{\eta=1,2} \left\langle \boldsymbol{\Sigma}^{(0)}_{\eta\text{lin}} \right\rangle_\eta$ into Equation (110), the coupling between the flow rule and the momentum balance law (106) becomes evident. Indeed, the particularly simple structure of Equation (110) concentrates the interaction between the remodeling distortions and the displacement in the (averaged) Mandel stress tensor $\sum_{\eta=1,2} \left\langle \boldsymbol{\Sigma}^{(0)}_{\eta\text{lin}} \right\rangle_\eta$, thereby providing a "tangible" example of the *"Eshelbian coupling"* advocated in [83] in the case of growth and remodeling of biological tissues. It is through the averaged Mandel stress tensor that the microstructural fields $\boldsymbol{\xi}_\eta$ and $\boldsymbol{\omega}_\eta$ concur to determine the macroscopic remodeling distortions.

Finally, we work our Equation (110) by applying the commutativity of DevSym and $\text{Div}_{\tilde{X}}$ as well as the property, granted by the constraints (42a) and (42b), that $\boldsymbol{L}^{(0)}_{\boldsymbol{K}}$ is deviatoric by itself, that is, $\text{DevSym}\boldsymbol{L}^{(0)}_{\boldsymbol{K}} \equiv \boldsymbol{L}^{(0)}_{\boldsymbol{K}}$. This yields

$$\gamma^{\text{eff}} \boldsymbol{L}^{(0)}_{\boldsymbol{K}} - \sum_{\eta=1,2} \left\langle \text{DevSym}\boldsymbol{\Sigma}^{(0)}_{\eta\text{lin}} \right\rangle_\eta - \frac{1}{L_0^2} \text{Div}_{\tilde{X}} \left[(\text{DevSym}\mathbb{D}^{\text{eff}}) \vdots \text{Grad}_{\tilde{X}} \boldsymbol{L}^{(0)}_{\boldsymbol{K}} \right] = \boldsymbol{O}, \tag{114}$$

where, by using Equation (111b), $\text{DevSym}\mathbb{D}^{\text{eff}}$ is given by

$$\text{DevSym}\mathbb{D}^{\text{eff}} := \sum_{\eta=1,2} \ell_\eta^2 \sigma_\eta \tau_\eta \left(\varphi_\eta \text{DevSym}\mathbb{I}_6 + \langle T\text{Grad}_{\tilde{Y}} (\text{DevSym}\boldsymbol{\Lambda}_\eta) \rangle_\eta \right). \tag{115}$$

Remark 6.3 (Non-dimensionalization of the macroscopic flow rule)**.** To us, an interesting aspect of the study presented in this work, which has led to Equation (114), is that it is possible to identify two non-dimensional numbers, each of which represents the ratio between the elastic forces and the corresponding viscous forces that characterize our mechanical problem [128]. The first one of these numbers is known as Weissenberg number [128], while the second one is a generalization of it. Both non-dimensional quantities contribute to determine the dynamic regime of the system under study, together with the concomitant effective viscosity and effective generalized viscosity. To proceed, we introduce the characteristic viscosity $\gamma_{\text{c}} > 0$, which can be expressed as a function of characteristic yield stresses σ_η, timescales τ_η, and volumetric fractions φ_η, with $\eta = 1, 2$, respectively; the characteristic time of the remodeling distortions, denoted by t_{c}; the characteristic Mandel stress $\Sigma_{\text{c}} > 0$; and the characteristic coefficient of generalized viscosity D_{c}, which, as for γ_{c}, can be defined as a function of ℓ_η, σ_η, τ_η and φ_η, with $\eta = 1, 2$. Hence, we can rewrite Equation (114) as

10991476, 2025, 1, Downloaded from https://onlinelibrary.wiley.com/doi/10.1002/nma.10367 by Politecnico Di Torino Sist. Bibl Del Polit Di Torino, Wiley Online Library on [12/02/2025]. See the Terms and Conditions (https://onlinelibrary.wiley.com/terms-and-conditions) on Wiley Online Library for rules of use; OA articles are governed by the applicable Creative Commons License

$$\begin{aligned}&\frac{\gamma_c}{t_c}\check{\gamma}^{\text{eff}}\check{\boldsymbol{L}}_{\boldsymbol{K}}^{(0)}-\Sigma_c\sum_{\eta=1,2}\left\langle \text{DevSym}\check{\boldsymbol{\Sigma}}_{\eta\text{lin}}^{(0)}\right\rangle_\eta-\frac{D_c}{L_0^2t_c}\text{Div}_{\check{X}}\left[\left(\text{DevSym}\check{\mathbb{D}}^{\text{eff}}\right)\vdots\text{Grad}_{\check{X}}\check{\boldsymbol{L}}_{\boldsymbol{K}}^{(0)}\right]=\boldsymbol{O}\\ \Rightarrow\ &\frac{\gamma_c}{\Sigma_c t_c}\check{\gamma}^{\text{eff}}\check{\boldsymbol{L}}_{\boldsymbol{K}}^{(0)}-\sum_{\eta=1,2}\left\langle \text{DevSym}\check{\boldsymbol{\Sigma}}_{\eta\text{lin}}^{(0)}\right\rangle_\eta-\frac{D_c/L_0^2}{\Sigma_c t_c}\text{Div}_{\check{X}}\left[\left(\text{DevSym}\check{\mathbb{D}}^{\text{eff}}\right)\vdots\text{Grad}_{\check{X}}\check{\boldsymbol{L}}_{\boldsymbol{K}}^{(0)}\right]=\boldsymbol{O},\end{aligned}\tag{116}$$

where the physical quantities marked with the symbol "ˇ" are non-dimensional, that is, for any quantity Φ, $\check{\Phi}:=\Phi_c^{-1}\Phi$ is its non-dimensional counterpart, while $\Phi_c>0$ is its characteristic value. We notice now that the non-dimensional quantities

$$\text{Wi}_{\text{std}}:=\frac{\Sigma_c t_c}{\gamma_c}\in]0,+\infty[,\qquad\qquad \text{Wi}_{\text{grad}}:=\frac{\Sigma_c t_c}{D_c/L_0^2}\in]0,+\infty[,\tag{117}$$

consist of the ratios between the characteristic "viscosity" induced by the Mandel stress Σ_c and characteristic viscosities associated with the flow of the remodeling distortions. In particular, we distinguish between Wi_{std}, in which the characteristic viscosity is the one characterizing a model of grade zero in $\boldsymbol{L}_{\boldsymbol{K}}$, from Wi_{grad}, in which the characteristic viscosity D_c/L_0^2 is due to the introduction of a model of grade one in $\boldsymbol{L}_{\boldsymbol{K}}$. The two non-dimensional numbers Wi_{std} and Wi_{grad} are referred to as Weissenberg numbers and permit to recast the flow rule in the form

$$\frac{1}{\text{Wi}_{\text{std}}}\check{\gamma}^{\text{eff}}\check{\boldsymbol{L}}_{\boldsymbol{K}}^{(0)}-\frac{1}{\text{Wi}_{\text{grad}}}\text{Div}_{\check{X}}\left[\left(\text{DevSym}\check{\mathbb{D}}^{\text{eff}}\right)\vdots\text{Grad}_{\check{X}}\check{\boldsymbol{L}}_{\boldsymbol{K}}^{(0)}\right]=\sum_{\eta=1,2}\left\langle \text{DevSym}\check{\boldsymbol{\Sigma}}_{\eta\text{lin}}^{(0)}\right\rangle_\eta.\tag{118}$$

This result shows that the flow rule is modulated by the two non-dimensional quantities expressed by Wi_{std} and Wi_{grad}, rather than the sole Wi_{std}, as is the case for grade zero theories.

A limit regime, which, however, requires further investigations, is the one in which Wi_{std} is sufficiently smaller than unity and smaller than the ratio $\text{Wi}_{\text{std}}/\text{Wi}_{\text{grad}}$ in such a way that the order of magnitude of the ratio is, for example, between 10^{-1} and 10^{1}. In this circumstance, indeed, Equation (118) could be approximated as

$$\check{\gamma}^{\text{eff}}\check{\boldsymbol{L}}_{\boldsymbol{K}}^{(0)}-\frac{\text{Wi}_{\text{std}}}{\text{Wi}_{\text{grad}}}\text{Div}_{\check{X}}\left[\left(\text{DevSym}\check{\mathbb{D}}^{\text{eff}}\right)\vdots\text{Grad}_{\check{X}}\check{\boldsymbol{L}}_{\boldsymbol{K}}^{(0)}\right]=0,\tag{119}$$

so that the trigger of the rate of remodeling distortions is the inhomogeneity of their spatial distribution rather than the Mandel stress, as standard grade zero theories prescribe. Should this be the case, a regime would be found in which there occurs the scenario suggested by Epstein [125] in a completely different setting.

We close this section noticing that if an energetic contribution linear in the Burgers tensor were considered, as would be the case by linearizing the "defect" energy density, we could introduce for it an *Ansatz* analogous to the one for $\boldsymbol{u}_\eta^{(1)}$, provided in Equation (62a), and we would thus find an additional term accounting for this effect in Equation (118).

6.3 | Comparison with conventional flow rules

The gradient flow rule put forward in [42] represents a generalization of a more conventional type of flow rules having the form [44, 53, 113]

$$\dot{\boldsymbol{B}}_{\boldsymbol{K}}=\frac{1}{\gamma_{\boldsymbol{K}}}\text{DevSym}\left\{\boldsymbol{B}_{\boldsymbol{K}}\boldsymbol{\Sigma}_R\right\},\tag{120}$$

and prescribing the evolution of the symmetric plastic metric tensor $\boldsymbol{B}_{\boldsymbol{K}}=\boldsymbol{K}^{-1}\boldsymbol{K}^{-T}$ in terms of the Mandel stress tensor $\boldsymbol{\Sigma}_R:=J_{\boldsymbol{K}}\boldsymbol{K}^T\boldsymbol{\Sigma}\boldsymbol{K}^{-T}$ associated with the reference placement of the composite (we recall that $\boldsymbol{\Sigma}_R$ satisfies the symmetry relation $\boldsymbol{B}_{\boldsymbol{K}}\boldsymbol{\Sigma}_R=(\boldsymbol{B}_{\boldsymbol{K}}\boldsymbol{\Sigma}_R)^T$). In Equation (120) $\gamma_{\boldsymbol{K}}$ designates a generalized viscosity whose mathematical expression can be, in general, very complicated. We notice that Equation (120) preserves the symmetry of $\boldsymbol{B}_{\boldsymbol{K}}$, and we refer to [129] for a discussion on symmetry-preserving homogenization.

In fact, by neglecting the divergence term in Equation (110), one recovers the homogenized equation

$$\dot{\boldsymbol{B}}_{\boldsymbol{K}}^{(0)}=\frac{1}{\gamma^{\text{eff}}}\text{DevSym}\left\{\boldsymbol{B}_{\boldsymbol{K}}^{(0)}\left\langle\boldsymbol{\Sigma}_R^{(0)}\right\rangle\right\},\tag{121}$$

10991476, 2025, 1, Downloaded from https://onlinelibrary.wiley.com/doi/10.1002/nma.10367 by Politecnico Di Torino Sist. Bibl Del Polit Di Torino, Wiley Online Library on [12/02/2025]. See the Terms and Conditions (https://onlinelibrary.wiley.com/terms-and-conditions) on Wiley Online Library for rules of use; OA articles are governed by the applicable Creative Commons License

where $\boldsymbol{B}_{\boldsymbol{K}}^{(0)} = \boldsymbol{Z}^{(0)}(\boldsymbol{Z}^{(0)})^{\mathrm{T}}$ is the leading term of the expansion of $\boldsymbol{B}_{\boldsymbol{K}}$, $\left\langle \boldsymbol{\Sigma}_{\mathrm{R}}^{(0)} \right\rangle = \boldsymbol{Z}^{(0)}\langle \boldsymbol{\Sigma}^{(0)} \rangle (\boldsymbol{Z}^{(0)})^{\mathrm{T}}$ is the homogenized Mandel stress tensor associated with the reference placement, and γ^{eff} can be identified with the effective viscosity defined in Equation (111a).

7 | MODEL SUMMARY AND COMPUTATION OF THE EFFECTIVE COEFFICIENTS

In this section, to ease the exposition of the model developed up to this point, we summarize the main results of our work, and we compute the effective coefficients of the composite under study. To begin with, we recall that the unknowns of the problem are the microscopic fields $\boldsymbol{\xi}_\eta$, $\boldsymbol{\omega}_\eta$ and $\boldsymbol{\Lambda}_\eta$, with $\eta = 1, 2$, introduced with the *Ansätze* (62a) and (62b), and the macroscopic fields $\boldsymbol{u}^{(0)}$ and $\boldsymbol{L}_{\boldsymbol{K}}^{(0)}$, from which $\boldsymbol{K}^{(0)}$ is computed.

The microscopic fields $\boldsymbol{\xi}_\eta$, $\boldsymbol{\omega}_\eta$ and $\boldsymbol{\Lambda}_\eta$, with $\eta = 1, 2$, are obtained by solving the three cell problems (87), (88), and (98), respectively, and are coupled both reciprocally and with the macroscale fields through the plastic Green–Lagrange strain tensor $\boldsymbol{E}_{\boldsymbol{K}}^{(0)}$. In fact, the scales are coupled, and the system altogether is multiscale in the sense that the cell problems affect the macroscale, and vice versa.

At the macroscopic level, the displacement field $\boldsymbol{u}^{(0)}$ and the remodeling tensor field $\boldsymbol{K}^{(0)}$ are obtained as the solutions of the respective macroscopic homogenized problems. Since we averaged over the reference cell, we denote by $\mathscr{B}_{\mathrm{R}}^{\mathrm{hom}}$ the homogenized counterpart of the composite over which we solve the homogenized problems. The first one reads (see Equation (106))

$$\begin{cases} \mathrm{Div}_{\bar{X}}\left(\mathcal{C}_{\mathrm{R}}^{\mathrm{eff}} : \mathrm{Grad}_{\bar{X}}\boldsymbol{u}^{(0)}\right) = -\mathrm{Div}_{\bar{X}}\hat{\boldsymbol{D}}_{\mathrm{R}}, & \text{in } \mathscr{B}_{\mathrm{R}}^{\mathrm{hom}}, \\ \left(\mathcal{C}_{\mathrm{R}}^{\mathrm{eff}} : \mathrm{Grad}_{\bar{X}}\boldsymbol{u}^{(0)}\right)\boldsymbol{N} + \hat{\boldsymbol{D}}_{\mathrm{R}}\boldsymbol{N} = \bar{\boldsymbol{T}}, & \text{on } \partial_T\mathscr{B}_{\mathrm{R}}^{\mathrm{hom}}, \\ \boldsymbol{u}^{(0)} = \bar{\boldsymbol{u}}, & \text{on } \partial_u\mathscr{B}_{\mathrm{R}}^{\mathrm{hom}}, \end{cases} \tag{122}$$

where $\partial_T\mathscr{B}_{\mathrm{R}}^{\mathrm{hom}}$ identifies the portion of the boundary of $\mathscr{B}_{\mathrm{R}}^{\mathrm{hom}}$, that is, $\partial\mathscr{B}_{\mathrm{R}}^{\mathrm{hom}}$, on which the traction field $\bar{\boldsymbol{T}}$ is applied, and $\partial_u\mathscr{B}_{\mathrm{R}}^{\mathrm{hom}}$ is the portion of $\partial\mathscr{B}_{\mathrm{R}}^{\mathrm{hom}}$ on which the displacement field $\bar{\boldsymbol{u}}$ is prescribed. Finally, the upscaled problem for the evolution of the internal structure is (see Equation (114))

$$\begin{cases} \gamma^{\mathrm{eff}}\boldsymbol{L}_{\boldsymbol{K}}^{(0)} - \sum_{\eta=1,2}\left\langle \mathrm{DevSym}\boldsymbol{\Sigma}_{\eta\mathrm{lin}}^{(0)} \right\rangle_\eta - \frac{1}{L_0^2}\mathrm{Div}_{\bar{X}}\left[(\mathrm{DevSym}\mathbb{D}^{\mathrm{eff}}) : \mathrm{Grad}_{\bar{X}}\boldsymbol{L}_{\boldsymbol{K}}^{(0)}\right] = \boldsymbol{O}, & \text{in } \mathscr{B}_{\mathrm{R}}^{\mathrm{hom}}, \\ \boldsymbol{L}_{\boldsymbol{K}}^{(0)} - \left(\boldsymbol{L}_{\boldsymbol{K}}^{(0)}\right)^{\mathrm{T}} = \boldsymbol{O}, & \text{in } \mathscr{B}_{\mathrm{R}}^{\mathrm{hom}}, \\ \left[\left(\mathrm{DevSym}\mathbb{D}^{\mathrm{eff}}\right) : \mathrm{Grad}_{\bar{X}}\boldsymbol{L}_{\boldsymbol{K}}^{(0)}\right]\boldsymbol{N} = \boldsymbol{O}, & \text{on } \partial\mathscr{B}_{\mathrm{R}}^{\mathrm{hom}}. \end{cases} \tag{123}$$

Remark 7.1 (Self-similarity of the homogenized problems)**.** The dynamic equation presented in the macroscopic problem (123), which is obtained at the end of the homogenization procedure, is "self-similar" to the dynamic equation that represents the balance of forces power conjugate with $\boldsymbol{L}_{\boldsymbol{K}}$ [42]. Thus, the leading term $\boldsymbol{K}^{(0)}$ of the asymptotic expansion of $\boldsymbol{K}^{\epsilon}$ is the solution of a problem that has the same structure as its counterpart before the asymptotic expansion was conducted. However, a difference resides in the presence of the effective coefficients, which are calculated by using the solutions of the cell problems (87), (88) and (98). Moreover, self-similarity does not occur for the balance of linear momentum, since its homogenized version is given by Equation (122), in which the right-hand side is a result of homogenization and, as such, is not present in the original balance law.

Remark 7.2 (Influence of microscale plastic distortions through the effective coefficients)**.** The homogenized problems (122) and (123) describe the upscaled inelastic behavior of the composite under investigation. Their simultaneous solution allows to determine the coarse-scale fields $\boldsymbol{u}^{(0)}$ and $\boldsymbol{K}^{(0)}$. In particular, $\boldsymbol{u}^{(0)}$ inherits the information on the composite's internal structure from the effective elastic coefficient $\mathcal{C}_{\mathrm{R}}^{\mathrm{eff}}$ and the "forcing term" $\hat{\boldsymbol{D}}_{\mathrm{R}}$ [19] (see Equation (122)). To this end, it is important to notice that each of these quantities depends on the internal geometry of the composite and on the composite's microscale elastic properties through the elasticity tensors $\mathcal{C}_{\mathrm{R}\eta}^{(0)}$. The former emerges through the averaging operators, which require integrating over the volumes $\mathscr{V}_{\mathrm{R}\eta}$, and through the auxiliary fields $\boldsymbol{\xi}_\eta$ and $\boldsymbol{\omega}_\eta$, which solve the cell problems (87) and (88), respectively. In fact, the fields $\boldsymbol{\xi}_\eta$ and $\boldsymbol{\omega}_\eta$ are driven by the remodeling distortions through the remodeling tensor $\boldsymbol{K}^{(0)}$, which, thus, exerts an indirect influence on $\mathcal{C}_{\mathrm{R}}^{\mathrm{eff}}$ and, consequently,

10991476, 2025, 1, Downloaded from https://onlinelibrary.wiley.com/doi/10.1002/nma.10367 by Politecnico Di Torino Sist. Bibl Del Polit Di Torino, Wiley Online Library on [12/02/2025]. See the Terms and Conditions (https://onlinelibrary.wiley.com/terms-and-conditions) on Wiley Online Library for rules of use; OA articles are governed by the applicable Creative Commons License

an even more indirect influence on $\boldsymbol{u}^{(0)}$ [19]. On top of that, as pointed out in [19], and as shown in Equations (103a) and (103b), both $C_{\mathrm{R}}^{\mathrm{eff}}$ and $\hat{\boldsymbol{D}}_{\mathrm{R}}$ evolve in time due to $\boldsymbol{K}^{(0)}$, so that the remodeling distortions produce also a direct influence on the change of the composite's effective elastic properties. For what concerns $\boldsymbol{K}^{(0)}$, we notice that the solution to the problem (123), that is, $\boldsymbol{K}^{(0)}$ itself, is directly influenced by the effective "viscosity" γ^{eff} and by the upscaled tensor field $\mathbb{D}^{\mathrm{eff}}$ (see Equations (111a) and (111b)). More in detail, while γ^{eff} is "simply" the volume average over the composite's unit cell of the viscosities of the phases, $\mathbb{D}^{\mathrm{eff}}$ requires the knowledge of the auxiliary fifth-order tensor fields $\boldsymbol{\Lambda}_\eta$. This result cannot be obtained within the standard theory of plasticity, and, in our context, it arises as a consequence of the asymptotic expansion of the strain-gradient plastic flow rule proposed in [42]. In this respect, it constitutes the main novelty of our work, and it indicates the way in which the fine-scale gradient of the rate of the tensor of remodeling distortions, that is, $\boldsymbol{L}_{\boldsymbol{K}\eta}^{(1)}$, influences $\boldsymbol{K}^{(0)}$. In turn, this influence reflects also on $\boldsymbol{u}^{(0)}$, thereby providing an additional effect that cannot be captured by standard models of plasticity, or remodeling, and an estimate of the weight of such effect. Once the shape of the periodic reference cell and the material properties of the composite's constituents are known, the three effective coefficients $C_{\mathrm{R}}^{\mathrm{eff}}$, γ^{eff}, and $\mathbb{D}^{\mathrm{eff}}$ can be computed with the formulation given by

$$C_{\mathrm{R}}^{\mathrm{eff}} = \sum_{\eta=1,2} \left(C_{\mathrm{R}\eta}^{(0)} - \boldsymbol{I} \underline{\otimes} \left(C_{\mathrm{R}\eta}^{(0)} : \boldsymbol{E}_{\boldsymbol{K}}^{(0)} \right) \right) : \left(\varphi_\eta \mathbb{I}_4 + \langle T\mathrm{Grad}_{\tilde{Y}} \boldsymbol{\xi}_\eta \rangle_\eta \right), \tag{124a}$$

$$\gamma^{\mathrm{eff}} = \sum_{\eta=1,2} \varphi_\eta \sigma_\eta \tau_\eta, \tag{124b}$$

$$\mathbb{D}^{\mathrm{eff}} = \sum_{\eta=1,2} \ell_\eta^2 \sigma_\eta \tau_\eta \left(\varphi_\eta \mathbb{I}_6 + \langle T\mathrm{Grad}_{\tilde{Y}} \boldsymbol{\Lambda}_\eta \rangle_\eta \right). \tag{124c}$$

Remark 7.3 (Remodeling as a design opportunity)**.** With this work and, in particular, with the determination of $C_{\mathrm{R}}^{\mathrm{eff}}$ and its dependence on $\boldsymbol{E}_{\boldsymbol{K}}^{(0)}$, we have an explicit expression of what remodeling is in the present context. The determination of the deformation fields and of the internal stresses depends on the direct and indirect influences of the remodeling distortions at both scales, as summarized in Figure 1.

In a sense, one may use our results to *design* a remodeling composite medium, which changes its internal structure according to the dynamics described by the problems (122) and (123). This amounts to solving the inverse problem in which one starts with a target stress-strain curve, which could be indicated in response to a specific need, for example, in the biomedical context, the devising a graft [130], and finds which material properties and geometry of the microstructure the composite should possess.

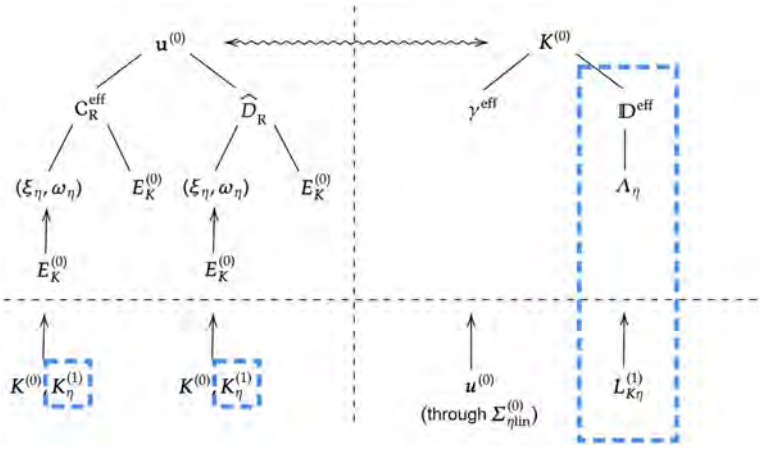


FIGURE 1 A schematic representation that highlights both the direct and indirect influences of the fine plastic distortions tensor $\boldsymbol{K}^{(1)}$. The dashed blue boxes enclose the contributions that would be absent within a standard theory of plasticity. [Colour figure can be viewed at wileyonlinelibrary.com]

10991476, 2025, 1, Downloaded from https://onlinelibrary.wiley.com/doi/10.1002/mma.10367 by Politecnico Di Torino Sist. Bibl Del Polit Di Torino, Wiley Online Library on [12/02/2025]. See the Terms and Conditions (https://onlinelibrary.wiley.com/terms-and-conditions) on Wiley Online Library for rules of use; OA articles are governed by the applicable Creative Commons License

8 | MULTILAYERED ELASTO-VISCOPLASTIC COMPOSITE UNDER AXIAL STRETCH

In this section, we consider the case in which the elasto-viscoplastic composite under study, described by the systems of equations in Section 7, possesses a layered structure, that is, a structure with a very regular pattern, which offers the possibility of simplifying significantly the problem at hand. We perform numerical simulations to investigate the potentialities of our model, which enriches the setting described in [19].

8.1 | Working hypotheses

In the forthcoming description of the composite's geometry, the space variables X and Y are not dimensionless. However, in this description, the displacement fields and the fields of remodeling distortions and of the rate of remodeling distortions are assumed to be functions of X and Y through their non-dimensional counterparts $\tilde{X}$ and $\tilde{Y}$.

To ease the computational burden, and to highlight the most essential features of the present model, we introduce the following hypotheses, which adhere the ones specified in [19]:

(a) The biphasic composite under investigation has a layered three-dimensional structure in which each phase occupies a single layer in alternating fashion: If the phase $\eta = 1$ occupies a given layer, the phase $\eta = 2$ occupies the preceding and the succeeding one. The reference shape of the composite is assumed to be a parallelepiped, so that its reference placement can be written as $\mathscr{B}_{\mathrm{R}} = \mathscr{S}_{\mathrm{R}} \times [0, L_0]$, with $\mathscr{S}_{\mathrm{R}}$ being its rectangular cross section. Given a global Cartesian reference frame $(O, \{\mathcal{E}_{\boldsymbol{A}}\}_{A=1}^{3})$, the origin O is the center of the bottom surface $\mathscr{S}_{\mathrm{R}}$ of the lowermost layer, the unit vector $\mathcal{E}_3$ is parallel to the vertical axis of the composite and is orthogonal to its layers, and the unit vectors $\mathcal{E}_1$ and $\mathcal{E}_2$ are parallel to the sides of $\mathscr{S}_{\mathrm{R}}$. Accordingly, in the associated system of macroscopic Cartesian coordinates (X_1, X_2, X_3), the unit vector $\mathcal{E}_3$ corresponds to the X_3-axis. The reference cell of the composite consists of two consecutive layers, each of which is occupied exclusively by one phase of the composite, and has geometry $\mathscr{S}_{\mathrm{R}} \times [0, \ell_0]$. To describe the reference cell, we take a Cartesian reference frame with axes collinear with those of the global frame, and an associated system of microscopic Cartesian coordinates (Y_1, Y_2, Y_3), with the Y_3-axis parallel to the X_3-axis. In addition to this very particular structural setting, we also assume that *all* the material properties and *all* the fields featuring in the cell problems (87), (88), and (98) are functions of space only along the direction orthogonal to the layers, and that, within each layer, they are homogeneous on each plane parallel to the layers themselves and, thus, to $\mathscr{S}_{\mathrm{R}}$. Consequently, a given quantity is a function of space only through Y_3 and/or X_3. More in detail, the averaged material properties of the body $\mathscr{B}_{\mathrm{R}}$ and the macroscopic quantities, such as, for example, $\boldsymbol{L}_{\boldsymbol{K}}^{(0)}$, are functions of space only through X_3, while the components of the elasticity tensors $C_{\mathrm{R1}}^{(0)}$ and $C_{\mathrm{R2}}^{(0)}$ are, in principle, functions both of the microscale variable Y_3 and of the macroscale variable X_3. As a result of this setting, the evolution of the three-dimensional composite material, featuring two sharply separated scales, is reformulated as a problem with spatial resolution only along the composite's axis both for the upscaled problems (122) and (123) and for the cell problems (87), (88), and (98). Moreover, the boundary conditions that, in this work, will be prescribed to the homogenized problems (122) and (123) are such that the current shape of the composite continues to be a rectangular parallelepiped with the same cross section as $\mathscr{B}_{\mathrm{R}}$ and different axial length. This very special hypothesis, added to the setting developed so far, makes it possible to study the evolution of the composite in the interval $[0, L_0]$, uniformly with respect to $\mathscr{S}_{\mathrm{R}}$, although both the homogenized problems and the cell problems remain three dimensional. Analogously, at the microscale, the cell problems formulated in the reference cell $\mathscr{Y}_{\mathrm{R}} = \mathscr{S}_{\mathrm{R}} \times [0, \ell_0]$, which is divided into the two subdomains $\mathscr{Y}_{\mathrm{R1}} = \mathscr{S}_{\mathrm{R}} \times [0, Y_\Gamma[$ and $\mathscr{Y}_{\mathrm{R2}} = \mathscr{S}_{\mathrm{R}} \times]Y_\Gamma, \ell_0]$, can be studied in the intervals $[0, Y_\Gamma[$ and $]Y_\Gamma, \ell_0]$, thereby dropping $\mathscr{S}_{\mathrm{R}}$.

(b) All the *intrinsic* material properties of each layer are assumed to be *homogeneous* inside the layer itself, so that the material properties of the composite as a whole are piece-wise constant along the direction of the geometric symmetry axis of the parallelepiped. Within this setting, the composite material turns out to be *transversely homogeneous*. In addition, each layer is hypothesized to consist of an *isotropic* hyperelastic material. Therefore, the aforementioned geometric symmetry axis coincides with the overall symmetry axis of the composite material as a whole. This description refers to the composite material in the absence of deformation. This means that, at this stage, each constituent of the composite, in each layer, finds itself in its undeformed state. The material properties of the constituents in their natural state are independent of the macroscopic variable X_3. In particular, we refer to the elasticity tensors C_η, and to the parameters τ_η and σ_η, which are associated with the viscoplastic behavior of the phases of the composite. Furthermore, because of isotropy, the elasticity tensor of each phase depends exclusively

10991476, 2025, 1, Downloaded from https://onlinelibrary.wiley.com/doi/10.1002/mma.10367 by Politecnico Di Torino Sist. Bibl Del Polit Di Torino, Wiley Online Library on [12/02/2025]. See the Terms and Conditions (https://onlinelibrary.wiley.com/terms-and-conditions) on Wiley Online Library for rules of use; OA articles are governed by the applicable Creative Commons License

on Lamé's parameters λ_η and μ_η, and the following equalities hold true [19]:

$$\mathcal{C}_\eta = \lambda_\eta \boldsymbol{I}\otimes\boldsymbol{I} + 2\mu_\eta \frac{\boldsymbol{I}\underline{\otimes}\boldsymbol{I} + \boldsymbol{I}\overline{\otimes}\boldsymbol{I}}{2}, \tag{125a}$$

$$[\mathcal{C}_\eta]_{1111} = [\mathcal{C}_\eta]_{2222} = [\mathcal{C}_\eta]_{3333} = \lambda_\eta + 2\mu_\eta, \tag{125b}$$

$$[\mathcal{C}_\eta]_{1122} = [\mathcal{C}_\eta]_{1133} = [\mathcal{C}_\eta]_{2233} = \lambda_\eta, \tag{125c}$$

$$[\mathcal{C}_\eta]_{2323} = [\mathcal{C}_\eta]_{1313} = [\mathcal{C}_\eta]_{1212} = \frac{1}{2}([\mathcal{C}_\eta]_{1111} - [\mathcal{C}_\eta]_{1122}) = \mu_\eta. \tag{125d}$$

Moreover, Lamé's parameters and τ_η and σ_η are taken to be piece-wise constant, as in [19], that is,

$$\lambda_\eta(Y) = \bar{\lambda}_\eta(Y_3) = \begin{cases} \lambda_1 & \text{in } \mathscr{Y}_{\mathrm{R1}}, \\ \lambda_2 & \text{in } \mathscr{Y}_{\mathrm{R2}}, \end{cases} \qquad \mu_\eta(Y) = \bar{\mu}_\eta(Y_3) = \begin{cases} \mu_1 & \text{in } \mathscr{Y}_{\mathrm{R1}}, \\ \mu_2 & \text{in } \mathscr{Y}_{\mathrm{R2}}, \end{cases} \tag{126a}$$

$$\tau_\eta(Y) = \bar{\tau}_\eta(Y_3) = \begin{cases} \tau_1 & \text{in } \mathscr{Y}_{\mathrm{R1}}, \\ \tau_2 & \text{in } \mathscr{Y}_{\mathrm{R2}}, \end{cases} \qquad \sigma_\eta(Y) = \bar{\sigma}_\eta(Y_3) = \begin{cases} \sigma_1 & \text{in } \mathscr{Y}_{\mathrm{R1}}, \\ \sigma_2 & \text{in } \mathscr{Y}_{\mathrm{R2}}. \end{cases} \tag{126b}$$

Finally, the elasticity tensor of the ηth constituent, pulled-back to the reference placement, that is, $\mathcal{C}^{(0)}_{\mathrm{R}\eta}$, is given by

$$\begin{aligned} \mathcal{C}^{(0)}_{\mathrm{R}\eta} &= (\det \boldsymbol{K}^{(0)})\boldsymbol{Z}^{(0)}\underline{\otimes}\boldsymbol{Z}^{(0)} : \mathcal{C}_\eta : (\boldsymbol{Z}^{(0)})^{\mathrm{T}}\underline{\otimes}(\boldsymbol{Z}^{(0)})^{\mathrm{T}} \\ &= \lambda_\eta \boldsymbol{B}^{(0)}_{\boldsymbol{K}}\otimes\boldsymbol{B}^{(0)}_{\boldsymbol{K}} + 2\mu_\eta \frac{\boldsymbol{B}^{(0)}_{\boldsymbol{K}}\underline{\otimes}\boldsymbol{B}^{(0)}_{\boldsymbol{K}} + \boldsymbol{B}^{(0)}_{\boldsymbol{K}}\overline{\otimes}\boldsymbol{B}^{(0)}_{\boldsymbol{K}}}{2}, \end{aligned} \tag{127}$$

with $\boldsymbol{B}^{(0)}_{\boldsymbol{K}} = ((\boldsymbol{K}^{(0)})^{\mathrm{T}}\boldsymbol{K}^{(0)})^{-1} = \boldsymbol{Z}^{(0)}(\boldsymbol{Z}^{(0)})^{\mathrm{T}}$, and where, as already mentioned, it holds that $\det \boldsymbol{K}^{(0)} = 1$, because of the hypothesis of isochoric plastic-like distortions.

(c) In a fashion similar to [19], we impose a purely diagonal tensor $\boldsymbol{K}^{(0)}$, and in compliance with the assumption of isochoric remodeling distortions, we assign it, for example, as $[\boldsymbol{K}^{(0)}]_{11} = \frac{1}{\sqrt{p}}$, $[\boldsymbol{K}^{(0)}]_{22} = \frac{1}{\sqrt{p}}$, and $[\boldsymbol{K}^{(0)}]_{33} = p$, where $p > 0$ is said to be the *remodeling parameter*. By doing so, the constraint of vanishing plastic spin is automatically satisfied, and the only non-vanishing components of $\boldsymbol{L}^{(0)}_{\boldsymbol{K}}$ are

$$\left[\boldsymbol{L}^{(0)}_{\boldsymbol{K}}\right]_{AA} = \left[\dot{\boldsymbol{K}}^{(0)}\right]_{AA}[\boldsymbol{Z}^{(0)}]_{AA} = -\frac{1}{2}\frac{\dot{p}}{p}, \qquad \text{for } A = 1, 2, \text{ no sum over } A, \tag{128a}$$

$$\left[\boldsymbol{L}^{(0)}_{\boldsymbol{K}}\right]_{33} = \left[\dot{\boldsymbol{K}}^{(0)}\right]_{33}[\boldsymbol{Z}^{(0)}]_{33} = \frac{\dot{p}}{p}. \tag{128b}$$

We do not assign $\boldsymbol{K}^{(1)}_\eta$ because it can be computed a posteriori, if needed, by integrating in time Equation (40b), in which the left-hand side is written as $\boldsymbol{L}^{(1)}_{\boldsymbol{K}\eta} = \boldsymbol{\Lambda}_\eta \vdots \mathrm{Grad}_{\mathrm{X}}\boldsymbol{L}^{(0)}_{\boldsymbol{K}}$ and the right-hand side is a combination of $\boldsymbol{K}^{(0)}$, $\dot{\boldsymbol{K}}^{(0)}$, $\boldsymbol{K}^{(1)}_\eta$, and $\dot{\boldsymbol{K}}^{(1)}_\eta$. This way, the information on the microstructure is embedded in $\boldsymbol{\Lambda}_\eta$.

Based on the definition of $\boldsymbol{K}^{(0)}$, the matrix representations of $\boldsymbol{B}^{(0)}_{\boldsymbol{K}}$ and of $\boldsymbol{E}^{(0)}_{\boldsymbol{K}}$ are

$$\left[\boldsymbol{B}^{(0)}_{\boldsymbol{K}}\right](X,t) = \mathrm{diag}\left\{p(X_3,t), p(X_3,t), [p(X_3,t)]^{-2}\right\}, \tag{129a}$$

$$\left[\boldsymbol{E}^{(0)}_{\boldsymbol{K}}\right](X,t) = \mathrm{diag}\left\{\frac{[p(X_3,t)]^{-1}-1}{2}, \frac{[p(X_3,t)]^{-1}-1}{2}, \frac{[p(X_3,t)]^{2}-1}{2}\right\}. \tag{129b}$$

Hence, the nonzero coefficients of $\mathcal{C}^{(0)}_{\mathrm{R}\eta}$ read

$$\left[\mathcal{C}^{(0)}_{\mathrm{R}\eta}\right]_{1111} = \left[\mathcal{C}^{(0)}_{\mathrm{R}\eta}\right]_{2222} = (\lambda_\eta + 2\mu_\eta)p^2, \qquad \left[\mathcal{C}^{(0)}_{\mathrm{R}\eta}\right]_{3333} = \frac{\lambda_\eta + 2\mu_\eta}{p^4}, \tag{130a}$$

$$\left[\mathcal{C}^{(0)}_{\mathrm{R}\eta}\right]_{1122} = \lambda_\eta p^2, \qquad \left[\mathcal{C}^{(0)}_{\mathrm{R}\eta}\right]_{1133} = \left[\mathcal{C}^{(0)}_{\mathrm{R}\eta}\right]_{2233} = \frac{\lambda_\eta}{p}, \tag{130b}$$

10991476, 2025, 1, Downloaded from https://onlinelibrary.wiley.com/doi/10.1002/nme.10367 by Politecnico Di Torino Sist. Bibl Del Polit Di Torino, Wiley Online Library on [12/02/2025]. See the Terms and Conditions (https://onlinelibrary.wiley.com/terms-and-conditions) on Wiley Online Library for rules of use; OA articles are governed by the applicable Creative Commons License

$$\left[C^{(0)}_{\mathrm{R}\eta}\right]_{2323} = \left[C^{(0)}_{\mathrm{R}\eta}\right]_{1313} = \frac{\mu_\eta}{p}, \qquad \left[C^{(0)}_{\mathrm{R}\eta}\right]_{1212} = \mu_\eta p^2. \tag{130c}$$

We notice that although the remodeling distortions, being such that $\boldsymbol{B}^{(0)}_{\boldsymbol{K}}$ is diagonal, preserve the symmetries of the elasticity tensor C_η, the components of the pulled-back tensor $C^{(0)}_{\mathrm{R}\eta}$ are different from those of C_η, and vary in time and *space* driven by the evolution of p. An important consequence of this result is that, although we have assumed that the spatial distribution of the components of the elasticity tensor C_η is resolved by the *fast variable* Y_3 only, the components of $C^{(0)}_{\mathrm{R}\eta}$ depend *both* on the slow variable X_3 *and* on the fast variable Y_3 [19]. However, because of Equations (126a) and (126b), the dependence on Y_3 is eliminated by choosing piece-wise constant Lamé's parameters.

By virtue of these results, for each $\eta = 1, 2$, the elasticity tensor $C^{(0)}_{\mathrm{R}\eta}$ defined in Equation (127) depends only on X_3 and t, and so does the term $C^{(0)}_{\mathrm{R}\eta} : \boldsymbol{E}^{(0)}_{\boldsymbol{K}}$. In particular, the latter quantity acquires the expression

$$C^{(0)}_{\mathrm{R}\eta} : \boldsymbol{E}^{(0)}_{\boldsymbol{K}} = \lambda_\eta \mathrm{tr}\left(\boldsymbol{B}^{(0)}_{\boldsymbol{K}}\boldsymbol{E}^{(0)}_{\boldsymbol{K}}\right)\boldsymbol{B}^{(0)}_{\boldsymbol{K}} + 2\mu_\eta \boldsymbol{B}^{(0)}_{\boldsymbol{K}}\boldsymbol{E}^{(0)}_{\boldsymbol{K}}\boldsymbol{B}^{(0)}_{\boldsymbol{K}}, \tag{131}$$

and its matrix representation is diagonal.

(d) We simulate a stretch test for the elasto-viscoplastic composite material under study. We remark that, since the procedure that we have followed for obtaining the upscaled equations, that is, prior to the introduction of the simplifying hypotheses described above, did not call for boundary conditions, the homogenization procedure does not depend on them [19], provided they maintain the symmetries implied by the simplifying hypotheses themselves. However, boundary conditions do play a role in solving the two upscaled, coupled, boundary-value problems (122) and (123). To this end, we prescribe two sets of boundary conditions, one for the determination of the motion of the system and one for the remodeling parameter. For the former, we assign Dirichlet boundary conditions on the overall boundary of the body. In particular, we require the vanishing of the transversal components of the displacement field at all times and at all points of the lateral boundary of the composite, that is, we set $[\boldsymbol{u}]_1(X,t) = [\boldsymbol{u}]_2(X,t) = 0$ for all $X \in \partial\mathscr{S}_\mathrm{R} \times [0, L_0]$, with $\partial\mathscr{S}_\mathrm{R}$ being the boundary of the lower surface of the body. Analogously, we set $[\boldsymbol{u}]_3(X,t) = 0$ for all $X \in \mathscr{S}_\mathrm{R}$, that is, at all points of the lower surface of the composite. These conditions are assumed to be respected exactly, that is, at all orders of the asymptotic expansion of the displacement. Furthermore, for the Dirichlet condition applied to the axial component of the displacement evaluated at the upper boundary of the composite, we prescribe the linear displacement ramp $\frac{u_\mathrm{L}}{T}t$, where u_L is a target displacement, and T is the required time to reach u_L. In this case, however, we enforce this condition to the boundary of the homogenized composite $\mathscr{B}^{\mathrm{hom}}_\mathrm{R}$, thereby involving only the leading order of the asymptotic expansion of the displacement. Hence, we write $[\boldsymbol{u}^{(0)}]_3(\tilde{X},t) = \frac{u_\mathrm{L}}{T}t$ at $\tilde{X}_3 = 1$ (i.e., $X_3 = L_0$).

For the problem (123), we prescribe homogeneous boundary conditions for the remodeling distortions, which, in accordance with Remark 4.3, amounts to requiring $\mathfrak{E}_{\mathrm{rem}} = \mathbf{O}$. Moreover, we study two cases of initial distributions for the remodeling parameter: first, we consider $p_{\mathrm{in}}(\tilde{X}_3) = \alpha + \beta\cos(16\pi\tilde{X}_3)$, with $\alpha > \beta > 0$, which amounts to studying the evolution of a composite that has already experienced "controlled" remodeling; second, we consider $p_{\mathrm{in}}(\tilde{X}_3) = 1+\theta(\tilde{X}_3)$, where θ is random variable with probability distribution of uniform type, so that $\theta(\tilde{X}_3) \in (-\beta, \beta)$, which aims to represent a heterogeneous material in which there is no information prior to the experiment.

In accordance with the boundary conditions discussed above, the zeroth-order displacement field $\boldsymbol{u}^{(0)}$, and the auxiliary fields $\boldsymbol{\xi}_\eta$ and $\boldsymbol{\omega}_\eta$ are prescribed to be

$$[\boldsymbol{u}^{(0)}]_I(\tilde{X},t) = 0, \qquad \sum_{B,C=1}^{3}[\boldsymbol{\xi}_\eta]_{IBC}(\tilde{X},\tilde{Y},t)\frac{\partial[\boldsymbol{u}^{(0)}]_B}{\partial\tilde{X}_C}(\tilde{X},t) = 0,\ [\boldsymbol{\omega}_\eta]_I(\tilde{X},\tilde{Y},t) = 0,\ I = 1,2, \tag{132a}$$

$$[\boldsymbol{u}^{(0)}]_3(\tilde{X},t) \equiv [\bar{\boldsymbol{u}}^{(0)}]_3(\tilde{X}_3,t), \tag{132b}$$

so that the conditions $\left[\boldsymbol{u}^{(1)}_\eta\right]_1(\tilde{X},\tilde{Y},t) = \left[\boldsymbol{u}^{(1)}_\eta\right]_2(\tilde{X},\tilde{Y},t) = 0$ are identically satisfied. Therefore, the *Ansatz* (62a), and Equations (132a) and (132b) imply that the only non-vanishing component of the first-order displacement field is

$$\begin{aligned}\left[\boldsymbol{u}^{(1)}_\eta\right]_3(\tilde{X},\tilde{Y},t) &= \sum_{B=1}^{3}\sum_{C=1}^{3}[\boldsymbol{\xi}_\eta]_{3BC}(\tilde{X},\tilde{Y},t)\frac{\partial[\boldsymbol{u}^{(0)}]_B}{\partial\tilde{X}_C}(\tilde{X},t) + [\boldsymbol{\omega}_\eta]_3(\tilde{X},\tilde{Y},t)\\ &= [\boldsymbol{\xi}_\eta]_{333}(\tilde{X},\tilde{Y},t)\frac{\partial[\bar{\boldsymbol{u}}^{(0)}]_3}{\partial\tilde{X}_3}(\tilde{X}_3,t) + [\boldsymbol{\omega}_\eta]_3(\tilde{X},\tilde{Y},t).\end{aligned} \tag{133}$$

10991476, 2025, 1, Downloaded from https://onlinelibrary.wiley.com/doi/10.1002/nma.10367 by Politecnico Di Torino Sist. Bibl Del Polit Di Torino, Wiley Online Library on [12/02/2025]. See the Terms and Conditions (https://onlinelibrary.wiley.com/terms-and-conditions) on Wiley Online Library for rules of use; OA articles are governed by the applicable Creative Commons License

We notice that due to the form of the matrix representation of the gradient of the displacement field, the sum in Equation (133) involves only the 333-component of $\boldsymbol{\xi}_\eta$. Moreover, to preserve the symmetries of the original problem and, in particular, to eliminate shear deformations both at the microscale and at the macroscale, the functions $[\boldsymbol{\xi}_\eta]_{333}$ and $[\boldsymbol{\omega}_\eta]_3$ are required to exhibit the following dependence:

$$[\boldsymbol{\xi}_\eta]_{333}(\tilde{X},\tilde{Y},t) = \left[\bar{\boldsymbol{\xi}}_\eta\right]_{333}(\tilde{X}_3,\tilde{Y}_3,t), \tag{134a}$$

$$[\boldsymbol{\omega}_\eta]_3(\tilde{X},\tilde{Y},t) = [\bar{\boldsymbol{\omega}}_\eta]_3(\tilde{X}_3,\tilde{Y}_3,t). \tag{134b}$$

Finally, Equations (132a), (132b), (133), (134a), and (134b) yield a zeroth-order deformation gradient tensor $\boldsymbol{F}_\eta^{(0)}$ with diagonal matrix representation given by

$$\begin{aligned}[\boldsymbol{F}_\eta^{(0)}](\tilde{X},t) &= \operatorname{diag}\left\{1,1,1+\frac{u_c}{L_0}\left[\left(1+\frac{\partial\left[\bar{\boldsymbol{\xi}}_\eta\right]_{333}}{\partial\tilde{Y}_3}(\tilde{X}_3,\tilde{Y}_3,t)\right)\frac{\partial[\bar{\boldsymbol{u}}^{(0)}]_3}{\partial\tilde{X}_3}(\tilde{X}_3,t)+\frac{\partial[\bar{\boldsymbol{\omega}}_\eta]_3}{\partial\tilde{Y}_3}(\tilde{X}_3,\tilde{Y}_3,t)\right]\right\}\\ &= \operatorname{diag}\left\{1,1,1+\frac{u_c}{L_0}\frac{\partial[\bar{\boldsymbol{u}}^{(0)}]_3}{\partial\tilde{X}_3}(\tilde{X}_3,t)\right\}\\ &\quad+\operatorname{diag}\left\{0,0,\frac{u_c}{L_0}\left(\frac{\partial\left[\bar{\boldsymbol{\xi}}_\eta\right]_{333}}{\partial\tilde{Y}_3}(\tilde{X}_3,\tilde{Y}_3,t)\frac{\partial[\bar{\boldsymbol{u}}^{(0)}]_3}{\partial\tilde{X}_3}(\tilde{X}_3,t)+\frac{\partial[\bar{\boldsymbol{\omega}}_\eta]_3}{\partial\tilde{Y}_3}(\tilde{X}_3,\tilde{Y}_3,t)\right)\right\},\end{aligned} \tag{135}$$

where the first term on the right-hand side is independent of η and represents the effective part of the deformation gradient tensor, while the second term depends on η since it is related to the perturbation to the deformation due to the microstructure.

8.2 | Solution of the upscaled boundary-value problems and numerical results

In this section, we solve analytically the cell problems that we have formulated for both $\boldsymbol{u}_\eta^{(1)}$ and $\boldsymbol{L}_{\boldsymbol{K}\eta}^{(1)}$, so that we can compute the composite's effective coefficients (124a)-(124c) by hand. To this end, we remark that, since we are imposing some stringent conditions on the components of the deformation, we do not directly employ the systems of equations described in Section 7 for the balance of linear momentum. In fact, they are obtained in general circumstances and without constraints on the motion. Rather, we follow the procedure delineated in the sequel to formulate the appropriate cell problems stemming from the balance of linear momentum. Afterwards, we solve for the effective coefficient of the remodeling parameter, and we write the upscaled model for the multilayered composite under study.

8.2.1 | Computation of the effective elastic coefficients

Under the hypotheses specified so far, the gradient $\operatorname{Grad}_{\tilde{X}}\boldsymbol{u}^{(0)}$ is independent of $\tilde{Y}$ and, thus, Equation (59a) can be rewritten as

$$\operatorname{Div}_{\tilde{Y}}\left\{\mathcal{C}_{\mathrm{R}\eta}^{(0)} : \operatorname{Grad}_{\tilde{Y}}\boldsymbol{u}_\eta^{(1)}\right\} - \operatorname{Div}_{\tilde{Y}}\left\{\left(\operatorname{Grad}_{\tilde{Y}}\boldsymbol{u}_\eta^{(1)}\right)\left(\mathcal{C}_{\mathrm{R}\eta}^{(0)} : \boldsymbol{E}_{\boldsymbol{K}}^{(0)}\right)\right\} = \boldsymbol{0}. \tag{136}$$

In index notation, Equation (136) reads

$$\sum_{B=1}^{3}\frac{\partial}{\partial\tilde{Y}_B}\left\{\sum_{C=1}^{3}\sum_{D=1}^{3}\left[\mathcal{C}_{\mathrm{R}\eta}^{(0)}\right]_{ABCD}\frac{\partial\left[\boldsymbol{u}_\eta^{(1)}\right]_C}{\partial\tilde{Y}_D}\right\} - \sum_{B=1}^{3}\frac{\partial}{\partial\tilde{Y}_B}\left\{\sum_{L=1}^{3}\frac{\partial\left[\boldsymbol{u}_\eta^{(1)}\right]_A}{\partial\tilde{Y}_L}\left[\mathcal{C}_{\mathrm{R}\eta}^{(0)} : \boldsymbol{E}_{\boldsymbol{K}}^{(0)}\right]_{LB}\right\} = 0. \tag{137}$$

Then, since the components of $\mathcal{C}_{\mathrm{R}\eta}^{(0)}$ and $\mathcal{C}_{\mathrm{R}\eta}^{(0)} : \boldsymbol{E}_{\boldsymbol{K}}^{(0)}$ are independent of the microscale variables, and since $\boldsymbol{B}_{\boldsymbol{K}}^{(0)}$, $\boldsymbol{E}_{\boldsymbol{K}}^{(0)}$, and $\mathcal{C}_{\mathrm{R}\eta}^{(0)} : \boldsymbol{E}_{\boldsymbol{K}}^{(0)}$ are second-order tensors with diagonal matrix representation, Equation (137) can be rewritten as a generalized Navier–Cauchy equation (no sum over A)

$$(\lambda_\eta+\mu_\eta)\left[\boldsymbol{B}_{\boldsymbol{K}}^{(0)}\right]_{AA}\sum_{LL=11}^{33}\left[\boldsymbol{B}_{\boldsymbol{K}}^{(0)}\right]_{LL}\frac{\partial^2\left[\boldsymbol{u}_\eta^{(1)}\right]_L}{\partial\tilde{Y}_L\partial\tilde{Y}_A} + \sum_{LL=11}^{33}\left(\mu_\eta\left[\boldsymbol{B}_{\boldsymbol{K}}^{(0)}\right]_{AA}\left[\boldsymbol{B}_{\boldsymbol{K}}^{(0)}\right]_{LL} - \left[\mathcal{C}_{\mathrm{R}\eta}^{(0)} : \boldsymbol{E}_{\boldsymbol{K}}^{(0)}\right]_{LL}\right)\frac{\partial^2\left[\boldsymbol{u}_\eta^{(1)}\right]_A}{\partial\tilde{Y}_L\partial\tilde{Y}_L} = 0, \tag{138}$$

10991476, 2025, 1, Downloaded from https://onlinelibrary.wiley.com/doi/10.1002/mma.10367 by Politecnico Di Torino Sist. Bibl Del Polit Di Torino, Wiley Online Library on [12/02/2025]. See the Terms and Conditions (https://onlinelibrary.wiley.com/terms-and-conditions) on Wiley Online Library for rules of use; OA articles are governed by the applicable Creative Commons License

which has been obtained by requiring the all the components of $\boldsymbol{u}_\eta^{(1)}$ are of class C^2. With respect to the "classic" Navier–Cauchy equation, the generalization consists in the *remodeling-driven modulation* of Lamé's elastic constants λ_η and μ_η due to the components of $\boldsymbol{B}_{\boldsymbol{K}}^{(0)}$, and in the *additive rescaling* of the coefficient of the second derivatives $\partial^2\left[\boldsymbol{u}_\eta^{(1)}\right]_A/\partial\tilde{Y}_L\partial\tilde{Y}_L$ due to $C_{\mathrm{R}\eta}^{(0)} : \boldsymbol{E}_{\boldsymbol{K}}^{(0)}$.

By working out Equation (138) with the aid of the *Ansatz* (62a), and the results (132a), (132b), (133), (134a), (134b), and (135), we obtain one generalized Navier–Cauchy equation for the 333-component of $\boldsymbol{\xi}_\eta$ and, analogously, one Navier–Cauchy equation for the 3-component of $\boldsymbol{\omega}_\eta$, with $\eta = 1, 2$. Thanks to the simplification introduced so far, each of these equations becomes

$$\left\{(\lambda_\eta + 2\mu_\eta)\left[\boldsymbol{B}_{\boldsymbol{K}}^{(0)}\right]_{33}\left[\boldsymbol{B}_{\boldsymbol{K}}^{(0)}\right]_{33} - \left[C_{\mathrm{R}\eta}^{(0)} : \boldsymbol{E}_{\boldsymbol{K}}^{(0)}\right]_{33}\right\}\frac{\partial^2\left[\bar{\boldsymbol{\xi}}_\eta\right]_{333}}{\partial\tilde{Y}_3\partial\tilde{Y}_3} = 0, \tag{139a}$$

$$\left\{(\lambda_\eta + 2\mu_\eta)\left[\boldsymbol{B}_{\boldsymbol{K}}^{(0)}\right]_{33}\left[\boldsymbol{B}_{\boldsymbol{K}}^{(0)}\right]_{33} - \left[C_{\mathrm{R}\eta}^{(0)} : \boldsymbol{E}_{\boldsymbol{K}}^{(0)}\right]_{33}\right\}\frac{\partial^2[\bar{\boldsymbol{\omega}}_\eta]_3}{\partial\tilde{Y}_3\partial\tilde{Y}_3} = 0, \tag{139b}$$

and admits general solutions

$$\left[\bar{\boldsymbol{\xi}}_\eta\right]_{333}(\tilde{X}_3, \tilde{Y}_3, t) = [\boldsymbol{\mathfrak{X}}_\eta]_{3333}(\tilde{X}_3, t)\tilde{Y}_3 + [\boldsymbol{\Xi}_\eta]_{333}(\tilde{X}_3, t), \tag{140a}$$

$$[\bar{\boldsymbol{\omega}}_\eta]_3(\tilde{X}_3, \tilde{Y}_3, t) = [\boldsymbol{\mathfrak{W}}_\eta]_{33}(\tilde{X}_3, t)\tilde{Y}_3 + [\boldsymbol{\Omega}_\eta]_3(\tilde{X}_3, t). \tag{140b}$$

Note that the coefficient of the second-order derivatives of $\left[\bar{\boldsymbol{\xi}}_\eta\right]_{333}$ and $[\bar{\boldsymbol{\omega}}_\eta]_3$ in Equations (139a) and (139b) is a generalized, remodeling-dependent *P-wave modulus* and has to be positive definite for the admissible values of the scalar remodeling variable p (see the definition of $\boldsymbol{K}^{(0)}$ given above as well as Equations (129a)–(130c)). In other words, not all values of p are admissible for the overall well-posedness of the problem under investigation. This issue will be discussed in Remark 8.1 below.

The pairs $[\boldsymbol{\mathfrak{X}}_\eta]_{3333}(\tilde{X}_3, t)$ and $[\boldsymbol{\Xi}_\eta]_{333}(\tilde{X}_3, t)$, and $[\boldsymbol{\mathfrak{W}}_\eta]_{33}(\tilde{X}_3, t)$ and $[\boldsymbol{\Omega}_\eta]_3(\tilde{X}_3, t)$ are integration "constants" to be determined by imposing the set of auxiliary conditions that are enforced along with the cell problems. Such conditions require (i) periodicity of the fields $\boldsymbol{\xi}_\eta$ and $\boldsymbol{\omega}_\eta$ at the boundaries of the reference cell that are orthogonal to the overall symmetry axis (the vertical axis) of the composite; (ii) no jump of the fields $\boldsymbol{\xi}_\eta$ and $\boldsymbol{\omega}_\eta$ across the interface separating the composite's constituents inside the reference cell (recall that the interface is orthogonal to the symmetry axis); (iii) no jump of the stress-like quantities associated with $\boldsymbol{\xi}_\eta$ and $\boldsymbol{\omega}_\eta$ at the reference cell's interface (these quantities are, in fact, the arguments of the divergence operators in Equations (87) and (88); and (iv) the fulfillment of an additional condition for the uniqueness of the solutions of the cell problems (139a) and (139b), which amounts to imposing the vanishing of the averages $\sum_{\eta=1,2}\langle\boldsymbol{\xi}_\eta\rangle_\eta$ and $\sum_{\eta=1,2}\langle\boldsymbol{\omega}_\eta\rangle_\eta$.

Condition (iii) descends from the physical consideration (30b), stating that the tractions at the interface of the reference cell, determined by $\boldsymbol{P}_{\eta\mathrm{lin}}^{(0)}\boldsymbol{N}_\Gamma \equiv \boldsymbol{P}_{\eta\mathrm{lin}}^{(0)}\mathcal{E}_3$ for each $\eta = 1, 2$, equal each other. In our context, since the representation of $\boldsymbol{P}_{\eta\mathrm{lin}}^{(0)}$ is diagonal, this condition amounts to requiring that the stresses $[\boldsymbol{P}_{1\mathrm{lin}}^{(0)}]_{33}$ and $[\boldsymbol{P}_{2\mathrm{lin}}^{(0)}]_{33}$ are the same at the cell's interface. Hence, given the expression of $\boldsymbol{P}_{\eta\mathrm{lin}}^{(0)}$ specified in Equation (85a), we find

$$\left[\boldsymbol{P}_{\eta\mathrm{lin}}^{(0)}\right]_{33} = \left(\left[C_{\mathrm{R}\eta}^{(0)}\right]_{3333} - \left[C_{\mathrm{R}\eta}^{(0)} : \boldsymbol{E}_{\boldsymbol{K}}^{(0)}\right]_{33}\right)\left[\left(1 + \frac{\partial\left[\bar{\boldsymbol{\xi}}_\eta\right]_{333}}{\partial\tilde{Y}_3}\right)\frac{\partial[\bar{\boldsymbol{u}}^{(0)}]_3}{\partial\tilde{X}_3} + \frac{\partial[\bar{\boldsymbol{\omega}}_\eta]_3}{\partial\tilde{Y}_3}\right] - \frac{L_0}{u_\mathrm{c}}\left[C_{\mathrm{R}\eta}^{(0)} : \boldsymbol{E}_{\boldsymbol{K}}^{(0)}\right]_{33}, \tag{141}$$

and, by employing the general expressions of $\left[\bar{\boldsymbol{\xi}}_\eta\right]_{333}$ and $[\bar{\boldsymbol{\omega}}_\eta]_3$ reported in Equations (140a) and (140b), respectively, factorizing $\partial[\bar{\boldsymbol{u}}^{(0)}]_3/\partial\tilde{X}_3$, and separating the contributions associated with $\bar{\boldsymbol{\xi}}_\eta$ from those associated with $\bar{\boldsymbol{\omega}}_\eta$, we obtain

$$\mathcal{Q}_1\left(1 + [\boldsymbol{\mathfrak{X}}_1]_{3333}\right) = \mathcal{Q}_2\left(1 + [\boldsymbol{\mathfrak{X}}_2]_{3333}\right), \tag{142a}$$

$$\mathcal{Q}_1[\boldsymbol{\mathfrak{W}}_1]_{33} - \frac{L_0}{u_\mathrm{c}}\left[C_{\mathrm{R1}}^{(0)} : \boldsymbol{E}_{\boldsymbol{K}}^{(0)}\right]_{33} = \mathcal{Q}_2[\boldsymbol{\mathfrak{W}}_2]_{33} - \frac{L_0}{u_\mathrm{c}}\left[C_{\mathrm{R2}}^{(0)} : \boldsymbol{E}_{\boldsymbol{K}}^{(0)}\right]_{33}, \text{ with } \mathcal{Q}_\eta := \left[C_{\mathrm{R}\eta}^{(0)}\right]_{3333} - \left[C_{\mathrm{R}\eta}^{(0)} : \boldsymbol{E}_{\boldsymbol{K}}^{(0)}\right]_{33}. \tag{142b}$$

Furthermore, for the special case considered in this section, conditions (i), (ii), and (iv) read:

Periodicity

$$[\bar{\boldsymbol{\xi}}_1]_{333}(\tilde{X}_3, 0, t) = [\bar{\boldsymbol{\xi}}_2]_{333}(\tilde{X}_3, 1, t), \qquad \Rightarrow\ [\boldsymbol{\Xi}_1]_{333} = [\boldsymbol{\mathfrak{X}}_2]_{3333} + [\boldsymbol{\Xi}_2]_{333}, \tag{143a}$$

10991476, 2025, 1, Downloaded from https://onlinelibrary.wiley.com/doi/10.1002/nma.10367 by Politecnico Di Torino Sist. Bibl Del Polit Di Torino, Wiley Online Library on [12/02/2025]. See the Terms and Conditions (https://onlinelibrary.wiley.com/terms-and-conditions) on Wiley Online Library for rules of use; OA articles are governed by the applicable Creative Commons License

$$[\bar{\boldsymbol{\omega}}_1]_3(\tilde{X}_3,0,t)=[\bar{\boldsymbol{\omega}}_2]_3(\tilde{X}_3,1,t),\qquad\Rightarrow\ [\boldsymbol{\Omega}_1]_3=[\mathfrak{W}_2]_{33}+[\boldsymbol{\Omega}_2]_3, \tag{143b}$$

No jump of the fields at the interface

$$[\bar{\boldsymbol{\xi}}_1]_{333}(\tilde{X}_3,\tilde{Y}_\Gamma,t)=[\bar{\boldsymbol{\xi}}_2]_{333}(\tilde{X}_3,\tilde{Y}_\Gamma,t),\qquad\Rightarrow\ [\boldsymbol{\mathfrak{X}}_1]_{3333}\tilde{Y}_\Gamma+[\boldsymbol{\Xi}_1]_{333}=[\boldsymbol{\mathfrak{X}}_2]_{3333}\tilde{Y}_\Gamma+[\boldsymbol{\Xi}_2]_{333}, \tag{143c}$$

$$[\bar{\boldsymbol{\omega}}_1]_3(\tilde{X}_3,\tilde{Y}_\Gamma,t)=[\bar{\boldsymbol{\omega}}_2]_3(\tilde{X}_3,\tilde{Y}_\Gamma,t),\qquad\Rightarrow\ [\mathfrak{W}_1]_{33}\tilde{Y}_\Gamma+[\boldsymbol{\Omega}_1]_3=[\mathfrak{W}_2]_{33}\tilde{Y}_\Gamma+[\boldsymbol{\Omega}_2]_3, \tag{143d}$$

Solvability condition

$$\sum_{\eta=1,2}\langle\left[\bar{\boldsymbol{\xi}}_\eta\right]_{333}(\tilde{X}_3,\cdot,t)\rangle_\eta=0,\qquad\Rightarrow\ \tilde{Y}_\Gamma\left\{[\boldsymbol{\mathfrak{X}}_1]_{3333}\frac{\tilde{Y}_\Gamma}{2}+[\boldsymbol{\Xi}_1]_{333}\right\}+(1-\tilde{Y}_\Gamma)\left\{[\boldsymbol{\mathfrak{X}}_2]_{3333}\frac{1+\tilde{Y}_\Gamma}{2}+[\boldsymbol{\Xi}_2]_{333}\right\}=0, \tag{143e}$$

$$\sum_{\eta=1,2}\langle[\bar{\boldsymbol{\omega}}_\eta]_{333}(\tilde{X}_3,\cdot,t)\rangle_\eta=0,\qquad\Rightarrow\ \tilde{Y}_\Gamma\left\{[\mathfrak{W}_1]_{33}\frac{\tilde{Y}_\Gamma}{2}+[\boldsymbol{\Omega}_1]_3\right\}+(1-\tilde{Y}_\Gamma)\left\{[\mathfrak{W}_2]_{33}\frac{1+\tilde{Y}_\Gamma}{2}+[\boldsymbol{\Omega}_2]_3\right\}=0, \tag{143f}$$

where the dependence of the integration "constants" on $\tilde{X}_3$ and t has been suppressed to save space, but it is understood. By solving the system (143a)–(143f), we obtain the following integration "constants":

$$[\boldsymbol{\mathfrak{X}}_1]_{3333}=(1-\tilde{Y}_\Gamma)\frac{\mathcal{Q}_2-\mathcal{Q}_1}{(1-\tilde{Y}_\Gamma)\mathcal{Q}_1+\tilde{Y}_\Gamma\mathcal{Q}_2},\qquad [\boldsymbol{\Xi}_1]_{333}=-\frac{\tilde{Y}_\Gamma(1-\tilde{Y}_\Gamma)}{2}\frac{\mathcal{Q}_2-\mathcal{Q}_1}{(1-\tilde{Y}_\Gamma)\mathcal{Q}_1+\tilde{Y}_\Gamma\mathcal{Q}_2}, \tag{144a}$$

$$[\boldsymbol{\mathfrak{X}}_2]_{3333}=-\tilde{Y}_\Gamma\frac{\mathcal{Q}_2-\mathcal{Q}_1}{(1-\tilde{Y}_\Gamma)\mathcal{Q}_1+\tilde{Y}_\Gamma\mathcal{Q}_2},\qquad [\boldsymbol{\Xi}_2]_{333}=\frac{\tilde{Y}_\Gamma(1+\tilde{Y}_\Gamma)}{2}\frac{\mathcal{Q}_2-\mathcal{Q}_1}{(1-\tilde{Y}_\Gamma)\mathcal{Q}_1+\tilde{Y}_\Gamma\mathcal{Q}_2}, \tag{144b}$$

$$[\mathfrak{W}_1]_{33}=(1-\tilde{Y}_\Gamma)\frac{\frac{L_0}{u_c}\left[\mathcal{C}^{(0)}_{\mathrm{R1}}:\boldsymbol{E}^{(0)}_{\boldsymbol{K}}\right]_{33}-\frac{L_0}{u_c}\left[\mathcal{C}^{(0)}_{\mathrm{R2}}:\boldsymbol{E}^{(0)}_{\boldsymbol{K}}\right]_{33}}{(1-\tilde{Y}_\Gamma)\mathcal{Q}_1+\tilde{Y}_\Gamma\mathcal{Q}_2},\qquad [\boldsymbol{\Omega}_1]_3=-\frac{\tilde{Y}_\Gamma(1-\tilde{Y}_\Gamma)}{2}\frac{\frac{L_0}{u_c}\left[\mathcal{C}^{(0)}_{\mathrm{R1}}:\boldsymbol{E}^{(0)}_{\boldsymbol{K}}\right]_{33}-\frac{L_0}{u_c}\left[\mathcal{C}^{(0)}_{\mathrm{R2}}:\boldsymbol{E}^{(0)}_{\boldsymbol{K}}\right]_{33}}{(1-\tilde{Y}_\Gamma)\mathcal{Q}_1+\tilde{Y}_\Gamma\mathcal{Q}_2}, \tag{144c}$$

$$[\mathfrak{W}_2]_{33}=-\tilde{Y}_\Gamma\frac{\frac{L_0}{u_c}\left[\mathcal{C}^{(0)}_{\mathrm{R1}}:\boldsymbol{E}^{(0)}_{\boldsymbol{K}}\right]_{33}-\frac{L_0}{u_c}\left[\mathcal{C}^{(0)}_{\mathrm{R2}}:\boldsymbol{E}^{(0)}_{\boldsymbol{K}}\right]_{33}}{(1-\tilde{Y}_\Gamma)\mathcal{Q}_1+\tilde{Y}_\Gamma\mathcal{Q}_2},\qquad [\boldsymbol{\Omega}_2]_3=\frac{\tilde{Y}_\Gamma(1+\tilde{Y}_\Gamma)}{2}\frac{\frac{L_0}{u_c}\left[\mathcal{C}^{(0)}_{\mathrm{R1}}:\boldsymbol{E}^{(0)}_{\boldsymbol{K}}\right]_{33}-\frac{L_0}{u_c}\left[\mathcal{C}^{(0)}_{\mathrm{R2}}:\boldsymbol{E}^{(0)}_{\boldsymbol{K}}\right]_{33}}{(1-\tilde{Y}_\Gamma)\mathcal{Q}_1+\tilde{Y}_\Gamma\mathcal{Q}_2}, \tag{144d}$$

where, again, the dependence of all the integration "constants" on $\tilde{X}_3$ and t is omitted, but understood.
The very special choice of the displacement field is such that Equation (122) becomes (in index notation)

$$\frac{\partial}{\partial\tilde{X}_3}\left\{\left[\mathcal{C}^{\mathrm{eff}}_{\mathrm{R}}\right]_{3333}\frac{\partial[\bar{\boldsymbol{u}}^{(0)}]_3}{\partial\tilde{X}_3}\right\}=-\frac{\partial\left[\hat{\boldsymbol{D}}_{\mathrm{R}}\right]_{33}}{\partial\tilde{X}_3}. \tag{145}$$

Therefore, only the coefficient $\left[\mathcal{C}^{\mathrm{eff}}_{\mathrm{R}}\right]_{3333}$ and the additional term $\left[\hat{\boldsymbol{D}}_{\mathrm{R}}\right]_{33}$ have to be determined. Looking at Equation (103a) and (103b), enforcing all the results obtained so far, and noticing that the volumetric fractions are $\varphi_1=\tilde{Y}_\Gamma$ and $\varphi_2=1-\tilde{Y}_\Gamma$, we find

$$\begin{aligned}\left[\mathcal{C}^{\mathrm{eff}}_{\mathrm{R}}\right]_{3333}&=\sum_{\eta=1,2}\left\{\left(\left[\mathcal{C}^{(0)}_{\mathrm{R}\eta}\right]_{3333}-\left[\mathcal{C}^{(0)}_{\mathrm{R}\eta}:\boldsymbol{E}^{(0)}_{\boldsymbol{K}}\right]_{33}\right)\left(\varphi_\eta+\left\langle\frac{\partial\left[\bar{\boldsymbol{\xi}}_\eta\right]_{333}}{\partial\tilde{Y}_3}\right\rangle_\eta\right)\right\}\\&=\sum_{\eta=1,2}\varphi_\eta\left\{\left(\left[\mathcal{C}^{(0)}_{\mathrm{R}\eta}\right]_{3333}-\left[\mathcal{C}^{(0)}_{\mathrm{R}\eta}:\boldsymbol{E}^{(0)}_{\boldsymbol{K}}\right]_{33}\right)(1+[\boldsymbol{\mathfrak{X}}_\eta]_{3333})\right\}\\&=\frac{\mathcal{Q}_1\mathcal{Q}_2}{(1-\tilde{Y}_\Gamma)\mathcal{Q}_1+\tilde{Y}_\Gamma\mathcal{Q}_2},\end{aligned} \tag{146a}$$

$$\begin{aligned}\left[\hat{\boldsymbol{D}}_{\mathrm{R}}\right]_{33}&=\sum_{\eta=1,2}\left\{\left(\left[\mathcal{C}^{(0)}_{\mathrm{R}\eta}\right]_{3333}-\left[\mathcal{C}^{(0)}_{\mathrm{R}\eta}:\boldsymbol{E}^{(0)}_{\boldsymbol{K}}\right]_{33}\right)\left\langle\frac{\partial[\bar{\boldsymbol{\omega}}_\eta]_3}{\partial\tilde{Y}_3}\right\rangle_\eta-\varphi_\eta\frac{L_0}{u_c}\left[\mathcal{C}^{(0)}_{\mathrm{R}\eta}:\boldsymbol{E}^{(0)}_{\boldsymbol{K}}\right]_{33}\right\}\\&=\sum_{\eta=1,2}\varphi_\eta\left\{\left(\left[\mathcal{C}^{(0)}_{\mathrm{R}\eta}\right]_{3333}-\left[\mathcal{C}^{(0)}_{\mathrm{R}\eta}:\boldsymbol{E}^{(0)}_{\boldsymbol{K}}\right]_{33}\right)[\mathfrak{W}_\eta]_{33}-\frac{L_0}{u_c}\left[\mathcal{C}^{(0)}_{\mathrm{R}\eta}:\boldsymbol{E}^{(0)}_{\boldsymbol{K}}\right]_{33}\right\}\\&=-\frac{(1-\tilde{Y}_\Gamma)\mathcal{Q}_1\frac{L_0}{u_c}\left[\mathcal{C}^{(0)}_{\mathrm{R2}}:\boldsymbol{E}^{(0)}_{\boldsymbol{K}}\right]_{33}+\tilde{Y}_\Gamma\mathcal{Q}_2\frac{L_0}{u_c}\left[\mathcal{C}^{(0)}_{\mathrm{R1}}:\boldsymbol{E}^{(0)}_{\boldsymbol{K}}\right]_{33}}{(1-\tilde{Y}_\Gamma)\mathcal{Q}_1+\tilde{Y}_\Gamma\mathcal{Q}_2}.\end{aligned} \tag{146b}$$

10991476, 2025, 1, Downloaded from https://onlinelibrary.wiley.com/doi/10.1002/nme.10367 by Politecnico Di Torino Sist. Bibl Del Polit Di Torino, Wiley Online Library on [12/02/2025]. See the Terms and Conditions (https://onlinelibrary.wiley.com/terms-and-conditions) on Wiley Online Library for rules of use; OA articles are governed by the applicable Creative Commons License

Remark 8.1 (Generalized P-wave modulus and strong ellipticity)**.** For the problem under investigation, the coefficient of the second-order derivatives of $\left[\bar{\boldsymbol{\xi}}_\eta\right]_{333}$ and $[\bar{\boldsymbol{\omega}}_\eta]_3$ in Equations (139a) and (139b) generalizes the "classical" P-wave modulus of the ηth phase of the composite and makes it dependent, in an algebraic way, on the scalar variable $p > 0$ describing the remodeling distortions in the considered setting. In explicit form, the generalized P-wave modulus obtained in Equations (139a) and (139b) takes on the form

$$\mathcal{Q}_\eta = \hat{\mathcal{Q}}_\eta(p) := \left[C^{(0)}_{\mathrm{R}\eta}\right]_{3333} - \left[C^{(0)}_{\mathrm{R}\eta} : \boldsymbol{E}^{(0)}_{\boldsymbol{K}}\right]_{33} = \frac{1}{2p^4}\left[2\lambda_\eta p^3 - 3\kappa_\eta p^2 + 3m_\eta\right],\ \eta = 1,2,\ p \in]0,+\infty[, \tag{147}$$

where $\kappa_\eta := \lambda_\eta + \frac{2}{3}\mu_\eta > 0$ and $m_\eta := \lambda_\eta + 2\mu_\eta > 0$ are the "classical" (i.e., independent of remodeling) bulk modulus and P-wave modulus of the ηth phase of the composite, respectively, both associated with its natural state.

In general, requiring the positivity of $\hat{\mathcal{Q}}_\eta(p)$, for $\eta = 1,2$, places restrictions on the physical admissibility of the values that can be attained by p (granted, of course, that $p > 0$ applies). In fact, these restrictions depend on Lamé's constants and, if we assume, for simplicity, the positivity of λ_η (μ_η is greater than 0), they can be expressed in terms of the ratio μ_η/λ_η. In particular, based on Equation (147), we define *critical value* of μ_η/λ_η the strictly positive real number $(\mu_\eta/\lambda_\eta)_{\mathrm{cr}}$ such that, for all ratios $\mu_\eta/\lambda_\eta \geq (\mu_\eta/\lambda_\eta)_{\mathrm{cr}}$, there exists a non-empty subset of $]0,+\infty[$ such that $\hat{\mathcal{Q}}_\eta(p) \leq 0$ for all the values of p belonging to this subset. This leads us to an important result, which we formalize in terms of a theorem and its associated corollary.

Theorem 1. *Let $\mathscr{C}_\eta = \lambda_\eta \boldsymbol{I}\otimes\boldsymbol{I} + \mu_\eta\left(\boldsymbol{I}\underline{\otimes}\boldsymbol{I} + \boldsymbol{I}\overline{\otimes}\boldsymbol{I}\right)$ be the elasticity tensor of the η-phase of a layered composite in its natural state. If Lamé's constants λ_η and μ_η satisfy the conditions*

$$\lambda_\eta > 0 \ \textit{and}\ \frac{\mu_\eta}{\lambda_\eta} \in]0,(\mu_\eta/\lambda_\eta)_{cr}[,\ \textit{with}\ (\mu_\eta/\lambda_\eta)_{cr} > 0, \tag{148}$$

and

$$\boldsymbol{K}^{(0)} = diag(p^{-1/2}, p^{-1/2}, p),\ with\ \ p \in]0,+\infty[, \tag{149}$$

then, the generalized P-wave modulus $\hat{\mathcal{Q}}_\eta(p)$ is strictly positive. Furthermore, there exists a locally periodic solution for Equation (139a) and for Equation (139b).

Proof. We slightly rephrase Equation (147) in terms of the ratio μ_η/λ_η, for $\lambda_\eta > 0$, as

$$\hat{\mathcal{Q}}_\eta(p) = \frac{\lambda_\eta}{2p^4}\left[2p^3 - 3\left(1 + \frac{2}{3}\frac{\mu_\eta}{\lambda_\eta}\right)p^2 + 3\left(1 + 2\frac{\mu_\eta}{\lambda_\eta}\right)\right],\ \eta = 1,2, \tag{150}$$

and we study the positivity of $\hat{\mathcal{Q}}_\eta(p)$ by looking at the sign of the expression between square brackets, which is a cubic polynomial in p, and is indicated with $\hat{f}_\eta(p)$ in this proof. This can be done by determining the roots of this polynomial and the values of $p \in]0,+\infty[$ for which the inequality $\hat{\mathcal{Q}}_\eta(p) > 0$ is fulfilled for given values of λ_η and μ_η. However, it can be shown that, since $\lambda_\eta > 0$, $\hat{f}_\eta$ admits a global minimum at $p = p_{\min} = 1 + \frac{2}{3}\frac{\mu_\eta}{\lambda_\eta} > 0$, that is,

$$\min_{p\in]0,+\infty[}\{\hat{f}_\eta(p)\} = \hat{f}_\eta(p_{\min}) = 3\left(1 + 2\frac{\mu_\eta}{\lambda_\eta}\right) - \left(1 + \frac{2}{3}\frac{\mu_\eta}{\lambda_\eta}\right)^3. \tag{151}$$

Now, to prove that $\hat{f}_\eta(p)$, and thus, $\hat{\mathcal{Q}}_\eta(p)$, is strictly greater than zero, it suffices to show that $\hat{f}_\eta(p_{\min}) > 0$. Since this condition is satisfied if the hypothesis $(148)_2$ is respected, then $\hat{\mathcal{Q}}_\eta(p)$ is strictly positive for all $p \in]0,+\infty[$. □

Corollary 1. *In the nearly incompressible case, that is, when the ratio μ_η/λ_η is sufficiently small, it holds that $\min_{p\in]0,+\infty[}\hat{f}_\eta(p) > 0$, where $\hat{f}_\eta(p)$ is the expression between squared brackets in Equation (151). Thus, $\hat{\mathcal{Q}}_\eta(p)$ is strictly positive for all values of p.*

Proof. It follows from Equation (151) by taking the limit for $\lambda_\eta \to +\infty$. □

Since the condition $\mu_\eta/\lambda_\eta \in]0,\left(\frac{\mu_\eta}{\lambda_\eta}\right)_{\mathrm{cr}}[$ is automatically satisfied by the material parameters considered in the present model, we conclude that the rescaled elasticity tensor for the case of the layered medium is strongly elliptic for all $p > 0$,

10991476, 2025, 1, Downloaded from https://onlinelibrary.wiley.com/doi/10.1002/nma.10367 by Politecnico Di Torino Sist. Bibl Del Polit Di Torino, Wiley Online Library on [12/02/2025]. See the Terms and Conditions (https://onlinelibrary.wiley.com/terms-and-conditions) on Wiley Online Library for rules of use; OA articles are governed by the applicable Creative Commons License

which guarantees the well-posedness of Equations (139a), (139b), and (145). We find that the critical value $\left(\frac{\mu_\eta}{\lambda_\eta}\right)_{\text{cr}}$ is approximately 2.376.

8.2.2 | Determination of $\text{DevSym}\mathbb{D}^{\text{eff}}$

To solve the cell problem for the remodeling variable, we start by looking at Equations (76) and (78), which is, in index notation, the bulk equation of the cell problem (97). Since tensor $\boldsymbol{L}_{\boldsymbol{K}}^{(0)}$ is diagonal, only the case in which $I = J$ has to be considered. Moreover, since $\boldsymbol{K}^{(0)}$ has only one independent coefficient, which can be identified with $[\boldsymbol{K}^{(0)}]_{33} = p$, we can consider the component $\left[\boldsymbol{L}_{\boldsymbol{K}}^{(0)}\right]_{33} = \dot{p}/p$ and disregard $\left[\boldsymbol{L}_{\boldsymbol{K}}^{(0)}\right]_{11}$ and $\left[\boldsymbol{L}_{\boldsymbol{K}}^{(0)}\right]_{22}$. Finally, since p depends only on $\tilde{X}_3$, we can take $\left[\text{Grad}_{\tilde{X}}\boldsymbol{L}_{\boldsymbol{K}}^{(0)}\right]_{333} = \frac{\partial}{\partial \tilde{X}_3}\left(\frac{\dot{p}}{p}\right)$ as the sole independent component of $\text{Grad}_{\tilde{X}}\boldsymbol{L}_{\boldsymbol{K}}^{(0)}$. Therefore, by also recalling the fact that all physical quantities are assumed to depend on space exclusively through $\tilde{X}_3$ and $\tilde{Y}_3$, Equation (78) becomes

$$
\begin{aligned}
&-\left[\text{Grad}_{\tilde{X}}\boldsymbol{L}_{\boldsymbol{K}}^{(0)}\right]_{333}\frac{\partial}{\partial \tilde{Y}_3}\left\{\frac{\ell_\eta^2}{L_0^2}\sigma_\eta\tau_\eta\left[\frac{\delta_{3A}\delta_{3B}+\delta_{3A}\delta_{3B}}{2}-\frac{1}{3}\delta_{AB}\right.\right.\\
&\left.\left.+\frac{\partial}{\partial \tilde{Y}_3}\left(\frac{[\boldsymbol{\Lambda}_\eta]_{AB333}+[\boldsymbol{\Lambda}_\eta]_{BA333}}{2}\right)-\frac{1}{3}\frac{\partial[\boldsymbol{\Lambda}_\eta]_{MM333}}{\partial \tilde{Y}_3}\delta_{AB}\right]\right\}=0
\end{aligned}
\tag{152}
$$

and can be turned into a set of ordinary differential equations in $[\boldsymbol{\Lambda}_\eta]_{AB333}$, whose general solution is

$$
[\text{DevSym}\boldsymbol{\Lambda}_\eta]_{AB333}(\tilde{X}_3,\tilde{Y}_3,t)=[\mathfrak{S}_\eta]_{AB3333}(\tilde{X}_3,t)\tilde{Y}_3+[\Theta_\eta]_{AB333}(\tilde{X}_3,t),\ \text{for } A,B=1,2,3,
\tag{153}
$$

where for each $\eta = 1, 2$, $[\mathfrak{S}_\eta(\tilde{X}_3,t)]_{AB3333}$ and $[\Theta_\eta(\tilde{X}_3,t)]_{AB333}$ are unknown functions representing the components of tensor fields that are symmetric and deviatoric in the first pair of indices. These functions are identified by imposing the following auxiliary conditions:

$$
[\text{DevSym}\boldsymbol{\Lambda}_1]_{AB333}(\tilde{X}_3,0,t)=[\text{DevSym}\boldsymbol{\Lambda}_2]_{AB333}(\tilde{X}_3,1,t),\qquad \text{Periodicity,}
\tag{154a}
$$

$$
[\text{DevSym}\boldsymbol{\Lambda}_1]_{AB333}(\tilde{X}_3,\tilde{Y}_\Gamma,t)=[\text{DevSym}\boldsymbol{\Lambda}_2]_{AB333}(\tilde{X}_3,\tilde{Y}_\Gamma,t),\qquad \text{No jump of } \boldsymbol{\Lambda}_\eta \text{ at the interface,}
\tag{154b}
$$

$$
\left[\!\!\left[\frac{\ell_\eta^2}{L_0^2}\sigma_\eta\tau_\eta\left([\text{DevSym}\mathbb{I}_6]_{AB3333}+\frac{\partial[\text{DevSym}\boldsymbol{\Lambda}_\eta]_{AB333}}{\partial \tilde{Y}_3}(\tilde{X}_3,\tilde{Y}_\Gamma,t)\right)\right]\!\!\right]=0,\qquad \text{No jump of the "fluxes,"}
\tag{154c}
$$

$$
\sum_{\eta=1,2}\left\langle[\text{DevSym}\boldsymbol{\Lambda}_\eta]_{AB333}\right\rangle_\eta=0,\qquad \text{Solvability condition,}
\tag{154d}
$$

which yield

$$
[\mathfrak{S}_1]_{AB3333}(\tilde{X}_3,t)=(1-\tilde{Y}_\Gamma)\frac{\ell_2^2\sigma_2\tau_2-\ell_1^2\sigma_1\tau_1}{(1-\tilde{Y}_\Gamma)\ell_1^2\sigma_1\tau_1+\tilde{Y}_\Gamma\ell_2^2\sigma_2\tau_2}[\text{DevSym}\mathbb{I}_6]_{AB3333},
\tag{155a}
$$

$$
[\mathfrak{S}_2]_{AB3333}(\tilde{X}_3,t)=-\tilde{Y}_\Gamma\frac{\ell_2^2\sigma_2\tau_2-\ell_1^2\sigma_1\tau_1}{(1-\tilde{Y}_\Gamma)\ell_1^2\sigma_1\tau_1+\tilde{Y}_\Gamma\ell_2^2\sigma_2\tau_2}[\text{DevSym}\mathbb{I}_6]_{AB3333},
\tag{155b}
$$

$$
[\Theta_1]_{AB333}(\tilde{X}_3,t)=-\frac{\tilde{Y}_\Gamma(1-\tilde{Y}_\Gamma)}{2}\frac{\ell_2^2\sigma_2\tau_2-\ell_1^2\sigma_1\tau_1}{(1-\tilde{Y}_\Gamma)\ell_1^2\sigma_1\tau_1+\tilde{Y}_\Gamma\ell_2^2\sigma_2\tau_2}[\text{DevSym}\mathbb{I}_6]_{AB3333},
\tag{155c}
$$

$$
[\Theta_2]_{AB333}(\tilde{X}_3,t)=\frac{\tilde{Y}_\Gamma(1+Y_\Gamma)}{2}\frac{\ell_2^2\sigma_2\tau_2-\ell_1^2\sigma_1\tau_1}{(1-\tilde{Y}_\Gamma)\ell_1^2\sigma_1\tau_1+\tilde{Y}_\Gamma\ell_2^2\sigma_2\tau_2}[\text{DevSym}\mathbb{I}_6]_{AB3333}.
\tag{155d}
$$

It is worthwhile to remark that because of the particularly simple choice of the coefficients σ_η and τ_η, the functions determined in Equations (155a)–(155d) are *independent of* $\tilde{X}_3$ and time, and, consequently, $[\text{DevSym}\boldsymbol{\Lambda}_\eta]_{AB333}$ depends only on $\tilde{Y}_3$ as indicated in Equation (153).

10991476, 2025, 1, Downloaded from https://onlinelibrary.wiley.com/doi/10.1002/nma.10367 by Politecnico Di Torino Sist. Bibl Del Polit Di Torino, Wiley Online Library on [12/02/2025]. See the Terms and Conditions (https://onlinelibrary.wiley.com/terms-and-conditions) on Wiley Online Library for rules of use; OA articles are governed by the applicable Creative Commons License

On the basis of the results obtained in Equations (155a) and (155b), the Cartesian components of interest of the "true" effective coefficient $\mathrm{DevSym}\mathbb{D}^{\mathrm{eff}}$ defined in Equation (115), that is, $\left[\mathrm{DevSym}\mathbb{D}^{\mathrm{eff}}\right]_{AB3333}$, read

$$\begin{aligned}[\mathrm{DevSym}\ \mathbb{D}^{\mathrm{eff}}]_{AB3333} &= \sum_{\eta=1,2} \ell_\eta^2 \sigma_\eta \tau_\eta \left(\varphi_\eta [\mathrm{DevSym}\mathbb{I}]_{AB3333} + \left\langle \frac{\partial [\mathrm{DevSym}\boldsymbol{\Lambda}_\eta]_{AB333}}{\partial \tilde{Y}_3} \right\rangle_\eta \right) \\ &= \sum_{\eta=1,2} \ell_\eta^2 \sigma_\eta \tau_\eta \varphi_\eta \left([\mathrm{DevSym}\mathbb{I}_6]_{AB3333} + [\mathfrak{S}_\eta]_{AB3333} \right) \\ &= \frac{[\mathrm{DevSym}\mathbb{I}_6]_{AB3333}}{\frac{\tilde{Y}_\Gamma}{\ell_1^2 \sigma_1 \tau_1} + \frac{1-\tilde{Y}_\Gamma}{\ell_2^2 \sigma_2 \tau_2}} = \left\langle \frac{1}{\ell_\eta^2 \sigma_\eta \tau_\eta} \right\rangle^{-1} [\mathrm{DevSym}\mathbb{I}_6]_{AB3333},\end{aligned} \tag{156}$$

where the expression $\langle \cdot \rangle$ is the cell average over $\tilde{\mathscr{Y}}_{\mathrm{R}}$ defined in Equation (10).

By substituting Equation (156) into Equation (114), and recalling that by virtue of the symmetries of the problem under investigation, that is, because of the special case of the displacement field and of remodeling tensor that we are considering, the evolution of the remodeling variable p is prescribed by the equation

$$(\tilde{Y}_\Gamma \sigma_1 \tau_1 + (1-\tilde{Y}_\Gamma)\sigma_2 \tau_2) \left[\boldsymbol{L}_{\boldsymbol{K}}^{(0)} \right]_{33} - \left[\left\langle \mathrm{DevSym}\boldsymbol{\Sigma}_{\eta\mathrm{lin}}^{(0)} \right\rangle \right]_{33} - \frac{1}{L_0^2} \left[\mathrm{DevSym}\mathbb{D}^{\mathrm{eff}} \right]_{333333} \frac{\partial^2 \left[\boldsymbol{L}_{\boldsymbol{K}}^{(0)} \right]_{33}}{\partial \tilde{X}_3 \partial \tilde{X}_3} = 0, \tag{157}$$

where we recall that the identity $\left[\boldsymbol{L}_{\boldsymbol{K}}^{(0)} \right]_{33} = \dot{p}/p$ (see Equation (128b)) permits to solve for the remodeling variable p.

Hence, the evolution of the homogenized multilayered material under consideration is described by the coupled Equations (145) and (157), which allow to determine the homogenized displacement $\boldsymbol{u}^{(0)}$ and the remodeling distortion p.

8.2.3 | Upscaled model and numerical simulations

We remark that including the contribution of the microscopic remodeling dislocations, encoded in the homogenized model through the effective coefficient $\mathbb{D}^{\mathrm{eff}}$, is an element of novelty in the study of remodeling at different scales. In our work, this is obtained as a natural consequence of the gradient flow rule put forward by Gurtin and Anand [42] and adapted to the context of AH.

The purpose of the numerical simulations presented in the sequel is to explore and emphasize the additional effects that our homogenized model is able to catch (see Table 1 for the list of parameters). In particular, with respect to a zeroth-order theory in the remodeling strain (see, e.g., [19]), the dissipative length scales ℓ_1 and ℓ_2 are among the material parameters considered in the model, and, in the general context of strain-gradient plasticity, they play a relevant role in fitting the experimental data for bending and torsion tests (see, e.g., [50] for a review on the argument and on the lack of a clear way to link ℓ_η to the phenomenology). However, since our simulations aim at showing the potentialities of our model in a simplified setting—indeed, for the time being, we do not have enough data to reproduce experiments conducted in a laboratory—we take the macroscopic parameters of the model from the literature, while we guess or impose the other ones beforehand.

In the following, the composite material comprises two phases: one, denoted by $\mathscr{F}_1$, has the material properties of the bone tissue [26, 28], with realistic elastic and viscous properties, while the other phase, indicated with $\mathscr{F}_2$, could represent a bio-engineered material with scaffolds compatible with those of the bone tissue. Moreover, the phase $\mathscr{F}_2$ is softer than

Parameter	Unit	Value	Reference	Parameter	Unit	Value	Reference
L_0	(cm)	10.0000	-	τ_1	(s)	1.0000	[28]
u_L	(cm)	0.1000	-	τ_2	(s)	100.0000	-
α	(-)	1.1	-	σ_1	(GPa)	2.0	[28]
β	(-)	0.1	-	σ_2	(GPa)	1.0	-
λ_1	(GPa)	17.6	[26]	ℓ_1	(mm)	5.00	-
λ_2	(GPa)	1.0	-	ℓ_2	(mm)	10.0	-
μ_1	(GPa)	1.0	[26]	t_0	(s)	0.0	
μ_2	(GPa)	0.4	-	T	(s)	50.0	
$\tilde{Y}_\Gamma$	(-)	0.4	-				

TABLE 1 Material parameters of the constituents of the composite material used for the simulations of the homogenized equations.

10991476, 2025, 1, Downloaded from https://onlinelibrary.wiley.com/doi/10.1002/mma.10367 by Politecnico Di Torino Sist. Bibl Del Polit Di Torino, Wiley Online Library on [12/02/2025]. See the Terms and Conditions (https://onlinelibrary.wiley.com/terms-and-conditions) on Wiley Online Library for rules of use; OA articles are governed by the applicable Creative Commons License

$\mathscr{F}_1$, that is, it exhibits elastic moduli lower than those associated with $\mathscr{F}_1$, but it is more viscous, thereby opposing higher resistance to the remodeling flow.

It is important to remark that, even if the phase $\mathscr{F}_1$ features the material parameters of the bone, this is not an accurate modeling, since the phenomenology associated with porosity or fluid flow is not present [131]. Thus, a precise description, and the employment of such description to predict the behavior of a realistic composite material, which could be of interest, for example, to study the elasto-plastic behavior of bio-engineered biphasic grafts, is out of scope for this work, but is in our research plans for the future.

The simulated multilayered composite, of initial height $L_0 = 10$ cm, is subjected to a stretch test of 1% of its initial length over a time window of $T = 50$s. Each cell comprises 40% of the first constituent and 60% of the second one. Since we refer to a bio-engineered material with similar microstructural properties as the bone tissue, we hypothesize that the height of the elementary cell is $\ell_0 = 5\mu$m, so that the composite consists of 20000 elementary cells. Under this assumption, we can study the evolution of the macroscopic fields $[\bar{\boldsymbol{u}}^{(0)}]_3$ and p independently of the miscrostructural heterogeneity. We consider two different initial conditions for the spatial distribution of p: in the first case, $p_{\text{in}}(\tilde{X}_3) = \alpha + \beta\cos(16\pi\tilde{X}_3)$, with $\alpha \geq 1 + \beta$ and $\beta > 0$, so that $p_{\text{in}}(\tilde{X}_3) \geq 1$; in the second case, $p_{\text{in}}(\tilde{X}_3) = 1 + \theta(\tilde{X}_3)$, with θ being a random variable having uniform probability distribution (so that $|\theta(\tilde{X}_3)| < 1$), zero average, and standard deviation $\zeta > 0$. Finally, we draw a comparison between our model and a more conventional model in p, in which the evolution of the remodeling distortions is given by Equation (121).

In Figure 2, we report the evolution of the homogenized kinematic descriptors $[\bar{\boldsymbol{u}}]_3$ and p for the two models, with and without gradient effects, for the initial distribution of remodeling distortions $p_{\text{in}}(\tilde{X}_3) = \alpha+\beta\cos(16\pi\tilde{X}_3)$. The displacement is calculated with respect to the *initial* placement, and not with respect to the reference placement, because of the presence of residual stresses at the initial time of the simulation (see [9] for a detailed analysis on the difference between reference and initial placement—*"configuration"* in the jargon of [9]).

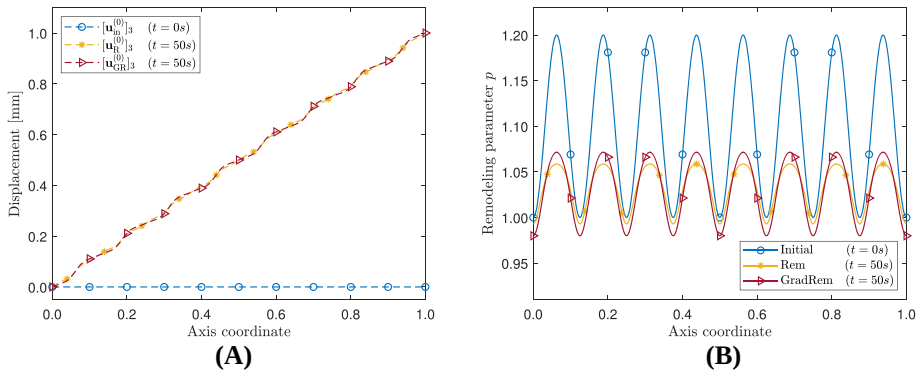


FIGURE 2 Spatial distribution of the displacement field (A) and of the remodeling parameter (B) at the end of the simulation, for both the model with and without gradient effects, for the initial condition $p_{\text{in}}(\tilde{X}_3) = \alpha + \beta\cos(16\pi\tilde{X}_3)$. In the figures, the labels R and GR mean "remodeling" and "strain-gradient remodeling," respectively. [Colour figure can be viewed at wileyonlinelibrary.com]

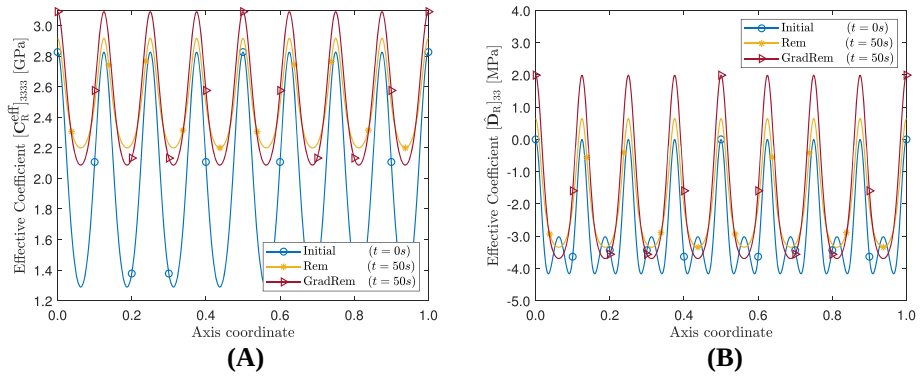


FIGURE 3 Spatial distribution of $[C_{\text{R}}^{\text{eff}}]_{3333}$ (A) and of $[\hat{\boldsymbol{D}}_{\text{R}}]_{33}$ (B) at the end of the simulation, for both the model with and without gradient effects, for the initial condition $p_{\text{in}}(\tilde{X}_3) = \alpha + \beta\cos(16\pi\tilde{X}_3)$. In the figures, the labels R and GR mean "remodeling" and "strain-gradient remodeling," respectively. [Colour figure can be viewed at wileyonlinelibrary.com]

10991476, 2025, 1, Downloaded from https://onlinelibrary.wiley.com/doi/10.1002/nme.10367 by Politecnico Di Torino Sist. Bibl Del Polit Di Torino, Wiley Online Library on [12/02/2025]. See the Terms and Conditions (https://onlinelibrary.wiley.com/terms-and-conditions) on Wiley Online Library for rules of use; OA articles are governed by the applicable Creative Commons License

At the end of the simulation, the influence of the homogenized strain-gradient flow rule manifests in the form of small corrections in the values of the macroscopic axial displacement field and remodeling parameter. Both models predict a decrease of the oscillations in the spatial distribution of p, which evolves towards a space-periodic distribution that features a lower amplitude than the initial one. In addition, the size effects manifest themselves in more pronounced peaks and valleys of the spatial distribution of the remodeling variable. This may seem to suggest that for a plastically stretched medium, that is, with $p_{\text{in}}(\tilde{X}_3) \geq 1$, that undergoes even more stretching in the course of the simulation, the strain-gradient effects make it possible that the model sustains a slower decrease of remodeling. This is seen by a smaller amplitude of the oscillations in the case in which the strain-gradient remodeling is not considered. In this sense, each transition between a maximum and a minimum in the spatial distribution of p occurs more smoothly when the strain-gradient term is active. Such differences in the distribution of p are reflected in the determination of the effective coefficients, in particular in $[C_{\text{R}}^{\text{eff}}]_{3333}$, which features an oscillatory behavior (see Figure 3).

In the second case, $p_{\text{in}}(\tilde{X}_3)$ is taken as a realization of a random variable of uniform probability distribution, with average 1 and standard deviation ζ. Thus, our interest resides in studying the occurrence of different patterns in the evolution of the displacement and of the remodeling variable depending on an highly oscillating initial datum. The random values are assigned for each node of the mesh in such a way that each value of $p_{\text{in}}(\tilde{X}_3)$ for the homogenized model encompasses 200 elementary cells of the composite. However, other choices for the discretization are possible, but have not been investigated here.

As can be seen in Figure 4, at the end of the simulation the two models predict considerable differences in both the displacement field and in the remodeling parameter. The irregular distribution of macroscopic heterogeneities, in fact, increases the relevance of the gradient effects within the medium for the remodeling parameter, the initial value of which is the only difference in input between the two simulated benchmarks.

Furthermore, our simulations show that the predicted evolution of $[C_{\text{R}}^{\text{eff}}]_{3333}$ changes depending on whether or not the constituents of the composite obey the gradient flow rule (14) (see Figure 5). In fact, the difference between the two spatial distributions ranges from almost 0 GPa up to 1 GPa, which is of the same order of magnitude of the effective elastic coefficient itself. Besides, we remark that, at the end of the second simulation, both $[C_{\text{R}}^{\text{eff}}]_{3333}$ and $[\hat{\boldsymbol{D}}_{\text{R}}]_{33}$ exhibit a variability in their spatial distribution higher than the one obtained with the first simulation.

To further examine the two models with and without strain-gradient remodeling, we compare the generalized stresses that feature in Equations (114) and (121), that is, $\gamma^{\text{eff}}\left[\boldsymbol{L}_{\boldsymbol{K}}^{(0)}\right]_{33}$ and $-\left[\text{DevSym}\mathbb{D}^{\text{eff}}\right]_{333333}/L_0^2\partial^2_{\tilde{X}_3\tilde{X}_3}\left[\boldsymbol{L}_{\boldsymbol{K}}^{(0)}\right]_{33}$. With the material properties of the constituents described in Table 1, it results that $\gamma^{\text{eff}} \approx 60.8$ GPa and $\left[\text{DevSym}\mathbb{D}^{\text{eff}}\right]_{333333}/L_0^2 \approx 12.4$ MPa, which means that, with the values of the parameters alone, if no significative macroscopic spatial heterogeneities were present, the gradient term would be negligible with respect to $\gamma^{\text{eff}}\left[\boldsymbol{L}_{\boldsymbol{K}}^{(0)}\right]_{33}$. However, for the cases that we are considering, the generalized stresses are comparable with each other (see Figure 6). In particular, we notice that for the model with strain-gradient remodeling, the total stress, that is,

$$\gamma^{\text{eff}}\left[\boldsymbol{L}_{\boldsymbol{K}}^{(0)}\right]_{33} - \frac{1}{L_0^2}\left[\text{DevSym}\mathbb{D}^{\text{eff}}\right]_{333333}\frac{\partial^2}{\partial\tilde{X}_3\partial\tilde{X}_3}\left[\boldsymbol{L}_{\boldsymbol{K}}^{(0)}\right]_{33}, \tag{158}$$

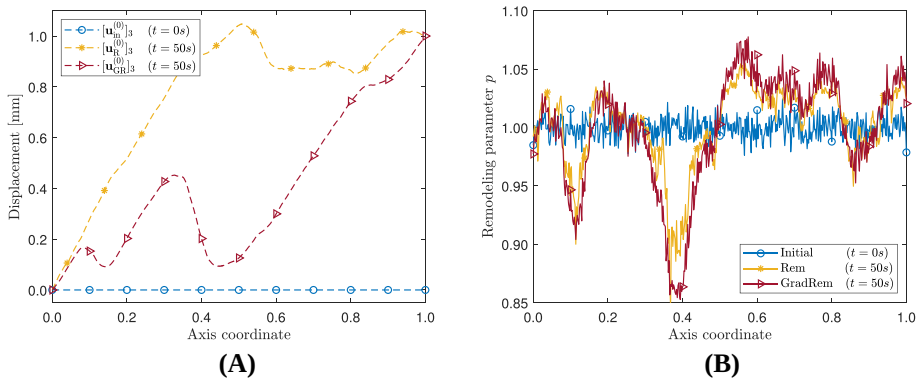


FIGURE 4 Spatial distribution of the displacement field (A) and of the remodeling parameter (B) at the end of the simulation, for both the model with and without gradient effects, for the initial condition $p_{\text{in}}(\tilde{X}_3) = 1 + \theta(\tilde{X}_3)$. In the figures, the labels R and GR mean "remodeling" and "strain-gradient remodeling," respectively. [Colour figure can be viewed at wileyonlinelibrary.com]

10991476, 2025, 1, Downloaded from https://onlinelibrary.wiley.com/doi/10.1002/nme.10367 by Politecnico Di Torino Sist. Bibl Del Polit Di Torino, Wiley Online Library on [12/02/2025]. See the Terms and Conditions (https://onlinelibrary.wiley.com/terms-and-conditions) on Wiley Online Library for rules of use; OA articles are governed by the applicable Creative Commons License

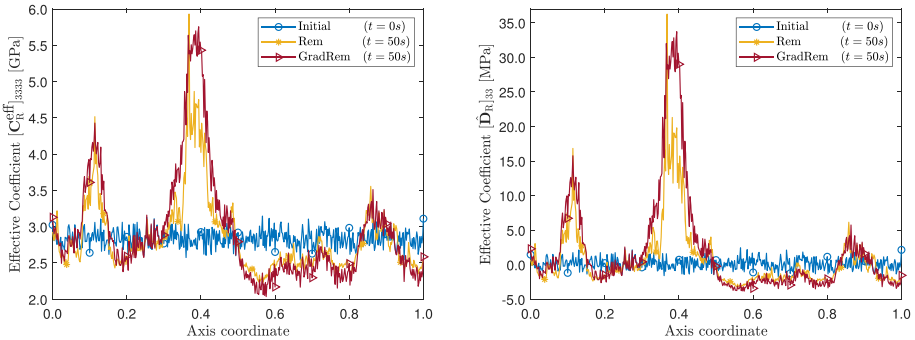


FIGURE 5 Spatial distribution of $[C_R^{\text{eff}}]_{3333}$ (A) and of $[\hat{\boldsymbol{D}}_R]_{33}$ (B) at the end of the simulation, for both the model with and without gradient effects, for the initial condition $p_{\text{in}}(\tilde{X}_3) = 1 + \theta(\tilde{X}_3)$. In the figures, the labels R and GR mean "remodeling" and "strain-gradient remodeling," respectively. [Colour figure can be viewed at wileyonlinelibrary.com]

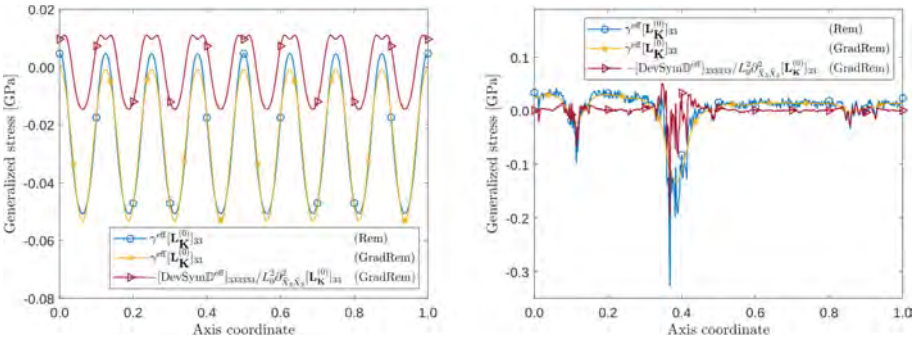


FIGURE 6 Spatial distribution at the end of the simulation of the generalized stresses $\gamma^{\text{eff}}\left[\boldsymbol{L}_{\boldsymbol{K}}^{(0)}\right]_{33}$ for the case of grade zero remodeling, $\gamma^{\text{eff}}\left[\boldsymbol{L}_{\boldsymbol{K}}^{(0)}\right]_{33}$ and $-\left[\text{DevSym}\mathbb{D}^{\text{eff}}\right]_{333333}/L_0^2\partial^2_{\tilde{X}_3\tilde{X}_3}\left[\boldsymbol{L}_{\boldsymbol{K}}^{(0)}\right]_{33}$ for the case of strain-gradient remodeling, respectively. The generalized stress associated with the remodeling flow is taken with the minus sign so that the overall generalizes stress is obtained by adding it to $\gamma^{\text{eff}}\left[\boldsymbol{L}_{\boldsymbol{K}}^{(0)}\right]_{33}$. On the left (a), the initial condition $p_{\text{in}}(\tilde{X}_3) = \alpha + \beta\cos(16\pi\tilde{X}_3)$, with $\alpha > \beta > 0$ is prescribed, whereas on the right (b) th initial condition is $p_{\text{in}}(\tilde{X}_3) = 1 + \theta(\tilde{X}_3)$. [Colour figure can be viewed at wileyonlinelibrary.com]

is sufficiently close to that of the standard model, especially for the random case (data not shown). In doing this comparison, we take into account the fact that the second summand of Equation (158) is relatively small, as one would expect, and that the two models predict two different distributions of p (see Figures 2b and 4b). By looking at Figures 6a and 6b, we notice also that, in the presence of strong macroscopic spatial inhomogeneities for p, it is the term associated with the macroscopic remodeling flux that captures the "oscillations" and drives the evolution of the remodeling distortions. As a consequence, the spatial distribution of the generalized stress $\gamma^{\text{eff}}\left[\boldsymbol{L}_{\boldsymbol{K}}^{(0)}\right]_{33}$ is much smoother in the strain-gradient remodeling case than in the other one. However, as seen in Figures 2b and 4b, this does not amount to significant differences in the regularity of the distribution of p, since the increase in spatial smoothness of $\left[\boldsymbol{L}_{\boldsymbol{K}}^{(0)}\right]_{33}$ barely affects the irregularities in $p_{\text{in}}(\tilde{X}_3)$.

9 | CONCLUDING REMARKS

In our work, we employ the AH approach to describe the remodeling of a biphasic, solid–solid composite material constituted by two elasto-viscoplastic constituents subjected to a microforce balance. We briefly summarize the main physico-mathematical aspects and hypotheses of the problem under investigation:

- we consider a composite material with a periodic microstructure, which is well-separated from the overall size of the medium, and we indicate with ℓ_0 and with L_0 the characteristic lengths of the microscopic and macroscopic geometric features, respectively;

10991476, 2025, 1, Downloaded from https://onlinelibrary.wiley.com/doi/10.1002/nma.10367 by Politecnico Di Torino Sist. Bibl Del Polit Di Torino, Wiley Online Library on [12/02/2025]. See the Terms and Conditions (https://onlinelibrary.wiley.com/terms-and-conditions) on Wiley Online Library for rules of use; OA articles are governed by the applicable Creative Commons License

- the characteristic lengths of the periodic cell and of the macroscopic body, that is, ℓ_0 and L_0, respectively, are well-separated, and the length scales of the remodeling processes ℓ_η ($\eta = 1, 2$) are such to cover several elementary cells. The biological case of inspiration is the formation of plastic zones in the bone tissue in the proximity of large cracks [73] or due to networks of microcracks [74–76];
- no-jump conditions are prescribed at the interface for the deformation, the remodeling and the associated stress measures;
- we deal with a hard tissue that can be subjected to inelastic processes that alter significantly and irreversibly its mechanical properties (plasticity, osteoporosis, remodeling, aging, etc.); thus, we consider the problem as linearized with respect to the displacement, but not to the inelastic distortions;

Motivated by the implications that the problem studied in our work has in biomechanics [73–76] and in the mechanics of materials [55, 58], our main purpose is to show how to employ the theory of AH to solve one of these problems, especially in the framework of the strain-gradient remodeling (this being, to our knowledge, an element of novelty). This is because AH allows to obtain the effective coefficients of the composite under investigation from the knowledge, possibly approximated, of its microstructure. Like in other situations in which AH is employed, the advantage of such methodology resides in the possibility of obtaining physical quantities characterizing the composite in a self-consistent way, thereby offering a point of comparison with the entirely "constitutive" theories formulated directly at the scale of the composite.

Clearly, the use of AH requires some technical hypotheses that in comparison with macroscopic constitutive theories, are deemed restrictive. However, AH has shown to be able to produce results coherent with the experimental observations in different contexts [23, 90, 93] in spite of its own "limitations." For this reason, although we do not have an experimental term of comparison at the moment for our problem, we believe that our research could suggest how the effective coefficients for a material undergoing strain-gradient remodeling should look like. In doing this, we think we are moving a step forward with respect to the point of view of Gurtin and Anand [42]. Indeed, they do not give any expression for the dissipative characteristic lengths, but they regard them as *"phenomenological parameters that enter the theory to make it dimensionally consistent"* and that *"are expected to be determined by fitting the theory to particular experiments"* [42]. On the contrary, we are identifying our microscopic length scale ℓ_η with the characteristic size of the plastic zone in bone tissue, and we are predicting the effective macroscopic coefficients of the theory, which, however, must be tested against experiments. Finally, the results reported in our work, although simplified for the purpose of AH (we refer mainly of the linearization of the constitutive laws employed in our work), and particularized to a very basic benchmark problem for the ease of calculations, can be applied to more general settings, like, for instance, composites with much more difficult representative periodic cells and more complicated shapes.

In Section 4, we frame the dynamics of the composite by studying, for each phase, the balance of linear momentum and the *"microforce balance"* introduced in [42], the latter one being the strain-gradient flow rule for each phase. In addition, we prescribe interface conditions between the constituents of the composite. Whereas we use rather standard interface conditions for the displacements and mechanical stresses, we make dedicated assumptions for the gradient of the remodeling distortions.

In Sections 5 and 6, we determine the equations governing the evolution of the remodeling distortions both at the fine- and at the coarse scale. To this end, we adopt the technique of asymptotic expansions, applied to all balance laws and interface conditions, thereby obtaining averaged expressions of the kinematic constraints and of the gradient flow rule. For our purposes, we prescribe a De Saint-Venant strain energy density and, for the sake of completeness, a "defect" energy density for $\boldsymbol{K}_\eta$ ($\eta = 1, 2$) quadratic in the norm of the Burgers tensor. However, to reduce the complexity of the homogenization procedure, we consider the case in which the sole non-dissipative contribution to the flow rule is due to the average of the leading order of the Mandel stress tensor of the theory. Within this framework, we find that the cell problem (98) for the fine-scale remodeling distortions leads, together with the two cell problems (87) and (88) for the deformation [19], to the definition of three effective coefficients for the homogenized composite (see Equations (122) and (123)). Furthermore, we predict that the viscoplastic effective coefficients found through our procedure influence in additional and novel way both the elastic properties of the homogenized system and the evolution of the microscopic remodeling distortions (see Figure 1).

Finally, in Section 8, we present a specific example of how the remodeling distortions at both the fine- and the coarse-scale interact reciprocally. The theoretical setting developed in the previous sections is adapted to the case of a multilayered composite, and numerical simulations are performed for this very simple setting to provide a proof of concept. Our findings show that the evolution of the elastic effective coefficient can be affected significantly by the contribution of the remodeling strain gradient if the initial condition on $\boldsymbol{K}$ is highly heterogeneous.

10991476, 2025, 1, Downloaded from https://onlinelibrary.wiley.com/doi/10.1002/mma.10367 by Politecnico Di Torino Sist. Bibl Del Polit Di Torino, Wiley Online Library on [12/02/2025]. See the Terms and Conditions (https://onlinelibrary.wiley.com/terms-and-conditions) on Wiley Online Library for rules of use; OA articles are governed by the applicable Creative Commons License

For the time being, we prefer to focus on the search for a mathematically rigorous formulation of the considered problem, rather than on experiment-based numerical simulations, which require further investigations. However, we believe that we have provided a potentially useful framework for studying, with the aid of AH, the mechanical characterization of strain-gradient elasto-viscoplasticity in composite materials of both industrial and biomechanical interest.

AUTHOR CONTRIBUTIONS

Alessandro Giammarini: Methodology; software; data curation; investigation; validation; formal analysis; visualization; project administration; writing—original draft. **Ariel Ramírez-Torres:** Conceptualization; methodology; software; data curation; investigation; validation; formal analysis; supervision; visualization; project administration; writing—original draft. **Alfio Grillo:** Conceptualization; methodology; software; data curation; supervision; formal analysis; validation; investigation; visualization; project administration; writing—original draft.

ACKNOWLEDGEMENTS

The authors warmly thank Dr R. Penta for very useful discussions of the asymptotic homogenization technique, especially during the visit of A. Giammarini at the University of Glasgow. Open access publishing facilitated by Politecnico di Torino, as part of the Wiley - CRUI-CARE agreement.

CONFLICT OF INTEREST STATEMENT

The authors declare no potential conflict of interests.

ORCID

Ariel Ramírez-Torres https://orcid.org/0000-0002-5775-8985

REFERENCES

1. L. A. Taber, *Biomechanics of growth, remodeling, and morphogenesis*, Appl. Mech. Rev. **48** (1995), no. 8, 487–545.
2. P. Friedl and K. Wolf, *Tumour-cell invasion and migration: diversity and escape mechanisms*, Nat. Rev. Cancer **3** (2003), no. 5, 362–374.
3. P. Friedl, *Prespecification and plasticity: shifting mechanisms of cell migration*, Curr. Opin. Cell Biol. **16** (2004), no. 1, 14–23.
4. L. V. Garmanchuk, E. M. Perepelitsyna, M. V. Sydorenko, and L. I. Ostapchenko, *Formation of multicellular aggregates under different conditions of microenvironment*, Cytol. Genet. **44** (2010), no. 1, 19–22.
5. M. Epstein, *The split between remodelling and aging*, Int. J. Non-Linear Mech. **44** (2009), no. 6, 604–609.
6. M. Epstein, *Mathematical characterization and identification of remodeling, growth, aging and morphogenesis*, J. Mech. Phys. Solids **84** (2015), 72–84.
7. D. Garcia, P. K. Zysset, M. Charlebois, and A. Curnier, *A three-dimensional elastic plastic damage constitutive law for bone tissue*, Biomech. Model. Mechanobiol. **8** (2008), no. 2, 149–165.
8. H. Byrne, *Modelling solid tumour growth using the theory of mixtures*, Math. Med. Biol. **20** (2003), no. 4, 341–366.
9. M. V. Micunovic, *Thermomechanics of viscoplasticity—fundamentals and applications*, Springer, Heidelberg, Germany, 2009.
10. A. Yavari, *Compatibility equations of nonlinear elasticity for non-simply-connected bodies*, Arch. Ration. Mech. Anal. **209** (2013), no. 1, 237–253.
11. A. Yavari and A. Goriely, *Riemann–Cartan geometry of nonlinear dislocation mechanics*, Arch. Ration. Mech. Anal. **205** (2012), no. 1, 59–118.
12. A. Yavari and A. Goriely, *Weyl geometry and the nonlinear mechanics of distributed point defects*, Proc. R. Soc. A. Math. Phys. Eng. Sci. **468** (2012), no. 2148, 3902–3922.
13. A. Yavari and A. Goriely, *Nonlinear elastic inclusions in isotropic solids*, Proc. R. Soc. A. Math. Phys. Eng. Sci. **469** (2013), no. 2160, 20130415.
14. A. Yavari and A. Goriely, *Riemann–Cartan geometry of nonlinear disclination mechanics*, Math. Mech. Solids **18** (2012), no. 1, 91–102.
15. A. Yavari and A. Goriely, *On the stress singularities generated by anisotropic eigenstrains and the hydrostatic stress due to annular inhomogeneities*, J. Mech. Phys. Solids **76** (2015), 325–337.
16. A. Goriely, *The mathematics and mechanics of biological growth*, Springer, New York, NY, 2017.
17. E. Kröner, *Alleganeine kontinuumstheorie der verzetsmugen and eigenspannuugen*, Arch. Ration. Mech. Anal. **4** (1960), 273–334.
18. A. Yavari, *A geometric theory of growth mechanics*, J. Nonlinear Sci. **20** (2010), no. 6, 781–830.
19. A. Ramírez-Torres, S. Di Stefano, A. Grillo, R. Rodríguez-Ramos, J. Merodio, and R. Penta, *An asymptotic homogenization approach to the microstructural evolution of heterogeneous media*, Int. J. Non-Linear Mech. **106** (2018), 245–257.

10991476, 2025, 1, Downloaded from https://onlinelibrary.wiley.com/doi/10.1002/nma.10367 by Politecnico Di Torino Sist. Bibl Del Polit Di Torino, Wiley Online Library on [12/02/2025]. See the Terms and Conditions (https://onlinelibrary.wiley.com/terms-and-conditions) on Wiley Online Library for rules of use; OA articles are governed by the applicable Creative Commons License

20. H. S. Yoon and J. L. Katz, *Ultrasonic wave propagation in human cortical bone—I. Theoretical considerations for hexagonal symmetry*, J. Biomech. **9** (1976), no. 6, 407–IN3.
21. H. S. Yoon and J. Lawrence Katz, *Ultrasonic wave propagation in human cortical bone—II. Measurements of elastic properties and microhardness*, J. Biomech. **9** (1976), no. 7, 459–464.
22. W. J. Parnell, M. B. Vu, Q. Grimal, and S. Naili, *Analytical methods to determine the effective mesoscopic and macroscopic elastic properties of cortical bone*, Biomech. Model. Mechanobiol. **11** (2011), no. 6, 883–901.
23. R. Penta, K. Raum, Q. Grimal, S. Schrof, and A. Gerisch, *Can a continuous mineral foam explain the stiffening of aged bone tissue? A micromechanical approach to mineral fusion in musculoskeletal tissues*, Bioinspirat. Biomimet. **11** (2016), no. 3, 035004.
24. I. Giorgio, F. dell'Isola, U. Andreaus, and A. Misra, *An orthotropic continuum model with substructure evolution for describing bone remodeling: an interpretation of the primary mechanism behind Wolff's law*, Biomech. Model. Mechanobiol. **22** (2023), no. 6, 2135–2152.
25. T. N. Shepherd, J. Zhang, T. C. Ovaert, R. K. Roeder, and G. L. Niebur, *Direct comparison of nanoindentation and macroscopic measurements of bone viscoelasticity*, J. Mech. Behav. Biomed. Mater. **4** (2011), no. 8, 2055–2062.
26. M. Frank, D. Marx, V. Nedelkovski, J.-T. Fischer, D. H. Pahr, and P. J. Thurner, *Dehydration of individual bovine trabeculae causes transition from ductile to quasi-brittle failure mode*, J. Mech. Behav. Biomed. Mater. **87** (2018), 296–305.
27. S. Di Stefano, M. Carfagna, M. M. Knodel, K. Hashlamoun, S. Federico, and A. Grillo, *Anelastic reorganisation of fibre-reinforced biological tissues*, Comput. Vis. Sci. **20** (2019), no. 3–6, 95–109.
28. A. G. Reisinger, M. Bittner-Frank, P. J. Thurner, and D. H. Pahr, *The 2-layer elasto-visco-plastic rheological model for the material parameter identification of bone tissue extended by a damage law*, J. Mech. Behav. Biomed. Mater. **150** (2024), 106259.
29. P. Suquet, Elements of homogenization for inelastic solid mechanics, *Homogenization techniques for composite media*, E. Sanchez-Palencia and A. Zaoui, (eds.), Vol. **272**, Springer, Berlin Heidelberg, 1987, pp. 193–278.
30. J. Collis, D. L. Brown, M. E. Hubbard, and R. D. O'Dea, *Effective equations governing an active poroelastic medium*, Proc. R. Soc. A: Math. Phys. Eng. Sci. **473** (2017), no. 2198, 20160755.
31. M. Sarikaya, *Hierarchical structures of biological hard tissues*, Mater. Des. **13** (1992), no. 2, 101–102.
32. S. Mondal and U. Pal, *3D hydroxyapatite scaffold for bone regeneration and local drug delivery applications*, J. Drug Deliv. Sci. Technol. **53** (2019), 101131.
33. A. Ramírez-Torres, R. Penta, R. Rodríguez-Ramos, and A. Grillo, *Effective properties of hierarchical fiber-reinforced composites via a three-scale asymptotic homogenization approach*, Math. Mech. Solids **24** (2019), no. 11, 3554–3574.
34. S. Di Stefano, A. Giammarini, C. Giverso, and A. Grillo, *An elasto-plastic biphasic model of the compression of multicellular aggregates: the influence of fluid on stress and deformation*, Z. Angew. Math. Phys. **73** (2022), no. 2, 79.
35. P. Mascheroni, M. Carfagna, A. Grillo, D. P. Boso, and B. A. Schrefler, *An avascular tumor growth model based on porous media mechanics and evolving natural states*, Math. Mech. Solids **23** (2017), no. 4, 686–712.
36. S. Di Stefano, E. Benvenuti, and V. Coscia, *On the role of friction and remodelling in cell–matrix interactions: a continuum mechanical model*, Int. J. Non-Linear Mech. **142** (2022), 103966.
37. G. Papanicolaou, A. Bensoussan, and J.-L. Lions, *Asymptotic analysis for periodic structures*, AMS Chelsea Publishing, Providence, Rhode Island, 1978.
38. E. Sanchez-Palencia, *Non-homogeneous media and vibration theory*, Notes in Physics, Vol. **127**, Springer-Verlag, Berlin, 1980.
39. N. Bakhvalov and G. Panasenko, *Homogenization: averaging processes in periodic media*, Kluwer, Dordrecht, The Netherlands, 1989.
40. D. Cioranescu and P. Donato, *An introduction to homogenization*, Oxford University Press Inc., New York, 1999.
41. J. L. Auriault, C. Geindreau, and C. Boutin, *Homogenization of coupled phenomena in heterogenous media*, J. Wiley; ISTE, London, UK; Hoboken, NJ, 2009.
42. M. E. Gurtin and L. Anand, *A theory of strain-gradient plasticity for isotropic, plastically irrotational materials. Part II: finite deformations*, Int. J. Plast. **21** (2005), no. 12, 2297–2318.
43. D. Ambrosi and L. Preziosi, *Cell adhesion mechanisms and stress relaxation in the mechanics of tumours*, Biomech. Model. Mechanobiol. **8** (2009), 397–413.
44. L. Preziosi, D. Ambrosi, and C. Verdier, *An elasto-visco-plastic model of cell aggregates*, J. Theor. Biol. **262** (2010), no. 1, 35–47.
45. L. Preziosi and G. Vitale, *A multiphase model of tumor and tissue growth including cell adhesion and plastic reorganization*, Math. Models Methods Appl. Sci. **21** (2011), no. 9, 1901–1932.
46. A. Grillo, S. Federico, and G. Wittum, *Growth, mass transfer, and remodeling in fiber-reinforced, multi-constituent materials*, Int. J. Non-Linear Mech. **47** (2012), 388–401.
47. C. Voutouri, F. Mpekris, P. Papageorgis, A. D. Odysseos, and T. Stylianopoulos, *Role of constitutive behavior and tumor-host mechanical interactions in the state of stress and growth of solid tumors*, PLoS ONE **9** (2014), no. 8, e104717.
48. C. Giverso, M. Scianna, and A. Grillo, *Growing avascular tumours as elasto-plastic bodies by the theory of evolving natural configurations*, Mech. Res. Commun. **68** (2015), 31–39.
49. P. Mascheroni, C. Stigliano, M. Carfagna, D. P. Boso, L. Preziosi, P. Decuzzi, and B. A. Schrefler, *Predicting the growth of glioblastoma multiforme spheroids using a multiphase porous media model*, Biomech. Model. Mechanobiol. **15** (2016), no. 5, 1215–1228.
50. G. Z. Voyiadjis and Y. Song, *Strain gradient continuum plasticity theories: theoretical, numerical and experimental investigations*, Int. J. Plast. **121** (2019), 21–75.
51. N. A. Fleck, G. M. Muller, M. F. Ashby, and J. W. Hutchinson, *Strain gradient plasticity: theory and experiment*, Acta Metall. Mater. **42** (1994), no. 2, 475–487.

10991476, 2025, 1, Downloaded from https://onlinelibrary.wiley.com/doi/10.1002/nme.10367 by Politecnico Di Torino Sist. Bibl Del Polit Di Torino, Wiley Online Library on [12/02/2025]. See the Terms and Conditions (https://onlinelibrary.wiley.com/terms-and-conditions) on Wiley Online Library for rules of use; OA articles are governed by the applicable Creative Commons License

52. L. Anand, O. Aslan, and S. A. Chester, *A large-deformation gradient theory for elastic–plastic materials: strain softening and regularization of shear bands*, Int. J. Plast. **30–31** (2012), 116–143.
53. J. C. Simo and T. J. R. Hughes, *Computational inelasticity*, Springer, New York, NY, 1998.
54. R. K. A. Al-Rub and G. Z. Voyiadjis, *A physically based gradient plasticity theory*, Int. J. Plast. **22** (2006), no. 4, 654–684.
55. L. H. Poh, *Scale transition of a higher order plasticity model—a consistent homogenization theory from meso to macro*, J. Mech. Phys. Solids **61** (2013), no. 12, 2692–2710.
56. P. Gudmundson, *A unified treatment of strain gradient plasticity*, J. Mech. Phys. Solids **52** (2004), no. 6, 1379–1406.
57. R. Azizi, C. F. Niordson, and B. N. Legarth, *On the homogenization of metal matrix composites using strain gradient plasticity*, Acta Mech. Sin. **30** (2014), no. 2, 175–190.
58. D. Okumura, Y. Higashi, K. Sumida, and N. Ohno, *A homogenization theory of strain gradient single crystal plasticity and its finite element discretization*, Int. J. Plast. **23** (2007), no. 7, 1148–1166.
59. B. N. Legarth, *Plasticity dependent damage evolution in composites with strain-gradient effects*, Int. J. Solids Struct. **63** (2015), 1–10.
60. H. Song, E. V. der Giessen, and X. Liu, *Strain gradient plasticity analysis of elasto-plastic contact between rough surfaces*, J. Mech. Phys. Solids **96** (2016), 18–28.
61. V. Monchiet, N. Auffray, and J. Yvonnet, *Strain-gradient homogenization: a bridge between the asymptotic expansion and quadratic boundary condition methods*, Mech. Mater. **143** (2020), 103309.
62. H. Abdoul-Anziz and P. Seppecher, *Strain gradient and generalized continua obtained by homogenizing frame lattices*, Math. Mech. Complex Syst. **6** (2018), no. 3, 213–250.
63. N. A. Fleck and J. R. Willis, *Bounds and estimates for the effect of strain gradients upon the effective plastic properties of an isotropic two-phase composite*, J. Mech. Phys. Solids **52** (2004), no. 8, 1855–1888.
64. A. Giacomini and A. Musesti, *Two-scale homogenization for a model in strain gradient plasticity*, ESAIM: Control Optim. Calc. Var. **17** (2010), no. 4, 1035–1065.
65. A. Grillo, S. D. Stefano, A. Ramírez-Torres, and M. Loverre, *A study of growth and remodeling in isotropic tissues, based on the Anand-Aslan-Chester theory of strain-gradient plasticity*, GAMM-Mitteilungen **42** (2019), no. 4, e201900015.
66. Z. Louna, I. Goda, and J.-F. Ganghoffer, *Homogenized strain gradient remodeling model for trabecular bone microstructures*, Contin. Mech. Thermodyn. **31** (2019), no. 5, 1339–1367.
67. A. Grillo and S. D. Stefano, *A formulation of volumetric growth as a mechanical problem subjected to non-holonomic and rheonomic constraint*, Math. Mech. Solids **28** (2023), no. 10, 2215–2241.
68. A. Grillo and S. D. Stefano, *Addendum to "A formulation of volumetric growth as a mechanical problem subjected to non-holonomic and rheonomic constraint"*, Math. Mech Solids **29** (2024), no. 1, 62–70.
69. J. L. Auriault, *Effective macroscopic description for heat conduction in periodic composites*, Int. J. Heat Mass Transfer **26** (1983), no. 6, 861–869.
70. L.-E. Persson, L. Persson, N. Svanstedt, and J. Wyller, *The homogenization method: an introduction*, Studentlitteratur, Lund, 1993.
71. M. E. Gurtin, *Generalized Ginzburg-Landau and Cahn-Hilliard equations based on a microforce balance*, Phys. D. Nonlinear Phenom. **92** (1996), no. 3–4, 178–192.
72. Y. Huang, H. Gao, W. D. Nix, and J. W. Hutchinson, *Mechanism-based strain gradient plasticity—II. Analysis*, J. Mech. Phys. Solids **48** (2000), no. 1, 99–128.
73. D. M. Robertson, D. Robertson, and C. R. Barrett, *Fracture toughness, critical crack length and plastic zone size in bone*, J. Biomech. **11** (1978), no. 8–9, 359–364.
74. R. Ritchie, M. Buehler, and P. Hansma, *Plasticity and toughness in bone*, Phys. Today **62** (2009), no. 6, 41–47.
75. H. D. Barth, M. E. Launey, A. A. MacDowell, J. W. Ager, and R. O. Ritchie, *On the effect of X-ray irradiation on the deformation and fracture behavior of human cortical bone*, Bone **46** (2010), no. 6, 1475–1485.
76. E. A. Zimmermann, E. Schaible, H. Bale, H. D. Barth, S. Y. Tang, P. Reichert, B. Busse, T. Alliston, J. W. Ager, and R. O. Ritchie, *Age-related changes in the plasticity and toughness of human cortical bone at multiple length scales*, Proc. Nat. Acad. Sci. **108** (2011), no. 35, 14416–14421.
77. A. Ramírez-Torres, R. Penta, R. Rodríguez-Ramos, J. Merodio, F. J. Sabina, J. Bravo-Castillero, R. Guinovart-Díaz, L. Preziosi, and A. Grillo, *Three scales asymptotic homogenization and its application to layered hierarchical hard tissues*, Int. J. Solids Struct. **130-131** (2018), 190–198.
78. E. Pruchnicki, *Homogenized elastoplastic properties for a partially cohesive composite material*, Z. Angew. Math. Phys. **49** (1998), 568–589.
79. J. E. Marsden and T. J. R. Hughes, *Mathematical foundations of elasticity*, Dover Publications Inc., Mineola, New York, 1983.
80. S. Di Stefano, L. Miller, A. Grillo, and R. Penta, *Effective balance equations for electrostrictive composites*, Z. Angew. Math. Phys. **71** (2020), no. 5, 1–36.
81. E. K. Rodriguez, A. Hoger, and A. D. McCulloch, *Stress-dependent finite growth in soft elastic tissues*, J. Biomech. **27** (1994), no. 4, 455–467.
82. M. Epstein and G. A. Maugin, *Thermomechanics of volumetric growth in uniform bodies*, Int. J. Plast. **16** (2000), no. 7–8, 951–978.
83. A. DiCarlo and S. Quiligotti, *Growth and balance*, Mech. Res. Commun. **29** (2002), no. 6, 449–456.
84. T. Olsson and A. Klarbring, *Residual stresses in soft tissue as a consequence of growth and remodeling: application to an arterial geometry*, Eur. J. Mech.—A/Solids **27** (2008), no. 6, 959–974.
85. J.-F. Ganghoffer, *On Eshelby tensors in the context of the thermodynamics of open systems: application to volumetric growth*, Int. J. Eng. Sci. **48** (2010), no. 12, 2081–2098.

10991476, 2025, 1, Downloaded from https://onlinelibrary.wiley.com/doi/10.1002/mma.10367 by Politecnico Di Torino Sist. Bibl Del Polit Di Torino, Wiley Online Library on [12/02/2025]. See the Terms and Conditions (https://onlinelibrary.wiley.com/terms-and-conditions) on Wiley Online Library for rules of use; OA articles are governed by the applicable Creative Commons License

86. J.-F. Ganghoffer, *A kinematically and thermodynamically consistent volumetric growth model based on the stress-free configuration*, Int. J. Solids Struct. **50** (2013), no. 20–21, 3446–3459.
87. A. Javili, P. Steinmann, and E. Kuhl, *A novel strategy to identify the critical conditions for growth-induced instabilities*, J. Mech. Behav. Biomed. Mater. **29** (2014), 20–32.
88. A. Ramírez-Torres, R. Penta, and A. Grillo, *Two-scale, non-local diffusion in homogenised heterogeneous media*, Arch. Appl. Mech. **92** (2021), no. 2, 559–595.
89. O. L. Cruz-González, A. Ramírez-Torres, R. Rodríguez-Ramos, R. Penta, J. Bravo-Castillero, R. Guinovart-Díaz, J. Merodio, F. J. Sabina, and F. Lebon, *A hierarchical asymptotic homogenization approach for viscoelastic composites*, Mech. Adv. Mater. Struct. **28** (2020), no. 21, 2190–2201.
90. R. Penta, A. Ramírez-Torres, J. Merodio, and R. Rodríguez-Ramos, *Effective governing equations for heterogenous porous media subject to inhomogeneous body forces*, Math. Eng. **3** (2021), no. 4, 1–17.
91. R. Burridge and J. B. Keller, *Poroelasticity equations derived from microstructure*, J. Acoust. Soc. Am. **70** (1981), no. 4, 1140–1146.
92. M. H. Holmes, *Introduction to perturbation methods*, Springer Science & Business Media, Springer-Verlag, New York, 1995.
93. R. Penta, D. Ambrosi, and R. J. Shipley, *Effective governing equations for poroelastic growing media*, Q. J. Mech. Appl. Math. **67** (2014), no. 1, 69–91.
94. A. Leyrat, A. Duperray, and C. Verdier, *Adhesion mechanisms in cancer metastasis*, 2003.
95. D. A. Hammer and M. Tirrell, *Biological adhesion at interfaces*, Ann. Rev. Mater. Sci. **26** (1996), no. 1, 651–691.
96. M. Gei, F. Genna, and D. Bigoni, *An interface model for the periodontal ligament*, J. Biomech. Eng. **124** (2002), no. 5, 538–546.
97. Z. Hashin, *Thermoelastic properties of fiber composites with imperfect interface*, Mech. Mater. **8** (1990), no. 4, 333–348.
98. Z. Hashin, *Thin interphase/imperfect interface in elasticity with application to coated fiber composites*, J. Mech. Phys. Solids **50** (2002), no. 12, 2509–2537.
99. Y. Benveniste and T. Miloh, *Imperfect soft and stiff interfaces in two-dimensional elasticity*, Mech. Mater. **33** (2001), no. 6, 309–323.
100. Y. Benveniste, *A general interface model for a three-dimensional curved thin anisotropic interphase between two anisotropic media*, J. Mech. Phys. Solids **54** (2006), no. 4, 708–734.
101. M. Serpilli, *On modeling interfaces in linear micropolar composites*, Math. Mech. Solids **23** (2017), no. 4, 667–685.
102. Y. Espinosa-Almeyda, V. Yanes, R. Rodríguez–Ramos, J. A. Otero, C. F. Sánchez-Valdés, H. Camacho–Montes, P. P. Longoria, and F. J. Sabina, *Effect of imperfect interface on the effective properties of elastic micropolar multilaminated nanostructures*, ZAMM—J. Appl. Math. Mech./Z. Angew. Math. Mech. **103** (2023), no. 8, e202200368.
103. R. Guinovart-Díaz, R. Rodríguez-Ramos, J. Bravo-Castillero, J. C. López-Realpozo, F. J. Sabina, and I. Sevostianov, *Effective elastic properties of a periodic fiber reinforced composite with parallelogram-like arrangement of fibers and imperfect contact between matrix and fibers*, Int. J. Solids Struct. **50** (2013), no. 13, 2022–2032.
104. S. M. Hassanizadeh, *Derivation of basic equations of mass transport in porous media, Part 1. Macroscopic balance laws*, Adv. Water Resour. **9** (1986), no. 4, 196–206.
105. M. E. Gurtin, *On the plasticity of single crystals: free energy, microforces, plastic-strain gradients*, J. Mech. Phys. Solids **48** (2000), no. 5, 989–1036.
106. M. E. Gurtin, *A gradient theory of single-crystal viscoplasticity that accounts for geometrically necessary dislocations*, J. Mech. Phys. Solids **50** (2002), no. 1, 5–32.
107. M. E. Gurtin, *On a framework for small-deformation viscoplasticity: free energy, microforces, strain gradients*, Int. J. Plast. **19** (2003), no. 1, 47–90.
108. M. Gurtin, *A gradient theory of small-deformation isotropic plasticity that accounts for the burgers vector and for dissipation due to plastic spin*, J. Mech. Phys. Solids **52** (2004), no. 11, 2545–2568.
109. R. Russo, F. A. G. Mata, S. Forest, and D. Jacquin, *A review on strain gradient plasticity approaches in simulation of manufacturing processes*, J. Manufact. Mater. Process. **4** (2020), no. 3, 87.
110. P. Cermelli and M. E. Gurtin, *On the characterization of geometrically necessary dislocations in finite plasticity*, J. Mech. Phys. Solids **49** (2001), no. 7, 1539–1568.
111. P. Neff and I. Münch, *Curl bounds grad on SO(3)*, PAMM **6** (2006), no. 1, 501–502.
112. P. Cermelli, E. Fried, and S. Sellers, *Configurational stress, yield and flow in rate–independent plasticity*, Proc. R. Soc. Lond. Ser. A Math. Phys. Eng. Sci. **457** (2001), no. 2010, 1447–1467.
113. A. Grillo, R. Prohl, and G. Wittum, *A poroplastic model of structural reorganisation in porous media of biomechanical interest*, Contin. Mech. Thermodyn. **28** (2016), 579–601.
114. R. A. Foty, C. M. Pfleger, G. Forgacs, and M. S. Steinberg, *Surface tensions of embryonic tissues predict their mutual envelopment behavior*, Development **122** (1996), no. 5, 1611–1620.
115. R. Skalak, S. Zargaryan, R. K. Jain, P. A. Netti, and A. Hoger, *Compatability and the genesis of residual stress by volumetric growth*, J. Math. Biol. **34** (1996), 889–914.
116. G. Forgacs, R. A. Foty, Y. Shafrir, and M. S. Steinberg, *Viscoelastic properties of living embryonic tissues: a quantitative study*, Biophys. J. **74** (1998), no. 5, 2227–2234.
117. T. Stylianopoulos, J. D. Martin, V. P. Chauhan, S. R. Jain, B. Diop-Frimpong, N. Bardeesy, B. L. Smith, C. R. Ferrone, F. J. Hornicek, Y. Boucher, L. L. Munn, and R. K. Jain, *Causes, consequences, and remedies for growth-induced solid stress in murine and human tumors*, Proc. Nat. Acad. Sci. **109** (2012), no. 38, 15101–15108.

10991476, 2025, 1, Downloaded from https://onlinelibrary.wiley.com/doi/10.1002/nme.10367 by Politecnico Di Torino Sist. Bibl Del Polit Di Torino, Wiley Online Library on [12/02/2025]. See the Terms and Conditions (https://onlinelibrary.wiley.com/terms-and-conditions) on Wiley Online Library for rules of use; OA articles are governed by the applicable Creative Commons License

118. C. Giverso, S. Di Stefano, A. Grillo, and L. Preziosi, *A three dimensional model of multicellular aggregate compression*, Soft Matter **15** (2019), no. 48, 10005–10019.
119. G. A. Maugin, *The thermomechanics of plasticity and fracture*, Cambridge University Press, Cambridge, 1992.
120. A. Carden, R. M. Rajachar, M. D. Morris, and D. H. Kohn, *Ultrastructural changes accompanying the mechanical deformation of bone tissue: a Raman imaging study*, Calcif. Tissue Int. **72** (2003), no. 2, 166–175.
121. P. Marmottant, A. Mgharbel, J. Käfer, B. Audren, J.-P. Rieu, J.-C. Vial, B. van der Sanden, A. F. M. Marée, F. Graner, and H. Delanoë-Ayari, *The role of fluctuations and stress on the effective viscosity of cell aggregates*, Proc. Nat. Acad. Sci. **106** (2009), no. 41, 17271–17275.
122. T. V. Stirbat, S. Tlili, T. Houver, J.-P. Rieu, C. Barentin, and H. Delanoë-Ayari, *Multicellular aggregates: a model system for tissue rheology*, Eur. Phys. J. E, Soft Matter **36** (2013), 9898.
123. C. Lanczos, *The variational principles of mechanics*, Dover Publications, New York, 1970.
124. A. Curnier, Q.-C. He, and P. Zysset, *Conewise linear elastic materials*, J. Elast. **37** (1995), no. 1, 1–38.
125. M. Epstein, Self-driven continuous dislocations and growth, *Advances in mechanics and mathematics*, Springer, Boston, MA, pp. 129–139.
126. S. Salsa, *Partial differential equations in action*, Springer-Verlag, Italia, Milan, 2015.
127. G. A. Pavliotis and A. Stuart, *Multiscale methods: averaging and homogenization*, Springer, New York, 2008.
128. R. J. Poole, *The Deborah and Weissenberg numbers*, British Soc. Rheol. Rheol. Bull. **2** (2012), no. 53, 32–39.
129. G. G. Giusteri and R. Penta, *Periodic rhomboidal cells for symmetry-preserving homogenization and isotropic metamaterials*, Mech. Res. Commun. **126** (2022), 104001.
130. A. Madeo, T. Lekszycki, and F. dell'Isola, *A continuum model for the bio-mechanical interactions between living tissue and bio-resorbable graft after bone reconstructive surgery*, Comptes Rend. Mécan. **339** (2011), no. 10, 625–640.
131. N. Abbasi, S. Hamlet, R. M. Love, and N.-T. Nguyen, *Porous scaffolds for bone regeneration*, J. Sci. Adv. Mater. Devices **5** (2020), no. 1, 1–9.

How to cite this article: A. Giammarini, A. Ramírez-Torres, and A. Grillo, *Effective elasto-(visco)plastic coefficients of a bi-phasic composite material with scale-dependent size effects*, Math. Meth. Appl. Sci. **48** (2025), 926–979, DOI 10.1002/mma.10367.

10991476, 2025, 1, Downloaded from https://onlinelibrary.wiley.com/doi/10.1002/mma.10367 by Politecnico Di Torino Sist. Bibl Del Polit Di Torino, Wiley Online Library on [12/02/2025]. See the Terms and Conditions (https://onlinelibrary.wiley.com/terms-and-conditions) on Wiley Online Library for rules of use; OA articles are governed by the applicable Creative Commons License